Stem Cells International

Improving Stem and Progenitor Cell Therapeutics

Guest Editors: Kenichi Tamama, Kathryn McFadden, and Jianjun Guan

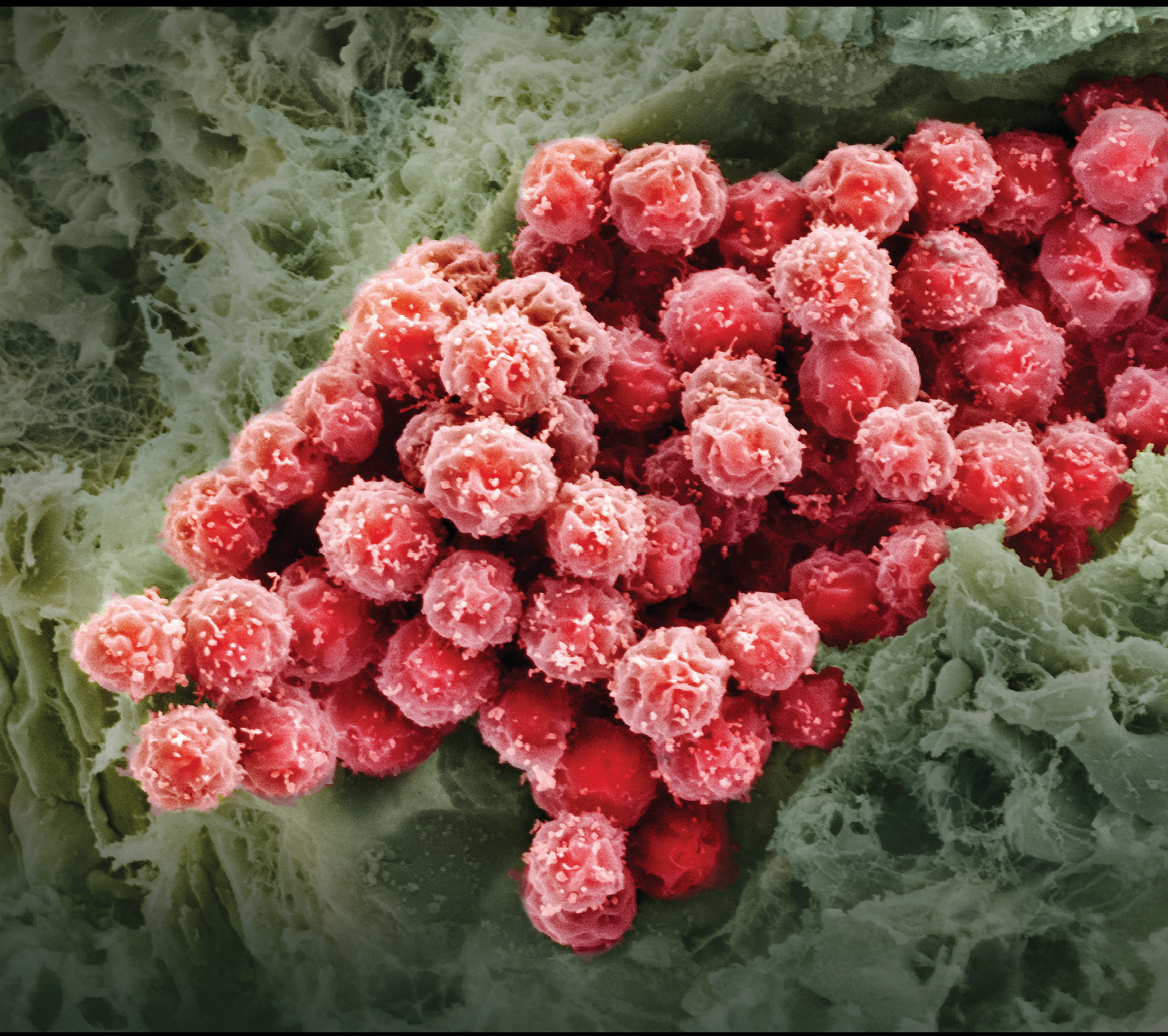

Improving Stem and Progenitor Cell Therapeutics

Stem Cells International

Improving Stem and Progenitor Cell Therapeutics

Guest Editors: Kenichi Tamama, Kathryn McFadden, and Jianjun Guan

Editorial Board

Contents

Hindawi Publishing Corporation
Stem Cells International
Volume 2016, Article ID 1409762, 2 pages
http://dx.doi.org/10.1155/2016/1409762

Editorial

Improving Stem and Progenitor Cell Therapeutics

Kenichi Tamama,[1,2] Kathryn McFadden,[3] and Jianjun Guan[4]

[1]*Department of Pathology, University of Pittsburgh School of Medicine, Pittsburgh, PA 15261, USA*
[2]*McGowan Institute for Regenerative Medicine, University of Pittsburgh, Pittsburgh, PA 15219, USA*
[3]*Department of Pathology, The University of Michigan Medical School, Ann Arbor, MI 48109, USA*
[4]*Department of Materials Science and Engineering, The Ohio State University, 2041 Collage Road, Columbus, OH 43210, USA*

Correspondence should be addressed to Kenichi Tamama; tamamakj@upmc.edu

Received 29 September 2015; Accepted 29 September 2015

Cell therapy with stem/progenitor cells is a new and promising therapeutic approach for many diseases that currently have few satisfying treatments. The prototype of stem cell-based therapy is bone marrow transplantation, which introduces hematopoietic stem cells (HSCs) to restore hematopoiesis after myeloablation in hematologic malignancy such as leukemia. Besides HSCs, other types of stem/progenitor cells, such as mesenchymal stem cells (MSCs) or induced pluripotent stem cells (iPSCs), are or will be applied in clinical studies.

There are various issues related to stem and progenitor cell therapeutics. First, the therapeutic effects of stem and progenitor cell therapeutics may be inadequate; the beneficial results of cell therapy in initial small-scale clinical studies have not always been reproduced by subsequent large-scale studies. For example, MSCs were shown to be no more effective than placebo in a large-scale, placebo-controlled phase III clinical trial for steroid-resistant graft-versus-host disease (GVHD) [1]. Moreover, autologous bone marrow mononuclear cells did not improve recovery of postmyocardial infarction left ventricular (post-MI LV) function in 2 randomized controlled trials with patients with ST-segment elevation myocardial infarction [2, 3]. These results strongly indicate the urgent needs of further optimization of cell-based therapy.

Safety is a second concern. For example, the original protocol of iPSC generation requires retrovirus-based transduction with 4 transcription factors (c-myc, oct4, klf4, and sos2) or Yamanaka factors [4, 5]. This means that iPSCs generated by the original protocol are potentially subject to insertional mutagenesis, as addressed in a review article by M. G. Cefalo et al. in this special issue. Obviously, there is still great room for improvement in stem/progenitor cell-based therapeutics, and this is the focus of this special issue.

Approaches and strategies to improve the therapeutic potential of stem/progenitor cells include enhancing treatment effect, improving cell delivery to target organs, and promoting cell engraftment and survival after implantation. In their original research article, R.-P. Zhang et al. demonstrated the combination of neurotrophin 3- (NT3-) transduction in a magnetically guided cell targeting system improves the neural regenerative effects of transplanted MSCs in a rat spinal cord injury model. C. Kiratipaiboon et al. showed in their original research article that a quinolone antibiotic ciprofloxacin improves the stemness of human dermal papilla cells by activating Wnt/β-catenin signaling, independently of its antimicrobial action. M. Chen et al. showed in their research article that polydactin, a glucoside of resveratrol widely used in traditional Chinese remedies, exerts antioxidative effects by activating the Nrf 2/ARE pathway. Finally, L. Wang et al. demonstrate the efficacy of transplanted umbilical cord mesenchymal stem cells, isolated according to their previously established novel protocol, in reducing standard measures of disease activity in clinical patients with juvenile idiopathic arthritis.

A promising technical approach is 3D-based cell culture. Mammalian cells have been traditionally cultured on the plastic in a 2D condition, but 3D spheroidal aggregates of MSCs

or MSC spheroids have been shown to possess enhanced therapeutic potential, as summarized by Z. Cesarz and K. Tamama. In their original research for this special issue, X. Zhao et al. additionally indicate transplanted adipose-derived MSC spheroids exert stronger tissue reparative effects with better graft survival in a rat renal ischemia-reperfusion injury model.

A biomaterial-based approach is another technical advance shown to improve both cell engraftment and survival after transplantation. This is well summarized by X. Li et al. in this issue. The original research by C. Uribe-Cruz et al. more specifically demonstrates whole bone marrow cells encapsulated by alginate-based hydrogel improve survival in rats after subtotal hepatectomy.

In summary, this special issue encompasses both comprehensive reviews and original research highlighting specific approaches, strategies, and techniques designed to improve stem and progenitor cell therapeutics.

Acknowledgment

We would like to thank all reviewers and authors for their contributions.

Kenichi Tamama
Kathryn McFadden
Jianjun Guan

References

[1] J. Galipeau, "The mesenchymal stromal cells dilemma-does a negative phase III trial of random donor mesenchymal stromal cells in steroid-resistant graft-versus-host disease represent a death knell or a bump in the road?" *Cytotherapy*, vol. 15, no. 1, pp. 2–8, 2013.

[2] S. Janssens, C. Dubois, J. Bogaert et al., "Autologous bone marrow-derived stem-cell transfer in patients with ST-segment elevation myocardial infarction: double-blind, randomised controlled trial," *The Lancet*, vol. 367, no. 9505, pp. 113–121, 2006.

[3] K. Lunde, S. Solheim, S. Aakhus et al., "Intracoronary injection of mononuclear bone marrow cells in acute myocardial infarction," *The New England Journal of Medicine*, vol. 355, no. 12, pp. 1199–1209, 2006.

[4] K. Takahashi, K. Tanabe, M. Ohnuki et al., "Induction of pluripotent stem cells from adult human fibroblasts by defined factors," *Cell*, vol. 131, no. 5, pp. 861–872, 2007.

[5] K. Takahashi and S. Yamanaka, "Induction of pluripotent stem cells from mouse embryonic and adult fibroblast cultures by defined factors," *Cell*, vol. 126, no. 4, pp. 663–676, 2006.

Hindawi Publishing Corporation
Stem Cells International
Volume 2016, Article ID 7168797, 11 pages
http://dx.doi.org/10.1155/2016/7168797

Review Article

Improving Cell Engraftment in Cardiac Stem Cell Therapy

Xiaofei Li,[1] Kenichi Tamama,[2,3] Xiaoyun Xie,[4] and Jianjun Guan[1,5]

[1]*Department of Materials Science and Engineering, The Ohio State University, 2041 College Road, Columbus, OH 43210, USA*
[2]*Department of Pathology, University of Pittsburgh School of Medicine, 3550 Terrace Street, Pittsburgh, PA 15261, USA*
[3]*McGowan Institute for Regenerative Medicine, University of Pittsburgh, Pittsburgh, PA 15219, USA*
[4]*Department of Gerontology, Tongji Hospital, Tongji University, Shanghai 200065, China*
[5]*Tongji Hospital, Tongji University, Shanghai 200065, China*

Correspondence should be addressed to Jianjun Guan; guan.21@osu.edu

Received 21 April 2015; Revised 22 July 2015; Accepted 11 August 2015

Academic Editor: Toru Hosoda

Myocardial infarction (MI) affects millions of people worldwide. MI causes massive cardiac cell death and heart function decrease. However, heart tissue cannot effectively regenerate by itself. While stem cell therapy has been considered an effective approach for regeneration, the efficacy of cardiac stem cell therapy remains low due to inferior cell engraftment in the infarcted region. This is mainly a result of low cell retention in the tissue and poor cell survival under ischemic, immune rejection and inflammatory conditions. Various approaches have been explored to improve cell engraftment: increase of cell retention using biomaterials as cell carriers; augmentation of cell survival under ischemic conditions by preconditioning cells, genetic modification of cells, and controlled release of growth factors and oxygen; and enhancement of cell survival by protecting cells from excessive inflammation and immune surveillance. In this paper, we review current progress, advantages, disadvantages, and potential solutions of these approaches.

1. Introduction

Heart disease has a high rate of morbidity and mortality [1]. Myocardial infarction (MI) is a major heart disease that causes massive cardiac cell death and partial loss of heart function. The infarcted heart tissue cannot effectively regenerate by itself because adult cardiomyocytes are unable to proliferate, and cardiac stem cells spontaneously generate only a limited number of cardiomyocytes [2]. Heart function thus cannot be restored. Following MI, the left ventricular wall progressively becomes thinner, and heart function gradually decreases. This adverse remodeling process leads to heart failure [3]. Heart transplantation is the only solution for patients with end-stage heart failure, but the number of donors available for transplantation is extremely limited, and the recipients require long-term immune suppressants to prevent organ rejection. Stem cell therapy is an alternate strategy. It aims to regenerate the infarcted heart tissue and/or improve heart function.

2. Stem Cells for Cardiac Therapy

Multiple cell types have been tested in animal models and clinical trials for cardiac therapy. Some stem cell types are capable of differentiating into cardiomyocytes to regenerate the heart tissue, leading to the restoration of heart function. These cells include cardiac stem cells [4–8] and pluripotent stem cell-derived cardiovascular progenitor cells [9, 10]. Some stem cell types cannot differentiate into functional cardiomyocytes but provide paracrine effects to augment the survival of resident cardiac cells, vascularize infarcted heart tissue, modulate immune response, recruit endogenous stem cells, and facilitate beneficial remodeling [11–17], resulting in an overall improvement of heart function. These stem cells include bone marrow-derived stem cells [18–23], adipose-derived stem cells [24–27], and cardiosphere-derived cells (CDCs) [28–35].

In the majority of current animal studies and clinical trials, stem cells are injected directly into the infarcted

heart. However approximately 90% of cells are lost to the circulation, leaked, or squeezed out of the injection site [36]. For those cells retained in the infarcted tissue, most of them die within the first few weeks [37]. Overall, cell engraftment of current stem cell therapy is low, and its therapeutic efficacy is limited.

3. Major Causes of Low Cell Engraftment in Infarcted Hearts

As discussed above, the major causes of the low cell engraftment are inferior cell retention and survival in the infarcted heart tissue. The commonly used saline solution has very low viscosity and cannot efficiently hold the cells in tissue. Transplanted cell death is mainly a result of inadequate cell attachment to the host tissue, severe ischemia, and excessive inflammation. Anoikis is a form of programmed cell death of adherent cells induced by poor or weak interaction between cell and extracellular matrix (ECM) [38]. In normal heart tissue, adherent cells attach strongly to the surrounding ECM. In the infarcted tissue, however, the ECM does not allow strong cell attachment [39]. Moreover, the saline used for cell transplantation does not provide cells with a matrix for attachment. These events cause anoikis [40].

Another factor is oxygen tension in the tissue. After MI, an extremely low oxygen and nutrient ischemic environment exists in the infarcted region. Although hypoxia is considered necessary to preserve the stem cell properties [41], the harsh ischemic environment activates cell death pathways, resulting in death of the transplanted cells [42].

Following MI, acute inflammation ensues with recruitment of inflammatory cells (neutrophils and monocytes) into the infarcted heart tissue. These recruited inflammatory cells are engaged in production of various inflammatory cytokines and chemokines to recruit more inflammatory cells, secretion of various proteolytic enzymes and reactive oxygen species (ROS), and phagocytosis to remove dead cells and tissue debris [43–45]. Both ROS and proinflammatory cytokines, such as tumor necrosis factor-α (TNF-α), can compromise survival of transplanted cells.

4. Approaches to Improve Stem Cell Engraftment

To increase cell engraftment in infarcted hearts, improving both cell retention and survival is necessary. The former may be achieved by using viscous, injectable hydrogels as cell carriers since low viscosity saline cannot efficiently hold cells in tissue. An injectable hydrogel can be delivered into the infarcted hearts through a minimal invasive injection approach (Figure 1) [49]. Seeding cells into scaffolds and patching them onto the heart may also increase cell retention (Figure 1). Both injectable hydrogels and scaffolds can augment cell survival. They provide an environment for cell attachment, which is required for cell survival. They can also be modified to promote stem cell survival under ischemic and inflammatory conditions [50]. In addition, the hydrogels and scaffolds offer mechanical support to the infarcted tissue to improve cardiac function.

To address the issue of cell survival under ischemic conditions, approaches including ischemic preexposure of cells, genetic modulation of cells, and delivery of growth factors and oxygen to cells have been used. To promote cell survival under inflammatory conditions, biomaterials have been modified to prevent immune proteins and proinflammatory cytokines from penetrating inside to attack the encapsulated stem cells.

4.1. Using Biomaterials and Cell Adhesion Molecules for Stem Cell Delivery. Biomaterials used for stem cell transplantation should be biodegradable and biocompatible [51]. Specifically, they should have a controlled biodegradation rate, which ideally coincides with the rate of new tissue regeneration [52]. The degradation products should be nontoxic. The biomaterials should ideally mimic mechanical properties of the heart tissue, for example, stiffness. This will decrease the elevated wall stress to improve cardiac function [53]. Both natural and synthetic polymers have been employed for stem cell transplantation. Natural polymers are biologically derived materials. Some of them, like fibrin [49, 54], alginate [55–57], collagen [58, 59], Matrigel [60], hyaluronic acid [61], and chitosan [62], have been used to deliver stem cells into infarcted hearts.

Synthetic polymers are generated via chemical method to pursue desired properties and functions. The properties can be controlled by composition and chemistry. The capability of endowing synthetic polymers with functional groups and tunable properties are advantages of using these polymers for stem cell transplantation [63]. Commonly used synthetic polymers include polyesters, such as polyglycolide (PGA), polylactide (PLA), poly(lactide-co-glycolide) (PLGA), polycaprolactone (PCL), and their copolymers [64]. These polymers are often used in the form of scaffold. PLGA scaffolds loaded with bFGF have been used to promote cardiac angiogenesis [65]. Porous PCL scaffolds have been used to deliver endothelial progenitor cells into heart tissue to promote vascularization [66].

Some synthetic polymers can be used in the form of hydrogel. For example, Li et al. generated thermosensitive hydrogels based on N-isopropylacrylamide (NIPAAm), acrylic acid (AAc), dimethyl-gamma-butyrolactone acrylate (DBA), and 2-hydroxyethyl methacrylate-poly(trimethylene carbonate) (HEMAPTMC) [46]. The hydrogels are injectable at room temperature and solidify at body temperature within 10 seconds. They can therefore quickly solidify to efficiently hold cells in the tissue. Interestingly, mesenchymal stem cells (MSCs) were able to proliferate inside (Figure 2). Other synthetic hydrogels developed for cardiac repair include poly(ethylene oxide)-b-poly(propylene oxide)-b-poly(ethylene oxide) (PEO-PPO-PEO) [67], poly(D-lysine) (PDL) [68], and MPEG-PCL-MPEG [69, 70].

Biomaterials can be modified with cell adhesive molecules to improve cell attachment, thus decreasing anoikis-induced stem cell death during transplantation [71]. Cell adhesive molecules are often mixed with or conjugated

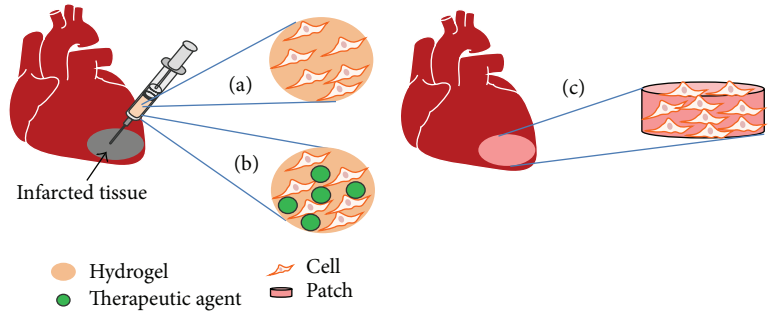

Figure 1: Strategies to improve cell retention in infarcted hearts. An injectable hydrogel can be used as a delivery vehicle for cells (a), or cells and therapeutic agents such as genes or proteins (b). A scaffold can be seeded with cells *in vitro* and then implanted to the infarcted region (c).

to the biomaterials. Karoubi et al. studied MSC survival in agarose with and without the addition of fibronectin and fibrinogen [72]. The results showed that cell survival was significantly increased after addition of fibronectin and fibrinogen. Similarly, fibrin glue remarkably improved cell survival in infarcted hearts [54]. Cooke et al. investigated cell adhesion on surfaces modified with several cell adhesive molecules, collagen I, collagen IV, fibronectin, and laminin, and found that cell attachment was increased [71]. Peptides YIGSR/IKVAV and RGD derived from laminin and fibronectin, respectively, have also been used to modify biomaterials to improve cell affinity [73].

4.2. Preexposure of Stem Cells for Enhanced Cell Survival. Preexposure of stem cells with ischemia or cytokines for cytoprotection is an alternate strategy to alleviate cell death. It enhances the cell tolerance to the harsh ischemic conditions. Murry et al. showed that cyclic exposure of stem cells to ischemia improved cell survival in ischemic myocardium [74]. Maulik et al. further demonstrated that ischemic preexposure allowed cells to adapt to ischemia, thus attenuating cell death under ischemia [75]. Grund et al. found that ischemically preexposed cells had reduced oxygen consumption [76]. In addition, ischemic preexposure enhanced cell secretion of growth factors [77, 78].

Cytokine preexposure can also improve cell survival [79–81]. MSCs pretreated with SDF-1α released antiapoptotic and angiogenic cytokines to improve cell survival and augment tissue angiogenesis [79]. Preexposure of endothelial progenitor cells with VEGF and bFGF enhanced cell paracrine effects, resulting in enhanced cell survival, angiogenesis, and reduced infarct size and left ventricle remodeling [80, 81]. Cells pretreated with IGF-1 showed cytoprotection effect both *in vitro* and *in vivo* [82, 83]. PI3K/Akt and MAPK/Erk1/2 pathways are responsible for the prosurvival effect.

4.3. Release of Growth Factors to Improve Cell Survival. High rates of both short-term and long-term cell survival are necessary for cardiac stem cell therapy. These may be achieved by using growth factors. Prosurvival growth factors allow for short-term cell survival, while angiogenic growth factors stimulate angiogenesis for long-term cell survival [84–86]. IGF-1 and HGF are two commonly used prosurvival growth factors. FGF [87], PDGF [88], and VEGF [89] are angiogenic growth factors used to promote angiogenesis in various tissues. bFGF also enhances cell survival under ischemic conditions [47]. In addition, specific growth factors can be used with prosurvival and angiogenic growth factors to promote stem cell differentiation into functional cells such as cardiomyocytes [90–92].

However, a concern for using growth factors in stem cell transplantation is that most of them have a relatively short half-life [93, 94]. Genetic modification of stem cells to promote the cells to secrete prosurvival and proangiogenic growth factors and sustained release of growth factors using biomaterials are commonly used approaches to address this concern.

Stem cells transfected with encoded genes of angiogenic growth factors like VEGF and FGF, and antiapoptotic factors like Akt and heme oxygenase-1, were able to secrete autocrine and paracrine growth factors [95, 96]. After transplanting these cells into infarcted hearts, cell survival, angiogenesis, and heart function were improved [97–99]. Matsumoto et al. transfected VEGF gene to MSCs and injected the modified cells into MI rat hearts [100]. High expression of VEGF was detected. This not only reduced cell death and increased capillary density, but also decreased the infarct size.

The growth factors are often encapsulated in biomaterials for controlled release [101–103]. Li et al. developed a bFGF release system based on a thermoresponsive and degradable hydrogel [47]. bFGF can be gradually released from the hydrogel for more than 2 weeks. The bFGF releasing system significantly increased MSC survival under low oxygen and nutrient conditions (Figure 3). It is expected that transplantation of stem cells using this bFGF release system will augment cell survival in the infarcted hearts. The release system may also promote angiogenesis due to the angiogenic effect of bFGF.

Padin-Iruega et al. tethered IGF-1 to self-assembling peptide nanofibers and used them for delivery of cardiac progenitor cells (CPCs) into infarcted hearts [104]. The IGF-1 was found to continuously release from the nanofibers to the myocardium. The released IGF-1 not only augmented CPC

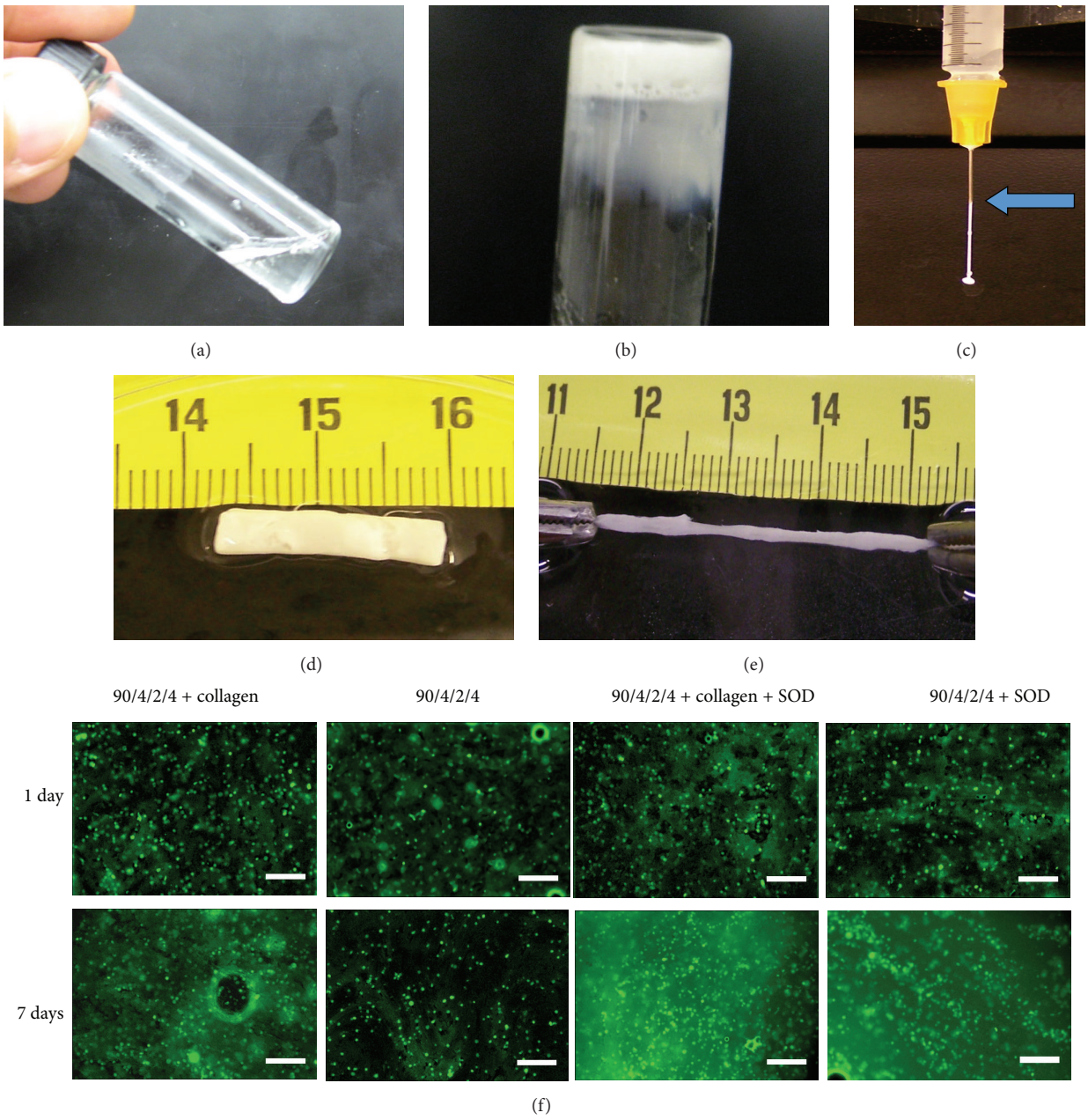

Figure 2: Macroscopic images of hydrogel and cells. The copolymer solution is flowable at 4°C (a) and forms gel after gelation at 37°C (b). The copolymer solution can be injected through a 26-gauge needle (c). At 37°C, the formed gel is flexible and can be stretched: (d) before stretching; (e) after stretching; (f) fluorescence images of MSCs encapsulated in hydrogels with or without collagen and superoxide dismutase (SOD, 4 mg/mL) after 1 and 7 days of culture. The cells were stained with live cell stain CMFDA before encapsulation. Scale bar = 100 μm. This figure is adopted from [46].

survival but also promoted cardiac differentiation, leading to enhanced cardiac regeneration.

4.4. Augmentation of Cell Survival by Releasing Oxygen to Transplanted Cells. Oxygen is critical for cell survival. The extremely low oxygen concentration in the infarcted heart results in significant cell death [105, 106]. Transplantation of stem cells with an oxygen release system is considered a feasible strategy to improve cell survival [107].

An oxygen release system can be generated using inorganic peroxide. Oh et al. developed a calcium peroxide-based oxygen release system by incorporating calcium peroxide into PLGA scaffold [108]. The system can continuously release oxygen for 10 days. The released oxygen enhanced cell survival under hypoxic conditions *in vitro*. However, this approach is not well suited for cardiac application since the Ca^{2+} generated together with oxygen may lead to abnormal Ca^{2+} transient in cardiomyocytes [109]. To avoid

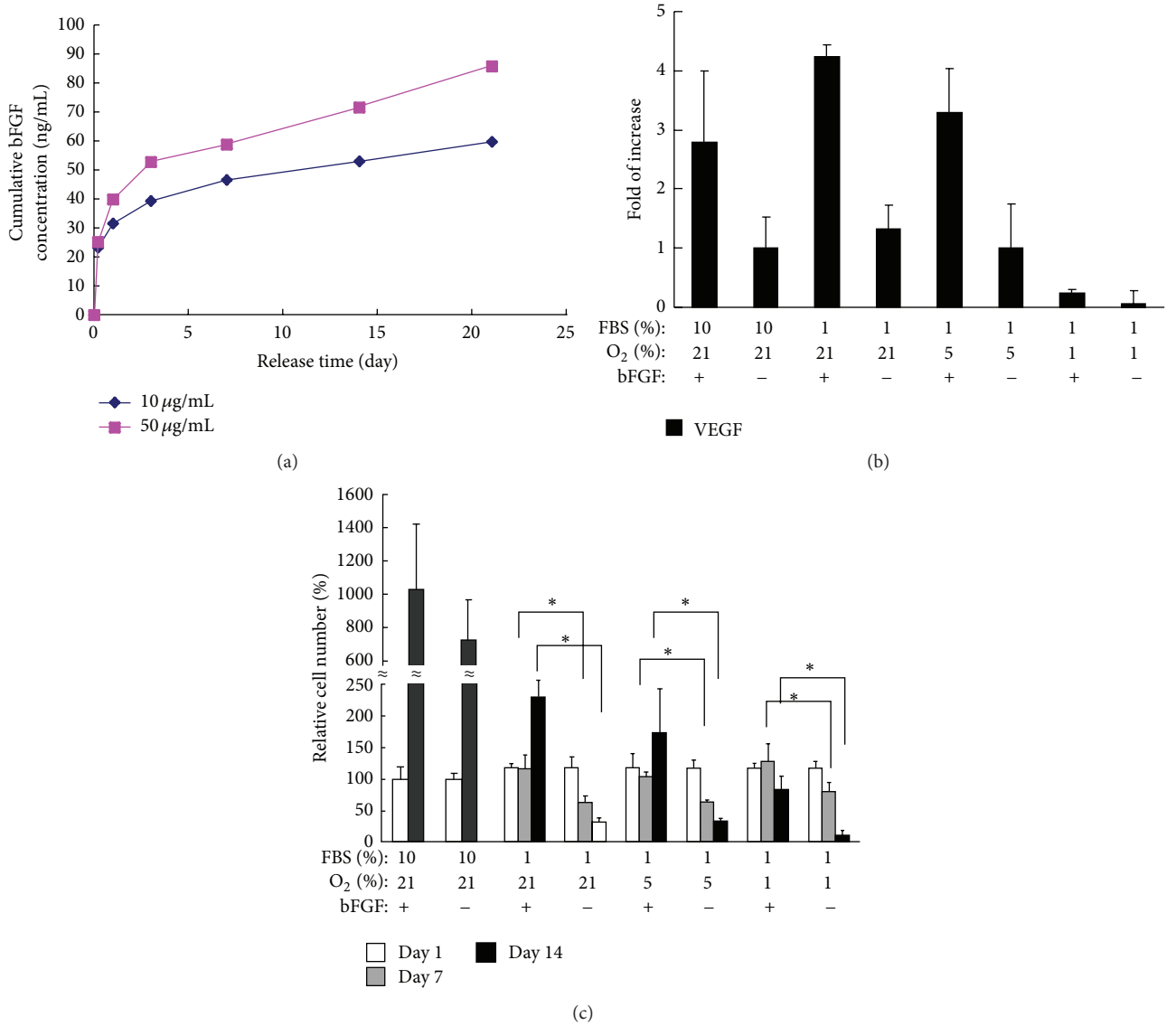

Figure 3: (a) Release kinetics of bFGF loaded in the hydrogels. bFGF loading was 10 and 50 μg/mL, respectively. The error bars are small. (b) VEGF expression of MSCs in the hydrogels under different culture conditions. Cells were cultured under conditions of 10% FBS and 21% oxygen, 1% FBS and 21% oxygen, 1% FBS and 5% oxygen, and 1% FBS and 1% oxygen, respectively. The expression was normalized by that under 10% FBS with 21% oxygen culture condition. (c) MSC survival in hydrogels cultured under different conditions. Culture conditions: 10% FBS and 21% oxygen, 1% FBS and 21% oxygen, 1% FBS and 5% oxygen, and 1% FBS and 1% oxygen. Double stranded DNA (dsDNA) content was used to quantify live cell number in the hydrogels. The dsDNA content at day 1 (100%) was used for normalization. This figure is adopted from [47].

the ion effect, organic molecules-based oxygen release systems, such as pyridine endoperoxide oxygen release system [110], hydrogen peroxide/poly(methyl methacrylate) microcapsule oxygen release system [111], and porphyrin-hemoprotein (rHSA(FeP-Glu)) oxygen release system [112], were developed and found to enhance cell survival. However, these oxygen release systems can release oxygen for less than 24 hours [108, 110–112].

To achieve longer term oxygen release, Abdi et al. encapsulated hydrogen peroxide into PLGA microspheres and obtained oxygen release for 7 days [113]. Li et al. encapsulated hydrogen peroxide/PVP complex in the PLGA microspheres and achieved sustained oxygen release at a relatively high oxygen level for 2 weeks (Figure 4) [48]. This oxygen release system significantly improved cell survival under hypoxic conditions *in vitro*. It has a great potential to augment cell survival in infarcted hearts for an extended period of time. Yet the concentration of released oxygen needs to be controlled so as not to overproduce ROS.

4.5. Modification of Biomaterials to Enhance Cell Survival under Immune Rejection and Inflammation Conditions. Immune rejection and excessive inflammation also decrease the survival rate of transplanted cells. Proinflammatory

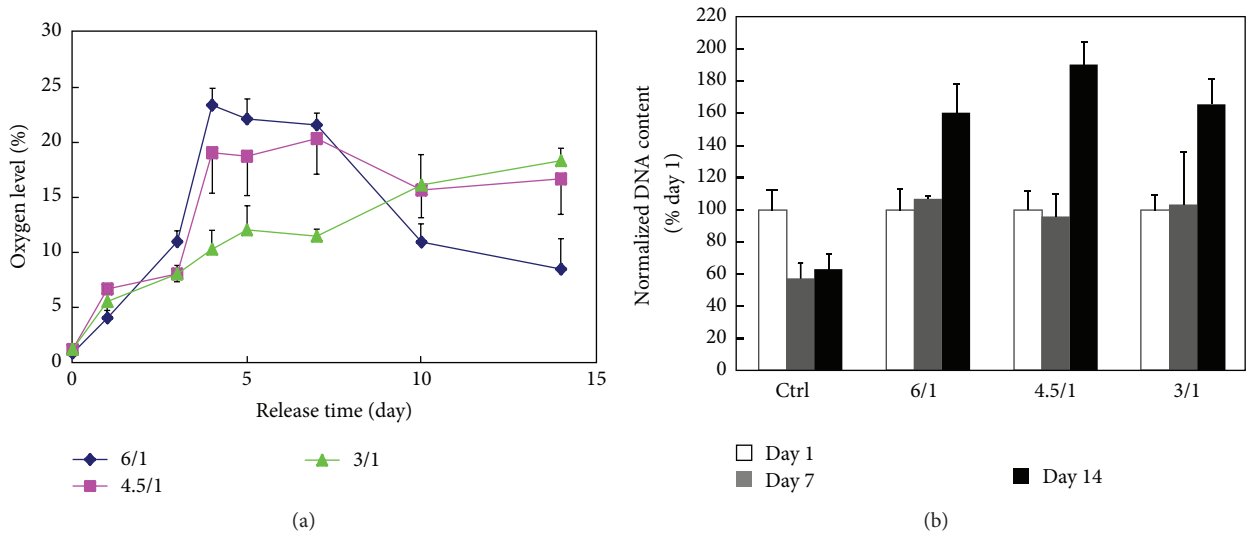

FIGURE 4: (a) Oxygen release kinetics of the H_2O_2 -releasing microspheres with different H_2O_2/VP ratio; (b) dsDNA content of live CDCs encapsulated in hydrogels with or without oxygen release. The higher dsDNA content represents higher live cell number. Cells were cultured under 1% oxygen condition. Hydrogels with oxygen release had microspheres with H_2O_2/VP ratio of 6/1, 4.5/1, and 3/1, respectively. This figure is adopted from [48].

cytokines like TNF-α and IL-1 induce excessive inflammation and create a noxious microenvironment, in addition to causing apoptosis of the cells [114]. Optimization of biomaterial properties and introduction of anti-inflammatory molecules into biomaterials may provide protection for the transplanted cells. By controlling pore size of the biomaterials, transplanted cells can be immunoisolated, leading to better cell survival of the transplanted cells [115–119]. However, small cytotoxic molecules such as TNF-α and IL-1β can still diffuse into the biomaterials [120, 121]. To address this issue, approaches like increasing degree of cross-linking and matrix concentration were used. However, these approaches may impede nutrient transport to cells. An alternate approach is to modify the biomaterials with anti-inflammatory molecules. For example, anti-TNF-peptide WP9QY (YCWSQYLCY) may be conjugated into hydrogel to prevent TNF from penetrating inside [122].

After MI, ROS content in the failing heart is upregulated [123], which can be cytotoxic against the transplanted cells. To decrease the cytotoxic effects of ROS, Hume and Anseth incorporated superoxide dismutase mimetic (SODm) into PEG hydrogel. This largely protected cells from oxidative stress damage and improved cell survival [124].

5. Conclusions and Prospects

Stem cell therapy is considered a potent and promising approach for cardiac therapy. However, the efficacy is limited as only a small percentage of transplanted cells engrafted in the infarcted tissue. Low cell retention and inferior cell survival are mainly responsible for the limited cell engraftment. Hydrogels and scaffolds can be utilized to improve cell retention. Injectable hydrogels may be more convenient for cell delivery than scaffolds as they can be delivered by a minimally invasive injection approach. Injectable hydrogels increase cell retention because of their high viscosity. Yet, long gelation time may not allow the hydrogels to largely increase cell retention, as they may be squeezed out of heart tissue or washed into circulation before gelation. Some hydrogels require UV radiation, pH changing, or ion addition to solidify, which may cause potential harm to cells. Thermosensitive and biodegradable hydrogels that have a fast gelation rate (in seconds) may address this issue.

Different approaches have been explored to enhance cell survival in infarcted hearts. While they can improve cell survival to some extent, different types of stem cells may require dissimilar optimization approaches for preparation, activation, transplantation procedures, and maintenance *in vivo*. There are also disadvantages associated with these approaches. Ischemic preexposure may damage cells in the process, and the transplanted cells may not survive under ischemic conditions for a long enough period. Genetic modification of cells may raise safety concerns. Controlled release of growth factors and oxygen and immune protection appear to be more effective to promote cell survival. However, further studies on the long-term effect of these approaches on cell survival, functioning, and differentiation are needed.

From a clinical point of view, safety and efficacy are still paramount issues. More studies on animals are required in order to develop a reliable cell-biomaterial delivery system with long-term safety and efficacy. Biomaterial type, degradation product toxicity, dose, and timing must be well studied before clinical application.

Conflict of Interests

The authors declare that there is no conflict of interests regarding the publication of this paper.

Acknowledgments

This work was supported by US National Science Foundation (1006734 and 1160122), American Heart Association (15GRNT25830058 and 13GRNT17150041), National Science Foundation of China (81471788), Institute for Materials Research Seed Grant at The Ohio State University, and Competitive Medical Research Fund from University of Pittsburgh Medical Center Health System.

References

[1] D. Mozaffarian, E. J. Benjamin, A. S. Go et al., "Heart disease and stroke statistics—2015 update: a report from the American Heart Association," *Circulation*, vol. 131, no. 4, pp. e29–e322, 2015.

[2] S. Etzion, L. H. Kedes, R. A. Kloner, and J. Leor, "Myocardial regeneration: present and future trends," *American Journal of Cardiovascular Drugs*, vol. 1, no. 4, pp. 233–244, 2001.

[3] J. N. Cohn, R. Ferrari, and N. Sharpe, "Cardiac remodeling—concepts and clinical implications: a consensus paper from an International Forum on Cardiac Remodeling," *Journal of the American College of Cardiology*, vol. 35, no. 3, pp. 569–582, 2000.

[4] T. Hosoda, H. Zheng, M. Cabral-Da-Silva et al., "Human cardiac stem cell differentiation is regulated by a mircrine mechanism," *Circulation*, vol. 123, no. 12, pp. 1287–1296, 2011.

[5] A. R. Chugh, G. M. Beache, J. H. Loughran et al., "Administration of cardiac stem cells in patients with ischemic cardiomyopathy: the SCIPIO trial: surgical aspects and interim analysis of myocardial function and viability by magnetic resonance," *Circulation*, vol. 126, no. 11, pp. S54–S64, 2012.

[6] R. Bolli, X.-L. Tang, S. K. Sanganalmath et al., "Intracoronary delivery of autologous cardiac stem cells improves cardiac function in a porcine model of chronic ischemic cardiomyopathy," *Circulation*, vol. 128, no. 2, pp. 122–131, 2013.

[7] N. Latham, B. Ye, R. Jackson et al., "Human blood and cardiac stem cells synergize to enhance cardiac repair when cotransplanted into ischemic myocardium," *Circulation*, vol. 128, supplement 1, no. 1, pp. S105–S112, 2013.

[8] A. R. Williams, K. E. Hatzistergos, B. Addicott et al., "Enhanced effect of combining human cardiac stem cells and bone marrow mesenchymal stem cells to reduce infarct size and to restore cardiac function after myocardial infarction," *Circulation*, vol. 127, no. 2, pp. 213–223, 2013.

[9] D. Später, M. K. Abramczuk, K. Buac et al., "A HCN4+ cardiomyogenic progenitor derived from the first heart field and human pluripotent stem cells," *Nature Cell Biology*, vol. 15, no. 9, pp. 1098–1106, 2013.

[10] A. Nsair, K. Schenke-Layland, B. van Handel et al., "haracterization and therapeutic potential of induced pluripotent stem cell-derived cardiovascular progenitor cells," *PLoS ONE*, vol. 7, no. 10, Article ID e45603, 2012.

[11] J. S. Forrester, R. R. Makkar, and E. Marbán, "Long-term outcome of stem cell therapy for acute myocardial infarction: right results, wrong reasons," *Journal of the American College of Cardiology*, vol. 53, no. 24, pp. 2270–2272, 2009.

[12] F. Wang and J. Guan, "Cellular cardiomyoplasty and cardiac tissue engineering for myocardial therapy," *Advanced Drug Delivery Reviews*, vol. 62, no. 7-8, pp. 784–797, 2010.

[13] C. W. Don and C. E. Murry, "Improving survival and efficacy of pluripotent stem cell-derived cardiac grafts," *Journal of Cellular and Molecular Medicine*, vol. 17, no. 11, pp. 1355–1362, 2013.

[14] Y. L. Tang, Y. J. Wang, L. J. Chen, Y. H. Pan, L. Zhang, and N. L. Weintraub, "Cardiac-derived stem cell-based therapy for heart failure: Progress and clinical applications," *Experimental Biology and Medicine*, vol. 238, no. 3, pp. 294–300, 2013.

[15] J. C. Garbern and R. T. Lee, "Cardiac stem cell therapy and the promise of heart regeneration," *Cell Stem Cell*, vol. 12, no. 6, pp. 689–698, 2013.

[16] M. R. Rosen, R. J. Myerburg, D. P. Francis, G. D. Cole, and E. Marbán, "Translating stem cell research to cardiac disease therapies: pitfalls and prospects for improvement," *Journal of the American College of Cardiology*, vol. 64, no. 9, pp. 922–937, 2014.

[17] J. H. van Berlo and J. D. Molkentin, "An emerging consensus on cardiac regeneration," *Nature Medicine*, vol. 20, no. 12, pp. 1386–1393, 2014.

[18] N. Nagaya, K. Kangawa, T. Itoh et al., "Transplantation of mesenchymal stem cells improves cardiac function in a rat model of dilated cardiomyopathy," *Circulation*, vol. 112, no. 8, pp. 1128–1135, 2005.

[19] M. Gnecchi, H. He, N. Noiseux et al., "Evidence supporting paracrine hypothesis for Akt-modified mesenchymal stem cell-mediated cardiac protection and functional improvement," *The FASEB Journal*, vol. 20, no. 6, pp. 661–669, 2006.

[20] R. S. Ripa, M. Haack-Sørensen, Y. Wang et al., "Bone marrow-derived mesenchymal cell mobilization by granulocyte-colony stimulating factor after acute myocardial infarction: results from the Stem Cells in Myocardial Infarction (STEMMI) trial," *Circulation*, vol. 116, no. 11, pp. I24–I30, 2007.

[21] J. M. Hare, J. H. Traverse, T. D. Henry et al., "A randomized, double-blind, placebo-controlled, dose-escalation study of intravenous adult human mesenchymal stem cells (Prochymal) after acute myocardial infarction," *Journal of the American College of Cardiology*, vol. 54, no. 24, pp. 2277–2286, 2009.

[22] J. H. Traverse, D. H. McKenna, K. Harvey et al., "Results of a phase 1, randomized, double-blind, placebo-controlled trial of bone marrow mononuclear stem cell administration in patients following ST-elevation myocardial infarction," *American Heart Journal*, vol. 160, no. 3, pp. 428–434, 2010.

[23] J. M. Duran, C. A. Makarewich, T. E. Sharp et al., "Bone-derived stem cells repair the heart after myocardial infarction through transdifferentiation and paracrine signaling mechanisms," *Circulation Research*, vol. 113, no. 5, pp. 539–552, 2013.

[24] M. Mazo, V. Planat-Bénard, G. Abizanda et al., "Transplantation of adipose derived stromal cells is associated with functional improvement in a rat model of chronic myocardial infarction," *European Journal of Heart Failure*, vol. 10, no. 5, pp. 454–462, 2008.

[25] M. Mazo, S. Hernández, J. J. Gavira et al., "Treatment of reperfused ischemia with adipose-derived stem cells in a preclinical Swine model of myocardial infarction," *Cell Transplantation*, vol. 21, no. 12, pp. 2723–2733, 2012.

[26] E. K. Shevchenko, P. I. Makarevich, Z. I. Tsokolaeva et al., "Transplantation of modified human adipose derived stromal cells expressing VEGF165 results in more efficient angiogenic response in ischemic skeletal muscle," *Journal of Translational Medicine*, vol. 11, no. 1, article 138, 2013.

[27] M. Rigol, N. Solanes, S. Roura et al., "Allogeneic adipose stem cell therapy in acute myocardial infarction," *European Journal of Clinical Investigation*, vol. 44, no. 1, pp. 83–92, 2014.

[28] R. R. Smith, L. Barile, H. C. Cho et al., "Regenerative potential of cardiosphere-derived cells expanded from percutaneous endomyocardial biopsy specimens," *Circulation*, vol. 115, no. 7, pp. 896–908, 2007.

[29] D. R. Davis, Y. Zhang, R. R. Smith et al., "Validation of the cardiosphere method to culture cardiac progenitor cells from myocardial tissue," *PLoS ONE*, vol. 4, no. 9, Article ID e7195, 2009.

[30] P. V. Johnston, T. Sasano, K. Mills et al., "Engraftment, differentiation, and functional benefits of autologous cardiosphere-derived cells in porcine ischemic cardiomyopathy," *Circulation*, vol. 120, no. 12, pp. 1075–1083, 2009.

[31] I. Chimenti, R. R. Smith, T.-S. Li et al., "Relative roles of direct regeneration versus paracrine effects of human cardiosphere-derived cells transplanted into infarcted mice," *Circulation Research*, vol. 106, no. 5, pp. 971–980, 2010.

[32] R. Mishra, K. Vijayan, E. J. Colletti et al., "Characterization and functionality of cardiac progenitor cells in congenital heart patients," *Circulation*, vol. 123, no. 4, pp. 364–373, 2011.

[33] T.-S. Li, K. Cheng, K. Malliaras et al., "Direct comparison of different stem cell types and subpopulations reveals superior paracrine potency and myocardial repair efficacy with cardiosphere-derived cells," *Journal of the American College of Cardiology*, vol. 59, no. 10, pp. 942–953, 2012.

[34] H. Maxeiner, S. Mufti, N. Krehbiehl et al., "Interleukin-6 contributes to the paracrine effects of cardiospheres cultured from human, murine and rat hearts," *Journal of Cellular Physiology*, vol. 229, no. 11, pp. 1681–1689, 2014.

[35] Y. Xie, A. Ibrahim, K. Cheng et al., "Importance of cell-cell contact in the therapeutic benefits of cardiosphere-derived cells," *Stem Cells*, vol. 32, no. 9, pp. 2397–2406, 2014.

[36] J. Leor, S. Aboulafia-Etzion, A. Dar et al., "Bioengineered cardiac grafts: a new approach to repair the infarcted myocardium?" *Circulation*, vol. 102, no. 19, pp. III56–III61, 2000.

[37] H. Reinecke and C. E. Murry, "Taking the death toll after cardiomyocyte grafting: a reminder of the importance of quantitative biology," *Journal of Molecular and Cellular Cardiology*, vol. 34, no. 3, pp. 251–253, 2002.

[38] S. M. Frisch and R. A. Screaton, "Anoikis mechanisms," *Current Opinion in Cell Biology*, vol. 13, no. 5, pp. 555–562, 2001.

[39] K. Imanaka-Yoshida, M. Hiroe, and T. Yoshida, "Interaction between cell and extracellular matrix in heart disease: multiple roles of tenascin-C in tissue remodeling," *Histology and Histopathology*, vol. 19, no. 2, pp. 517–525, 2004.

[40] S. M. Frisch and H. Francis, "Disruption of epithelial cell-matrix interactions induces apoptosis," *Journal of Cell Biology*, vol. 124, no. 4, pp. 619–626, 1994.

[41] M. Csete, "Oxygen in the cultivation of stem cells," *Annals of the New York Academy of Sciences*, vol. 1049, pp. 1–8, 2005.

[42] H. K. Haider and M. Ashraf, "Strategies to promote donor cell survival: combining preconditioning approach with stem cell transplantation," *Journal of Molecular and Cellular Cardiology*, vol. 45, no. 4, pp. 554–566, 2008.

[43] J. L. Mehta, W. W. Nichols, and P. Mehta, "Neutrophils as potential participants in acute myocardial ischemia: relevance to reperfusion," *Journal of the American College of Cardiology*, vol. 11, no. 6, pp. 1309–1316, 1988.

[44] M. Nahrendorf, F. K. Swirski, E. Aikawa et al., "The healing myocardium sequentially mobilizes two monocyte subsets with divergent and complementary functions," *The Journal of Experimental Medicine*, vol. 204, no. 12, pp. 3037–3047, 2007.

[45] M. Nahrendorf, S. Frantz, F. K. Swirski et al., "Imaging systemic inflammatory networks in ischemic heart disease," *Journal of the American College of Cardiology*, vol. 65, no. 15, pp. 1583–1591, 2015.

[46] Z. Li, F. Wang, S. Roy, C. K. Sen, and J. Guan, "Injectable, highly flexible, and thermosensitive hydrogels capable of delivering superoxide dismutase," *Biomacromolecules*, vol. 10, no. 12, pp. 3306–3316, 2009.

[47] Z. Li, X. Guo, and J. Guan, "A thermosensitive hydrogel capable of releasing bFGF for enhanced differentiation of mesenchymal stem cell into cardiomyocyte-like cells under ischemic conditions," *Biomacromolecules*, vol. 13, no. 6, pp. 1956–1964, 2012.

[48] Z. Li, X. Guo, and J. Guan, "An oxygen release system to augment cardiac progenitor cell survival and differentiation under hypoxic condition," *Biomaterials*, vol. 33, no. 25, pp. 5914–5923, 2012.

[49] K. L. Christman and R. J. Lee, "Biomaterials for the treatment of myocardial infarction," *Journal of the American College of Cardiology*, vol. 48, no. 5, pp. 907–913, 2006.

[50] M. S. Shoichet, "Polymer scaffolds for biomaterials applications," *Macromolecules*, vol. 43, no. 2, pp. 581–591, 2009.

[51] B. L. Seal, T. C. Otero, and A. Panitch, "Polymeric biomaterials for tissue and organ regeneration," *Materials Science & Engineering: R: Reports*, vol. 34, no. 4-5, pp. 147–230, 2001.

[52] H. Shin, S. Jo, and A. G. Mikos, "Biomimetic materials for tissue engineering," *Biomaterials*, vol. 24, no. 24, pp. 4353–4364, 2003.

[53] K. L. Christman, H. H. Fok, R. E. Sievers, Q. Fang, and R. J. Lee, "Fibrin glue alone and skeletal myoblasts in a fibrin scaffold preserve cardiac function after myocardial infarction," *Tissue Engineering*, vol. 10, no. 3-4, pp. 403–409, 2004.

[54] K. L. Christman, A. J. Vardanian, Q. Fang, R. E. Sievers, H. H. Fok, and R. J. Lee, "Injectable fibrin scaffold improves cell transplant survival, reduces infarct expansion, and induces neovasculature formation in ischemic myocardium," *Journal of the American College of Cardiology*, vol. 44, no. 3, pp. 654–660, 2004.

[55] N. Landa, L. Miller, M. S. Feinberg et al., "Effect of injectable alginate implant on cardiac remodeling and function after recent and old infarcts in rat," *Circulation*, vol. 117, no. 11, pp. 1388–1396, 2008.

[56] R. G. Gomez-Mauricio, A. Acarregui, F. M. Sánchez-Margallo et al., "A preliminary approach to the repair of myocardial infarction using adipose tissue-derived stem cells encapsulated in magnetic resonance-labelled alginate microspheres in a porcine model," *European Journal of Pharmaceutics and Biopharmaceutics*, vol. 84, no. 1, pp. 29–39, 2013.

[57] E. T. Roche, C. L. Hastings, S. A. Lewin et al., "Comparison of biomaterial delivery vehicles for improving acute retention of stem cells in the infarcted heart," *Biomaterials*, vol. 35, no. 25, pp. 6850–6858, 2014.

[58] W. Dai, L. E. Wold, J. S. Dow, and R. A. Kloner, "Thickening of the infarcted wall by collagen injection improves left ventricular function in rats: a novel approach to preserve cardiac function after myocardial infarction," *Journal of the American College of Cardiology*, vol. 46, no. 4, pp. 714–719, 2005.

[59] E. J. Suuronen, J. P. Veinot, S. Wong et al., "Tissue-engineered injectable collagen-based matrices for improved cell delivery and vascularization of ischemic tissue using CD133+ progenitors expanded from the peripheral blood," *Circulation*, vol. 114, supplement, no. 1, pp. I138–I144, 2006.

[60] C. Xu, M. S. Inokuma, J. Denham et al., "Feeder-free growth of undifferentiated human embryonic stem cells," *Nature Biotechnology*, vol. 19, no. 10, pp. 971–974, 2001.

[61] C. Y. Chang, A. T. Chan, P. A. Armstrong et al., "Hyaluronic acid-human blood hydrogels for stem cell transplantation," *Biomaterials*, vol. 33, no. 32, pp. 8026–8033, 2012.

[62] M. Ishihara, K. Nakanishi, K. Ono et al., "Photocrosslinkable chitosan as a dressing for wound occlusion and accelerator in healing process," *Biomaterials*, vol. 23, no. 3, pp. 833–840, 2002.

[63] N. Zhang and D. H. Kohn, "Using polymeric materials to control stem cell behavior for tissue regeneration," *Birth Defects Research, Part C—Embryo Today: Reviews*, vol. 96, no. 1, pp. 63–81, 2012.

[64] R. C. Thomson, M. C. Wake, M. J. Yaszemski et al., "Biodegradable polymer scaffolds to regenerate organs," in *Biopolymers II*, N. Peppas and R. Langer, Eds., pp. 245–274, Springer, Berlin, Germany, 1995.

[65] Y. Wang, X.-C. Liu, J. Zhao et al., "Degradable PLGA scaffolds with basic fibroblast growth factor: experimental studies in myocardial revascularization," *Texas Heart Institute Journal*, vol. 36, no. 2, pp. 89–97, 2009.

[66] S. Singh, B. M. Wu, and J. C. Y. Dunn, "Accelerating vascularization in polycaprolactone scaffolds by endothelial progenitor cells," *Tissue Engineering Part: A*, vol. 17, no. 13-14, pp. 1819–1830, 2011.

[67] P. Bawa, V. Pillay, Y. E. Choonara, and L. C. D. Toit, "Stimuli-responsive polymers and their applications in drug delivery," *Biomedical Materials*, vol. 4, no. 2, Article ID 022001, 2009.

[68] K. E. Crompton, J. D. Goud, R. V. Bellamkonda et al., "Polylysine-functionalised thermoresponsive chitosan hydrogel for neural tissue engineering," *Biomaterials*, vol. 28, no. 3, pp. 441–449, 2007.

[69] X.-J. Jiang, T. Wang, X.-Y. Li et al., "Injection of a novel synthetic hydrogel preserves left ventricle function after myocardial infarction," *Journal of Biomedical Materials Research A*, vol. 90, no. 2, pp. 472–477, 2009.

[70] H. Tseng, D. S. Puperi, E. J. Kim et al., "Anisotropic poly(ethylene glycol)/polycaprolactone hydrogel–fiber composites for heart valve tissue engineering," *Tissue Engineering Part A*, vol. 20, no. 19-20, pp. 2634–2645, 2014.

[71] M. J. Cooke, S. R. Phillips, D. S. H. Shah, D. Athey, J. H. Lakey, and S. A. Przyborski, "Enhanced cell attachment using a novel cell culture surface presenting functional domains from extracellular matrix proteins," *Cytotechnology*, vol. 56, no. 2, pp. 71–79, 2008.

[72] G. Karoubi, M. L. Ormiston, D. J. Stewart, and D. W. Courtman, "Single-cell hydrogel encapsulation for enhanced survival of human marrow stromal cells," *Biomaterials*, vol. 30, no. 29, pp. 5445–5455, 2009.

[73] L. Jongpaiboonkit, W. J. King, and W. L. Murphy, "Screening for 3D environments that support human mesenchymal stem cell viability using hydrogel arrays," *Tissue Engineering Part A*, vol. 15, no. 2, pp. 343–353, 2009.

[74] C. E. Murry, R. B. Jennings, and K. A. Reimer, "Preconditioning with ischemia: a delay of lethal cell injury in ischemic myocardium," *Circulation*, vol. 74, no. 5, pp. 1124–1136, 1986.

[75] N. Maulik, T. Yoshida, R. M. Engelman et al., "Ischemic preconditioning attenuates apoptotic cell death associated with ischemia/reperfusion," *Molecular and Cellular Biochemistry*, vol. 186, no. 1-2, pp. 139–145, 1998.

[76] F. Grund, H. T. Sommerschild, K. A. Kirkebøen, and A. Ilebekk, "Preconditioning with ischaemia reduces both myocardial oxygen consumption and infarct size in a graded pattern," *Journal of Molecular and Cellular Cardiology*, vol. 29, no. 11, pp. 3067–3079, 1997.

[77] M. Ii, H. Nishimura, A. Iwakura et al., "Endothelial progenitor cells are rapidly recruited to myocardium and mediate protective effect of ischemic preconditioning via 'imported' nitric oxide synthase activity," *Circulation*, vol. 111, no. 9, pp. 1114–1120, 2005.

[78] S. Addya, K. Shiroto, T. Turoczi et al., "Ischemic preconditioning-mediated cardioprotection is disrupted in heterozygous Flt-1 (VEGFR-1) knockout mice," *Journal of Molecular and Cellular Cardiology*, vol. 38, no. 2, pp. 345–351, 2005.

[79] S. Vandervelde, M. J. A. van Luyn, R. A. Tio, and M. C. Harmsen, "Signaling factors in stem cell-mediated repair of infarcted myocardium," *Journal of Molecular and Cellular Cardiology*, vol. 39, no. 2, pp. 363–376, 2005.

[80] S. Shintani, K. Kusano, M. Ii et al., "Synergistic effect of combined intramyocardial $CD34^+$ cells and VEGF2 gene therapy after MI," *Nature Clinical Practice Cardiovascular Medicine*, vol. 3, supplement 1, pp. S123–S128, 2006.

[81] Z. Pasha, Y. Wang, R. Sheikh, D. Zhang, T. Zhao, and M. Ashraf, "Preconditioning enhances cell survival and differentiation of stem cells during transplantation in infarcted myocardium," *Cardiovascular Research*, vol. 77, no. 1, pp. 134–142, 2008.

[82] M. Párrizas, A. R. Saltiel, and D. LeRoith, "Insulin-like growth factor 1 inhibits apoptosis using the phosphatidylinositol 3'-kinase and mitogen-activated protein kinase pathways," *The Journal of Biological Chemistry*, vol. 272, no. 1, pp. 154–161, 1997.

[83] S. Humbert, E. A. Bryson, F. P. Cordelières et al., "The IGF-1/Akt pathway is neuroprotective in Huntington's disease and involves huntingtin phosphorylation by Akt," *Developmental Cell*, vol. 2, no. 6, pp. 831–837, 2002.

[84] J. E. Nör, J. Christensen, D. J. Mooney, and P. J. Polverini, "Vascular endothelial growth factor (VEGF)-mediated angiogenesis is associated with enhanced endothelial cell survival and induction of Bcl-2 expression," *The American Journal of Pathology*, vol. 154, no. 2, pp. 375–384, 1999.

[85] T. Deuse, C. Peter, P. W. M. Fedak et al., "Hepatocyte growth factor or vascular endothelial growth factor gene transfer maximizes mesenchymal stem cell-based myocardial salvage after acute myocardial infarction," *Circulation*, vol. 120, no. 1, pp. S247–S254, 2009.

[86] T.-J. Lee, S. H. Bhang, H. S. Yang et al., "Enhancement of long-term angiogenic efficacy of adipose stem cells by delivery of FGF2," *Microvascular Research*, vol. 84, no. 1, pp. 1–8, 2012.

[87] F. Ma, Z. Xiao, B. Chen et al., "Accelerating proliferation of neural stem/progenitor cells in collagen sponges immobilized with engineered basic fibroblast growth factor for nervous system tissue engineering," *Biomacromolecules*, vol. 15, no. 3, pp. 1062–1068, 2014.

[88] Y. Chen, H. Xu, J. Liu, C. Zhang, A. Leutz, and X. Mo, "The c-Myb functions as a downstream target of PDGF-mediated survival signal in vascular smooth muscle cells," *Biochemical and Biophysical Research Communications*, vol. 360, no. 2, pp. 433–436, 2007.

[89] H. K. Haider, L. Ye, S. Jiang et al., "Angiomyogenesis for cardiac repair using human myoblasts as carriers of human vascular endothelial growth factor," *Journal of Molecular Medicine*, vol. 82, no. 8, pp. 539–549, 2004.

[90] K.-C. Choi, D.-S. Yoo, K.-S. Cho, P.-W. Huh, D.-S. Kim, and C.-K. Park, "Effect of single growth factor and growth factor combinations on differentiation of neural stem cells," *Journal of Korean Neurosurgical Society*, vol. 44, no. 6, pp. 375–381, 2008.

[91] A. Minato, H. Ise, M. Goto, and T. Akaike, "Cardiac differentiation of embryonic stem cells by substrate immobilization of insulin-like growth factor binding protein 4 with elastin-like polypeptides," *Biomaterials*, vol. 33, no. 2, pp. 515–523, 2012.

[92] Y. Xue, Y. Yan, H. Gong et al., "Insulin-like growth factor binding protein 4 enhances cardiomyocytes induction in murine-induced pluripotent stem cells," *Journal of Cellular Biochemistry*, vol. 115, no. 9, pp. 1495–1504, 2014.

[93] S. E. Lynch, G. R. de Castilla, R. C. Williams et al., "The effects of short-term application of a combination of platelet-derived and insulin-like growth factors on periodontal wound healing," *Journal of Periodontology*, vol. 62, no. 7, pp. 458–467, 1991.

[94] A. J. Nixon, B. D. Brower-Toland, S. J. Bent et al., "Insulinlike growth factor-I gene therapy applications for cartilage repair," *Clinical Orthopaedics and Related Research*, no. 379, pp. S201–S213, 2000.

[95] V. J. Dzau, M. Gnecchi, and A. S. Pachori, "Enhancing stem cell therapy through genetic modification," *Journal of the American College of Cardiology*, vol. 46, no. 7, pp. 1351–1353, 2005.

[96] T. M. Yau, C. Kim, D. Ng et al., "Increasing transplanted cell survival with cell-based angiogenic gene therapy," *Annals of Thoracic Surgery*, vol. 80, no. 5, pp. 1779–1786, 2005.

[97] T. Kofidis, J. L. de Bruin, T. Yamane et al., "Insulin-like growth factor promotes engraftment, differentiation, and functional improvement after transfer of embryonic stem cells for myocardial restoration," *Stem Cells*, vol. 22, no. 7, pp. 1239–1245, 2004.

[98] N. Kanemitsu, K. Tambara, G. U. Premaratne et al., "Insulin-like growth factor-1 enhances the efficacy of myoblast transplantation with its multiple functions in the chronic myocardial infarction rat model," *Journal of Heart and Lung Transplantation*, vol. 25, no. 10, pp. 1253–1262, 2006.

[99] L. Ye, H. K. Haider, S. Jiang et al., "Improved angiogenic response in pig heart following ischaemic injury using human skeletal myoblast simultaneously expressing VEGF165 and angiopoietin-1," *European Journal of Heart Failure*, vol. 9, no. 1, pp. 15–22, 2007.

[100] R. Matsumoto, T. Omura, M. Yoshiyama et al., "Vascular endothelial growth factor-expressing mesenchymal stem cell transplantation for the treatment of acute myocardial infarction," *Arteriosclerosis, Thrombosis, and Vascular Biology*, vol. 25, no. 6, pp. 1168–1173, 2005.

[101] J. E. Babensee, L. V. McIntire, and A. G. Mikos, "Growth factor delivery for tissue engineering," *Pharmaceutical Research*, vol. 17, no. 5, pp. 497–504, 2000.

[102] T. P. Martens, A. F. G. Godier, J. J. Parks et al., "Percutaneous cell delivery into the heart using hydrogels polymerizing in situ," *Cell Transplantation*, vol. 18, no. 3, pp. 297–304, 2009.

[103] Z. Li and J. Guan, "Thermosensitive hydrogels for drug delivery," *Expert Opinion on Drug Delivery*, vol. 8, no. 8, pp. 991–1007, 2011.

[104] M. E. Padin-Iruega, Y. Misao, M. E. Davis et al., "Cardiac progenitor cells and biotinylated insulin-like growth factor-1 nanofibers improve endogenous and exogenous myocardial regeneration after infarction," *Circulation*, vol. 120, no. 10, pp. 876–887, 2009.

[105] M. Egred, A. Al-Mohammad, G. D. Waiter et al., "Detection of scarred and viable myocardium using a new magnetic resonance imaging technique: blood oxygen level dependent (BOLD) MRI," *Heart*, vol. 89, no. 7, pp. 738–744, 2003.

[106] T. E. Robey, M. K. Saiget, H. Reinecke, and C. E. Murry, "Systems approaches to preventing transplanted cell death in cardiac repair," *Journal of Molecular and Cellular Cardiology*, vol. 45, no. 4, pp. 567–581, 2008.

[107] G. Camci-Unal, N. Alemdar, N. Annabi, and A. Khademhosseini, "Oxygen releasing biomaterials for tissue engineering," *Polymer International*, vol. 62, no. 6, pp. 843–848, 2013.

[108] S. H. Oh, C. L. Ward, A. Atala, J. J. Yoo, and B. S. Harrison, "Oxygen generating scaffolds for enhancing engineered tissue survival," *Biomaterials*, vol. 30, no. 5, pp. 757–762, 2009.

[109] X. Ai, "Ca^{2+}/calmodulin-dependent protein kinase modulates cardiac ryanodine receptor phosphorylation and sarcoplasmic reticulum Ca^{2+} leak in heart failure," *Circulation Research*, vol. 97, no. 12, pp. 1314–1322, 2005.

[110] S. Benz, S. Nötzli, J. S. Siegel, D. Eberli, and H. J. Jessen, "Controlled oxygen release from pyridone endoperoxides promotes cell survival under anoxic conditions," *Journal of Medicinal Chemistry*, vol. 56, no. 24, pp. 10171–10182, 2013.

[111] R. R. Mallepally, C. C. Parrish, M. A. M. Mc Hugh, and K. R. Ward, "Hydrogen peroxide filled poly(methyl methacrylate) microcapsules: potential oxygen delivery materials," *International Journal of Pharmaceutics*, vol. 475, no. 1-2, pp. e130–e137, 2014.

[112] R.-M. Wang, T. Komatsu, A. Nakagawa, and E. Tsuchida, "Human serum albumin bearing covalently attached iron(II) porphyrins as O_2-coordination sites," *Bioconjugate Chemistry*, vol. 16, no. 1, pp. 23–26, 2005.

[113] S. I. H. Abdi, S. M. Ng, and J. O. Lim, "An enzyme-modulated oxygen-producing micro-system for regenerative therapeutics," *International Journal of Pharmaceutics*, vol. 409, no. 1-2, pp. 203–205, 2011.

[114] M. Hedayat, M. J. Mahmoudi, N. R. Rose, and N. Rezaei, "Proinflammatory cytokines in heart failure: double-edged swords," *Heart Failure Reviews*, vol. 15, no. 6, pp. 543–562, 2010.

[115] R. H. Li, "Materials for immunoisolated cell transplantation," *Advanced Drug Delivery Reviews*, vol. 33, no. 1-2, pp. 87–109, 1998.

[116] J. T. Wilson and E. L. Chaikof, "Challenges and emerging technologies in the immunoisolation of cells and tissues," *Advanced Drug Delivery Reviews*, vol. 60, no. 2, pp. 124–145, 2008.

[117] L. M. Weber, K. N. Hayda, and K. S. Anseth, "Cell-matrix interactions improve beta-cell survival and insulin secretion in three-dimensional culture," *Tissue Engineering—Part A*, vol. 14, no. 12, pp. 1959–1968, 2008.

[118] L. M. Weber and K. S. Anseth, "Hydrogel encapsulation environments functionalized with extracellular matrix interactions increase islet insulin secretion," *Matrix Biology*, vol. 27, no. 8, pp. 667–673, 2008.

[119] C.-C. Lin and K. S. Anseth, "Glucagon-like peptide-1 functionalized PEG hydrogels promote survival and function of encapsulated pancreatic β-cells," *Biomacromolecules*, vol. 10, no. 9, pp. 2460–2467, 2009.

[120] P. de Vos and P. Marchetti, "Encapsulation of pancreatic islets for transplantation in diabetes: the untouchable islets," *Trends in Molecular Medicine*, vol. 8, no. 8, pp. 363–366, 2002.

[121] J. Y. Jang, D. Y. Lee, S. J. Park, and Y. Byun, "Immune reactions of lymphocytes and macrophages against PEG-grafted pancreatic islets," *Biomaterials*, vol. 25, no. 17, pp. 3663–3669, 2004.

[122] C.-C. Lin, A. T. Metters, and K. S. Anseth, "Functional PEG-peptide hydrogels to modulate local inflammation induced by the pro-inflammatory cytokine TNFα," *Biomaterials*, vol. 30, no. 28, pp. 4907–4914, 2009.

[123] T. Inoue, T. Ide, M. Yamato et al., "Time-dependent changes of myocardial and systemic oxidative stress are dissociated after

myocardial infarction," *Free Radical Research*, vol. 43, no. 1, pp. 37–46, 2009.

[124] P. S. Hume and K. S. Anseth, "Polymerizable superoxide dismutase mimetic protects cells encapsulated in poly(ethylene glycol) hydrogels from reactive oxygen species-mediated damage," *Journal of Biomedical Materials Research - Part A*, vol. 99, no. 1, pp. 29–37, 2011.

Hindawi Publishing Corporation
Stem Cells International
Volume 2016, Article ID 9165267, 7 pages
http://dx.doi.org/10.1155/2016/9165267

Clinical Study

Clinical Observation of Employment of Umbilical Cord Derived Mesenchymal Stem Cell for Juvenile Idiopathic Arthritis Therapy

Liming Wang,[1] Yu Zhang,[2,3] Hongtao Li,[2,3] Jingxin Hong,[3] Xiaobo Chen,[3] Ming Li,[1] Wen Bai,[1] Jiangang Wang,[2,3] Yongjun Liu,[2,3] and Mingyuan Wu[2,3,4]

[1]*Cell Therapy Center, 323 Hospital of People's Liberation Army, Xi'an 710054, China*
[2]*Zhongyuan Union Cell & Gene Engineering Corporation Company, Tianjin 300304, China*
[3]*Alliancells Institute of Stem Cells and Translational Regenerative Medicine & Alliancells Bioscience Co., Ltd., Tianjin 300381, China*
[4]*Harold Hamm Oklahoma Diabetes Center and Section of Endocrinology and Diabetes in the Department of Internal Medicine, University of Oklahoma Health Sciences Center, Oklahoma City, OK 73104, USA*

Correspondence should be addressed to Mingyuan Wu; wumingyuan@vcanbio.com

Received 28 April 2015; Revised 31 July 2015; Accepted 6 August 2015

Academic Editor: Kathryn McFadden

Juvenile idiopathic arthritis (JIA), known as Juvenile rheumatoid arthritis, is the most common type of arthritis in children aged under 17. It may cause sequelae due to lack of effective treatment. The goal of this study is to explore the therapeutic effect of umbilical cord mesenchymal stem cells (UC-MSCs) for JIA. Ten JIA patients were treated with UC-MSCs and received second infusion three months later. Some key values such as 28-joint disease activity score (DAS28), TNF-α, IL-6, and regulatory T cells (Tregs) were evaluated. Data were collected at 3 months and 6 months after first treatment. DAS28 score of 10 patients was between 2.6 and 3.2 at three months after infusion. WBC, ESR, and CRP were significantly decreased while Tregs were remarkably increased and IL-6 and TNF-α were declined. Similar changes of above values were found after 6 months. At the same time, the amount of NSAIDS and steroid usage in patients was reduced. However, no significant changes were found comparing the data from 3 and 6 months. These results suggest that UC-MSCs can reduce inflammatory cytokines, improve immune network effects, adjust immune tolerance, and effectively alleviate the symptoms and they might provide a safe and novel approach for JIA treatment.

1. Introduction

Juvenile idiopathic arthritis (JIA) is a common rheumatic disease and is the primary cause of disability and blindness in childhood [1]. The main feature of JIA is chronic arthritis accompanied by systemic multiorgan involvement. This disease can be divided into three types: systemic, polyarticular, and oligoarticular [2]. JIA commonly occurs in 2–16-year-old children with characteristics of long-term fever, rash, joint pain, and leukocytosis. It can affect growth and development of the victims and is a formidable disease to treat [3]. New treatment is urgently needed. Mesenchymal stem cells (MSCs) could be harvested from a variety of tissues such as bone marrow, adipose tissue, umbilical cord, placenta, and muscle [4, 5]. MSCs showed the ability to differentiate towards multiple cell lineages including osteoblasts and chondrocytes [6, 7]. On the other hand, MSCs were immunosuppressive and immunoprivileged, display high migration and motility, and could secret cytokines to improve the repair of damaged tissues; therefore MSCs have been used to treat various diseases in clinic trials [8, 9]. Previously we have reported data harvested from adult patients with Active Rheumatoid Arthritis treated by UC-MSC [10]. Here we report the first attempt to our knowledge to use umbilical cord mesenchymal stem cell (UC-MSC) to treat JIA. In this study, 10 cases of JIA patients aged 2–15 were treated with UC-MSC at two time points.

Table 1: List of patient information.

Number	Sex	Age	Course of disease	Symptom	Exterior sign
1	Female	4	2 years	Repeated pain in the joints, mainly in the knee, difficulty in walking	Knee joint deformity, swelling
2	Male	15	5 years	Repeated fever with pain in metacarpophalangeal joint	The right joint deformity
3	Male	14	3 years	Repeated fever with pain in arm and leg joints	
4	Male	9	4 years	Repeated fever with pain in hip and metacarpophalangeal joints	Bilateral femoral head necrosis in phase 2
5	Male	11	5 years	Fever in the early stage, later pain in the joints	Limited squat with knee, restricted movement in elbow
6	Female	10	3 years	Fever in the early stage, later pain in the joints	
7	Female	14	3 years	Pain in the joints	Limited squat with knee, deformity in metacarpophalangeal joints
8	Female	2	1 year	Fever in the early stage, later pain in the joints	The knee joint deformity
9	Male	15	12 years	Repeated fever with pain in arm and leg joints	Metacarpophalangeal joint deformity, necrosis in the right femoral head in phase 2
10	Male	9	4 years	Fever in the early stage, later pain in the joints	Developmental retardation, limited squat with knee

2. Materials and Methods

2.1. Patients. Ten JIA inpatients were selected from our department dating from October 2011 to November 2012, according to the American College of Rheumatology criteria, ARA [11]. The patients consisted of 6 males and 4 females, aged 2–15 years. The course of disease ranged from 1 to 12 years. Six cases were systemic type JIA, three cases were polyarticular type, and one case was oligoarticular type. The detailed information is listed in Table 1. The patients were evaluated by 28-joint disease activity score (DAS28). All patients were above 3.2. DSA28 were between 3.2 and 5.1 points in eight cases and were above 5.1 points in two cases. Erythrocyte sedimentation rate (ESR) of eight patients was between 40 and 100 mm/h and was above 100 mm/h in the other two cases. C-reactive protein (CRP) was between 50 and 100 mg/L in five cases and above 100 mg/L in the other five. The white blood cell count (WBC) of all the patients was between 10.0×10^9/L and 26.0×10^9/L. All the patients had been treated repeatedly with steroids, nonsteroidal anti-inflammatory drugs (NSAIDS), disease modifying antirheumatic drugs (DMAIDS), and biological agents, but the treatments showed no significantly beneficial effects.

2.2. Pretesting. Level of cytokines in peripheral blood was tested before and after treatments. Peripheral blood was collected in procoagulant tube and centrifuged in 3500 rpm/min for 5 minutes. Serum was then transferred into EP tubes. Each tube contained 200 microliters of serum and was saved in −80°C freezer for further testing. BD Multitest_IMK kit was used to detect the level of TNF-α and IL-6 in serum, and multifunction streaming LUMINEX 200 was used for analysis and detection.

Regulatory T cells (Tregs) were stained with anti-CD4 (BD, number 340133) fluorescein isothiocyanate, anti-CD25-Allophycocyanin (BD, number 340939), and anti-Foxp3-PE (eBioscience, number 12-4776-42). Isotype control antibodies were used alternatively. Samples were incubated in the dark for 15 minutes and analyzed with flow cytometer (BD, FACS Calibur, USA). Image and data were acquired and saved.

2.3. Preparation of the UC-MSCs. UC-MSCs were obtained from Alliancells Institute of Stem Cells and Translational Regenerative Medicine. UC-MSC was harvested according to our previous study [12]. Briefly, the newborn umbilical cord was collected and cut to about 1 mm × 1 mm × 1 mm in dimension and then was digested with 0.1% collagenase and 0.125% trypsin in 37°C for 30 min. Undigested tissues were removed with filters. After filtration, the cells were seeded by $1 \times 10^6/\text{cm}^2$ in plastic culture flasks containing DMEM-LG/F12 (Sigma, USA), 5% FCS (Gibco BRL, USA) medium, and then were placed into the incubator. The medium was changed after 5 days and nonadherent cells were discarded. Half medium was changed every 3 days. The cells were able to adhere to the plastic and showed fibroblast-like morphology. Harvested cells were characterized according to our previous study [12], which is suggested by the ISCT [13]. The characterization procedure was performed according to our previous procedure. Cell surface markers such as CD29, CD31, CD34, CD73, CD90, and HLA-DR were analyzed by flow cytometry (BD, FACS Calibur, USA). Isotype-matched normal mouse IgGs were used as controls. Image and data were acquired and saved.

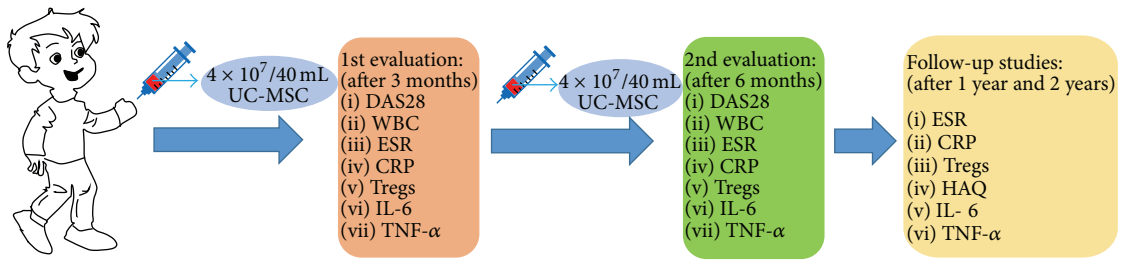

Figure 1: UC-MSC treatment and evaluation procedure. All the 10 patients received infusion with $4 \times 10^7/40$ mL MSCs. After 3 months, DAS28 value was measured and peripheral blood of each patient was obtained for WBC, ESR, CRP, Tregs, IL-6, and TNF-α measurement. The patients were given the second cell infusion later, and the second measurement was done three months later. Follow-up studies were carried out for 1 year and 2 years.

2.4. Cell Quality Control of MSCs. All used MSCs will be firstly analyzed for tumor formation with agar cloning assay *in vitro*. HeLa cells were used as positive control. Before injection, MSCs will be investigated with several tests for cell viability, bacteria, fungus, mycoplasma, and endoxin. Cell viability assay was performed by 2% trypan blue staining; the percentage of living cells must be more than 95%. For bacteria detection, bacterial automatic reporting system BacT/ALERT-3D (Merieux) was used. When the detection result is negative (−) and other detection indexes are qualified, the cell culture process will be continued; when result is positive (+), the cells will be abandoned. For fungal detection, acridine orange staining was used with MSC numbers 1–3 × 10^6. Fluorescence was tested with the 500 nm excitation light. For mycoplasma detection, Hoechst 33258 staining was used and pictures were taken in 340 mm ultraviolet light. For endotoxin detection, samples from all culture media will be detected with Limulus amebocyte lysate gel; the standard is not more than 50 EU/agent. MSCs will proceed to clinical application only if all above test results are qualified. Finally, MSCs with a passage number less than 6 were used for all patients.

2.5. Treatment. All the 10 patients received the treatment of UC-MSC with intravenous infusion and the number of cells delivered was $4 \times 10^7/40$ mL. At the same time of infusion, the patients were given 2–5 mg (by weight) of dexamethasone for antiallergy. Before the infusion, the patients individually took NSAIDS, DMAIDS, and prednisone in the dose of 10–20 mg per day following the ACR guidelines. All patients were given the second cell infusion three months later. The detailed procedures were shown in Figure 1.

2.6. Efficacy Evaluation. DAS28 was used for evaluation of clinical efficacy. A score of DAS28 below 2.6 indicates that disease is in remission, a score between 2.6 and 3.2 points indicates that disease is in low activity, a score between 3.2 and 5.1 points indicates that disease is in moderate activity, and a score above 5.1 points indicates that disease is in high activity. CRP, ESR, inflammatory related factors (TNF-α and IL-6), and Treg were evaluated for laboratory efficacy. Follow-up was carried out before and after three months or six months after the cell treatment.

2.7. Safety Assessment. Side effect events were recorded during each follow-up. Liver and kidney function, ECG, X-ray, blood pressure, and other indicators were checked regularly in order to detect the side effects and observe the outcome of the situation. Discomfort reaction was graded as the following: 0 is no discomfort, 1 is mild discomfort with no effects on their daily life, 2 is moderate discomfort with negative effects on daily life and learning, 3 is moderate discomfort with daily life significantly affected and immobilized, and 4 is severe discomfort with life-threatening events.

2.8. Statistical Analysis. Statistical analysis was performed with Microsoft Office program Excel and SPSS (17.0) software. Measurements were repeated at least three times for each donor. The probability (P) value was calculated using t-test to assess differences between two groups. Levels of significance were labeled as follows: $^*P < 0.05$ and $^{**}P < 0.01$. Significance was given with the appropriate number of asterisks or in numbers.

2.9. Ethic Statement. The use of human umbilical cord materials for isolation, differentiation, and characterization of human umbilical cord derived mesenchymal stem cells was approved by the Ethics Committee in Alliancells Institute of Stem Cells and Translational Regenerative Medicine. The cell therapy was approved by the Ethic Committee in 323 Hospital of People's Liberation Army, and the parents of the patients signed consent to the treatment of UC-MSC.

3. Results

3.1. Characterization of UC-MSCs. The isolated UC-MSCs were evaluated if they meet the minimal criteria suggested by the International Society for Cellular Therapy [13], which are plastic adherence, the multipotent differentiation potential into their respective mesenchymal lineages (osteo- and adipogenic), and the expression of the mesenchymal cell markers. To do so, isolated cells showed a fibroblast-like cell morphology and were further differentiated towards adipocytes and osteoblasts as our previous study [12]. The osteogenic differentiation was identified using Alizarin Red S staining of calcium deposits and adipogenic differentiation was verified using Oil Red O staining (Figure 2(a)). In addition to this,

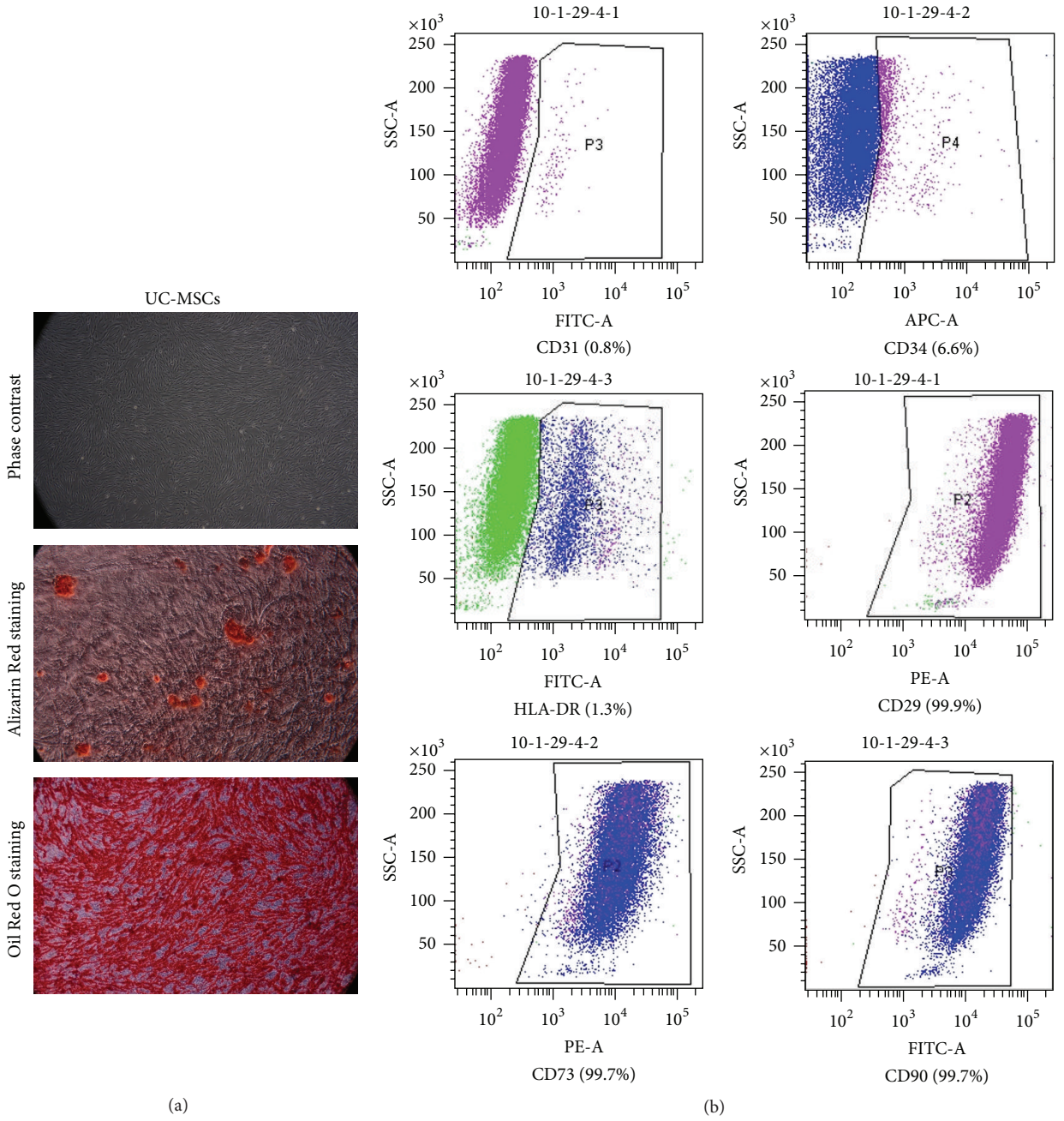

Figure 2: Verification with MSC characters. MSCs were isolated from human umbilical cord materials. Isolated cells displayed fibroblast-like morphology on the plastic surface and were positive for Alizarin Red staining and Oil Red O staining (a). At the same time, isolated cells were analyzed with MSC specific markers by FACS and cells were positive for CD29, CD73, and CD90 but negative for CD31, CD34, and HLA-DR (b).

FACS analysis was performed for MSC specific markers. Data showed that the isolated cells expressed the mesenchymal cell markers CD29 (99.9%), CD73 (99.7%), and CD90 (99.7%) and as expected, these cells were negative for CD31 (0.8%), CD34 (6.6%), and HLA-DR (1.3%) (Figure 2(b)).

3.2. Cell Quality Control of the MSCs. The viability of all MSC samples was above 98%. MSCs cultured on the agar showed no clone formation compared with HeLa, which indicates MSCs has very low ability to from tumors *in vitro* (as shown in Figure 3(a)). With acridine orange and hoechst staining, only MSCs were stained with green and blue, respectively, (as shown in Figures 3(b) and 3(c)). Other signals were not detected suggesting cells were not contaminated by fungal and mycoplasma.

3.3. DAS Value at 3 Months after the First Treatment. No side effects were detected in 10 patients after the UC-MSC

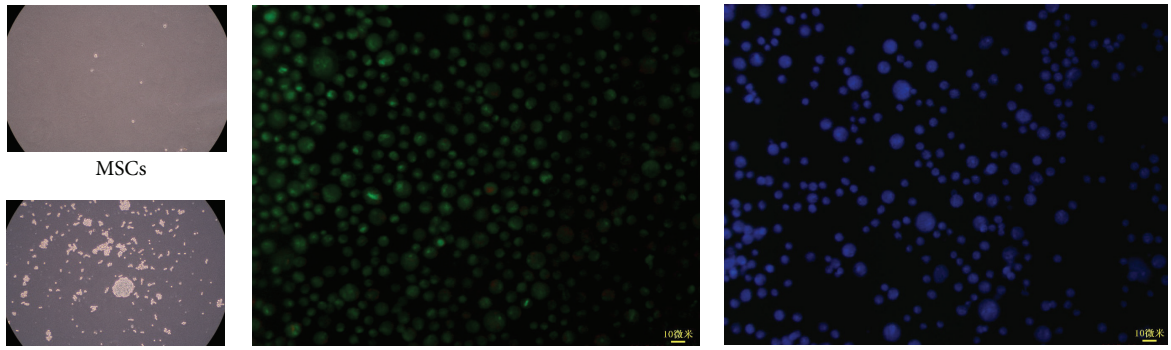

Figure 3: Cell quality of MSCs. MSCs were analyzed with agar cloning assay, acridine orange staining, and hoechst staining, respectively. In the cloning assay, MSCs showed no significant clones compared with HeLa (a). Acridine orange staining showed that only MSCs were stained indicating no fungal contamination (b). Hoechst 33258 staining showed that only MSCs were stained suggesting no mycoplasma contamination (c). This result was taken from one of the ten samples for patients.

treatment. Data for urine routine tests, liver function, and renal function test showed no significant difference. After the first UC-MSC treatment, symptoms such as fever or rash were not observed in all patients, while joint pain was alleviated significantly. Four of the six systemic type patients, two of the three multijoint type patients, and the oligoarticular type patient achieved remission. The DAS28 value of 10 patients was between 2.6 and 3.2. WBC of all the patients declined to $4.0–11.0 \times 10^9$/L. In seven patients, it dropped significantly and showed no difference with the normal children. ESR and CRP also declined significantly. ESR value was between 20 and 50 mm/h and CRP value was between 20 and 60 mg/L. On average, Tregs showed significant increase in 10 patients. In eight of the 10 patients, Treg increased very significantly ($P < 0.01$), while in the other two cases it did not increase by comparing pre- and posttreatment. Levels of IL-6 and TNF-α decreased with the overall comparison before and after treatment (as shown in Figure 4 with orange column).

3.4. DAS Value at 6 Months after the First Treatment. All the patients received the second infusion with UC-MSC at three months after the first infusion. Follow-up observations were carried out three months after the second infusion. DAS28 value was between 2.6 and 3.2. WBC, ESR, and CRP showed a continued declining trend and were significant compared with the values before infusion. However, it is not significant compared to the three months after the first treatment. Tregs continued to increase, but there was no statistical significance compared to the three months after the first treatment. Levels of IL-6 and TNF-α decreased compared to the three months after the first treatment and there was no statistical significance (as shown in Figure 4 with green column). The doses of rheumatism drugs, such as NSAIDS and prednisone, were reduced gradually after the second cell treatment.

3.5. Follow-Up Study Data on DIA. The 1-year follow-up studies were done for all the patients after the second

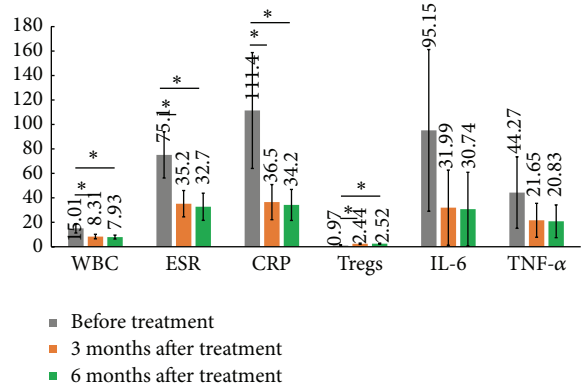

Figure 4: Laboratory measurement before/after UC-MSC treatment in JIA patients. To test the effect of MSC treatment on JIA patients, two-time measurements were done at three months after the first MSC infusion (orange column) and at three months after the second infusion (green column). Values such as WBC, ESR, CRP, Tregs, IL-6, and TNF-α were analyzed and differences were compared with the values obtained before the MSC infusion (grey column). WBC, ESR, and CRP showed significant decreases, while Tregs showed a significant increase. The expression of IL-6 and TNF-α was declined at three months after the first and second UC-MSC infusion.

treatment; four of them were further tracked with 2 years. ESR and CRP value kept in the low level after 1 year. Tregs percentage in the whole T cell family showed no significant changes, HAQ and DAS28 values declined, joint symptoms improved significantly, and the expression of IL-6 and TNF-α kept in low levels.

Four patients were kept tracking for 2 years; HAQ and DAS28 values declined. Two of them were unable to walk but now can walk to school independently. Ten patients showed enhanced speed in growth and development with an average of 5–10 cm increase in height. Two patients with necrosis in the femoral head show no aggregations.

4. Discussion

JIA is one of connective tissue malignancies, which affects approximately 1 in 1000 children in any given year and with about 1 in 10000 having a more severe form [14]. JIA has been reported to be related to environment, infection, immunology, metabolism, endocrine, and other factors; however the detailed etiology is still unclear. There are two reactions which may coexist for pathogenesis. One is humoral immune response caused by immune complex formed mainly by the rheumatoid factor, which is the major factor causing damage to the articular synovia. The other is cellular immune response, which secretes and releases lymphocyte factors including a variety of globulins, forms immune complexes with rheumatoid factors, and further activates the inflammatory response of the complement system [15]. The traditional treatments are not effective because they cannot completely adjust the immune responses in JIA patients. It may explain why clinical symptoms of JIA occur repeatedly. It also gives our new perspective to look for exploring approaches to repair the patient immune responses. MSCs belong to adult stem cells and mainly derived from early mesoderm and ectoderm. MSC was first found in bone marrow and later in adipose tissue and umbilical cord [16]. MSCs were shown as a potential cell source for regenerative medicine because they are multipotent and more importantly can secret cytokines to regulate immune response and repair the damaged tissue [17, 18]. For example, MSCs were shown to inhibit leukemia/lymphoma cell proliferation *in vitro* and in allogeneic bone marrow transplant in mice [19]. More bodies of evidence were demonstrated to uncover the detailed regulation of MSCs on immune system. The autologous or allogeneic MSCs can significantly inhibit the proliferation and activation of T lymphocytes [20]. UC-MSCs are the undifferentiated primitive cells. UC-MSCs have low immunogenicity because they do not express the mature antigens of the cells and will not be recognized by the immune system [10]. On the other hand, UC-MSCs have a long survival time in the host and can express a variety of cytokines and growth factors such as stem cell growth factor, keratinocyte growth factor, Ghrelin, interleukin-15, and growth hormone to improve the tissue repair [21, 22]. They can also reduce the activation of macrophages and the expression of inflammatory cytokines [23]. Therefore, UC-MSCs are a promising cell candidate for the transplantation treatment of JIA patients [24, 25].

In this study, 10 JIA patients were treated with UC-MSCs. No side effect was observed after MSC infusion. Patients continued to take NSAIDS, DMAIDS, and prednisone. Follow-up data at 3 months after the first treatment showed significant improvement. DAS28 scored lower and reached a low activity of the disease. Laboratory results also showed improvements: WBC, ESR, CRP, and inflammatory cytokines IL-6 and TNF-α reduced, whereas Tregs increased significantly. At three months after the second MSC infusion, DAS28 score maintained a low activity level and the laboratory results remained stable. WBC, ESR, CRP, and inflammatory cytokines IL-6 and TNF-α decreased while Tregs increased continuously. UC-MSCs can increase the output of mature T cells in the thymus and the number of Tregs in peripheral blood [26]. However, there was no statistical significance between the data from 3 months after the first infusion and 3 months after the second infusion. The reason required further investigations. The dose of antirheumatic drugs decreased with good tolerance. The data for the 1- and 2-year follow-up study showed that the patients with stable condition promote physical development substantially, which indicated the long-term efficacy with UC-MSC treatment.

5. Conclusion

Our data demonstrated for the first time that UC-MSC treatment could alleviate the symptom and pain in JIA patients. This might be regulated via repairing patient's immune system by MSC released cytokines. The further studies could be focusing on which factors are the major regulators and downstream transduction pathways.

Conflict of Interests

All authors declare that there is no conflict of interests and agree with the contents of the paper.

Authors' Contribution

Liming Wang, Yu Zhang, and Hongtao Li contributed equally to this study and share first authorship.

Acknowledgment

This study was supported by Military Medicine and Public Health Plan (CLZ120GA23).

References

[1] S. Ringold, A. Burke, and R. M. Glass, "Juvenile idiopathic arthritis," *The Journal of the American Medical Association*, vol. 294, no. 13, p. 1722, 2005.

[2] J. M. Burnham, J. Shults, S. E. Dubner, H. Sembhi, B. S. Zemel, and M. B. Leonard, "Bone density, structure, and strength in juvenile idiopathic arthritis: importance of disease severity and muscle deficits," *Arthritis and Rheumatism*, vol. 58, no. 8, pp. 2518–2527, 2008.

[3] P. J. Hashkes and R. M. Laxer, "Medical treatment of juvenile idiopathic arthritis," *Journal of the American Medical Association*, vol. 294, no. 13, pp. 1671–1684, 2005.

[4] D. J. Prockop, "Marrow stromal cells as stem cells for non-hematopoietic tissues," *Science*, vol. 276, no. 5309, pp. 71–74, 1997.

[5] Y. Zhang, D. Khan, J. Delling, and E. Tobiasch, "Mechanisms underlying the osteo- and adipo-differentiation of human mesenchymal stem cells," *The Scientific World Journal*, vol. 2012, Article ID 793823, 14 pages, 2012.

[6] O. K. Lee, T. K. Kuo, W.-M. Chen, K.-D. Lee, S.-L. Hsieh, and T.-H. Chen, "Isolation of multipotent mesenchymal stem cells from umbilical cord blood," *Blood*, vol. 103, no. 5, pp. 1669–1675, 2004.

[7] N. Zippel, C. A. Limbach, N. Ratajski et al., "Purinergic receptors influence the differentiation of human mesenchymal stem cells," *Stem Cells and Development*, vol. 21, no. 6, pp. 884–900, 2012.

[8] H. K. Salem and C. Thiemermann, "Mesenchymal stromal cells: current understanding and clinical status," *Stem Cells*, vol. 28, no. 3, pp. 585–596, 2010.

[9] A. J. Nauta and W. E. Fibbe, "Immunomodulatory properties of mesenchymal stromal cells," *Blood*, vol. 110, no. 10, pp. 3499–3506, 2007.

[10] L. Wang, L. Wang, X. Cong et al., "Human umbilical cord mesenchymal stem cell therapy for patients with active rheumatoid arthritis: safety and efficacy," *Stem Cells and Development*, vol. 22, no. 24, pp. 3192–3202, 2013.

[11] D. M. F. M. Van Der Heijde, M. Van't Hof, P. L. C. M. Van Riel, and L. B. A. Van De Putte, "Development of a disease activity score based on judgment in clinical practice by rheumatologists," *Journal of Rheumatology*, vol. 20, no. 3, pp. 579–581, 1993.

[12] Y. Xu, H. Meng, C. Li et al., "Umbilical cord-derived mesenchymal stem cells isolated by a novel explantation technique can differentiate into functional endothelial cells and promote revascularization," *Stem Cells and Development*, vol. 19, no. 10, pp. 1511–1522, 2010.

[13] M. Dominici, K. Le Blanc, I. Mueller et al., "Minimal criteria for defining multipotent mesenchymal stromal cells. The International Society for Cellular Therapy position statement," *Cytotherapy*, vol. 8, no. 4, pp. 315–317, 2006.

[14] C. William and J. R. Shiel, Eds., *Juvenile Rheumatoid Arthritis*, MedicineNet, 2012.

[15] A. Woerner, A. von Scheven-Gête, R. Cimaz, and M. Hofer, "Complications of systemic juvenile idiopathic arthritis: risk factors and management recommendations," *Expert Review of Clinical Immunology*, vol. 11, no. 5, pp. 575–588, 2015.

[16] W. Zhao, D. G. Phinney, D. Bonnet, M. Dominici, and M. Krampera, "Mesenchymal stem cell biodistribution, migration, and homing in vivo," *Stem Cells International*, vol. 2014, Article ID 292109, 2 pages, 2014.

[17] I. Ullah, R. B. Subbarao, and G. J. Rho, "Human mesenchymal stem cells—current trends and future prospective," *Bioscience Reports*, vol. 35, no. 2, Article ID e00191, 2015.

[18] K. Nemeth, "Mesenchymal stem cell therapy for immune-modulation: the donor, the recipient, and the drugs in-between," *Experimental Dermatology*, vol. 23, no. 9, pp. 625–628, 2014.

[19] N. Song, L. Gao, H. Qiu et al., "Mouse bone marrow-derived mesenchymal stem cells inhibit leukemia/lymphoma cell proliferation in vitro and in a mouse model of allogeneic bone marrow transplant," *International Journal of Molecular Medicine*, vol. 36, no. 1, pp. 139–149, 2015.

[20] A. Del Fattore, R. Luciano, L. Pascucci et al., "Immunoregulatory effects of mesenchymal stem cell-derived extracellular vesicles on T lymphocytes," *Cell Transplantation*, 2015.

[21] I. Perea-Gil, M. Monguió-Tortajada, C. Gálvez-Montón, A. Bayes-Genis, F. E. Borràs, and S. Roura, "Preclinical evaluation of the immunomodulatory properties of cardiac adipose tissue progenitor cells using umbilical cord blood mesenchymal stem cells: a direct comparative study," *BioMed Research International*, vol. 2015, Article ID 439808, 9 pages, 2015.

[22] S. Shawki, T. Gaafar, H. Erfan, E. E. Khateeb, A. E. Sheikhah, and R. E. Hawary, "Immunomodulatory effects of umbilical cord-derived mesenchymal stem cells," *Microbiology and Immunology*, vol. 59, no. 6, pp. 348–356, 2015.

[23] L.-L. Lu, Y.-J. Liu, S.-G. Yang et al., "Isolation and characterization of human umbilical cord mesenchymal stem cells with hematopoiesis-supportive function and other potentials," *Haematologica*, vol. 91, no. 8, pp. 1017–1026, 2006.

[24] R. Atoui and R. C. J. Chiu, "Immune responses after mesenchymal stem cell implantation," in *Cellular Cardiomyoplasty*, vol. 1036 of *Methods in Molecular Biology*, pp. 107–120, Humana Press, 2015.

[25] K. A. T. de Carvalho, G. Steinhoff, and J. C. Chachques, "Mesenchymal stem cell therapy in nonhematopoietic diseases," *Stem Cells International*, vol. 2015, Article ID 676903, 2 pages, 2015.

[26] L. Sun, D. Wang, J. Liang et al., "Umbilical cord mesenchymal stem cell transplantation in severe and refractory systemic lupus erythematosus," *Arthritis & Rheumatism*, vol. 62, no. 8, pp. 2467–2475, 2010.

Hindawi Publishing Corporation
Stem Cells International
Volume 2016, Article ID 9394150, 10 pages
http://dx.doi.org/10.1155/2016/9394150

Research Article

Polydatin Protects Bone Marrow Stem Cells against Oxidative Injury: Involvement of Nrf 2/ARE Pathways

Meihui Chen, Yu Hou, and Dingkun Lin

Research Laboratory of Spine Degenerative Disease, Guangdong Provincial Hospital of Traditional Chinese Medicine, Guangzhou 510120, China

Correspondence should be addressed to Dingkun Lin; lindingkun@126.com

Received 29 April 2015; Revised 20 July 2015; Accepted 2 August 2015

Academic Editor: Kenichi Tamama

Polydatin, a glucoside of resveratrol, has been reported to possess potent antioxidative effects. In the present study, we aimed to investigate the effects of polydatin in bone marrow-derived mesenchymal stem cells (BMSCs) death caused by hydrogen peroxide (H_2O_2), imitating the microenvironment surrounding transplanted cells in the injured spinal cord in vitro. In our study, MTT results showed that polydatin effectively prevented the decrease of cell viability caused by H_2O_2. Hochest 33258, Annexin V-PI, and Western blot assay showed H_2O_2-induced apoptosis in BMSCs, which was attenuated by polydatin. Further studies indicated that polydatin significantly protects BMSCs against apoptosis due to its antioxidative effects and the regulation of Nrf 2/ARE pathway. Taken together, our results indicate that polydatin could be used in combination with BMSCs for the treatment of spinal cord injury by improving the cell survival and oxidative stress microenvironments.

1. Introduction

Among central nervous system (CNS) disorders, spinal cord injury (SCI) is the most devastating and traumatic [1, 2]. 40 cases per million individuals are diagnosed as SCI [3]. Bone marrow-derived mesenchymal stem cells (BMSCs), which possess immunosuppressive properties and the capacity for unlimited self-amplification and for terminal differentiation [4, 5], play a privileged role in ameliorating neuronal damage in CNS disease models including SCI [6]. Cellular replacement with MSCs in different SCI animal models has showed functional recovery [7, 8]. However, attempts to transplant BMSCs into animal and human subjects are hampered mainly due to the poor survival of BMSCs [9]. After being transplanted, BMSCs are facing a complicated environment with risk factors that may lead to cell death including oxidative stress [4, 9, 10]. The increased reactive oxygen species (ROS) resulting in sustained oxidative stress in damaged spinal cord is one of the key factors that challenged the survival of donor BMSCs. BMSCs may unavoidably result in apoptosis under oxidative circumstance. Therefore, drugs with antioxidative effects and antiapoptosis may be crucial for the successful transplantation of BMSCs in SCI [10].

Polydatin (Figure 2(a)), isolated from the roots of *Polygonum cuspidatum*, is widely used in traditional Chinese remedies [11–14]. Polydatin has been shown to protect heart function, prevent the development of diabetic renal fibrosis, and ameliorate Alzheimer's disease due to its multiple pharmacological actions, such as antioxidation, anti-inflammation, immunoregulation, antitumor, and neuroprotection [15–18]. However, the protective activity of polydatin on transplanted BMSCs after SCI is unknown.

In this study, we demonstrated for the first time that polydatin might protect BMSCs against H_2O_2-induced apoptosis due to enhancing the resistance of BMSCs against oxidative injury and activate the nuclear factor E2-related factor 2 (Nrf 2)/antioxidant response element (ARE) pathway, which has been reported to have key roles in regulating endogenous antioxidants and phase II detoxification enzymes, suggesting that polydatin could be a promising approach to increase the cell survival in cell replacement therapy for SCI.

2. Materials and Methods

2.1. Materials. Male Sprague-Dawley (SD) rats (100 ± 20 g) were supplied by the Center of Experimental Animals,

Guangzhou University of Chinese Medicine (Guangzhou, China, Certificate number 00100561). All procedures were performed according to animal guidelines of Guangzhou University of Chinese Medicine. Polydatin was purchased in Aladdin (Shanghai, China). Trypsin, 3-(4,5-dimethylthiazol-2-yl)-2,5-diphenyltetrazolium bromide (MTT), dimethyl sulfoxide (DMSO), Hochest 33258, and dichlorofluorescein diacetate (H_2DCF-DA) were purchased from Sigma-Aldrich (MO, USA). Low-glucose Dulbecco's modified Eagle's medium (LG-DMEM) and fetal bovine serum (FBS) were obtained from Gibco-BRL (NY, USA). Hydrogen peroxide, lactate dehydrogenase (LDH), Annexin V FITC/PI, Cell-Light 5-ethynyl-2′-deoxyuridine (EdU) Apollo594 in vitro Image kit, and glutathione (GSH) assay kits were purchased from Keygen (Nanjing, China). Brusatol was bought from Chengdu PureChem-Standard Co., Ltd. (Chengdu, China). Polydatin (Aladdin) was dissolved in DMSO before dilution with the culture medium. The final concentration of DMSO was 0.1%.

2.2. Cell Culture and Treatment. Culture of rat BMSCs was performed as previously described [19]. Briefly, all bone marrow was flushed out with a 10 mL syringe using LG-DMEM supplemented with 10% FBS. The whole marrow washouts were collected, centrifuged, and plated into a culture flask in 37°C under 5% CO_2. All cells used in the assay were of passages 3–5. The phenotypic properties of BMSCs were identified by flow cytometry as previously reported [20]. Cells were pretreated with polydatin for 2 h and then treated with H_2O_2 (600 μM) for 24 h.

2.3. Cell Viability Assay. Cell viability was measured by MTT assay. Cells were plated on 96-well plates at a density of 1×10^4 for 24 h. After incubation with H_2O_2 for 24 h, 10 μL MTT (5 mg/mL) was then added to each well and the mixture was incubated for 3 h at 37°C. MTT reagent was then replaced with DMSO (100 μL per well) to dissolve formazan crystals. After the mixture was shaken at 37°C for 15 min, absorbance was determined at 570 nm using a microplate reader. Results were expressed as the percentage of MTT reduction and the absorbance of control cells was set as 100%.

2.4. LDH Release Assay. The cytotoxicity was measured by LDH release assay. LDH is a cytoplasmic enzyme retained by viable cells with intact plasma membrane and released from cells with damaged membranes. After the indicated treatment of BMSCs, the medium was collected and assayed for LDH activity as previously reported [21]. Briefly, the release of LDH is measured with a coupled enzymatic reaction that results in the conversion of a tetrazolium salt into red-colored formazan, which is correlated with LDH activity. The formazan was measured with a microplate reader at 450 nm. Results were expressed as the percentage of LDH release and the absorbance of control cells was set as 100%.

2.5. Hochest 33258 Assay. To detect morphological evidence of apoptosis, cell nuclei were visualized by DNA staining with the fluorescent dye Hochest 33258. After treatment, BMSCs were stained with Hochest 33258 (1 μg/mL) for 15 min in the dark. Results were tested by visual observation of nuclear morphology through fluorescence microscopy (Olympus, Japan) equipped with a UV filter.

2.6. Annexin V-FITC Assay. The apoptotic ratios of cells were determined with the Annexin V-FITC apoptosis detection kit. Briefly, BMSCs were collected and washed twice with cold PBS buffer, resuspended in 500 μL of binding buffer, incubated with 5 μL of Annexin V-FITC, conjugated to FITC and 5 μL PI for 15 min at room temperature, and analyzed by flow cytometry I (BD Biosciences). Cells treated with DMSO were used as the negative control.

2.7. Measurement of ROS. Intracellular ROS formation was measured using H_2DCF-DA as reported [22]. Briefly, after treatment, cells were washed with warm PBS three times and then stained with 10 μM H_2DCF-DA in serum-free medium for 30 min at 37°C in the dark. DCF fluorescence was analyzed by visual observation of cell morphology through fluorescence microscopy equipped with a UV filter.

2.8. Detection of Intracellular GSH. Intracellular GSH concentration was tested by a GSH assay kit. By reacting with dithiobis-nitrobenzoic acid, reduced GSH could form a yellow compound, which is quantifiable at 405 nm and is related to the concentration of the reduced GSH. In brief, whole-cell lysate was prepared according to manufacturer's instructions. The basal contents of GSH in control cells were taken as 100%.

2.9. Cell Proliferation. The proliferation of BMSCs was tested with EdU assay. BMSCs were planted into 6-well plate, and then cells were allowed to adhere for 24 h. After the treatment, BMSCs were incubated with EdU for 4 h before fluorescent detection. Cells were fixed with 2% paraformaldehyde for 15 min and stained with EdU kit according to the manufacturer's instructions. Finally, cells were placed under a laser-scanning confocal microscope (LSM710, Carl Zeiss, Germany) for image acquisition.

2.10. Western Blot Analysis. Western blotting analysis was performed as previously described [22]. In brief, cellular protein was collected and lysed in lysis buffer. The protein concentration was measured using the BCA assay (Keygen, Nanjing, China). Equal amounts of total protein were separated on SDS-PAGE gel and transferred onto the PVDF membranes (Millipore, Billerica, MA). After blocking with 5% skim milk, the membranes were incubated with primary antibodies Bcl-2, Bax, Nrf 2, and NQO-1 (Cell Signaling Technology, Beverly, MA, USA) overnight at 4°C, followed by sequential incubation with horseradish peroxidase-conjugated secondary antibodies for 2 h. The bands were visualized by an enhanced chemiluminescence detection kit (ECL, Amersham Arlington Heights, IL, USA) and exposed to gel imaging system. The intensities of bands were performed using Quantity One Software (Bio-Rad, Hercules, CA).

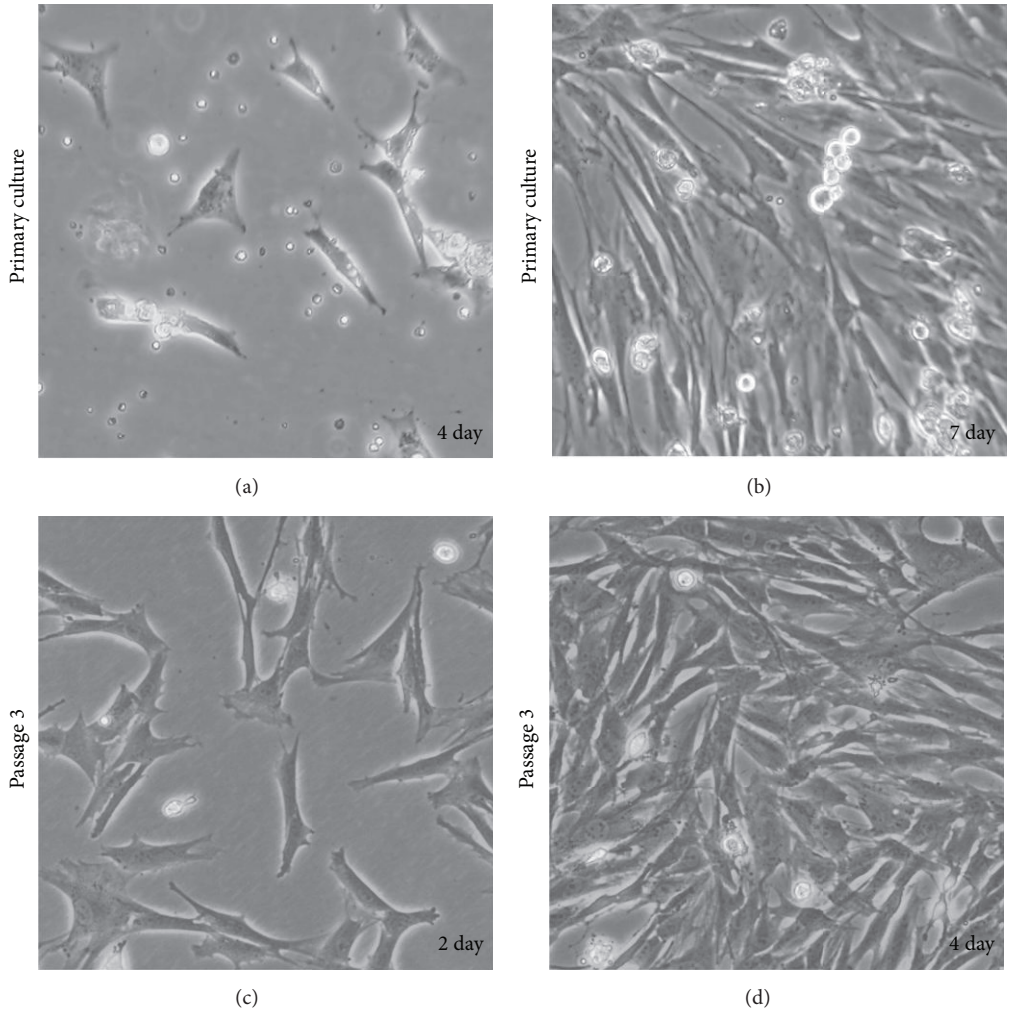

Figure 1: Representative fields of BMSCs morphologies.

2.11. Statistical Analysis. The data were presented as mean ± S.E.M. Statistical analyses between two groups were performed by unpaired Student's t-test. Differences among groups were tested by one-way analysis of variance (ANOVA). A probability value of $p < 0.05$ was accepted to be statistically significant.

3. Results

3.1. Characterization of BMSCs. BMSCs were isolated from rat bone marrow, expanded in primary culture and passaged for three times. At initial phase, BMSCs of growth contained attached spindle-shaped cells with colonies and floating cells (Figure 1(a)), reaching confluence at day 7 (Figure 1(b)). The floating cells were completely abolished at passage 3 (Figures 1(c) and 1(d)).

3.2. Effects of Polydatin on BMSCs Exposed to H_2O_2. The viability of BMSCs treated with H_2O_2, ranging from 400 to 800 μM for 24 h, decreased dose-dependently. 600 μM H_2O_2 caused approximately cell death by 50% (Figure 2(b)) and the concentration was chosen for the following experiments. To investigate the effects of polydatin on H_2O_2-induced cell death, MTT and LDH assays were applied. The results showed that polydatin significantly increased cell viability (Figures 2(c) and 2(d)) and decreased cell death (Figure 2(e)).

3.3. Polydatin Reduced H_2O_2-Induced Apoptosis-Like Cell Death. Hochest 33258 staining and Annexin V-propidium iodide (PI) staining assay were used to observe whether H_2O_2 induced apoptotic death. Our results showed that H_2O_2 induced nuclear condensation (Figure 3(a)), which was blocked by polydatin. The total apoptotic rate (total rate of the cells that are Annexin V positive and PI positive) of H_2O_2 group (10.95% ± 1.25) was significantly increased compared with control group (4.45% ± 0.15), and polydatin effectively reduced the apoptotic rate (5.15% ± 0.75) (Figures 3(b) and 3(c)). Furthermore, after treatment with H_2O_2, upregulation of proapoptotic protein Bax and cleaved caspase-3 and downregulation of antiapoptotic protein Bcl-2 were observed in BMSCs, which were reversed by polydatin pretreatment.

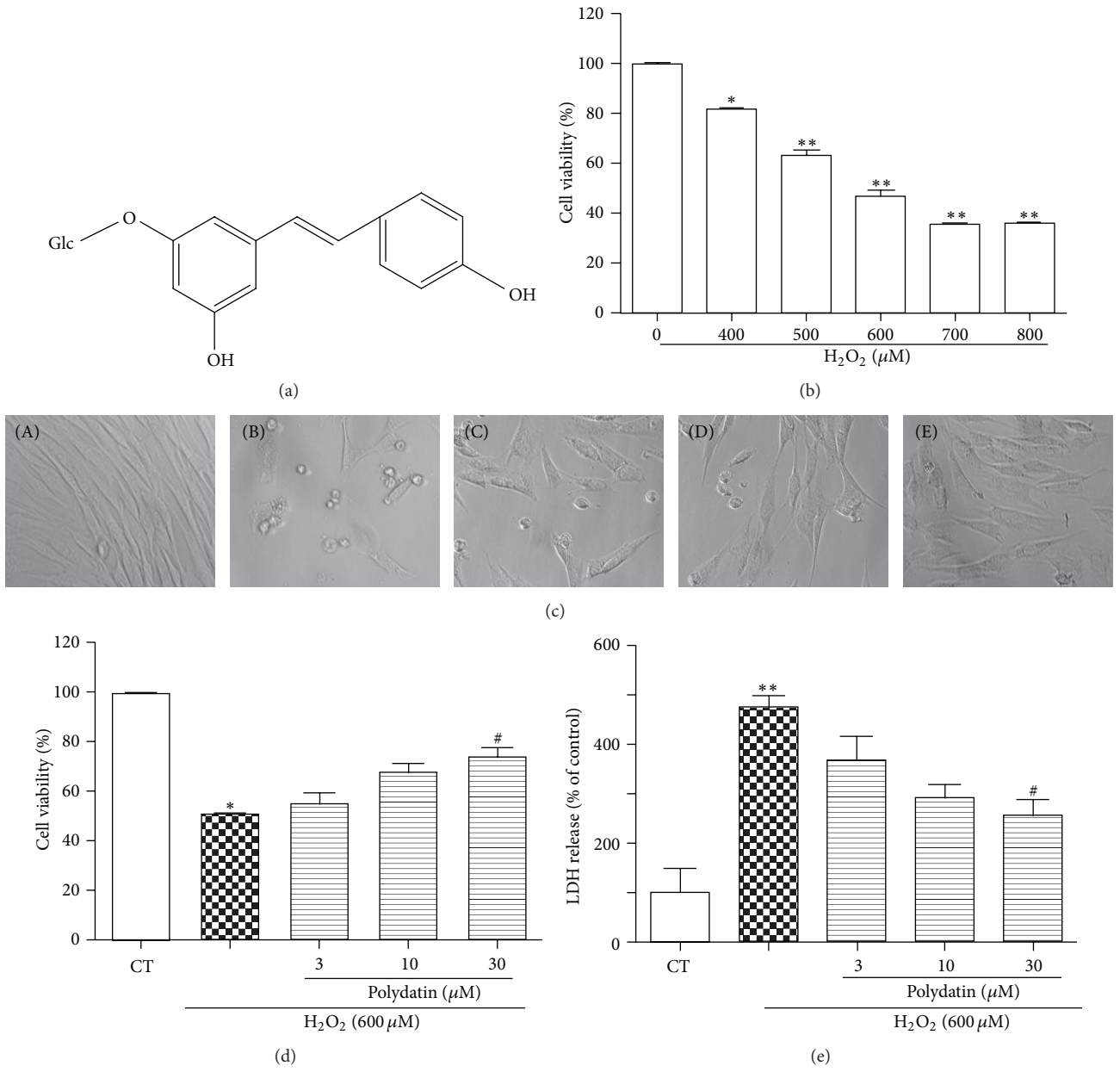

Figure 2: Effects of polydatin on the cell viability of BMSCs exposed to H_2O_2. Cells were pretreated with different concentrations of polydatin for 2 h followed with H_2O_2 (600 μM) for 24 h. (a) Structure of polydatin. (b) Cells were treated with different concentrations of H_2O_2 for 24 h. (c, d) Cell viability was measured by MTT assay and cells were photographed under phase-contrast optics. (A) CT, (B) H_2O_2, (C) polydatin 3 μM + H_2O_2, (D) polydatin 10 μM + H_2O_2, and (E) polydatin 30 μM + H_2O_2. (e) Cell death was measured by LDH assay. Bar graph represents independent experiments, each performed in triplicate. One-way ANOVA followed by Tukey's test. Data are presented as means ± S.D. $^{*}p < 0.05$ and $^{**}p < 0.01$ versus control group. $^{\#}p < 0.05$ versus H_2O_2-treated group.

3.4. Polydatin Decreased the Intracellular ROS Formation. To further disclosure the protective mechanism of polydatin, we detected its effects on the formation of intracellular ROS by H_2DCF-DA staining, a ROS probe, and the endogenous antioxidant glutathione (GSH) using a GSH assay kit. As shown in Figures 4(a) and 4(b), compared with the control group, H_2O_2-treated group cause significant increase of ROS, which was attenuated by polydatin. Moreover, polydatin also improve the intracellular GSH which was depleted by H_2O_2 (Figure 4(c)).

3.5. Effects of Polydatin on the Cell Cycle of BMSCs. It is reported that polydatin, the natural precursor of resveratrol, inhibits proliferation of tumor cells caused by the cell cycle arrest [23, 24]. Thus, the survival effect of polydatin indicated in the study might simply be a switch of MSCs into

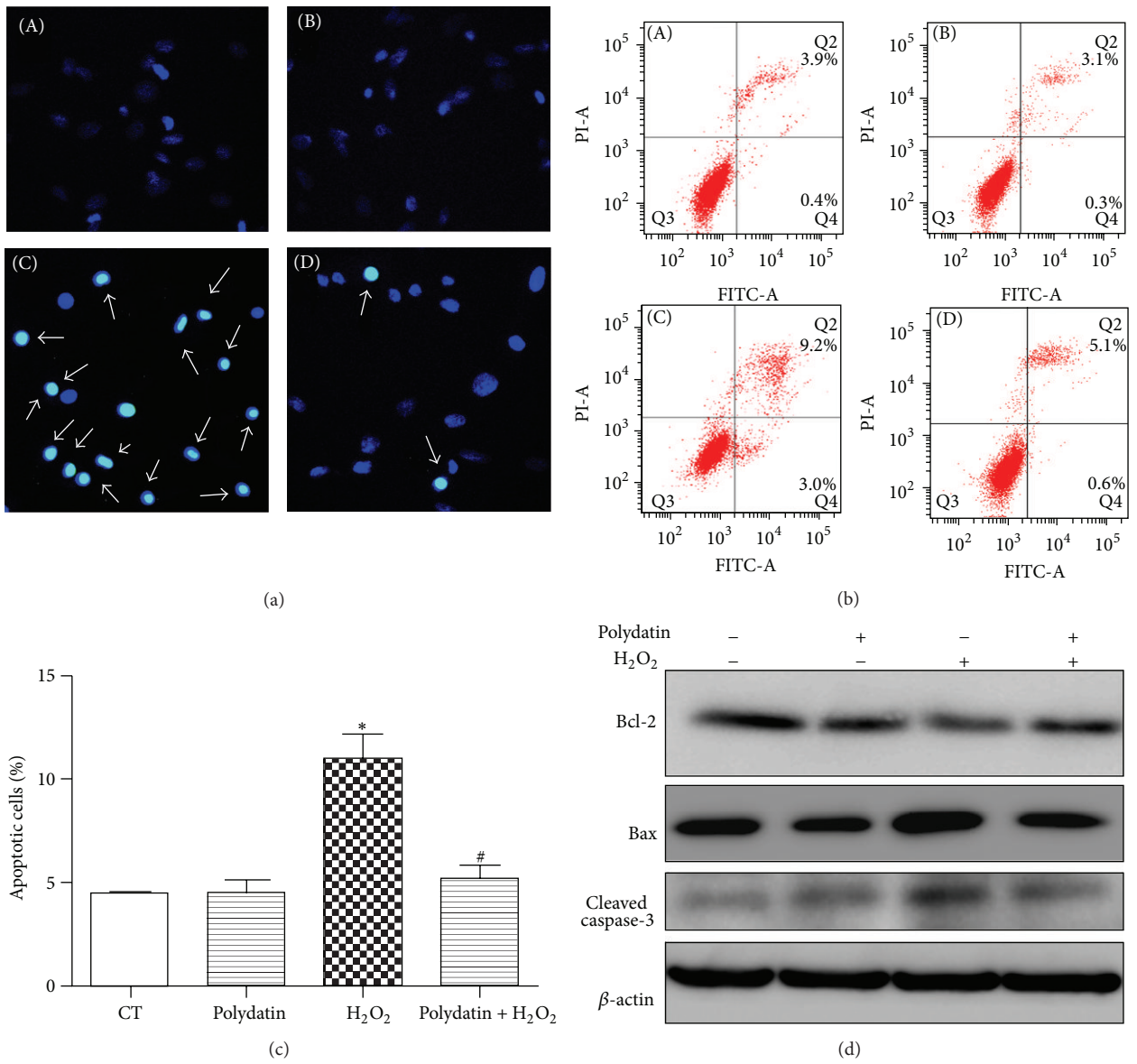

FIGURE 3: Polydatin attenuated H_2O_2-induced apoptosis in BMSCs. (a) Hochest 33258 staining was applied to detect the nuclear condensation of BMSCs, pretreated with polydatin in presence of H_2O_2. Fluorescence images (A–D) were observed by fluorescence microscope. (A)–(D) represented CT, polydatin, H_2O_2, and H_2O_2 + polydatin group, respectively. (b) BMSCs were pretreated with 30 μM polydatin for 2 h and followed by exposing to H_2O_2 (600 μM) for 12 h. The induction of apoptosis was determined using Annexin V-FITC/PI staining. (c) Quantitative analysis of apoptotic cells in Figure 3(b). (d) The expression of Bcl-2, cleaved caspase-3, and Bax of BMSCs exposed to H_2O_2 with or without polydatin. Data are presented as means ± S.D. $^*p < 0.05$ versus control group; $^\#p < 0.05$ versus H_2O_2-treated group.

quiescence. To examine whether the protective effects are related to polydatin cell cycle arrest activities, EdU assay was applied. Our results showed that H_2O_2 significantly reduced the proliferation rate of BMSCs compared with control group; polydatin at 30 μM did not cause proliferation inhibition on BMSCs, which suggests that polydatin may not lead to cell cycle arrest on BMSCs at the concentration (Figure 5).

3.6. Polydatin Prevented BMSCs from H_2O_2-Induced Apoptosis through Nrf 2/ARE Pathway. Polydatin has been reported to quench ROS overproduction by activating Nrf 2/ARE pathway, which has been reported to have key roles in regulating a battery of endogenous antioxidants and phase II detoxification enzymes, including NAD(P)H quinone oxidoreductase-1 (NQO-1) [25]. To explore whether Nrf 2/ARE pathway was involved in the protection of polydatin against oxidative injury, Western blotting was applied. As shown in Figures 6(a)–6(c), H_2O_2 significantly decreased the protein levels of p-Nrf 2 and NQO-1 protein, which was partly reversed by polydatin.

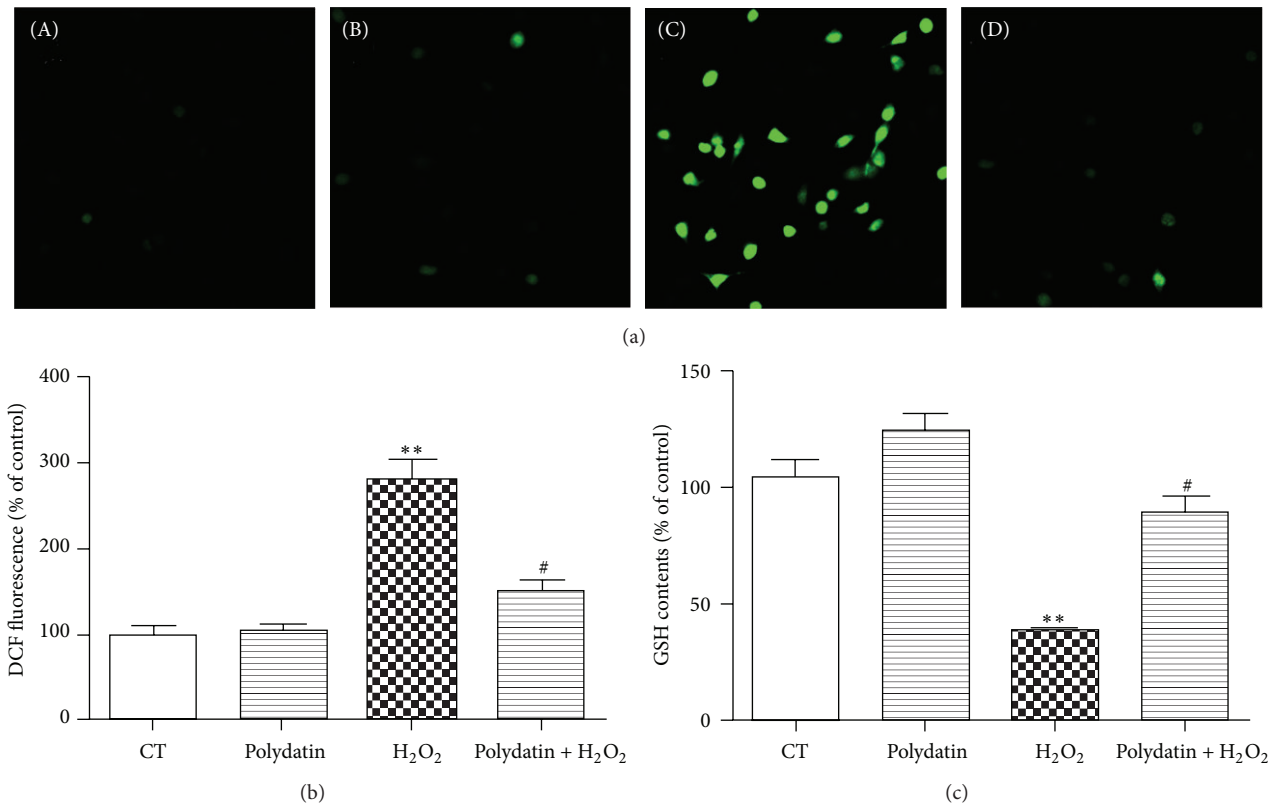

Figure 4: Polydatin scavenges ROS produced by H_2O_2. (a) ROS production induced by H_2O_2 was detected by H_2DCF-DA staining. (b) Quantitative analysis of DCF fluorescent intensity. (c) The level of GSH was measured using GSH assay kit. The basal contents of GSH in untreated control cells were taken as 100%. Data are collected from 3 independent experiments and presented as means ± S.D. One-way ANOVA followed by Tukey's test. $^{*}p < 0.05$ and $^{**}p < 0.001$ versus control group; $^{\#}p < 0.05$ versus H_2O_2-treated group.

To further confirm the involvement of Nrf 2/ARE pathway in the protective effects of polydatin, brusatol, a unique inhibitor of the Nrf 2 pathway, which selectively reduces the protein level of Nrf 2 through enhanced degradation and ubiquitination of Nrf 2, was applied [26, 27]. As shown in Figure 6(d), brusatol at 100 nM significantly reduced phosphorylation of Nrf 2 and did not cause cell death in BMSCs. Therefore, the concentration was chosen for the next experiment. Our results showed that polydatin attenuated cell viability decrease caused by H_2O_2, which was reversed by brusatol (Figure 6(h)). Moreover, brusatol also blocked the ROS scavenging activities of polydatin (Figures 6(f) and 6(i)).

4. Discussion

To the best of our knowledge, this is the first report about the effects of polydatin on the oxidative injury induced by H_2O_2 in BMSCs. We observed that polydatin dramatically attenuated H_2O_2-induced ROS generation, GSH depletion, LDH release, and subsequent cell death. Further studies showed that polydatin also enhanced phosphorylation of Nrf 2 and upregulation of NQO-1 which was downregulated by H_2O_2, suggesting that polydatin might protect BMSCs against H_2O_2 partly via Nrf 2/ARE pathway.

BMSCs, which are capable of self-renewal and differentiation into a variety of mesodermal cell lineages, including osteocytes, chondrocytes, myoblasts, and adipocytes [28, 29] are considered as an ideal source of cells for cell replacement therapy. BMSCs transplantation has shown great promises for treating vast CNS disorders, including SCI. However, poor viability of transplanted BMSCs in injured spinal cord has limited the therapeutic efficiency. Oxidative stress is one of the key mechanisms underlying the pathogenesis of CNS disorders including SCI. Sustained oxidative stress could reduce the survival of donor BMSCs, causing limited reparative capacity of BMSCs. Therefore, it is rational to improve the poor oxidative environment and protect the BMSCs against oxidative stress for the successful transplantation of BMSCs in SCI.

Polydatin, an active stilbene compound isolated from the roots of *Polygonum cuspidatum* Sieb. and Zucc., has been shown to prevent the development of diabetic renal fibrosis, ameliorate Alzheimer's disease, and protect ischemia/reperfusion damage in heart and diabetic nephropathy. It has also been reported to have antiapoptosis and antioxidation activities in many cellular systems. However, protective effects of polydatin on BMSCs are unknown. We used H_2O_2 to induce oxidative injury on BMSCs, imitating the

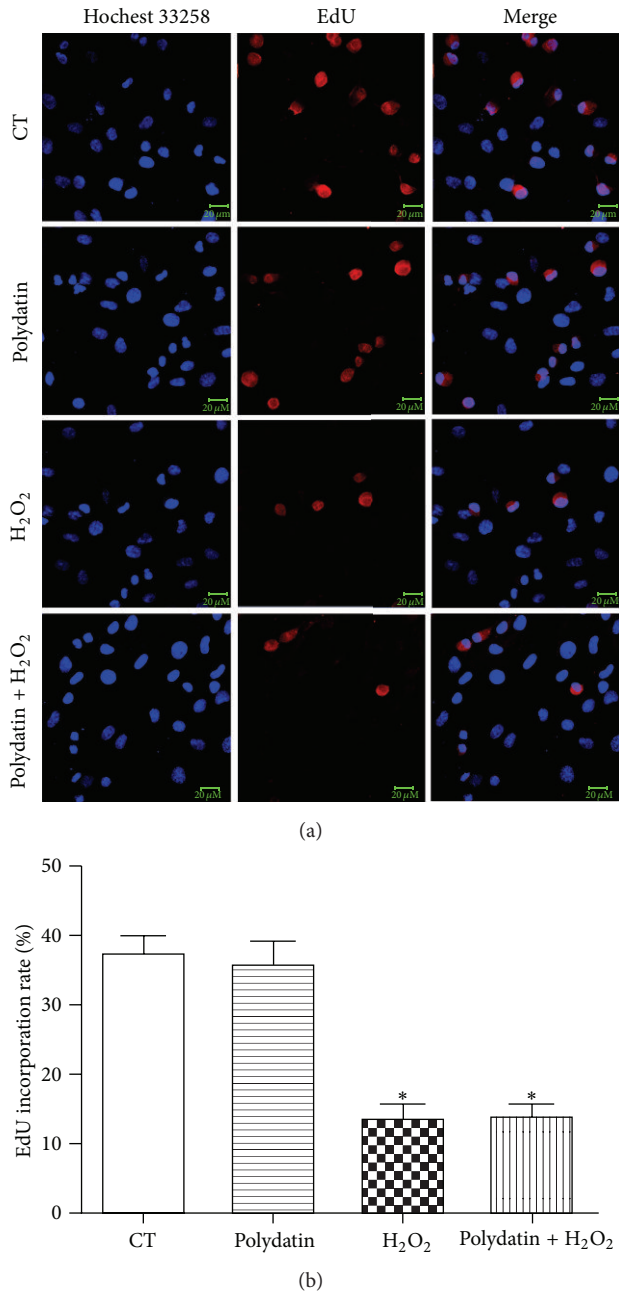

Figure 5: Polydatin did not inhibit the proliferation of BMSCs. (a) Proliferation rate of BMSCs was detected by EdU and Hochest 33258 staining. Fluorescence was visualized by a laser-scanning confocal microscope. Scale bar represents 20 μM. (b) Quantitative analysis of the EdU incorporation rate of BMSCs. $^*p < 0.05$ versus control group.

poor microenvironment of the spinal cord after SCI. Our results showed that H_2O_2 reduced cell viability of BMSCs dose-dependently and caused a robust ROS generation and GSH depletion as previously reported [10]. Polydatin, at a concentration of 30 μM, effectively suppressed H_2O_2-induced cell death, scavenged the ROS, and reversed the depletion of GSH, indicating that polydatin exerts beneficial effects on BMSCs as well.

Bcl-2 and Bax are two members of the Bcl-2 family, which are crucial regulatory factors in apoptosis. Bcl-2, the antiapoptotic protein, inhibits apoptosis by preventing cytochrome c release into the cytoplasm [22], while Bax, the proapoptotic protein, promotes apoptosis by inducing mitochondrial membrane depolarization. The Bcl-2 family maintains mitochondrial stabilization by mediating the Bcl-2/Bax balance [30]. Caspase-3 is a pivotal executioner caspase, which triggers the cleavage of a number of proteins and ultimately leads to DNA fragmentation, and has long been considered as a key protease involved in cell apoptosis [31]. In the present study, we examined the underlying mechanism of the protection of polydatin against H_2O_2-induced apoptosis by detecting the expression of apoptosis-related proteins using Western blot. We observed the upregulation of Bax and cleaved caspase-3 and downregulation of Bcl-2 following treatment of H_2O_2, which were overtly reversed by polydatin, suggesting its antiapoptotic effects.

It is well established that polydatin (also named piceid) and resveratrol inhibit proliferation of tumor cells caused by the cell cycle arrest [23, 24]. Thus, the survival effect of polydatin indicated in the study might simply be a switch of MSCs into quiescence. To examine whether the protective effects are related to polydatin cell cycle arrest activities, we detected the proliferation rate of BMSCs pretreated with polydatin in the presence or absence of H_2O_2 using EdU assay. The results showed that polydatin at 30 μM did not cause proliferation inhibition on BMSCs, which suggests that polydatin may not lead to cell cycle arrest on BMSCs at the concentration. According to Su et al., polydatin induced the cell cycle arrest in the S phase at 300 μM on MDA-MB-231 cells but not MCF-7 cells and HepG2 cells, suggesting that polydatin only cause proliferation inhibition in certain cell lines at proper concentrations [23]. According to Su et al., polydatin protected MDA-MB-231 cells against H_2O_2 toxicity at 50 μM, a concentration which did not cause cell cycle arrest, indicating that the protective effects of polydatin were independent from its effects on cell cycle arrest. Therefore, the protective effects of polydatin reported in our paper may be just related to its antioxidative activities.

Nrf 2, a basic leucine zipper transcription factor, is reported to drive transcription of all kinds of genes involved in combating products of oxygen radicals and oxidation such as protein and DNA adducts from carbonyls or malondialdehyde [25, 32]. Under normal conditions, Nrf 2 binds to Kelch-like ECH associated protein-1 (Keap1) [33]. When oxidative stress occurs, Nrf 2 is released from Keap1, is translocated to the nucleus, is bound with ARE sequences, and results in transcriptional activation of antioxidant genes including NAD(P)H quinone oxidoreductase-1 (NQO-1) [34]. Huang et al. have reported that polydatin activated Nrf 2/ARE pathway in glomerular mesangial cells [16]. Herein, we found that H_2O_2 downregulated NQO-1 and the phosphorylation of Nrf 2 which was partly reversed by polydatin. To further confirm the involvement of Nrf 2/ARE pathway in the protection of polydatin, brusatol was applied. Previous studies reported

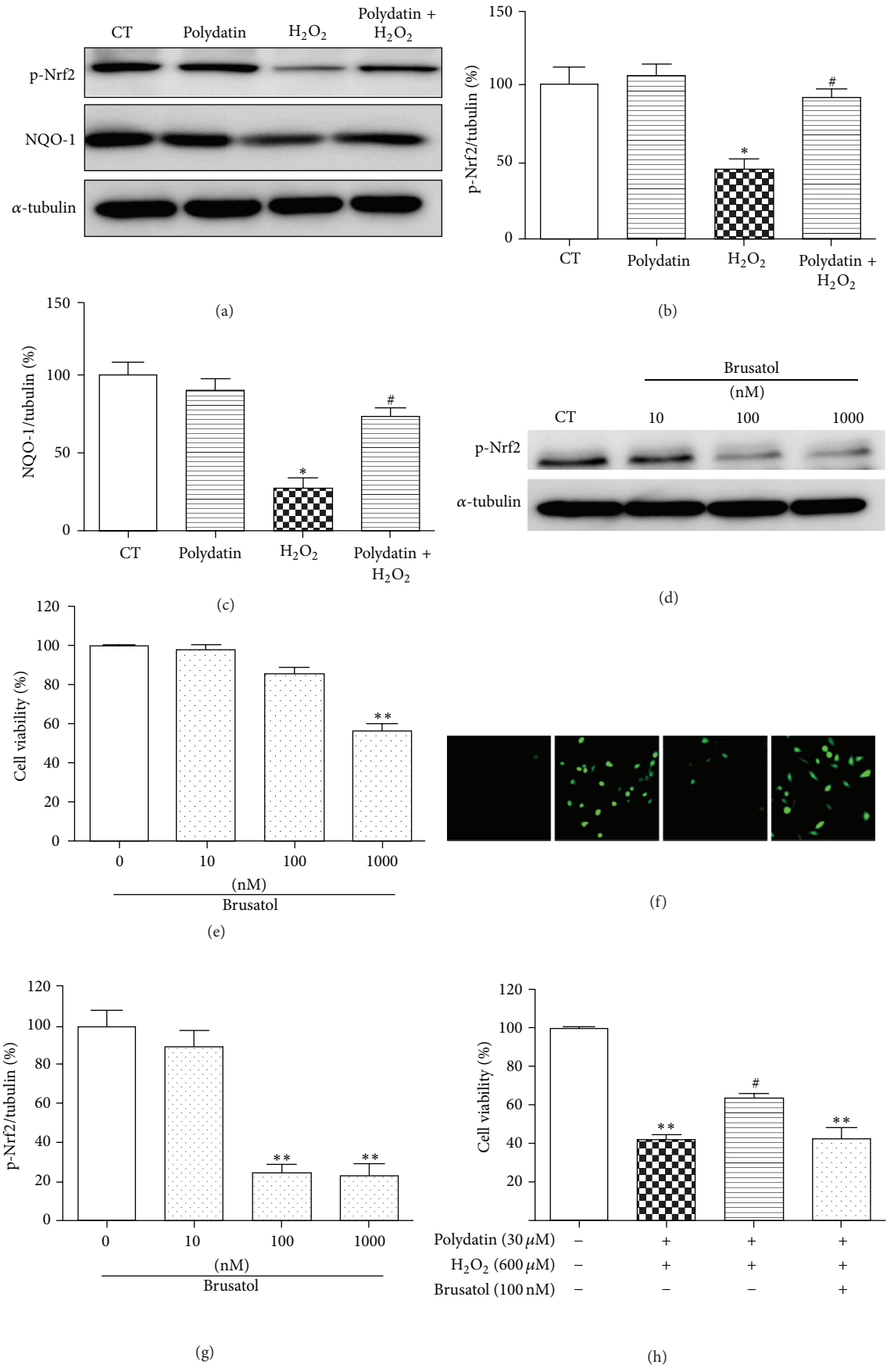

Figure 6: Continued.

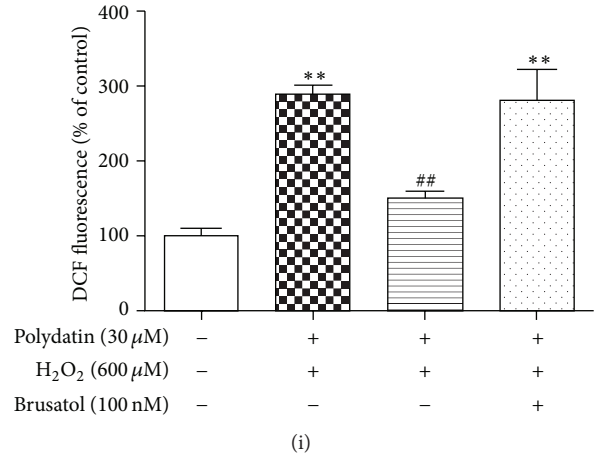

Figure 6: Polydatin protected BMSCs against H_2O_2-induced cell death partly through Nrf 2/ARE pathway. BMSCs were pretreated with polydatin for 2 h and further exposed to H_2O_2 for 12 h. (a) Effects of polydatin on NQO-1 and the phosphorylation of Nrf 2. (b, c) Quantitative analysis of the blots was shown in panel after being normalized by α-tubulin. (d) Cells were treated with different concentration of brusatol for 24 h. Effects of brusatol on phosphorylation of Nrf 2 were detected by Western blot and (g) the bands were normalized by α-tubulin. (e) Cell viability was tested in the presence of different concentration of brusatol. (h) BMSCs were pretreated with brusatol (100 μM) for 1 h followed by incubating with/without polydatin and H_2O_2 for 24 h. (f) ROS production was detected by H2DCF-DA staining. (b) Quantitative analysis of DCF fluorescent intensity. One-way ANOVA followed by Tukey's test. $^{*}p < 0.05$ and $^{**}p < 0.001$ versus control group; $^{\#}p < 0.05$ and $^{\#\#}p < 0.01$ versus H_2O_2-treated group.

brusatol as a unique inhibitor of the Nrf 2 pathway, which selectively downregulates the protein level of Nrf 2 via increasing ubiquitination and degradation of Nrf 2 [27]. Herein, we proved that coincubation with polydatin and brusatol reversed the protective and the ROS scavenging effects of polydatin, suggesting that Nrf 2/ARE pathway was involved in the protection and antioxidation of polydatin against H_2O_2-induced cell death.

5. Conclusion

Taken together, our results indicate that polydatin exerts strikingly protective effects against H_2O_2-induced cytotoxicity in BMSCs through activating the Nrf 2/ARE pathway, suggesting that polydatin could be a promising approach to increase the cell survival in cell replacement therapy for SCI.

Conflict of Interests

The authors declare that there is no conflict of interests regarding the publication of this paper.

Acknowledgment

This study was supported by National Natural Science Foundation of China (no. 81273782) to Dingkun Lin.

References

[1] H. L. Harkey III, E. A. White IV, R. E. Tibbs Jr., and D. E. Haines, "A clinician's view of spinal cord injury," *Anatomical Record Part B: New Anatomist*, vol. 271, no. 1, pp. 41–48, 2003.

[2] T. K. Ng, V. R. Fortino, D. Pelaez, and H. S. Cheung, "Progress of mesenchymal stem cell therapy for neural and retinal diseases," *World Journal of Stem Cells*, vol. 6, no. 2, pp. 111–119, 2014.

[3] A. Singh, L. Tetreault, S. Kalsi-Ryan, A. Nouri, and M. G. Fehlings, "Global prevalence and incidence of traumatic spinal cord injury," *Clinical Epidemiology*, vol. 6, pp. 309–331, 2014.

[4] H.-Y. Chen, X. Zhang, S.-F. Chen et al., "The protective effect of 17beta-estradiol against hydrogen peroxide-induced apoptosis on mesenchymal stem cell," *Biomedicine & Pharmacotherapy*, vol. 66, no. 1, pp. 57–63, 2012.

[5] R. Ju, W. Zeng, R. Wu, and Z. Feng, "Interaction between neural stem cells and bone marrow derived-mesenchymal stem cells during differentiation," *Biomedical Reports*, vol. 3, no. 2, pp. 242–246, 2015.

[6] M. Bacigaluppi, S. Pluchino, G. Martino, E. Kilic, and D. M. Hermann, "Neural stem/precursor cells for the treatment of ischemic stroke," *Journal of the Neurological Sciences*, vol. 265, no. 1-2, pp. 73–77, 2008.

[7] A. Hejčl, J. Šedý, M. Kapcalová et al., "HPMA-RGD hydrogels seeded with mesenchymal stem cells improve functional outcome in chronic spinal cord injury," *Stem Cells and Development*, vol. 19, no. 10, pp. 1535–1546, 2010.

[8] J. C. Ra, I. S. Shin, S. H. Kim et al., "Safety of intravenous infusion of human adipose tissue-derived mesenchymal stem cells in animals and humans," *Stem Cells and Development*, vol. 20, no. 8, pp. 1297–1308, 2011.

[9] F.-W. Wang, Z. Wang, Y.-M. Zhang et al., "Protective effect of melatonin on bone marrow mesenchymal stem cells against hydrogen peroxide-induced apoptosis in vitro," *Journal of Cellular Biochemistry*, vol. 114, no. 10, pp. 2346–2355, 2013.

[10] B. Sun, M. Feng, X. Tian et al., "Dl-3-n-Butylphthalide protects rat bone marrow stem cells against hydrogen peroxide-induced cell death through antioxidation and activation of PI3K-Akt pathway," *Neuroscience Letters*, vol. 516, no. 2, pp. 247–252, 2012.

[11] M. Dong, W. Ding, Y. Liao et al., "Polydatin prevents hypertrophy in phenylephrine induced neonatal mouse cardiomyocytes and pressure-overload mouse models," *European Journal of Pharmacology*, vol. 746, pp. 186–197, 2014.

[12] Q. Zhang, Y. Tan, N. Zhang, and F. Yao, "Polydatin supplementation ameliorates diet-induced development of insulin resistance and hepatic steatosis in rats," *Molecular Medicine Reports*, vol. 11, no. 1, pp. 603–610, 2014.

[13] X. Xie, J. Peng, K. Huang et al., "Polydatin ameliorates experimental diabetes-induced fibronectin through inhibiting the activation of NF-κB signaling pathway in rat glomerular mesangial cells," *Molecular and Cellular Endocrinology*, vol. 362, no. 1-2, pp. 183–193, 2012.

[14] L. Zhang, W.-F. Ma, J. Li et al., "Influence of processing on pharmacokinetic of typical constituents in radix polygoni multiflori after oral administration by LC-ESI-MS/MS," *Journal of Ethnopharmacology*, vol. 148, no. 1, pp. 246–253, 2013.

[15] J. Sun, Y. Qu, H. He et al., "Protective effect of polydatin on learning and memory impairments in neonatal rats with hypoxic-ischemic brain injury by up-regulating brain-derived neurotrophic factor," *Molecular Medicine Reports*, vol. 10, no. 6, pp. 3047–3051, 2014.

[16] K. Huang, C. Chen, J. Hao et al., "Polydatin promotes Nrf2-ARE anti-oxidative pathway through activating Sirt1 to resist AGEs-induced upregulation of fibronetin and transforming growth factor-beta1 in rat glomerular messangial cells," *Molecular and Cellular Endocrinology*, vol. 399, pp. 178–189, 2015.

[17] L. Chen, Z. Lan, Q. Lin et al., "Polydatin ameliorates renal injury by attenuating oxidative stress-related inflammatory responses in fructose-induced urate nephropathic mice," *Food and Chemical Toxicology*, vol. 52, pp. 28–35, 2013.

[18] X. Jiang, W. Liu, J. Deng et al., "Polydatin protects cardiac function against burn injury by inhibiting sarcoplasmic reticulum Ca^{2+} leak by reducing oxidative modification of ryanodine receptors," *Free Radical Biology and Medicine*, vol. 60, pp. 292–299, 2013.

[19] W. Zhang, N. Liu, H. Shi et al., "Upregulation of BMSCs osteogenesis by positively-charged tertiary amines on polymeric implants via charge/iNOS signaling pathway," *Scientific Reports*, vol. 5, article 9369, 2015.

[20] D. Cizkova, S. Devaux, F. Le Marrec-Croq et al., "Modulation properties of factors released by bone marrow stromal cells on activated microglia: an in vitro study," *Scientific Reports*, vol. 4, article 7514, 2014.

[21] Y. Huang, J. Qin, M. Chen et al., "Lithium prevents acrolein-induced neurotoxicity in HT22 mouse hippocampal Cells," *Neurochemical Research*, vol. 39, no. 4, pp. 677–684, 2014.

[22] M. Chen, M. Tan, M. Jing et al., "Berberine protects homocysteic acid-induced HT-22 cell death: involvement of Akt pathway," *Metabolic Brain Disease*, vol. 30, pp. 137–142, 2015.

[23] D. Su, Y. Cheng, M. Liu et al., "Comparision of piceid and resveratrol in antioxidation and antiproliferation activities in vitro," *PLoS ONE*, vol. 8, no. 1, Article ID e54505, 2013.

[24] Y. Zhang, Z. Zhuang, Q. Meng, Y. Jiao, J. Xu, and S. Fan, "Polydatin inhibits growth of lung cancer cells by inducing apoptosis and causing cell cycle arrest," *Oncology Letters*, vol. 7, no. 1, pp. 295–301, 2014.

[25] M. J. Calkins, D. A. Johnson, J. A. Townsend et al., "The Nrf2/ARE pathway as a potential therapeutic target in neurodegenerative disease," *Antioxidants & Redox Signaling*, vol. 11, no. 3, pp. 497–508, 2009.

[26] X.-J. Chao, Z.-W. Chen, A.-M. Liu et al., "Effect of tacrine-3-caffeic acid, a novel multifunctional anti-alzheimer's dimer, against oxidative-stress-induced cell death in HT22 hippocampal neurons: Involvement of Nrf2/HO-1 pathway," *CNS Neuroscience & Therapeutics*, vol. 20, no. 9, pp. 840–850, 2014.

[27] D. Ren, N. F. Villeneuve, T. Jiang et al., "Brusatol enhances the efficacy of chemotherapy by inhibiting the Nrf2-mediated defense mechanism," *Proceedings of the National Academy of Sciences of the United States of America*, vol. 108, no. 4, pp. 1433–1438, 2011.

[28] M. F. Pittenger, A. M. Mackay, S. C. Beck et al., "Multilineage potential of adult human mesenchymal stem cells," *Science*, vol. 284, no. 5411, pp. 143–147, 1999.

[29] D. J. Prockop, "Marrow stromal cells as stem cells for non-hematopoietic tissues," *Science*, vol. 276, no. 5309, pp. 71–74, 1997.

[30] J. Qiu, P. Shi, W. Mao, Y. Zhao, W. Liu, and Y. Wang, "Effect of apoptosis in neural stem cells treated with sevoflurane," *BMC Anesthesiology*, vol. 15, article 25, 2015.

[31] E. A. Slee, M. T. Harte, R. M. Kluck et al., "Ordering the cytochrome c-initiated caspase cascade: hierarchical activation of caspases-2, -3, -6, -7, -8, and -10 in a caspase-9-dependent manner," *The Journal of Cell Biology*, vol. 144, no. 2, pp. 281–292, 1999.

[32] R. M. Abdelsalam and M. M. Safar, "Neuroprotective effects of vildagliptin in rat rotenone Parkinson's disease model: role of RAGE-NFkappaB and Nrf2-antioxidant signaling pathways," *Journal of Neurochemistry*, vol. 133, no. 5, pp. 700–707, 2015.

[33] A. Yanaka, S. Zhang, M. Tauchi et al., "Role of the nrf-2 gene in protection and repair of gastric mucosa against oxidative stress," *Inflammopharmacology*, vol. 13, no. 1–3, pp. 83–90, 2005.

[34] L. Wang, R. Wang, M. Jin et al., "Carvedilol attenuates 6-hydroxydopamine-induced cell death in PC12 cells: involvement of Akt and Nrf2/ARE pathways," *Neurochemical Research*, vol. 39, pp. 1733–1740, 2014.

Hindawi Publishing Corporation
Stem Cells International
Volume 2016, Article ID 4869071, 11 pages
http://dx.doi.org/10.1155/2016/4869071

Review Article

Human iPSC for Therapeutic Approaches to the Nervous System: Present and Future Applications

Maria Giuseppina Cefalo,[1] Andrea Carai,[2] Evelina Miele,[3,4] Agnese Po,[3] Elisabetta Ferretti,[5] Angela Mastronuzzi,[1] and Isabelle M. Germano[6]

[1]*Department of Hematology/Oncology and Stem Cell Transplantation, Bambino Gesù Children's Hospital, IRCCS, Piazza Sant'Onofrio 4, 00165 Rome, Italy*
[2]*Department of Neuroscience and Neurorehabilitation, Neurosurgery Unit, Bambino Gesù Children's Hospital, IRCCS, Piazza Sant'Onofrio 4, 00165 Rome, Italy*
[3]*Department of Molecular Medicine, Sapienza University of Rome, 00161 Rome, Italy*
[4]*Center for Life Nano Science @Sapienza, Italian Institute of Technology, 00161 Rome, Italy*
[5]*Department of Experimental Medicine, Sapienza University of Rome, 00161 Rome, Italy*
[6]*Department of Neurosurgery, Icahn School of Medicine at Mount Sinai, New York, NY 10029, USA*

Correspondence should be addressed to Isabelle M. Germano; isabelle.germano@mountsinai.org

Received 27 February 2015; Revised 13 July 2015; Accepted 16 July 2015

Academic Editor: Tao-Sheng Li

Many central nervous system (CNS) diseases including stroke, spinal cord injury (SCI), and brain tumors are a significant cause of worldwide morbidity/mortality and yet do not have satisfying treatments. Cell-based therapy to restore lost function or to carry new therapeutic genes is a promising new therapeutic approach, particularly after human iPSCs became available. However, efficient generation of footprint-free and xeno-free human iPSC is a prerequisite for their clinical use. In this paper, we will first summarize the current methodology to obtain footprint- and xeno-free human iPSC. We will then review the current iPSC applications in therapeutic approaches for CNS regeneration and their use as vectors to carry proapoptotic genes for brain tumors and review their applications for modelling of neurological diseases and formulating new therapeutic approaches. Available results will be summarized and compared. Finally, we will discuss current limitations precluding iPSC from being used on large scale for clinical applications and provide an overview of future areas of improvement. In conclusion, significant progress has occurred in deriving iPSC suitable for clinical use in the field of neurological diseases. Current efforts to overcome technical challenges, including reducing labour and cost, will hopefully expedite the integration of this technology in the clinical setting.

1. Introduction

Several diseases affecting the central nervous system (CNS) including stroke, spinal cord injury (SCI), and brain tumors remain the leading causes of mortality and morbidity in the US and worldwide [1]. Current therapies are still not fully successful in restoring the damaged tissue, in the case of stroke and SCI, or in selectively killing tumor cells dispersed in otherwise normal parenchyma, while sparing the latter, in the case of brain tumors. Cell-based therapies offer the potential advantages to provide regenerative tissue or to provide "vectors" aimed at targeting diseased cells. One additional challenge to improve therapies for CNS diseases is a better understanding of their pathophysiology, particularly for neurodegenerative diseases, such as Parkinson's diseases [2] or amyotrophic lateral sclerosis (ALS) [3]. For this purpose, information that can be derived from patient's specific cells offers a great tool to accelerate the understanding of mechanisms at the base of these conditions, possibly providing new therapeutic approaches.

The isolation of embryonic stem cells (ESC) was initially considered the most innovative strategy to approach "cell-based regenerative medicine" [4] due to their pluripotent nature, their unrestricted power of self-renewal, and their

ability to autodifferentiate into any cellular type. Unfortunately, many aspects have limited their application in treating human diseases, including ethical and technical issues, such as their derivation from early-stage embryos and the immune rejection for nonautologous cell lines [5]. Subsequently, the elaboration of "nuclear cloning" [6] or mammalian somatic cell nuclear transfer seemed to solve some of these limitations by creating a cloned cell from which to isolate the nuclear transfer-derived ESC, as autologous donor cells for therapy. This strategy demonstrated feasibility in a mouse model of immunodeficiency [7] but was not successfully reproduced in humans.

In 2006, Takahashi and Yamanaka [8] developed a line of induced pluripotent stem cells (iPSCs) using fibroblasts. They identified 24 candidate genes highly expressed in ESC critical to confer and maintain pluripotency. These genes were introduced into the mouse fibroblasts by a retroviral vector, demonstrating the reprogramming of somatic cells back to an ESC-like pluripotent state. iPSCs were first induced by the transfer of only four genes [9], Oct4, Sox2, Klf4, and c-Myc. This approach was applied to adult human fibroblasts, leading to the creation of human iPSC [10]. Due to the potential genomic integration of transgenes resulting from the use of retroviruses containing the oncogene c-Myc, the original technique carried a significant risk of tumorigenesis. Recent improvements in nuclear reprogramming have made iPSC induction safer as genes transfer can be achieved with techniques other than viral transduction [11–14], thus eliminating the risk of genomic integration. This is clinically significant when iPSCs are considered for transplant, as they represent a promising tool for regenerative medicine, in pathologies such as cardiomyopathies [15], stroke [16], and SCI [17].

The main characteristic of iPSC is pluripotency [18], defining the ability to differentiate into three germ layers and all cell types. The advantage of patient-specific iPSC is twofold. In disease modelling, the effects of patient-relevant mutations can be studied in the correct genetic and cellular background. In cells-based therapy, patient-specific iPSC will obviate the needs of immune suppressors. The elaboration of disease-derived iPSC [19] was first obtained in 2008 from a patient with ALS. These patient-specific iPSCs were successfully directed to differentiate into motor neurons, representing a potentially novel platform for disease modelling. Advances in induction of patient-specific iPSCs allowed their use to model a widespread variety of patient-specific diseases, such as cardiomyopathies [16] and as recently reported chemotherapy induced neurotoxicity [20].

Finally, iPSC-derived cells can be used in cell-based therapy as vectors to carry genes to their original organ. This has been explored for brain tumors using ESC and NPC [21, 22]. The rationale for this approach relies on the fact that primary brain tumors are very aggressive, infiltrative, and invasive, thus requiring cell-based therapy that can target tumoral cells while sparing the normal brain [22].

To accomplish the goals of using iPSC in large scale, numerous technical advances need to be pursued including reducing labour and cost to produce iPSC in large scale. In 2009 in the US, the FDA approved the country's first human trial on ESC transplantation into patients suffering from SCI; the trial, however, came to a halt in November 2011 when the company financing the trial announced the discontinuation of the trial due to financial issues [23]. Additionally, iPSC should be "safe" and easily obtainable from body sources with minimal invasiveness and high efficiency of reprogramming, overcoming three major current obstacles. First, the risk of genomic modification due to viral transgenes needs to be overcome by insertion-free or "footprint-free" iPSC. Second, the risk of teratogenicity if undifferentiated iPSCs are engrafted requires full differentiation or reprogramming inactivation of iPSCs before transplant. Finally, the risks of transmission of nonhuman pathogens to humans and/or immune response concern triggered by contamination from nonhuman antigens, deriving from the xeno-cell-dependent culture systems, necessitate the development of xeno-free iPSCs. Techniques and results used to overcome these burdens are described below.

2. Methods

Figure 1 summarizes methods to obtain iPSC. Different somatic cells can be used for reprogramming (Figure 1, left column). Reprogramming techniques (Figure 1, center column) first used viral based genomic integration (Figure 1(a)) and then used footprint-free techniques (Figure 1(b)). Finally, culturing conditions (Figure 1, right column) at first requiring feeder cells evolved to xeno-free conditions to allow safer clinical translation. Methodologies summarized in the diagram are briefly reported below.

2.1. Reprogrammable Somatic Cells for iPSC. Ideally, cell sources of hiPSC should be acquired easily and noninvasively from patients and should be reprogrammed into iPSCs with high efficiency. Cell types successfully utilized for hIPSC production include dermal fibroblasts [10], bone marrow CD34+ cells [32], cord blood cells [33], peripheral blood cells [34], adipose-derived stromal cells [35], neural stem cells [36], and keratinocytes [37] (Figure 1, left column).

Recently, Nakagawa et al. [38] were able to obtain an adequate number of footprint-free, xeno-free hiPSC clones from both skin-derived fibroblasts and blood cells. Lee et al. [39] reported a method to generate footprint- and xeno-free iPSC from urine cells which can be obtained totally non-invasively using extracellular matrix-based xeno-free iPSC culture condition and episomal transfection.

2.2. "Footprint-Free" iPSC. The reprogramming of somatic cells to pluripotency implicates the risk of genomic modification when retroviral and lentiviral vectors are used. Indeed, although these vectors are feasible and efficient in iPSC production, they also cause insertional mutagenesis due to viral vector integration, prompting caution with their translation to clinical applications (Figure 1(a)).

Among the first attempts to produce footprint-free iPSC was the use of nonintegrating vectors encoding reprogramming factors (RF) based on adenovirus [40] and transient plasmid to be repeatedly transfected [41, 42]. However, this resulted in much lower reprogramming efficiency with still

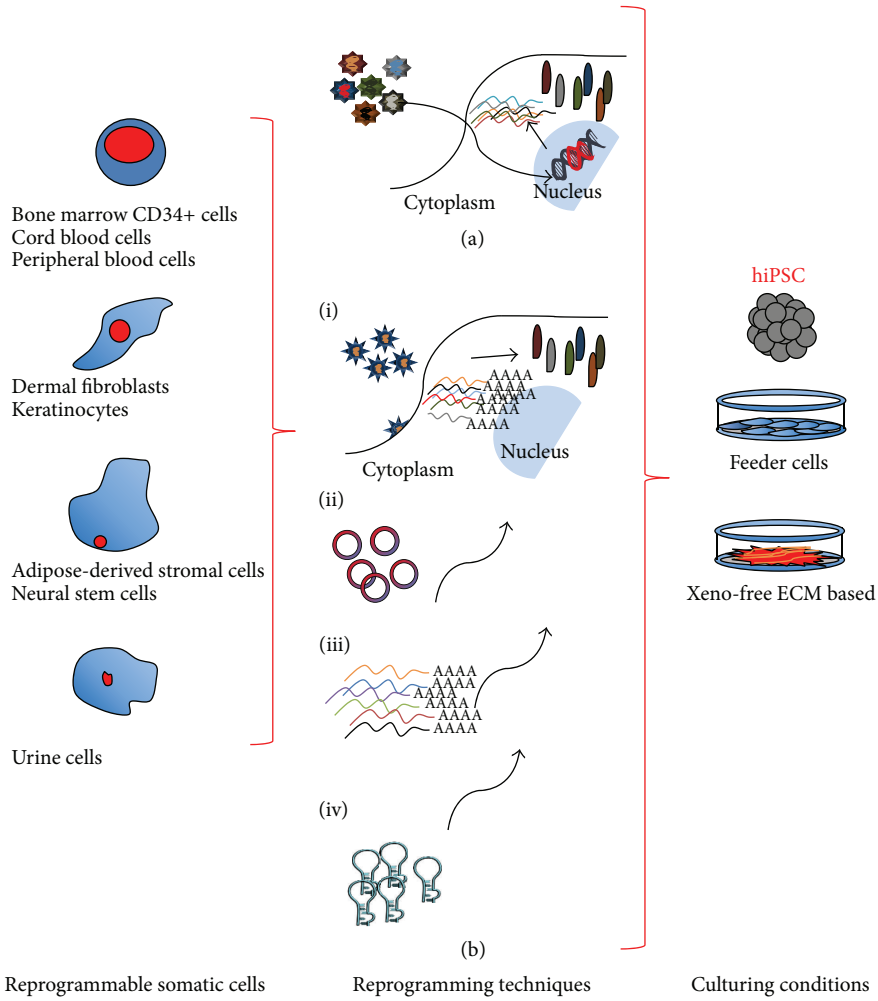

Figure 1: Diagrammatic representation of methods used to obtain human iPSC. Different somatic cells can be used for reprogramming (left column). Reprogramming techniques (center column) first used viral based genomic integration (a) and then used footprint-free techniques (b). Footprint-free iPSC induction can be obtained by Sendai virus (b(i)); episome (b(ii)); mRNA (b(iii)); siRNA (b(iv)). Finally, culturing conditions (right column) at first requiring feeder cells evolved to xeno-free conditions to allow safer clinical translation.

some residual risk of genomic alteration, thus necessitating PCR screening of iPSC colonies or sequencing before taking them forward to clinical application.

Another intriguing system is represented by episomes (Figure 1(b(ii))) [43, 44] where the expression vector is circular DNA encoding RF that is incorporated by cells through penetrating peptide moieties in culture media. The episomes show rapid and persistent RF expression, allowing a single transfection procedure to obtain iPSC, while they are lost by dilution over several weeks [45]. Nonetheless, episome-derived iPSCs need to be checked for genomic recombination and successful clearance of the RF, making their clinical applicability far from optimal.

Later on, new attracting methods to generate footprint-free iPSCs with higher reprogramming efficiency were developed: the RNA virus (Figure 1(b(i))), Sendai virus (SeV) [46], and mRNA or modified RNA (modRNA) [47] (Figure 1(b(iii))). In the SeV, RNA system RF are infected into cells by using a recombinant animal virus with a completely RNA-based replication cycle. Robust iPSC colonies are generated in 2-3 weeks, with efficiency even higher than the conventional retroviral and lentiviral protocols. As with the episomal method, the SeV RNA has the "one-shot" advantage and is lost from the iPSC between expansion passages. With the exception of the genomic recombination risk, SeV RNA method encounters the same concerns of episomal system for the clinical application, that is, the passive clearance of RF and false negative results. The mRNA method has been successfully applied in iPSC field, achieving high efficiency and rapid kinetics, without risk of accidental insertional mutagenesis and without the need for multiple passages to clear residual vector traces (Figure 1(b(iii))). Indeed, once transfection of RF is completed, ectopic expression in the cells soon ceases thanks to the rapid degradation of mRNA in the cytoplasm. Synthetic mRNA delivery to cells can occur by electroporation allowing diffusion into the cytoplasm by

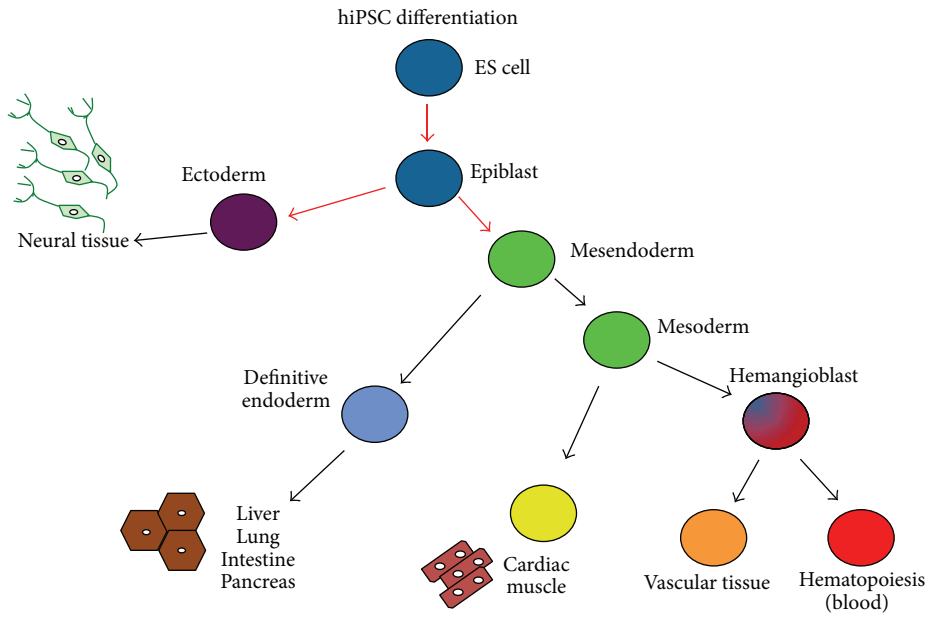

Figure 2: Human iPSC can be differentiated into all cell lineages.

creating pores in the cell membrane [48] and by complexing the RNA with cationic vehicles permitting internalization by endocytosis after the linkage to the negatively charged cell membrane [49]. Moreover, parallel to mRNA transfect other RNAs (siRNA, miRNA, and long noncoding RNA) can be codelivered with the same method, increasing the possibilities to control reprogramming and differentiation by supplying growth factors, cytokines, and small molecules in culture media [50] (Figure 1(b(iv))).

2.3. Xeno-Free iPSC. Another important safety-related issue to translate iPSC into the clinical setting is the need to reduce or eliminate the use of animal-derived materials, establishing xeno-free conditions for both iPSC derivation and expansion (Figure 1, right column).

All the initial culturing techniques for hiPSC utilized mouse embryonic fibroblast feeder cells and media containing other xeno-contaminated reagents, inheriting protocols developed for hESC cells over the last decade. The mouse feeder cell system bears in itself the risk of transmission of nonhuman pathogens to humans as well as immunological issues of rejection triggered by nonhuman antigens [50]. To overcome these obstacles, several protocols have been attempted. Almost all the approaches are based on media optimization toward xeno-free conditions and on the use of extracellular matrix- (ECM-) based feeder-independent culture system [50], substituting the routine system that includes bovine serum albumin (BSA) on Matrigel. Various matrices can be used to replace feeder cells, such as Matrigel, CELLstart, recombinant proteins, and synthetic polymers. Xeno-free media recently developed include TeSR2 and Essential E8 medium [39].

The former, developed by Sun et al. [51] for hESC culturing, is characterized by the complete absence of animal proteins and the inclusion of human serum albumin and human sourced matrix proteins. However, the prohibitively expensive costs of these media make their use not applicable for routine use. Additionally, the high variability of human serum albumin from batch to batch can impact the reprogramming results. When it was clarified that the need of albumin in ES and iPSC media is strictly linked to prevent the toxicity of another component, β-mercaptoethanol (BME), contained in the media, and is no longer necessary when BME is removed, a new medium was proposed, defined as E8 (eight components, including the DMEM/F12) [52]. Additionally, surfaces that efficiently support derivation and maintenance of hESC and iPSC were added such as laminin, vitronectin, and fibronectin purified from human plasma, or pericellular matrix of decidua-derived mesenchymal stem cells [52]. Several vitronectin variants were tested and in particular VTN-NC and VTN-N resulted to be efficient [40]. Nakagawa et al. [38] reported that recombinant laminin-511 E8 fragments are useful matrices for maintaining hESCs and footprint-free hiPSCs when used in combination with the StemFitTM medium, completely xeno-free. Their study showed that the Ff-hiPSCs established under footprint-free and xeno-free conditions from several types of somatic cells are similar to the hiPSCs established using the conventional system with feeders, showing equivalent growth and differentiation potential.

2.4. hiPSC Differentiation. hiPSC, obtained with the methods above, can be differentiated into all cell lineages as shown in Figure 2. Detailed protocols on how to differentiate footprint-free hiPSC were previously reported [16, 53].

3. Results

3.1. iPSC and Ischemic Stroke. Ischemic stroke, still causing high disability and mortality, prompted the investigation

of therapeutic approaches other than thrombolytic therapy and/or percutaneous intravascular interventions [54]. iPSCs have emerged as a promising tool for cell replacement in ischemic brain injuries. At least 4 synergistic mechanisms have been proposed to account for the beneficial effect of stem cells on experimental stroke: neuroprotection, neurogenesis, modulation of the immune response, and angiogenesis. The first [55] occurs by secretion of neuroprotective cytokines such as VEGF and NGF and neurotrophins and by causing paracrine effects, increasing dendritic plasticity and axonal rewriting. Endogenous neurogenesis [56] has been shown by increased number of cells expressing the early neuronal lineage marker Dcx in murine models. Modulation of immune and inflammatory response [57] is achieved by reducing the main inflammatory regulators in focal brain tissue, such as microglia, by inducing the downregulation of some inflammatory regulators, such as TNF-alpha, IL-6, and leptin receptors. Finally, angiogenesis [58] is stimulated with formation of brain microvessels and functional recovery has been demonstrated in peri-infarct regions after stem cell infusion in rat stroke model.

3.2. iPSC and SCI. SCI can be caused by a variety of factors, such as trauma, ischemia, and iatrogenic injury, resulting in sensory and motor dysfunctions. SCI [59] is the consequence of the primary irreversible damage caused by direct mechanical insult and the secondary injuries of trauma as inflammatory/immune response, cell necrosis and/or apoptosis, excitotoxins, oxygen free radical, ionic imbalance, and axon reaction. The therapeutic effects of iPSC in SCI can affect multiple mechanisms [60], such as the reconstruction of neural synaptic connections by neural cells derived by iPSC, axons remyelination by oligodendrocytes, and the neuroprotection due to neurotrophic factors secreted by neural cells. In mouse SCI model, data show that treating the damage with iPSC could restore the impaired function through these mechanisms [61]. Mouse iPSC-derived NPC transplanted into nonobese diabetic-severe combined immunodeficiency (NOD-SCID) mice's spinal cord 9 days after SCI differentiated into all three neural lineages did not give rise to teratoma and showed their neural differentiation capacity, participating in remyelination and inducing the axonal regrowth and promoting motor functional recovery [62]. Thus, iPSC clone-derived NPC may be a promising cell source for future transplantation therapy in SCI.

3.3. iPSC and Neurodegenerative Disease Modelling. Patient-specific iPSCs provide the unprecedented opportunity to study insights and potentially develop therapeutic options for neurodegenerative diseases, up to date difficult to target due to lack of experimental models. The generation of cell models of diseases is based on the differentiation of disease-specific iPSC into cell types relevant to the diseases [63]. The characterization of iPSC from patient-specific fibroblasts has been reported [64].

Table 1 summarizes the CNS disease-specific iPSCs that have been derived. Most diseases in which the phenotype could be recapitulated were congenital and paediatric disorders [63].

3.4. iPSC and Adrenoleukodystrophy Modelling. Jang et al. [24] generated X-linked adrenoleukodystrophy (ALD) iPSC, for both childhood cerebral ALD (CCALD) and adrenomyeloneuropathy (AMN). Both CCALD and AMN iPSC normally differentiated into oligodendrocytes, the cell type primarily affected in the X-linked ALD brain, indicating no developmental defect due to the ABCD1 mutations. Although low in X-ALD iPSC, very long chain fatty acid (VLCFA) level was significantly increased after oligodendrocyte differentiation. VLCFA accumulation was much higher in CCALD oligodendrocytes than AMN, indicating that the severe clinical manifestations in CCALD might be associated with abnormal VLCFA accumulation in oligodendrocytes. Furthermore, the abnormal accumulation of VLCFA in the X-ALD oligodendrocytes can be reduced by the upregulated ABCD2 gene expression after treatment with lovastatin or 4-phenylbutyrate. X-ALD iPSC model recapitulates the key events of disease pathophysiology, as VLCFA accumulation in oligodendrocytes, and allows for early diagnosis of the disease subtypes. X-ALD oligodendrocytes can be a useful cell model system to develop new therapeutics for treating X-ALD.

3.5. iPSC and Rett Syndrome Modelling. Using Rett syndrome (RTT) as an autism spectrum disorders genetic model, Marchetto et al. [28] developed a culture system using iPSC from RTT patients' fibroblasts, generating functional neurons. Neurons derived from RTT-iPSC had fewer synapses, reduced spine density, smaller soma size, altered calcium signalling, and electrophysiological defects. Finally, they used RTT neurons to test the effects of drugs in rescuing synaptic defects. Their model recapitulates early stages of a human neurodevelopmental disease.

3.6. iPSC and Familial Dysautonomia Modelling. Familial dysautonomia (FD) is a rare but fatal peripheral neuropathy, characterized by the depletion of autonomic and sensory neurons and caused by a point mutation in the *IKBKAP* gene, involved in transcriptional elongation. Lee et al. [27] elaborated the patient-specific FD-iPSCs and evidenced tissue-specific missplicing of *IKBKAP in vitro* by performing gene expression analysis in purified FD-iPSC-derived lineages. Patient-specific neural crest precursors express particularly low levels of normal *IKBKAP* transcript, as a mechanism for disease specificity. They also validated the potency of candidate drugs in reversing aberrant splicing and ameliorating neuronal differentiation. Finally, Koch et al. [30] illustrate that iPSCs enable the study of aberrant protein processing associated with late-onset neurodegenerative disorders in patient-specific neurons in Machado-Joseph disease model.

3.7. iPSCs as Gene Therapy Vectors for Brain Tumors. High grade gliomas (HGG), the most common primary brain tumors, remain a clinical challenge with an average life expectancy of 14 months for the most aggressive type after the best surgical, radiation, and chemotherapy treatments [65] due to the tumors' ability to diffusely invade and infiltrate the brain parenchyma. This coupled with the inability of most therapeutic compounds to penetrate the brain due to the blood-brain barrier raises the need to develop vectors

Table 1: Neurodegenerative specific iPSC for disease modelling.

CNS disease	Genetic defect	Phenotype
Adrenoleukodystrophy [24]	ABCD1	Increased level of VLCFA in oligodendrocytes
Alzheimer's disease [25]	Presenilin 1 Presenilin 2 APP duplication	Increased amyloid β (Aβ) secretion Increased Aβ40 production Increased phosphor-tau and GSK-3β activity
Amyotrophic lateral sclerosis [3]	SOD1, VAPB, and TDP43	Decreased VAPB in motor neurons Elevated levels of TDP43 protein
Huntington's disease [26]	CAG repeat expansion in HTT gene	Enhanced caspase activity upon growth factor deprivation
Familial dysautonomia [27]	IKBKAP	Decreased expression of genes involved in neurogenesis and neural differentiation
Parkinson's disease [3]	LRRK2, PINK1, and SNCA	Impaired mitochondrial function in PINK1-mutated dopaminergic neurons Increased sensitivity to oxidative stress in LRRK2 and SNCA-mutant neurons
Rett syndrome [28]	MeCP2 CDKL5	MeCP2: neuronal maturation defects, decreased synapse number CDKL5: aberrant dendritic spines
Spinal muscular atrophy [29]	SMN1	Decreased size, number, and survival of motor neurons
Machado-Joseph disease [30]	MJD1 (ATXN3)	Excitation-induced ataxin-3 aggregation in differentiated neurons
Schizophrenia [31]	Multifactorial	Reduced neuronal connectivity, increased consumption in extramitochondrial oxygen, and elevated levels of ROS

VLCFA: very long chain fatty acid; ROS: reactive oxygen species.

Table 2: Therapeutic agents delivered by SC for the treatment of HGG.

Agent delivered	Type of stem cells		
	ESC	NSC	MSC
Cytokines	Mda-7/IL24, TRAIL	IL-4, IL-12, IL-23, TRAIL +/− BMZ, and S-TRAIL +/− MIR/TMZ	IL-2, IL-12, IL-18, INFα, INF-β, and TRAIL +/− PI3KI
Enzyme/prodrug		Tk/GCV, CD/5FC +/− IFNβ	Tk/GCV
Viral particles		Mutant HSV-1, CRAd-survivin	CRAd-survivin, CRAd-CXCR4, and CRAd-Rb
Metalloproteinases		PEX	
Antibodies			EGFRvIII
Nanoparticles			Ferrociphenol lipid

that can infiltrate the brain in a fashion similar to glioma tumor cells delivering proapoptotic genes that spare normal parenchyma. Stem cells (SC) seem to be a logical choice as they maintain migratory capacity after transplant into the brain [66]. Table 2 summarizes the SC used as vectors to deliver specific therapeutic agents for HGG. Thus far, three types of SC have been tested as vehicle for therapeutic agents in brain tumors: ESC, mesenchymal SC (MSC), and NPC. Each strategy has specific advantages and disadvantages. ESC can be permanently and genetically modified using homologous recombination [67], but their use is held back by ethical and regulatory issues. NPC are the only SC native to the brain [68]; they have tumor tropism and infiltrative capacity across the blood-brain barrier; however, they are difficult to harvest and have risk of dedifferentiation with potential for tumorigenesis. MSC are easily obtainable from bone marrow and peripheral tissues or blood cells, but a major limitation is safety, due to the risk of promoting the growth potential of HGG cells [69]. Our published work shows that mESC-derived astrocytes maintain migration capacity after implant into the brain and in the presence of brain tumors they "home" within and around it [70]. We have also shown that a proapoptotic gene can be inserted prior to ECS differentiation into astrocytes downstream to a tetracycline inducible promoter ("tet-on") to regulate its expression with administration of doxycycline (Dox) [71]. Additionally, we have shown the proapoptotic effects of the mECS-derived astrocytes expressed gene *in vitro* and *in vivo* [72, 73]. Whereas most of the work using stem cells as vector is done on experimental models, there is a current FDA-approved phase 1 clinical trial using NPC engineered to convert the 5FU prodrug into active chemotherapy [74]. However, there are at least 4 significant limitations to this vector: (1) NPC are difficult to obtain and must be derived from fetal brain raising technical and ethical questions; (2) NPC are not fully differentiated and therefore are potentially tumorigenic; (3) viral vectors, used to engineer NPC, cause significant risk of insertional mutagenesis; (4) NPC are not autologous requiring potential immunosuppressive therapy. This prompted us to explore other vectors, such as iPSC.

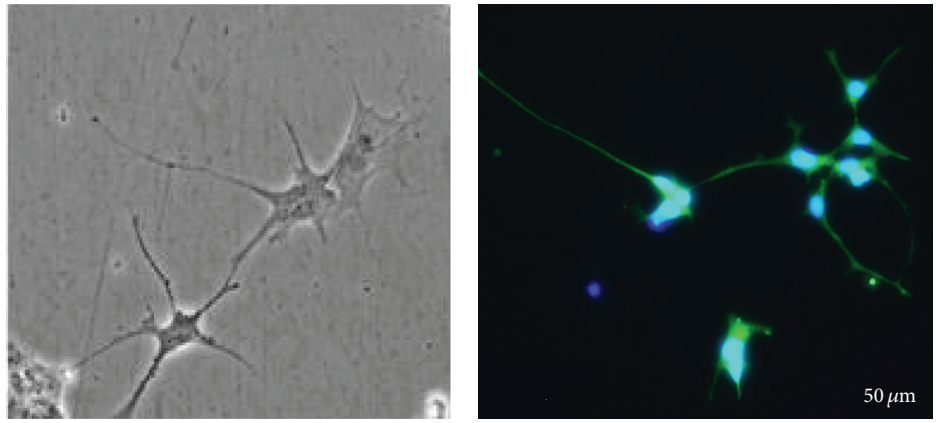

(a) (b)

Figure 3: Microphotographs of footprint-free iPSC-derived astrocytes. (a) Phase contrast and (b) immunocytochemistry for GFAP 9 days after MACS sorting of mRNA iPSC-derived astrocytes.

We have shown that we can differentiate astrocyte from iPSC in similar fashion to those obtained from ESC [21]. Recently, we have also shown that we can differentiate a pure population of footprint-free iPSC-derived astrocytes (Figure 3), which does not cause teratogenicity after implant into the brain [53]. We therefore propose that patient-specific cells can be reprogrammed into "footprint-free" hiPSC, their DNA engineered to carry proapoptotic genes, and then be differentiated into astrocytes and reimplanted in the same patient at the time of surgery for brain tumor recurrence (Figure 4). As discussed below, the ability to translate these exciting data to the clinical setting is still halted by technical obstacles, cost-effectiveness, and scalability.

4. Discussion

Human SC represent important cell resources and hold high promise for disease modelling, cell-based therapies, and drug and pharmaceutical applications [75]. iPSCs are the most appealing among SC due to the recent advances in reprogramming footprint-free and xeno-free iPSC [53]. They are a promising platform to pave the way for personalized medicine as they can be differentiated from the same patient to study his/her disease and/or response to new drugs and/or delivered back carrying proapoptotic genes/drugs. Current limitations, however, are still halting the translational use of hiPSC and need additional technical improvements. These are limited to not only the reprograming process, such as genetic/epigenetic abnormalities and immunogenicity, but also cost and labor of reprogramming process.

Genetic and epigenetic abnormalities may be reduced during reprogramming by improving efficiency to a level where iPSC could be derived without colony picking and colonial expansion, because the low efficiency and slow kinetics of iPSCs generation may give rise to the activation of cell growth pathways and suppression of tumor suppressor pathways. Therefore, using epigenetic small molecules to improve reprogramming efficiency could represent the key to ensure greater iPSCs safety. Reprogramming with mRNA could be highly immunogenic [76], since human cells have antiviral defence pathways triggered by exogenous RNA. These pathways can activate the suppression of translation, the degradation of foreign transcripts, and the priming of cytostatic and apoptotic pathways. To avoid such immunogenic response, several strategies have been tested, such as the incorporation of modified nucleobases (pseudouridine) into synthetic transcripts [77] or the supplementation of cell media with an extracellular decoy receptor for type I interferons [78] that blunt immune responses to infection.

A major obstacle in using iPSCs for clinical application resides in the risk of genomic modification when they are derived with viral transgenes, but the generation of "footprint-free" iPSC-derived astrocytes represents a promising innovation. Nonetheless, some drawbacks still exist even with mRNA reprogramming. First, certain cell types, including blood cells, are difficult to transfect [79]. Secondly, the approach works robustly if mRNA is transfected at frequent intervals to yield a steady state of protein expression over time. Cationic transfection reagents come to aid since they are well tolerated on repeat administration, while electroporation procedures are less feasible.

To achieve their full clinical and commercial potential, significant challenges must be overcome in order to produce iPSC-derived cells at commercially relevant scale. These include operational performances, economics, quality control and compliance, safety, and flexibility. Recent innovations in integrated bioprocesses design are helpful in improving hiPSC expansion. These include planar and three-dimensional culture systems. In particular, planar processing platforms are important for the production of autologous and patient-specific hiPSC-derived cells that necessitate a scale-out rather than a scale-up process [80]. Additional improvements are needed in the differentiation processes, including planar strategies and bioreactor-based systems. Finally, shorter reprogramming process and strategies to rapidly induce iPSC need to be developed as well as media

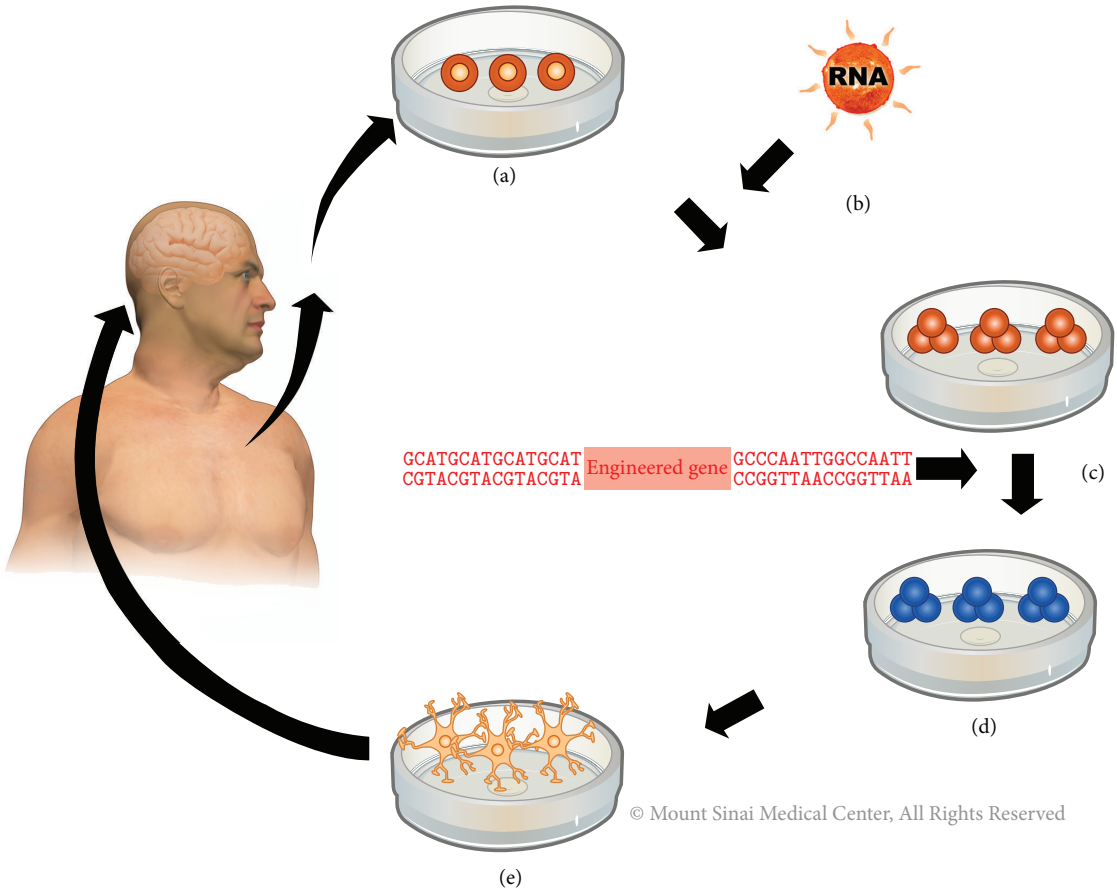

(a) Bone marrow cells removed from patient
(b) Ribonucleic acid added to the cells, which turns them into stem cells
(c) Tumor cells killer gene added to the stem cells
(d) Engineered cells cloned
(e) Engineered cells transformed to brain cells and implanted back in the same patient during brain surgery

FIGURE 4: Personalized medicine using patient-specific iPSC. Diagrammatic summary of reprogramming patient-specific cells into footprint-free hiPSC, engineering their DNA to carry proapoptotic genes, differentiating them into astrocytes, and reimplanting them at the time of surgery for brain tumor recurrence. (a) Dermal fibroblast cells obtained from patient. (b) Ribonucleic acid (RNA) added to cells, which turns them into stem cells. (c) Tumor cells killer gene added to stem cells. (d) Engineered cells cloned. (e) Engineered cells transformed to brain cells, astrocytes, and implanted back in the same patient at the time of surgical resection for recurrent tumor.

to improve iPSC efficiency without causing any aberrations of reprogrammed cells [81].

5. Conclusion

iPSCs provide a novel platform for CNS regenerative medicine, neurodegenerative disease modelling, pharmaceutical testing, and brain tumor treatments with a personalized medicine paradigm. The unique properties of iPSCs to self-renew and to differentiate into cells of three germ layers make them an invaluable tool for the present and the future of most neurologic disorders. Technical improvements in reprogramming with high efficiency induction systems and virus-free and integration-free strategies have greatly advanced iPSC therapeutic potentials. Additional efforts focused on refining reprogramming approaches will further enhance their clinical applications. Current efforts to reduce labour and cost are also instrumental for the integration of iPSC and iPSC-derived cells in the clinical setting.

Conflict of Interests

The authors declare that there is no conflict of interests regarding the publication of this paper.

References

[1] P. T. Donnan, D. W. T. Dorward, B. Mutch, and A. D. Morris, "Development and validation of a model for predicting emergency admissions over the next year (PEONY): a UK historical cohort study," *Archives of Internal Medicine*, vol. 168, no. 13, pp. 1416–1422, 2008.

[2] B. M. Jacobs, "Stemming the Hype: what can we learn from iPSC models of parkinson's disease and how can we learn it?" *Journal of Parkinson's Disease*, vol. 4, no. 1, pp. 15–27, 2014.

[3] M. C. Kiernan, S. Vucic, B. C. Cheah et al., "Amyotrophic lateral sclerosis," *The Lancet*, vol. 377, no. 9769, pp. 942–955, 2011.

[4] M. J. Evans and M. H. Kaufman, "Establishment in culture of pluripotential cells from mouse embryos," *Nature*, vol. 292, no. 5819, pp. 154–156, 1981.

[5] S. Das, M. Bonaguidi, K. Muro, and J. A. Kessler, "Generation of embryonic stem cells: limitations of and alternatives to inner cell mass harvest," *Neurosurgical Focus*, vol. 24, no. 3-4, article E3, 2008.

[6] A. Ogura, K. Inoue, and T. Wakayama, "Recent advancements in cloning by somatic cell nuclear transfer," *Philosophical Transactions of the Royal Society B: Biological Sciences*, vol. 368, no. 1609, Article ID 20110329, 2013.

[7] W. M. Rideout III, K. Hochedlinger, M. Kyba, G. Q. Daley, and R. Jaenisch, "Correction of a genetic defect by nuclear transplantation and combined cell and gene therapy," *Cell*, vol. 109, no. 1, pp. 17–27, 2002.

[8] K. Takahashi and S. Yamanaka, "Induction of pluripotent stem cells from mouse embryonic and adult fibroblast cultures by defined factors," *Cell*, vol. 126, no. 4, pp. 663–676, 2006.

[9] M. Wernig, A. Meissner, R. Foreman et al., "In vitro reprogramming of fibroblasts into a pluripotent ES-cell-like state," *Nature*, vol. 448, no. 7151, pp. 318–324, 2007.

[10] K. Takahashi, K. Tanabe, M. Ohnuki et al., "Induction of pluripotent stem cells from adult human fibroblasts by defined factors," *Cell*, vol. 131, no. 5, pp. 861–872, 2007.

[11] M. Wernig, A. Meissner, J. P. Cassady, and R. Jaenisch, "c-Myc is dispensable for direct reprogramming of mouse fibroblasts," *Cell Stem Cell*, vol. 2, no. 1, pp. 10–12, 2008.

[12] N. Maherali, R. Sridharan, W. Xie et al., "Directly reprogrammed fibroblasts show global epigenetic remodeling and widespread tissue contribution," *Cell Stem Cell*, vol. 1, no. 1, pp. 55–70, 2007.

[13] K. Okita, T. Ichisaka, and S. Yamanaka, "Generation of germline-competent induced pluripotent stem cells," *Nature*, vol. 448, no. 7151, pp. 313–317, 2007.

[14] M. Nakagawa, M. Koyanagi, K. Tanabe et al., "Generation of induced pluripotent stem cells without Myc from mouse and human fibroblasts," *Nature Biotechnology*, vol. 26, no. 1, pp. 101–106, 2008.

[15] T. Eschenhagen, C. Mummery, and B. C. Knollmann, "Modeling sarcomeric cardiomyopathies in the dish—from human heart samples to iPSC cardiomyocytes," *Cardiovascular Research*, vol. 105, no. 4, 2015.

[16] L. Hao, Z. Zou, H. Tian, Y. Zhang, H. Zhou, and L. Liu, "Stem cell-based therapies for ischemic stroke," *BioMed Research International*, vol. 2014, Article ID 468748, 17 pages, 2014.

[17] H. Wang, H. Fang, J. Dai, G. Liu, and Z. J. Xu, "Induced pluripotent stem cells for spinal cord injury therapy: current status and perspective," *Neurological Sciences*, vol. 34, no. 1, pp. 11–17, 2013.

[18] V. K. Singh, M. Kalsan, N. Kumar, A. Saini, and R. Chandra, "Induced pluripotent stem cells: applications in regenerative medicine, disease modeling, and drug discovery," *Frontiers in Cell and Developmental Biology*, vol. 3, no. 2, 2015.

[19] J. T. Dimos, K. T. Rodolfa, K. K. Niakan et al., "Induced pluripotent stem cells generated from patients with ALS can be differentiated into motor neurons," *Science*, vol. 321, no. 5893, pp. 1218–1221, 2008.

[20] H. E. Wheeler, C. Wing, S. M. Delaney, M. Komatsu, and M. E. Dolan, "Modeling chemotherapeutic neurotoxicity with human induced pluripotent stem cell-derived neuronal cells," *PLoS ONE*, vol. 10, no. 2, Article ID e0118020, 2015.

[21] E. Binello and I. M. Germano, "Stem cells as therapeutic vehicles for the treatment of high-grade gliomas," *Neuro-Oncology*, vol. 14, no. 3, pp. 256–265, 2012.

[22] M. Nakamura and H. Okano, "Cell transplantation therapies for spinal cord injury focusing on induced pluripotent stem cells," *Cell Research*, vol. 23, no. 1, pp. 70–80, 2013.

[23] M. Nakamura, O. Tsuji, S. Nori, Y. Toyama, and H. Okano, "Cell transplantation for spinal cord injury focusing on iPSCs," *Expert Opinion on Biological Therapy*, vol. 12, no. 7, pp. 811–821, 2012.

[24] J. Jang, H.-C. Kang, H.-S. Kim et al., "Induced pluripotent stem cell models from X-linked adrenoleukodystrophy patients," *Annals of Neurology*, vol. 70, no. 3, pp. 402–409, 2011.

[25] C. R. Muratore, H. C. Rice, P. Srikanth et al., "The familial Alzheimer's disease APPV717I mutation alters APP processing and Tau expression in iPSC-derived neurons," *Human Molecular Genetics*, vol. 23, no. 13, pp. 3523–3536, 2014.

[26] J. A. Kaye and S. Finkbeiner, "Modeling Huntington's disease with induced pluripotent stem cells," *Molecular and Cellular Neuroscience*, vol. 56, pp. 50–64, 2013.

[27] G. Lee, E. P. Papapetrou, H. Kim et al., "Modelling pathogenesis and treatment of familial dysautonomia using patient-specific iPSCs," *Nature*, vol. 461, no. 7262, pp. 402–406, 2009.

[28] M. C. N. Marchetto, C. Carromeu, A. Acab et al., "A model for neural development and treatment of rett syndrome using human induced pluripotent stem cells," *Cell*, vol. 143, no. 4, pp. 527–539, 2010.

[29] E. Frattini, M. Ruggieri, S. Salani et al., "Pluripotent stem cell-based models of spinal muscular atrophy," *Molecular and Cellular Neuroscience*, vol. 64, pp. 44–50, 2015.

[30] P. Koch, P. Breuer, M. Peitz et al., "Excitation-induced ataxin-3 aggregation in neurons from patients with Machado-Joseph disease," *Nature*, vol. 480, no. 7378, pp. 543–546, 2011.

[31] V. Hook, K. J. Brennand, Y. Kim et al., "Human iPSC neurons display activity-dependent neurotransmitter secretion: Aberrant catecholamine levels in schizophrenia neurons," *Stem Cell Reports*, vol. 3, no. 4, pp. 531–538, 2014.

[32] C. Takenaka, N. Nishishita, N. Takada, L. M. Jakt, and S. Kawamata, "Effective generation of iPS cells from $CD34^+$ cord blood cells by inhibition of p53," *Experimental Hematology*, vol. 38, no. 2, pp. 154–162, 2010.

[33] A. Haase, R. Olmer, K. Schwanke et al., "Generation of induced pluripotent stem cells from human cord blood," *Cell Stem Cell*, vol. 5, no. 4, pp. 434–441, 2009.

[34] Y.-H. Loh, O. Hartung, H. Li et al., "Reprogramming of T cells from human peripheral blood," *Cell Stem Cell*, vol. 7, no. 1, pp. 15–19, 2010.

[35] N. Sun, N. J. Panetta, D. M. Gupta et al., "Feeder-free derivation of induced pluripotent stem cells from adult human adipose stem cells," *Proceedings of the National Academy of Sciences of the United States of America*, vol. 106, no. 37, pp. 15720–15725, 2009.

[36] J. B. Kim, B. Greber, M. J. Araúzo-Bravo et al., "Direct reprogramming of human neural stem cells by OCT4," *Nature*, vol. 461, no. 7264, pp. 649–653, 2009.

[37] T. Aasen, A. Raya, M. J. Barrero et al., "Efficient and rapid generation of induced pluripotent stem cells from human keratinocytes," *Nature Biotechnology*, vol. 26, no. 11, pp. 1276–1284, 2008.

[38] M. Nakagawa, Y. Taniguchi, S. Senda et al., "A novel efficient feeder-free culture system for the derivation of human induced pluripotent stem cells," *Scientific Reports*, vol. 4, Article ID 03594, 2014.

[39] K.-I. Lee, H.-T. Kim, and D.-Y. Hwang, "Footprint- and xeno-free human iPSCs derived from urine cells using extracellular matrix-based culture conditions," *Biomaterials*, vol. 35, no. 29, pp. 8330–8338, 2014.

[40] M. Stadtfeld, N. Maherali, D. T. Breault, and K. Hochedlinger, "Defining molecular cornerstones during fibroblast to iPS cell reprogramming in mouse," *Cell Stem Cell*, vol. 2, no. 3, pp. 230–240, 2008.

[41] K. D. Wilson, S. Venkatasubrahmanyam, F. Jia, N. Sun, A. J. Butte, and J. C. Wu, "MicroRNA profiling of human-induced pluripotent stem cells," *Stem Cells and Development*, vol. 18, no. 5, pp. 749–757, 2009.

[42] K. Si-Tayeb, F. K. Noto, A. Sepac et al., "Generation of human induced pluripotent stem cells by simple transient transfection of plasmid DNA encoding reprogramming factors," *BMC Developmental Biology*, vol. 10, article 81, 2010.

[43] B. A. Tucker, K. R. Anfinson, R. F. Mullins, E. M. Stone, and M. J. Young, "Use of a synthetic xeno-free culture substrate for induced pluripotent stem cell induction and retinal differentiation," *Stem Cells Translational Medicine*, vol. 2, no. 1, pp. 16–24, 2013.

[44] J. Yu, M. A. Vodyanik, K. Smuga-Otto et al., "Induced pluripotent stem cell lines derived from human somatic cells," *Science*, vol. 318, no. 5858, pp. 1917–1920, 2007.

[45] L. Warren and J. Wang, "UNIT 4A.6 Feeder-free reprogramming of human fibroblasts with messenger RNA," in *Current Protocols in Stem Cell Biology*, pp. 13–27, John Wiley & Sons, 2013.

[46] C. C. MacArthur, A. Fontes, N. Ravinder et al., "Generation of human-induced pluripotent stem cells by a nonintegrating RNA Sendai virus vector in feeder-free or xeno-free conditions," *Stem Cells International*, vol. 2012, Article ID 564612, 9 pages, 2012.

[47] P. K. Mandal and D. J. Rossi, "Reprogramming human fibroblasts to pluripotency using modified mRNA," *Nature Protocols*, vol. 8, no. 3, pp. 568–582, 2013.

[48] V. F. I. Van Tendeloo, P. Ponsaerts, F. Lardon et al., "Highly efficient gene delivery by mRNA electroporation in human hematopoietic cells: superiority to lipofection and passive pulsing of mRNA and to electroporation of plasmid cDNA for tumor antigen loading of dendritic cells," *Blood*, vol. 98, no. 1, pp. 49–56, 2001.

[49] S. Audouy and D. Hoekstra, "Cationic lipid-mediated transfection in vitro and in vivo (review)," *Molecular Membrane Biology*, vol. 18, no. 2, pp. 129–143, 2001.

[50] A. Heiskanen, T. Satomaa, S. Tiitinen et al., "*N*-glycolylneuraminic acid xenoantigen contamination of human embryonic and mesenchymal stem cells is substantially reversible," *Stem Cells*, vol. 25, no. 1, pp. 197–202, 2007.

[51] N. Sun, A. Lee, and J. C. Wu, "Long term non-invasive imaging of embryonic stem cells using reporter genes," *Nature Protocols*, vol. 4, no. 8, pp. 1192–1201, 2009.

[52] H. Fukusumi, T. Shofuda, D. Kanematsu et al., "Feeder-free generation and long-term culture of human induced pluripotent stem cells using pericellular matrix of decidua derived mesenchymal cells," *PLoS ONE*, vol. 8, no. 1, Article ID e55226, 2013.

[53] E. Mormone, S. D'sousa, V. Alexeeva, M. M. Bederson, and I. M. Germano, "'Footprint-free' human induced pluripotent stem cell-derived astrocytes for in vivo cell-based therapy," *Stem Cells and Development*, vol. 23, no. 21, pp. 2626–2636, 2014.

[54] G. Thomalla, J. Sobesky, M. Köhrmann et al., "Two tales: hemorrhagic transformation but not parenchymal hemorrhage after thrombolysis is related to severity and duration of ischemia—MRI study of acute stroke patients treated with intravenous tissue plasminogen activator within 6 hours," *Stroke*, vol. 38, no. 2, pp. 313–318, 2007.

[55] R. H. Andres, N. Horie, W. Slikker et al., "Human neural stem cells enhance structural plasticity and axonal transport in the ischaemic brain," *Brain*, vol. 134, no. 6, pp. 1777–1789, 2011.

[56] K. Jin, L. Xie, X. Mao et al., "Effect of human neural precursor cell transplantation on endogenous neurogenesis after focal cerebral ischemia in the rat," *Brain Research*, vol. 1374, pp. 56–62, 2011.

[57] M. Bacigaluppi, S. Pluchino, L. P. Jametti et al., "Delayed post-ischaemic neuroprotection following systemic neural stem cell transplantation involves multiple mechanisms," *Brain*, vol. 132, no. 8, pp. 2239–2251, 2009.

[58] P. Zhang, J. Li, Y. Liu et al., "Human embryonic neural stem cell transplantation increases subventricular zone cell proliferation and promotes peri-infarct angiogenesis after focal cerebral ischemia," *Neuropathology*, vol. 31, no. 4, pp. 384–391, 2011.

[59] M. Ronaghi, S. Erceg, V. Moreno-Manzano, and M. Stojkovic, "Challenges of stem cell therapy for spinal cord injury: human embryonic stem cells, endogenous neural stem cells, or induced pluripotent stem cells?" *Stem Cells*, vol. 28, no. 1, pp. 93–99, 2010.

[60] O. Tsuji, K. Miura, Y. Okada et al., "Therapeutic potential of appropriately evaluated safe-induced pluripotent stem cells for spinal cord injury," *Proceedings of the National Academy of Sciences of the United States of America*, vol. 107, no. 28, pp. 12704–12709, 2010.

[61] R. D. Hawkins, G. C. Hon, L. K. Lee et al., "Distinct epigenomic landscapes of pluripotent and lineage-committed human cells," *Cell Stem Cell*, vol. 6, no. 5, pp. 479–491, 2010.

[62] S. Nori, O. Tsuji, Y. Okada, Y. Toyama, H. Okano, and M. Nakamura, "Therapeutic potential of induced pluripotent stem cells for spinal cord injury," *Brain and Nerve*, vol. 64, no. 1, pp. 17–27, 2012.

[63] J. Jang, J.-E. Yoo, J.-A. Lee et al., "Disease-specific induced pluripotent stem cells: a platform for human disease modeling and drug discovery," *Experimental and Molecular Medicine*, vol. 44, no. 3, pp. 202–213, 2012.

[64] D. Ito, H. Okano, and N. Suzuki, "Accelerating progress in induced pluripotent stem cell research for neurological diseases," *Annals of Neurology*, vol. 72, no. 2, pp. 167–174, 2012.

[65] R. Benveniste and I. M. Germano, "Evaluation of factors predicting accurate resection of high-grade gliomas by using frameless image-guided stereotactic guidance," *Neurosurgical Focus*, vol. 14, no. 2, article e5, 2003.

[66] R. J. Benveniste, G. Keller, and I. Germano, "Embryonic stem cell-derived astrocytes expressing drug-inducible transgenes: differentiation and transplantion into the mouse brain," *Journal of Neurosurgery*, vol. 103, no. 1, pp. 115–123, 2005.

[67] I. M. Germano, M. Uzzaman, and G. Keller, "Gene delivery by embryonic stem cells for malignant glioma therapy: hype or hope?" *Cancer Biology and Therapy*, vol. 7, no. 9, pp. 1341–1347, 2008.

[68] E. Binello and I. M. Germano, "Targeting glioma stem cells: a novel framework for brain tumors," *Cancer Science*, vol. 102, no. 11, pp. 1958–1966, 2011.

[69] K. Akimoto, K. Kimura, M. Nagano et al., "Umbilical cord blood-derived mesenchymal stem cells inhibit, but adipose tissue-derived mesenchymal stem cells promote, glioblastoma multiforme proliferation," *Stem Cells and Development*, vol. 22, no. 9, pp. 1370–1386, 2013.

[70] L. Emdad, S. L. D'Souza, H. P. Kothari, Z. A. Qadeer, and I. M. Germano, "Efficient differentiation of human embryonic and induced pluripotent stem cells into functional astrocytes," *Stem Cells and Development*, vol. 21, no. 3, pp. 404–410, 2012.

[71] I. M. Germano and E. Binello, "Gene therapy as an adjuvant treatment for malignant gliomas: from bench to bedside," *Journal of Neuro-Oncology*, vol. 93, no. 1, pp. 79–87, 2009.

[72] M. Uzzaman, G. Keller, and I. M. Germano, "In vivo gene delivery by embryonic-stem-cell-derived astrocytes for malignant gliomas," *Neuro-Oncology*, vol. 11, no. 2, pp. 102–108, 2009.

[73] M. Uzzaman, R. J. Benveniste, G. Keller, and I. M. Germano, "Embryonic stem cell-derived astrocytes: a novel gene therapy vector for brain tumors," *Neurosurgical Focus*, vol. 19, no. 3, article E6, 2005.

[74] K. S. Aboody, J. Najbauer, M. Z. Metz et al., "Neural stem cell-mediated enzyme/prodrug therapy for glioma: preclinical studies," *Science Translational Medicine*, vol. 5, no. 184, Article ID 184ra59, 2013.

[75] K. Aboody, "Researchers and the translational reality. Interview with Karen Aboody," *Regenerative Medicine*, vol. 7, no. 6, supplement, pp. 64–66, 2012.

[76] M. Uzzaman, G. Keller, and I. M. Germano, "Enhanced proapoptotic effects of tumor necrosis factor-related apoptosis-inducing ligand on temozolomide-resistant glioma cells," *Journal of Neurosurgery*, vol. 106, no. 4, pp. 646–651, 2007.

[77] K. Karikó, H. Muramatsu, F. A. Welsh et al., "Incorporation of pseudouridine into mRNA yields superior nonimmunogenic vector with increased translational capacity and biological stability," *Molecular Therapy*, vol. 16, no. 11, pp. 1833–1840, 2008.

[78] Z. Waibler, M. Anzaghe, T. Frenz et al., "Vaccinia virus-mediated inhibition of type I interferon responses is a multifactorial process involving the soluble type I interferon receptor B18 and intracellular components," *Journal of Virology*, vol. 83, no. 4, pp. 1563–1571, 2009.

[79] N. Malik and M. S. Rao, "A review of the methods for human iPSC derivation," *Methods in Molecular Biology*, vol. 997, pp. 23–33, 2013.

[80] M. J. Jenkins and S. S. Farid, "Human pluripotent stem cell-derived products: advances towards robust, scalable and cost-effective manufacturing strategies," *Biotechnology Journal*, vol. 10, no. 1, pp. 83–95, 2015.

[81] H. Inoue, N. Nagata, H. Kurokawa, and S. Yamanaka, "IPS cells: a game changer for future medicine," *The EMBO Journal*, vol. 33, no. 5, pp. 409–417, 2014.

Hindawi Publishing Corporation
Stem Cells International
Volume 2016, Article ID 9176357, 11 pages
http://dx.doi.org/10.1155/2016/9176357

Review Article

Spheroid Culture of Mesenchymal Stem Cells

Zoe Cesarz[1] and Kenichi Tamama[1,2]

[1]*Department of Pathology, University of Pittsburgh School of Medicine, Pittsburgh, PA 15261, USA*
[2]*McGowan Institute for Regenerative Medicine, University of Pittsburgh, Pittsburgh, PA 15219, USA*

Correspondence should be addressed to Kenichi Tamama; tamamakj@upmc.edu

Received 19 February 2015; Accepted 3 April 2015

Academic Editor: Ren-Ke Li

Compared with traditional 2D adherent cell culture, 3D spheroidal cell aggregates, or spheroids, are regarded as more physiological, and this technique has been exploited in the field of oncology, stem cell biology, and tissue engineering. Mesenchymal stem cells (MSCs) cultured in spheroids have enhanced anti-inflammatory, angiogenic, and tissue reparative/regenerative effects with improved cell survival after transplantation. Cytoskeletal reorganization and drastic changes in cell morphology in MSC spheroids indicate a major difference in mechanophysical properties compared with 2D culture. Enhanced multidifferentiation potential, upregulated expression of pluripotency marker genes, and delayed replicative senescence indicate enhanced stemness in MSC spheroids. Furthermore, spheroid formation causes drastic changes in the gene expression profile of MSC in microarray analyses. In spite of these significant changes, underlying molecular mechanisms and signaling pathways triggering and sustaining these changes are largely unknown.

1. Introduction

Multipotential stromal cells or mesenchymal stem cells (MSCs), originally isolated as single cell suspensions of bone marrow colonies of fibroblast-like cells adhering to plastic, carry multilineage differentiation potentials *in vitro* and *in vivo* after transplantation [1–6]. MSCs are relatively easy to obtain and to expand *in vitro* [7, 8].

Traditionally, two-dimensional (2D) adherent culture conditions have been used as a standard technique for *in vitro* expansion of MSCs. On the other hand, *in vitro* culture of multicellular aggregates was originally described for embryonic cells 70 years ago. Because of their spherical shape, these multicellular aggregates are now called multicellular spheroids, or spheroids. Spheroids have been utilized in the field of oncology [9, 10], stem cell biology [11–14], and tissue engineering [15, 16]. In this review, we will discuss an overview of spheroids and their significance in MSC biology.

2. Spheroids as Three-Dimensional (3D) Culture

2D cell culture is an easy and traditional culture condition; however, it is a highly artificial and less physiological environment, as some *in vivo* characteristics and traits are lost or compromised. In contrast, 3D cell culture is regarded as more physiological with these traits better preserved [10].

2.1. Spheroid Formation Techniques In Vitro. In the regular cell culture condition, anchorage dependent cells, including MSCs, in suspension will fall on the plastic surface by gravity and establish the cell adhesion to the plastic (strictly speaking, to the extracellular matrix (ECM) molecules such as fibronectin adsorbed on the plastic surface of cell culture plates and dishes via cell surface integrins) [17, 18]. In order to allow cells to form aggregates in suspension, these cells need to be cultured in a condition which does not allow them to adhere to a solid surface. Historically, the spinner flask method and the liquid overlay method had been used to facilitate cell aggregation [9]. The spinner flask method uses constant agitation of high density cell suspension to minimize cellular attachment to the solid surface and to maximize cell to cell contact, while the liquid overlay technique uses agar to prevent attachment. Early spinner flask and liquid overlay techniques result in a heterogeneous population of spheroids.

Later methods have improved upon the spinner flask and liquid overlay techniques to generate a more homogeneous population of spheroids. 96-well plates are now commercially available with low attachment surfaces for single spheroid production per well (e.g., 96 Well Ultra-Low Attachment Spheroid Plate from Corning in Corning, NY, or 3D-culture NanoCulture plate from Scivax in Tokyo, Japan); thus, spheroid size is determined by the number of cells in each well [19]. Another widely used technique for spheroid formation is the hanging drop method, which eliminates surface attachment by placing the cell suspension in a drop, allowing gravity to facilitate cellular aggregation at the bottom of the drop [20]. These cells spontaneously attach to each other to form cell aggregates if the possibility of surface attachment is abolished [20]. Another recent spheroid formation technique involves the use of chitosan membranes to initiate the 2D to 3D transition. Chitosan is a deacetylated derivative of a natural polysaccharide, chitin, and is often paired with another glycosaminoglycan, hyaluronan, known to have an impact on cell migration, proliferation, and matrix secretion [21, 22].

2.2. Spheroid Formation In Vitro. The formation process of multicellular spheroidal aggregates in low attachment conditions starts with the initial loose cell aggregate formation through integrin-ECM binding followed by the spheroid compaction through enhanced cell to cell connection via homophilic cadherin binding [15, 23, 24]. The formation of MSC spheroids was shown to be dependent on cadherins [25, 26] and the spheroid compaction was shown to rely on the actomyosin cytoskeleton [24]. Moreover, MSCs with intact endogenous ECM preserved by thermal lifting accelerate the initial cell aggregation process, as compared with trypsinized MSCs with degraded ECM [27]. Interestingly, the assembly process of MSC spheroids on the chitosan membrane is quite different from that in suspension or on nonadherent polymer surfaces. Rather than the self-aggregation present in other methods, MSCs attach and spread on chitosan membranes first and then retract their pseudopodia to form multicellular spheroids [21, 28].

2.3. Spheroid Culture in Oncology. Spheroidal cell culture has been used extensively in the field of oncology [9], as spheroidal cell culture exhibits both histological and physiological features similar to those of solid tumors in the body. Volume growth kinetics and spatial variation are better reproduced in 3D than in 2D culture [29–33]. Tumor spheroids synthesize ECM similar to original tumors *in vivo*, where the capacity for ECM production is reduced in the same cells in 2D culture conditions [34, 35]. The response of cancer cells to therapeutic interventions *in vivo* is better reproduced in *in vitro* spheroidal culture than in 2D adherent culture [29, 36–39]. In evaluating the efficacy of radiation therapy, spheroid culture of cancer cells produces a more comparable response to cells *in vivo* than cancer cells in 2D culture [9]. Additionally, tumor spheroids might possibly mimic circulating tumor cell aggregates [40–42].

2.4. Spheroid Culture in Stem Cell Biology. Spheroidal cell culture with pluripotent stem cells (PSCs), including embryonic stem cells (ESCs), is specifically called embryoid body [43–45]. Utilization of embryoid bodies is a standard protocol to produce specific cell lineages of interest *in vitro*, as the intercellular interactions of embryonic cells occurring during embryogenesis are recapitulated in the 3D culture setting [14]. Similarly, spheroidal cell culture of neural stem cells (NSCs), or neurospheres, has been used routinely for NSC isolation from embryonic and adult tissues and *in vitro* expansion and differentiation of NSCs into neurons, oligodendrocytes, and astrocytes [46, 47].

Differentiation capability and potential of stem and progenitor cells are generally enhanced in the 3D culture setting. For example, salivary gland-derived progenitor cells can differentiate into hepatocytic and pancreatic islet cell lineages, but these differentiations only take place when the cells are cultured in 3D cell aggregates, not in 2D monolayer [48]. Neuronal differentiation of ESCs is enhanced in embryoid body culture compared to 2D monolayer cell culture [49]. Moreover, *in vitro* reproduction of complex organ architecture, such as the optic cup, is made possible only in 3D culture, in which the inherent tissue self-organization capability of ESCs is maximized [11, 12].

2.5. Limitations in Spheroid Culture. There are some possible limitations known in the 3D spheroid culture technique. Because of the spheroidal structure, diffusion of nutrients, oxygen, and waste through the interior of the spheroids is compromised in a size-dependent manner [9, 10, 24]. Presence of these "stressors" can contribute to the characteristic gene expression profile of MSC spheroids; however, it can also compromise viability of the cells in the spheroid core, especially in harsh conditions [24] (see Section 3.4.5 and Section 4). Spinner flask techniques maximize the nutrient, oxygen, and waste diffusion through the spheroid, enabling larger spheroid culture and improving cell survival *in vitro* [9, 10, 24].

3. Significance of MSC Spheroids in Stem Cell Biology

3.1. Morphology and Mechanophysical Properties of MSC Spheroids. MSCs cultured in spheroids are spherical inside and elongated outside with an overall reduction of cytoskeletal molecules and ECM. The size of MSCs in spheroids is drastically smaller than cells in 2D monolayer, resulting in 75% reduction in individual cell volume [24, 50–52]. Cellular morphology is a key characteristic used to determine cellular phenotypes and fates of MSCs [53]. Small, rounded MSCs are prone to differentiate into an adipogenic lineage, whereas large, extended MSCs are prone to differentiate into an osteogenic lineage in both 2D and 3D culture system [54, 55]. Moreover, these differentiation preferences in MSC spheroids can be altered by myosin II inhibitor blebbistatin or constitutively active Rho kinase treatments, indicating the pivotal role of actomyosin cytoskeleton and myosin-generated mechanical tension in these processes [55].

Another major difference between 2D monolayer culture and 3D spheroid culture is Young's elasticity modulus of the materials surrounding the cells, which should also affect cell differentiation [56, 57]. The cells in 2D regular monolayer reside on plastic with an elasticity modulus in the gigapascal (GPa) range, whereas cells in 3D spheroids should be surrounded by the cells and ECM with a combined elasticity modulus of less than 0.1 kPa [52]. The biological significance of the elasticity modulus has only been addressed in 2D monolayer culture [56, 57], and it should also contribute to the altered gene expression and cell phenotype in 3D spheroids. All of these data indicate the clear difference in mechanophysical properties between spheroidal MSCs and MSCs in 2D monolayer culture on plastic [13].

3.2. Gene Expression Changes in MSC Spheroids. Microarray analysis showed a drastic change in the gene expression profile in the MSC spheroid culture when compared with MSCs in 2D monolayer culture with upregulation of 1,731 genes and downregulation of 1,387 genes [58]. The upregulated genes are associated with hypoxia, angiogenesis, inflammation, stress response, and redox signaling, including angiopoietin 2 (*ANGPT2*), bone morphogenetic protein 2 (*BMP2*), chemokine (C-X-C motif) receptor 4 (*CXCR4*), heme oxygenase 1 (*HMOX1*), interleukin 1α (*IL1A*), interleukin 1β (*IL1B*), interleukin 6 (*IL6*), interleukin 8 (*IL8*), interleukin 11 (*IL11*), interleukin 24 (*IL24*), leukemia inhibitory factor (*LIF*), prostaglandin-endoperoxide synthase 2/cyclooxygenase 2 (*PTGS2/COX2*), tumor necrosis factor α-induced protein 6/tumor necrosis factor α stimulated gene/protein 6 (*TNFAIP6/TSG6*), transforming growth factor-β3 (*TGFB3*), and vascular endothelial growth factor-A (*VEGFA*) [28, 50, 58–60]. Moreover, stronger induction of gene expression of key genes of interest, such as *BMP2*, *LIF*, *PTGS2/COX2*, and *TGFB3*, is observed in MSC spheroids formed on chitosan membranes than the ones formed on a nonadherent surface [28]. The molecular mechanisms responsible for the altered gene expression profiles in MSC spheroids are largely unknown (see below).

Quantitative reverse transcription- (qRT-) PCR is the major method for quantitative analysis of targeted gene expression in current cell biology research. As discussed earlier, gene expression of cytoskeletal molecules including β-actin (*ACTB*) is largely reduced in MSC spheroids [28, 50]. *ACTB* is frequently used as an endogenous normalizer in gene expression analysis; therefore, utilization of *ACTB* as an endogenous normalizer could lead to possible overinterpretation of upregulated genes in 3D MSC spheroids and thus data analysis and interpretation of gene expression need caution.

3.3. In Vivo Counterpart of MSC Spheroids. As discussed earlier, tumor spheroids are an *in vitro* imitation of the original tumors *in vivo*, whereas embryoid bodies are an *in vitro* imitation of the inner cell mass in blastocysts. However, an *in vivo* counterpart of MSC spheroids is not immediately clear. Intravenously administered single cell suspension MSCs form cell aggregates and are trapped as emboli in lung. These cells could possibly cause harmful effects to the recipients through MSC-derived pulmonary emboli, especially if a massive dose of MSCs is transplanted intravenously [61], but at the same time these cells also express *TNFAIP6/TSG6* very strongly, similar to MSC spheroids, exerting strong anti-inflammatory effects [50, 62]. Endogenous MSCs reside as a subfraction of pericytes surrounding the vasculature [63–68]. Pericytes in noninjured tissues are not activated, whereas cultured MSCs are counterparts of activated pericytes found in repairing and regenerating tissues, such as granulation tissues [69]. Granulation tissues are comprised of loose cellular aggregates, including pericytes embedded within provisional ECM, although compact spheroidal cell aggregates are not typically observed in granulation tissues [70].

3.4. Clinical Significance. MSC-based therapeutics is a promising approach in the field of autoimmune diseases, regenerative medicine, and tissue engineering. However, the beneficial effects of MSC-based therapeutics in initial small scale clinical studies are often not substantiated by large randomized-controlled clinical trials, strongly indicating the urgent need of further optimization of cell-based therapy [71–73]. There are various approaches to improve the efficacy of MSC-based therapeutics, and MSC preparation as spheroids represents one method of optimization. Spheroid formation has been shown to enhance anti-inflammatory effects, augment tissue regenerative and reparative effects with enhanced angiogenesis, facilitate differentiation potentials of multiple lineages, increase posttransplant survival of MSCs, improve MSC stemness, and delay *in vitro* replicative senescent processes, as discussed in detail below (Figure 1).

3.4.1. Enhanced Anti-Inflammatory Effects. MSCs exert strong anti-inflammatory or immunomodulatory effects and MSC-based therapeutics is regarded as promising approaches against immune-mediated diseases, such as graft versus host disease. Multiple molecules, such as indoleamine dioxygenase-1 (IDO1) or prostaglandin E_2 (PGE_2), have been identified to mediate MSCs' strong anti-inflammatory effects [71, 74–77]. Recently, MSC spheroids were shown to exert strong anti-inflammatory effects, presumably through upregulated TNFAIP6/TSG6 produced by MSC spheroids [50]. In this study, MSC spheroids reduced macrophage activation in a coculture system *in vitro* or mitigated zymosan-induced inflammation in a mouse zymosan-induced peritonitis model. PGE_2 is another molecule strongly upregulated in MSC spheroids [78].

Interestingly, strong upregulation of these mediators in MSC spheroids is observed when MSC spheroids are cultured in the regular cell culture medium (i.e., alpha MEM supplemented with FBS), but this upregulation is largely abolished if the MSC spheroids are cultured in the serum and animal component-free chemically defined medium (MesenCult-XF Medium, STEMCELL Technologies, Vancouver, Canada) [19]. The apparent reason for this difference is unknown, but this result clearly indicates the presence of unknown factors in serum pivotal for the upregulation of immunomodulatory mediators in MSC spheroids. Xeno-free chemically defined

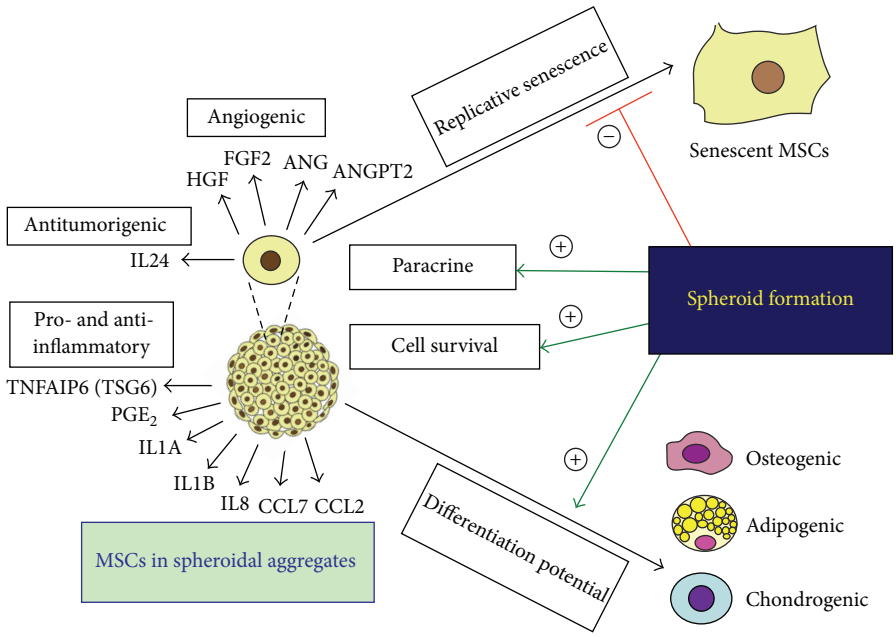

Figure 1: Clinical significance of MSC spheroids. Formation of spheroidal aggregates (1) enhances paracrine secretion of angiogenic, antitumorigenic, and pro- and anti-inflammatory factors, (2) improves cell survival, (3) increases differentiation potentials, and (4) delays replicative senescence of MSCs (ANG: angiogenin; ANGPT2: angiopoietin 2; CCL2: chemokine (C-C motif) ligand 2; CCL7: chemokine (C-C motif) ligand 7; FGF2: fibroblast growth factor 2; HGF: hepatocyte growth factor; IL1A: interleukin 1α; IL1B: interleukin 1β; IL8: interleukin 8; IL24: interleukin 24; PGE_2: prostaglandin E_2; TNFAIP6 (TSG6): tumor necrosis factor α-induced protein 6 (tumor necrosis factor α stimulated gene/protein 6); VEGFA: vascular endothelial growth factor-A).

media are ideal for *in vitro* preparation of clinical-grade MSCs [8], but anti-inflammatory or immunomodulatory effects might not be reproduced in MSCs cultured in chemically defined media [19, 79], indicating the importance in learning the underlying molecular mechanisms of MSCs' strong immunoregulatory properties.

As seen above, spheroidal formation upregulates proinflammatory cytokines (such as IL1A, IL1B, and IL8) and chemokines (such as chemokine (C-C motif) ligand 2 (CCL2) and chemokine (C-C motif) ligand 7 (CCL7)) that recruit inflammatory cells, indicating possible proinflammatory properties of MSCs [23, 28, 50, 58]. MSCs are required to be primed with proinflammatory cytokines to acquire anti-inflammatory properties [71, 74, 80], and MSCs in spheroids are self-stimulated by autocrined IL1 signaling to have enhanced anti-inflammatory effects [23]. In other words, MSC spheroids use autocrined proinflammatory cytokines as molecular switches of their anti-inflammatory properties. But at the same time it is also possible that these proinflammatory cytokines produced by MSC spheroids directly contribute to the inflammatory response of the host, though this possibility has not been shown experimentally. Moreover, recent studies have shown that MSCs promote recruitment of inflammatory cells. This can be interpreted as proinflammatory effects of MSCs [81–83], but it is also shown to be required for MSC-mediated anti-inflammatory effects [84]. Thus, underlying molecular mechanisms of MSC-mediated anti-inflammatory and possibly proinflammatory effects are very complicated. Further studies are required to address the possible proinflammatory roles of these proinflammatory cytokines and chemokines strongly produced by MSC spheroids, as these proinflammatory cytokines or chemokines could directly enhance inflammation around the MSC spheroids in certain situations.

3.4.2. Enhanced Angiogenic and Tissue Reparative/Regenerative Effects. Tissue repair and regeneration are an essential biological function for humans. In this complex biological process, numerous types of cells and bioactive mediators are regulated in a temporary and spatially sophisticated manner. The normal repair process of adult tissues, represented with skin in this case, takes place in three phases: inflammation, new tissue formation, and remodeling. *Inflammation* is an initial body's adaptive response to tissue damage, comprised of hemostasis and recruitment of inflammatory cells. The *new tissue formation* phase involves cellular proliferation and migration of various cells, such as endothelial cells or fibroblasts, and ECM production by these cells to form granulation tissues. New blood vessel formation or angiogenesis provides conduits of cellular and nutritional supports to the granulation tissues. The *remodeling* phase involves termination of the active repair process, reduction of these cells by emigration or apoptosis, and wound contraction by myofibroblasts to leave fibrous scar tissues consisting of disorganized ECM deposits in the end [85]. Contrary to adult wound healing, scar formation does not happen in

mammalian early fetuses (before day 16 of mice), which retain tissue regenerative capacity. The major difference in the tissue repair process between fetuses and adults lies in the inflammation phase, which does not take place in the tissue repair of early fetuses. Consistently, scar formation is reduced by inhibiting inflammation [86].

Gene expression of various growth factors and cytokines, including angiogenin (*ANG*), *ANGPT2*, fibroblast growth factor 2 (*FGF2*), hepatocyte growth factor (*HGF*), and *VEGFA*, is upregulated in MSC spheroids [28, 58, 59]. ANGPT2 activates endothelial cells and exerts a strong angiogenic response in the presence of VEGFA [87, 88]. FGF2 and HGF are also angiogenic molecules [89–91]. Thus, it is logical to speculate that MSC spheroids are more tissue reparative through their stronger angiogenic effects than MSCs cultured in monolayer, and it was indeed shown in various animal models [26, 51, 92–96].

HGF-mediated antifibrotic effects have been reported for MSCs [97]. Moreover, TGFB3 has been shown to be a key mediator for scar-free skin repair or skin regeneration [86]. Both HGF and TGFB3 are upregulated in MSC spheroids [28] and thus MSC spheroids might have stronger antifibrotic or even tissue regenerative effects than MSCs cultured in monolayer.

3.4.3. Enhanced Stemness and Delayed Replicative Senescence. A key feature of MSCs is their multilineage differentiation potentials, which have drawn attention in the field of regenerative medicine [1–6]. Initially, MSC spheroids or pellets were solely utilized for their chondrogenic differentiation capacity [98–100]. It was subsequently realized that differentiation potentials of MSC spheroids are enhanced not only to the chondrogenic lineage, but also to other lineages [21, 28, 60, 101–104].

Another interesting feature of MSC spheroids is that spheroidal formation prolongs replicative lifespan or delays cell senescence of MSCs *in vitro* [95]. This study also shows the increased gene expression of pluripotency marker genes (*NANOG*, *SOX2*, and *POU5F1/OCT4*) in MSC spheroids, consistent with previous studies [21, 102]. However, the degree of pluripotency gene upregulation is relatively weak in these studies and the role of OCT4 in adult stem cells has been questioned [105, 106]. Thus, interpretation of the roles of upregulated pluripotency marker genes in MSC spheroids needs caution.

Enhanced multilineage differentiation potentials, delayed cell senescent processes, and upregulation of pluripotency marker genes are indicative of enhanced stemness in MSC spheroids. This concept is supported by colony formation assays, which measure the proportion of early progenitors in culture [107]. Colony formation capability is increased with MSC suspension derived from spheroids as compared with that from MSCs cultured in monolayer, further indicating enhanced stemness in MSC spheroids [108]. MSC spheroids derived from thermally lifted cells have enhanced differentiation and colony formation potential, as compared with MSC spheroids from trypsinized MSCs, indicating the pivotal role of intact ECM for stemness preservation of MSC spheroids [27].

Although ease of *in vitro* preparation is a great strength of MSC-based therapeutics [5, 7, 8, 109], *in vitro* MSC expansion leads to replicative cell senescence, loss of differentiation potentials, and reduced paracrine capability so that organ protective effects become compromised [110–115]. *In vitro* preservation of MSC stemness is one of the clinical significant aspects of MSC spheroids.

3.4.4. Possible Enhancement of Antitumorigenic Effects. IL24 is a multifunctional cancer killing cytokine [116–118] that is a strongly upregulated gene in MSC spheroids [28, 50, 60]. Interestingly, MSC spheroids were shown to selectively reduce the viability of cancer cell lines but not that of noncancer-derived immortalized cell lines in an IL24-dependent mechanism, suggesting that MSC spheroids might be utilized in novel cancer therapeutics [60]. As seen earlier, MSC spheroids have enhanced production of growth factors and cytokines including mitogens [28, 50, 58–60]. Indeed MSCs have been shown to have protumorigenic effects by secreting growth factors and cytokines and directly contributing to tumor stroma, in addition to their antitumorigenic effects [119]. Moreover, transformation of MSCs themselves is another potential concern [120]. The concern might be more legitimate with MSC spheroids, as stemness of these cells is enhanced (see above). Overall, it appears that pro- or antitumorigenic effects of MSCs are largely context-dependent. Thus, it is very attractive to hypothesize MSC spheroids as novel therapeutics for certain cancers, but more rigorous studies are needed to address this hypothesis.

3.4.5. Improved Cell Survival after Transplantation. One of the factors limiting the efficacies of MSC therapeutics is posttransplant cell survival [8, 121]. An early study showed that >99% of MSCs transplanted to the uninjured heart are cleared within 4 days after cell injection [122], whereas another study showed that >85% of systematically injected MSCs are entrapped and lost in precapillaries [123]. Even though MSCs exert tissue reparative and regenerative effects presumably through a brief "hit and run" mechanism and thus long-term engraftment might not be a prerequisite for the tissue reparative and regenerative effects of MSCs [76, 124], initial survival of transplanted MSCs should nevertheless be a critical factor defining the overall efficacy of MSC-based therapeutics. MSC spheroids have been shown to have improved survival *in vivo* compared to single cell suspensions of MSCs [93], even though MSC spheroids are shown to have less survival advantage than MSCs in 2D regular condition *in vitro* [24] (see Section 2.5 and Section 4). Additionally, the antiapoptotic molecule Bcl-2 is upregulated while the proapoptotic molecule, Bax, is downregulated resulting in an overall prosurvival molecular profile in spheroidal cells [93]. Improved survival of posttransplanted MSCs contributes to the enhanced therapeutic efficacy of MSC spheroids *in vivo*.

4. Key Molecular Signals and Events in MSC Spheroids

Despite the promising potential that MSC spheroids have in regenerative medicine and autoimmune diseases, there is

limited research on the underlying molecular mechanisms and signaling pathways which initiate and mediate these drastic differences in the gene expression profile and phenotype of MSC spheroids.

Oxygen reaches the inside of spheroids through diffusion, which makes the internal core of spheroids hypoxic [9, 13, 15]. Consistently, hypoxia-associated genes, such as *VEGFA*, are overrepresented among the upregulated genes in MSC spheroids in the microarray analysis [28, 58]. Hypoxia inducible factor (HIF) is a master transcription factor that regulates expression of hypoxia-associated genes [125]. MSCs express HIF-2α in addition to ubiquitous HIF-1α [126], and we showed that HIF-1α and HIF-2α have a limited but important role in MSC self-renewal and production of growth factors and cytokines in hypoxia [127]. HIF-2α is also identified as one of the stemness genes in human MSCs [128]. Protein expression of both HIF-1α and HIF-2α is observed in MSC spheroids [51], and, thus, both HIF-1α and HIF-2α should serve as key transcription factors in MSC spheroids.

The self-aggregation process of MSCs initiates caspase-dependent IL1 autocrine signaling. We have previously shown that one of the signaling molecules upregulated by IL1 is early growth response gene-2 (EGR2), a zinc finger transcription factor that regulates PGE_2 levels through regulation of *PTGS2/COX2* gene expression in MSCs [7, 129]. *EGR2* expression is upregulated in MSC spheroids [28], presumably in response to autocrined IL1 stimulation [7, 129], and the enhanced anti-inflammatory properties of MSC spheroids should be attributable to upregulated *EGR2*, at least partly.

The IL1 autocrine signaling subsequently upregulates chemokine receptors, such as CXCR4, or immunomodulatory mediators, such as TNFAIP6/TSG6, IL6, and PGE_2 [23, 24]. Interestingly, spheroidal formation coincides with reduced mitochondrial membrane potential and ATP production, indicating the ongoing apoptosis process in MSCs in spheroidal aggregates [24]. Apoptotic cells are shown to process and release IL1 [130]. Furthermore, MSCs in spheroidal aggregates are shown to have higher fluorescent calcium uptake than MSCs in 2D culture [25], and intracellular calcium overload is regarded as apoptogenic [131–133]. Thus, the apoptotic process seems to trigger the IL1 autocrine signaling and induce the stress response in MSC spheroids [24]. However, it cannot reconcile well with their improved cell survival *in vivo* [93]. One possible explanation is quick disassembly of MSC spheroids after transplantation eliminating compromised oxygen and nutrient access to the interior of spheroids as a factor (see Section 2.5). In fact, disassembled MSCs from MSC spheroids have a survival advantage over MSCs cultured on regular 2D condition *in vitro*, supporting such an explanation [24, 95].

Even though a glimpse of key signaling pathways has been revealed, more studies of crucial molecular events and signaling need to be conducted. For example, the signaling pathways connecting the initial self-aggregation process and the apoptotic process are still unknown. Moreover, the upstream signaling events causing such a drastic change in the gene expression profiles in MSC spheroids [28, 50, 58–60] are largely unclear. As discussed earlier, the alteration in mechanophysical properties might be such a significant event in MSC spheroids [13], but it requires experimental validation.

Epigenetics is defined as an inheritable change in gene expression through DNA methylation, noncoding RNAs, and histone modification, without altering the DNA sequence itself [134–136]. It causes drastic changes in gene expression profiles, as best exemplified in the fertilization process and the somatic cell reprogramming process during the development of induced pluripotent stem cells (iPSCs) [137]. Indeed, MSC spheroids were shown to acquire epigenetic changes. In this study, histone H3 lysine 9 acetylation (H3K9ac), which favors transcriptional activation [138], increases in promoter regions of *NANOG*, *SOX2*, and *POU5F1/OCT4* and telomerase reverse transcriptase (*TERT*) in MSC spheroids, as compared with MSCs cultured in monolayer. Thus, epigenetic regulation appears to be one of the underlying molecular mechanisms causing the drastic change in the gene expression profile in MSC spheroids.

5. Epilogue

MSCs have shown promise in the field of regenerative medicine and 3D MSC culture further enhances such characteristics. Microarray analysis has shown a drastic change in the gene expression profile between monolayer and spheroid cultured MSCs; however, a critical lack of understanding exists with relation to the molecular signaling mediating the enhanced MSC spheroid properties or the improved cell survival. More mechanistic work is definitely needed at the molecular level to better understand and optimize MSC spheroids for clinical applications.

Conflict of Interests

The authors declare that there is no conflict of interests regarding the publication of this paper.

Acknowledgments

This study was supported by University of Pittsburgh Schools of Health Sciences (Bridge Funding Category One) and University of Pittsburgh Medical Center Health System (Competitive Medical Research Fund) (Kenichi Tamama).

References

[1] A. J. Friedenstein, U. F. Gorskaja, and N. N. Kulagina, "Fibroblast precursors in normal and irradiated mouse hematopoietic organs," *Experimental Hematology*, vol. 4, no. 5, pp. 267–274, 1976.

[2] M. Owen and A. J. Friedenstein, "Stromal stem cells: marrow-derived osteogenic precursors," *Ciba Foundation Symposium*, vol. 136, pp. 42–60, 1988.

[3] M. F. Pittenger, A. M. Mackay, S. C. Beck et al., "Multilineage potential of adult human mesenchymal stem cells," *Science*, vol. 284, no. 5411, pp. 143–147, 1999.

[4] D. J. Prockop, "Marrow stromal cells as stem cells for non-hematopoietic tissues," *Science*, vol. 276, no. 5309, pp. 71–74, 1997.

[5] K. Tamama, V. H. Fan, L. G. Griffith, H. C. Blair, and A. Wells, "Epidermal growth factor as a candidate for ex vivo expansion of bone marrow-derived mesenchymal stem cells," *Stem Cells*, vol. 24, no. 3, pp. 686–695, 2006.

[6] K. Tamama, C. K. Sen, and A. Wells, "Differentiation of bone marrow mesenchymal stem cells into the smooth muscle lineage by blocking ERK/MAPK signaling pathway," *Stem Cells and Development*, vol. 17, no. 5, pp. 897–908, 2008.

[7] K. Tamama and D. J. Barbeau, "Early growth response genes signaling supports strong paracrine capability of mesenchymal stem cells," *Stem Cells International*, vol. 2012, Article ID 428403, 7 pages, 2012.

[8] K. Tamama, H. Kawasaki, and A. Wells, "Epidermal growth factor (EGF) treatment on multipotential stromal cells (MSCs). Possible enhancement of therapeutic potential of MSC," *Journal of Biomedicine and Biotechnology*, vol. 2010, Article ID 795385, 10 pages, 2010.

[9] W. Mueller-Klieser, "Multicellular spheroids—a review on cellular aggregates in cancer research," *Journal of Cancer Research and Clinical Oncology*, vol. 113, no. 2, pp. 101–122, 1987.

[10] W. Mueller-Klieser, "Three-dimensional cell cultures: from molecular mechanisms to clinical applications," *American Journal of Physiology—Cell Physiology*, vol. 273, no. 4, pp. C1109–Cl123, 1997.

[11] Y. Sasai, "Next-generation regenerative medicine: organogenesis from stem cells in 3D culture," *Cell Stem Cell*, vol. 12, no. 5, pp. 520–530, 2013.

[12] Y. Sasai, "Cytosystems dynamics in self-organization of tissue architecture," *Nature*, vol. 493, no. 7432, pp. 318–326, 2013.

[13] S. Sart, A. C. Tsai, Y. Li, and T. Ma, "Three-dimensional aggregates of mesenchymal stem cells: cellular mechanisms, biological properties, and applications," *Tissue Engineering Part B: Reviews*, vol. 20, no. 5, pp. 365–380, 2014.

[14] L. Vallier and R. A. Pedersen, "Human embryonic stem cells: an in vitro model to study mechanisms controlling pluripotency in early mammalian development," *Stem Cell Reviews*, vol. 1, no. 2, pp. 119–130, 2005.

[15] R. Z. Lin and H. Y. Chang, "Recent advances in three-dimensional multicellular spheroid culture for biomedical research," *Biotechnology Journal*, vol. 3, no. 9-10, pp. 1172–1184, 2008.

[16] T.-M. Achilli, J. Meyer, and J. R. Morgan, "Advances in the formation, use and understanding of multi-cellular spheroids," *Expert Opinion on Biological Therapy*, vol. 12, no. 10, pp. 1347–1360, 2012.

[17] F. Grinnell and M. K. Feld, "Adsorption characteristics of plasma fibronectin in relationship to biological activity," *Journal of Biomedical Materials Research*, vol. 15, no. 3, pp. 363–381, 1981.

[18] E. Ruoslahti and M. D. Pierschbacher, "New perspectives in cell adhesion: RGD and integrins," *Science*, vol. 238, no. 4826, pp. 491–497, 1987.

[19] J. A. Zimmermann and T. C. Mcdevitt, "Pre-conditioning mesenchymal stromal cell spheroids for immunomodulatory paracrine factor secretion," *Cytotherapy*, vol. 16, no. 3, pp. 331–345, 2014.

[20] R. Foty, "A simple hanging drop cell culture protocol for generation of 3D spheroids," *Journal of Visualized Experiments*, no. 51, Article ID e2720, 2011.

[21] G.-S. Huang, L.-G. Dai, B. L. Yen, and S.-H. Hsu, "Spheroid formation of mesenchymal stem cells on chitosan and chitosan-hyaluronan membranes," *Biomaterials*, vol. 32, no. 29, pp. 6929–6945, 2011.

[22] S. Schmidt and P. Friedl, "Interstitial cell migration: integrin-dependent and alternative adhesion mechanisms," *Cell and Tissue Research*, vol. 339, no. 1, pp. 83–92, 2010.

[23] T. J. Bartosh, J. H. Ylöstalo, N. Bazhanov, J. Kuhlman, and D. J. Prockop, "Dynamic compaction of human mesenchymal stem/precursor cells into spheres self-activates caspase-dependent il1 signaling to enhance secretion of modulators of inflammation and immunity (PGE2, TSG6, and STC1)," *Stem Cells*, vol. 31, no. 11, pp. 2443–2456, 2013.

[24] A. C. Tsai, Y. Liu, X. Yuan, and T. Ma, "Compaction, fusion, and functional activation of three-dimensional human mesenchymal stem cell aggregate," *Tissue Engineering A*, 2015.

[25] H. Y. Yeh, B. H. Liu, and S. H. Hsu, "The calcium-dependent regulation of spheroid formation and cardiomyogenic differentiation for MSCs on chitosan membranes," *Biomaterials*, vol. 33, no. 35, pp. 8943–8954, 2012.

[26] E. J. Lee, S. J. Park, S. K. Kang et al., "Spherical bullet formation via E-cadherin promotes therapeutic potency of mesenchymal stem cells derived from human umbilical cord blood for myocardial infarction," *Molecular Therapy*, vol. 20, no. 7, pp. 1424–1433, 2012.

[27] J. Kim and T. Ma, "Endogenous extracellular matrices enhance human mesenchymal stem cell aggregate formation and survival," *Biotechnology Progress*, vol. 29, no. 2, pp. 441–451, 2013.

[28] H.-Y. Yeh, B.-H. Liu, M. Sieber, and S.-H. Hsu, "Substrate-dependent gene regulation of self-assembled human MSC spheroids on chitosan membranes," *BMC Genomics*, vol. 15, no. 1, article 10, 2014.

[29] H. Dertinger and C. L. Huhle, "A comparative study of post-irradiation growth kinetics of spheroids and monolayers," *International Journal of Radiation Biology*, vol. 28, no. 3, pp. 255–265, 1975.

[30] R. E. Durand, "Cell cycle kinetics in an in vitro tumor model," *Cell and Tissue Kinetics*, vol. 9, no. 5, pp. 403–412, 1976.

[31] M. Haji-Karim and J. Carlsson, "Proliferation and viability in cellular spheroids of human origin," *Cancer Research*, vol. 38, no. 5, pp. 1457–1464, 1978.

[32] J. M. Yuhas and A. P. Li, "Growth fraction as the major determinant of multicellular tumor spheroid growth rates," *Cancer Research*, vol. 38, no. 6, pp. 1528–1532, 1978.

[33] J. Carlsson, C.-G. Stålnacke, H. Acker, M. Haji-Karim, S. Nilsson, and B. Larsson, "The influence of oxygen on viability and proliferation in cellular spheroids," *International Journal of Radiation Oncology, Biology, Physics*, vol. 5, no. 11-12, pp. 2011–2020, 1979.

[34] J. C. Angello and H. L. Hosick, "Glycosaminoglycan synthesis by mammary tumor spheroids," *Biochemical and Biophysical Research Communications*, vol. 107, no. 3, pp. 1130–1137, 1982.

[35] T. Nederman, B. Norling, B. Glimelius, J. Carlsson, and U. Brunk, "Demonstration of an extracellular matrix in multicellular tumor spheroids," *Cancer Research*, vol. 44, no. 7, pp. 3090–3097, 1984.

[36] R. M. Sutherland, W. R. Inch, J. A. McCredie, and J. Kruuv, "A multi-component radiation survival curve using an in vitro tumour model," *International Journal of Radiation Biology and Related Studies in Physics, Chemistry, and Medicine*, vol. 18, no. 5, pp. 491–495, 1970.

[37] R. E. Durand and R. M. Sutherland, "Effects of intercellular contact on repair of radiation damage," *Experimental Cell Research*, vol. 71, no. 1, pp. 75–80, 1972.

[38] R. E. Durand and R. M. Sutherland, "Dependence of the radiation response of an *in vitro* tumor model on cell cycle effects," *Cancer Research*, vol. 33, no. 2, pp. 213–219, 1973.

[39] R. E. Durand and R. M. Sutherland, "Growth and radiation survival characteristics of V79-171b Chinese hamster cells: a possible influence of intercellular contact," *Radiation Research*, vol. 56, no. 3, pp. 513–527, 1973.

[40] G. Kats-Ugurlu, I. Roodink, M. de Weijert et al., "Circulating tumour tissue fragments in patients with pulmonary metastasis of clear cell renal cell carcinoma," *Journal of Pathology*, vol. 219, no. 3, pp. 287–293, 2009.

[41] E. H. Cho, M. Wendel, M. Luttgen et al., "Characterization of circulating tumor cell aggregates identified in patients with epithelial tumors," *Physical Biology*, vol. 9, no. 1, Article ID 016001, 2012.

[42] V. V. Glinsky, G. V. Glinsky, O. V. Glinskii et al., "Intravascular metastatic cancer cell homotypic aggregation at the sites of primary attachment to the endothelium," *Cancer Research*, vol. 63, no. 13, pp. 3805–3811, 2003.

[43] M. J. Evans and M. H. Kaufman, "Establishment in culture of pluripotential cells from mouse embryos," *Nature*, vol. 292, no. 5819, pp. 154–156, 1981.

[44] G. R. Martin, "Isolation of a pluripotent cell line from early mouse embryos cultured in medium conditioned by teratocarcinoma stem cells," *Proceedings of the National Academy of Sciences of the United States of America*, vol. 78, no. 12, pp. 7634–7638, 1981.

[45] A. Grover, R. G. Oshima, and E. D. Adamson, "Epithelial layer formation in differentiating aggregates of F9 embryonal carcinoma cells," *Journal of Cell Biology*, vol. 96, no. 6, pp. 1690–1696, 1983.

[46] S. Ahmed, "The culture of neural stem cells," *Journal of Cellular Biochemistry*, vol. 106, no. 1, pp. 1–6, 2009.

[47] J. B. Jensen and M. Parmar, "Strengths and limitations of the neurosphere culture system," *Molecular Neurobiology*, vol. 34, no. 3, pp. 153–161, 2006.

[48] K. Okumura, K. Nakamura, Y. Hisatomi et al., "Salivary gland progenitor cells induced by duct ligation differentiate into hepatic and pancreatic lineages," *Hepatology*, vol. 38, no. 1, pp. 104–113, 2003.

[49] K. Watanabe, D. Kamiya, A. Nishiyama et al., "Directed differentiation of telencephalic precursors from embryonic stem cells," *Nature Neuroscience*, vol. 8, no. 3, pp. 288–296, 2005.

[50] T. J. Bartosh, J. H. Ylöstalo, A. Mohammadipoor et al., "Aggregation of human mesenchymal stromal cells (MSCs) into 3D spheroids enhances their antiinflammatory properties," *Proceedings of the National Academy of Sciences of the United States of America*, vol. 107, no. 31, pp. 13724–13729, 2010.

[51] Q. Zhang, A. L. Nguyen, S. Shi et al., "Three-dimensional spheroid culture of human gingiva-derived mesenchymal stem cells enhances mitigation of chemotherapy-induced oral mucositis," *Stem Cells and Development*, vol. 21, no. 6, pp. 937–947, 2012.

[52] P. R. Baraniak, M. T. Cooke, R. Saeed, M. A. Kinney, K. M. Fridley, and T. C. McDevitt, "Stiffening of human mesenchymal stem cell spheroid microenvironments induced by incorporation of gelatin microparticles," *Journal of the Mechanical Behavior of Biomedical Materials*, vol. 11, pp. 63–71, 2012.

[53] E. Bellas and C. S. Chen, "Forms, forces, and stem cell fate," *Current Opinion in Cell Biology*, vol. 31, pp. 92–97, 2014.

[54] R. McBeath, D. M. Pirone, C. M. Nelson, K. Bhadriraju, and C. S. Chen, "Cell shape, cytoskeletal tension, and RhoA regulate stem cell lineage commitment," *Developmental Cell*, vol. 6, no. 4, pp. 483–495, 2004.

[55] S. A. Ruiz and C. S. Chen, "Emergence of patterned stem cell differentiation within multicellular structures," *Stem Cells*, vol. 26, no. 11, pp. 2921–2927, 2008.

[56] J. H. Wen, L. G. Vincent, A. Fuhrmann et al., "Interplay of matrix stiffness and protein tethering in stem cell differentiation," *Nature Materials*, vol. 13, no. 10, pp. 979–987, 2014.

[57] W. L. Murphy, T. C. McDevitt, and A. J. Engler, "Materials as stem cell regulators," *Nature Materials*, vol. 13, no. 6, pp. 547–557, 2014.

[58] I. A. Potapova, G. R. Gaudette, P. R. Brink et al., "Mesenchymal stem cells support migration, extracellular matrix invasion, proliferation, and survival of endothelial cells in vitro," *Stem Cells*, vol. 25, no. 7, pp. 1761–1768, 2007.

[59] I. A. Potapova, P. R. Brink, I. S. Cohen, and S. V. Doronin, "Culturing of human mesenchymal stem cells as three-dimensional aggregates induces functional expression of CXCR4 that regulates adhesion to endothelial cells," *The Journal of Biological Chemistry*, vol. 283, no. 19, pp. 13100–13107, 2008.

[60] J. E. Frith, B. Thomson, and P. G. Genever, "Dynamic three-dimensional culture methods enhance mesenchymal stem cell properties and increase therapeutic potential," *Tissue Engineering Part C: Methods*, vol. 16, no. 4, pp. 735–749, 2010.

[61] R. H. Lee, M. J. Seo, A. A. Pulin, C. A. Gregory, J. Ylostalo, and D. J. Prockop, "The CD34-like protein PODXL and α6-integrin (CD49f) identify early progenitor MSCs with increased clonogenicity and migration to infarcted heart in mice," *Blood*, vol. 113, no. 4, pp. 816–826, 2009.

[62] R. H. Lee, A. A. Pulin, M. J. Seo et al., "Intravenous hMSCs improve myocardial infarction in mice because cells embolized in lung are activated to secrete the anti-inflammatory protein TSG-6," *Cell Stem Cell*, vol. 5, no. 1, pp. 54–63, 2009.

[63] M. Crisan, S. Yap, L. Casteilla et al., "A perivascular origin for mesenchymal stem cells in multiple human organs," *Cell Stem Cell*, vol. 3, no. 3, pp. 301–313, 2008.

[64] D. T. Covas, R. A. Panepucci, A. M. Fontes et al., "Multipotent mesenchymal stromal cells obtained from diverse human tissues share functional properties and gene-expression profile with $CD146^+$ perivascular cells and fibroblasts," *Experimental Hematology*, vol. 36, no. 5, pp. 642–654, 2008.

[65] D. T. Covas, C. E. Piccinato, M. D. Orellana et al., "Mesenchymal stem cells can be obtained from the human saphena vein," *Experimental Cell Research*, vol. 309, no. 2, pp. 340–344, 2005.

[66] M. Abedin, Y. Tintut, and L. L. Demer, "Mesenchymal stem cells and the artery wall," *Circulation Research*, vol. 95, no. 7, pp. 671–676, 2004.

[67] A. I. Caplan, "All MSCs are pericytes?" *Cell Stem Cell*, vol. 3, no. 3, pp. 229–230, 2008.

[68] C. Lamagna and G. Bergers, "The bone marrow constitutes a reservoir of pericyte progenitors," *Journal of Leukocyte Biology*, vol. 80, no. 4, pp. 677–681, 2006.

[69] A. I. Caplan, "Why are MSCs therapeutic? New data: new insight," *Journal of Pathology*, vol. 217, no. 2, pp. 318–324, 2009.

[70] L. Diaz-Flores Jr., R. Gutierrez, J. F. Madrid, H. Varela, F. Valladares, and L. Diaz-Flores, "Adult stem cells and repair through granulation tissue," *Frontiers in Bioscience*, vol. 14, no. 4, pp. 1433–1470, 2009.

[71] K. English, A. French, and K. J. Wood, "Mesenchymal stromal cells: facilitators of successful transplantation?" *Cell Stem Cell*, vol. 7, no. 4, pp. 431–442, 2010.

[72] J. Galipeau, "The mesenchymal stromal cells dilemma—does a negative phase III trial of random donor mesenchymal stromal cells in steroid-resistant graft-versus-host disease represent a death knell or a bump in the road?" *Cytotherapy*, vol. 15, no. 1, pp. 2–8, 2013.

[73] J. Tongers, D. W. Losordo, and U. Landmesser, "Stem and progenitor cell-based therapy in ischaemic heart disease: promise, uncertainties, and challenges," *European Heart Journal*, vol. 32, no. 10, pp. 1197–1206, 2011.

[74] M. Krampera, "Mesenchymal stromal cell 'licensing': a multistep process," *Leukemia*, vol. 25, no. 9, pp. 1408–1414, 2011.

[75] A. Uccelli, L. Moretta, and V. Pistoia, "Mesenchymal stem cells in health and disease," *Nature Reviews Immunology*, vol. 8, no. 9, pp. 726–736, 2008.

[76] J. A. Ankrum, J. F. Ong, and J. M. Karp, "Mesenchymal stem cells: immune evasive, not immune privileged," *Nature Biotechnology*, vol. 32, no. 3, pp. 252–260, 2014.

[77] D. J. Prockop, "Concise review: two negative feedback loops place mesenchymal stem/stromal cells at the center of early regulators of inflammation," *Stem Cells*, vol. 31, no. 10, pp. 2042–2046, 2013.

[78] J. H. Ylöstalo, T. J. Bartosh, K. Coble, and D. J. Prockop, "Human mesenchymal stem/stromal cells cultured as spheroids are self-activated to produce prostaglandin E2 that directs stimulated macrophages into an anti-inflammatory phenotype," *Stem Cells*, vol. 30, no. 10, pp. 2283–2296, 2012.

[79] C. Menard, L. Pacelli, G. Bassi et al., "Clinical-grade mesenchymal stromal cells produced under various good manufacturing practice processes differ in their immunomodulatory properties: standardization of immune quality controls," *Stem Cells and Development*, vol. 22, no. 12, pp. 1789–1801, 2013.

[80] Y. Shi, J. Su, A. I. Roberts, P. Shou, A. B. Rabson, and G. Ren, "How mesenchymal stem cells interact with tissue immune responses," *Trends in Immunology*, vol. 33, no. 3, pp. 136–143, 2012.

[81] Y. Zhou, A. Day, S. Haykal, A. Keating, and T. K. Waddell, "Mesenchymal stromal cells augment CD4+ and CD8+ T-cell proliferation through a CCL2 pathway," *Cytotherapy*, vol. 15, no. 10, pp. 1195–1207, 2013.

[82] M. J. Hoogduijn, M. Roemeling-van Rhijn, A. U. Engela et al., "Mesenchymal stem cells induce an inflammatory response after intravenous infusion," *Stem Cells and Development*, vol. 22, no. 21, pp. 2825–2835, 2013.

[83] K. Anton, D. Banerjee, and J. Glod, "Macrophage-associated mesenchymal stem cells assume an activated, migratory, pro-inflammatory phenotype with increased IL-6 and CXCL10 secretion," *PLoS ONE*, vol. 7, no. 4, Article ID e35036, 2012.

[84] G. Ren, L. Zhang, X. Zhao et al., "Mesenchymal stem cell-mediated immunosuppression occurs via concerted action of chemokines and nitric oxide," *Cell Stem Cell*, vol. 2, no. 2, pp. 141–150, 2008.

[85] G. C. Gurtner, S. Werner, Y. Barrandon, and M. T. Longaker, "Wound repair and regeneration," *Nature*, vol. 453, no. 7193, pp. 314–321, 2008.

[86] M. W. J. Ferguson and S. O'Kane, "Scar-free healing: from embryonic mechanism to adult therapeutic intervention," *Philosophical Transactions of the Royal Society of London B: Biological Sciences*, vol. 359, no. 1445, pp. 839–850, 2004.

[87] D. Hanahan, "Signaling vascular morphogenesis and maintenance," *Science*, vol. 277, no. 5322, pp. 48–50, 1997.

[88] H. G. Augustin, G. Y. Koh, G. Thurston, and K. Alitalo, "Control of vascular morphogenesis and homeostasis through the angiopoietin—tie system," *Nature Reviews Molecular Cell Biology*, vol. 10, no. 3, pp. 165–177, 2009.

[89] Y. Cao, J. Arbiser, R. J. D'Amato et al., "Forty-year journey of angiogenesis translational research," *Science Translational Medicine*, vol. 3, no. 114, Article ID 114rv3, 2011.

[90] M. Nomi, H. Miyake, Y. Sugita, M. Fujisawa, and S. Soker, "Role of growth factors and endothelial cells in therapeutic angiogenesis and tissue engineering," *Current Stem Cell Research & Therapy*, vol. 1, no. 3, pp. 333–343, 2006.

[91] E. Gherardi, W. Birchmeier, C. Birchmeier, and G. V. Woude, "Targeting MET in cancer: rationale and progress," *Nature Reviews Cancer*, vol. 12, no. 2, pp. 89–103, 2012.

[92] M. W. Laschke, T. E. Schank, C. Scheuer et al., "Three-dimensional spheroids of adipose-derived mesenchymal stem cells are potent initiators of blood vessel formation in porous polyurethane scaffolds," *Acta Biomaterialia*, vol. 9, no. 6, pp. 6876–6884, 2013.

[93] S. H. Bhang, S. Lee, J.-Y. Shin, T.-J. Lee, and B.-S. Kim, "Transplantation of cord blood mesenchymal stem cells as spheroids enhances vascularization," *Tissue Engineering Part A*, vol. 18, no. 19-20, pp. 2138–2147, 2012.

[94] M. Fu, J. Zhang, Y. Lin, X. Zhu, M. U. Ehrengruber, and Y. E. Chen, "Early growth response factor-1 is a critical transcriptional mediator of peroxisome proliferator-activated receptor-γ1 gene expression in human aortic smooth muscle cells," *The Journal of Biological Chemistry*, vol. 277, no. 30, pp. 26808–26814, 2002.

[95] N.-C. Cheng, S.-Y. Chen, J.-R. Li, and T.-H. Young, "Short-term spheroid formation enhances the regenerative capacity of adipose-derived stem cells by promoting stemness, angiogenesis, and chemotaxis," *Stem Cells Translational Medicine*, vol. 2, no. 8, pp. 584–594, 2013.

[96] C. L. Rettinger, A. B. Fourcaudot, S. J. Hong, T. A. Mustoe, R. G. Hale, and K. P. Leung, "In vitro characterization of scaffold-free three-dimensional mesenchymal stem cell aggregates," *Cell and Tissue Research*, vol. 358, no. 2, pp. 395–405, 2014.

[97] W. M. Jackson, L. J. Nesti, and R. S. Tuan, "Mesenchymal stem cell therapy for attenuation of scar formation during wound healing," *Stem Cell Research & Therapy*, vol. 3, no. 3, article 20, 2012.

[98] B. Johnstone, T. M. Hering, A. I. Caplan, V. M. Goldberg, and J. U. Yoo, "In vitro chondrogenesis of bone marrow-derived mesenchymal progenitor cells," *Experimental Cell Research*, vol. 238, no. 1, pp. 265–272, 1998.

[99] J. U. Yoo, T. S. Barthel, K. Nishimura et al., "The chondrogenic potential of human bone-marrow-derived mesenchymal progenitor cells," *The Journal of Bone & Joint Surgery—American Volume*, vol. 80, no. 12, pp. 1745–1757, 1998.

[100] A. M. Mackay, S. C. Beck, J. M. Murphy, F. P. Barry, C. O. Chichester, and M. F. Pittenger, "Chondrogenic differentiation of cultured human mesenchymal stem cells from marrow," *Tissue Engineering*, vol. 4, no. 4, pp. 415–428, 1998.

[101] W. Wang, K. Itaka, S. Ohba et al., "3D spheroid culture system on micropatterned substrates for improved differentiation efficiency of multipotent mesenchymal stem cells," *Biomaterials*, vol. 30, no. 14, pp. 2705–2715, 2009.

[102] N.-C. Cheng, S. Wang, and T.-H. Young, "The influence of spheroid formation of human adipose-derived stem cells on

chitosan films on stemness and differentiation capabilities," *Biomaterials*, vol. 33, no. 6, pp. 1748–1758, 2012.

[103] M. C. Arufe, A. de La Fuente, I. Fuentes-Boquete, F. J. de Toro, and F. J. Blanco, "Differentiation of synovial CD-105$^+$ human mesenchymal stem cells into chondrocyte-like cells through spheroid formation," *Journal of Cellular Biochemistry*, vol. 108, no. 1, pp. 145–155, 2009.

[104] Y. Miyagawa, H. Okita, M. Hiroyama et al., "A microfabricated scaffold induces the spheroid formation of human bone marrow-derived mesenchymal progenitor cells and promotes efficient adipogenic differentiation," *Tissue Engineering A*, vol. 17, no. 3-4, pp. 513–521, 2011.

[105] C. J. Lengner, F. D. Camargo, K. Hochedlinger et al., "Oct4 expression is not required for mouse somatic stem cell self-renewal," *Cell Stem Cell*, vol. 1, no. 4, pp. 403–415, 2007.

[106] J. S. Berg and M. A. Goodell, "An argument against a role for Oct4 in somatic stem cells," *Cell Stem Cell*, vol. 1, no. 4, pp. 359–360, 2007.

[107] R. Pochampally, "Colony forming unit assays for MSCs," *Methods in Molecular Biology*, vol. 449, pp. 83–91, 2008.

[108] L. Guo, Y. Zhou, S. Wang, and Y. Wu, "Epigenetic changes of mesenchymal stem cells in three-dimensional (3D) spheroids," *Journal of Cellular and Molecular Medicine*, vol. 18, no. 10, pp. 2009–2019, 2014.

[109] I. Sekiya, B. L. Larson, J. R. Smith, R. Pochampally, J.-G. Cui, and D. J. Prockop, "Expansion of human adult stem cells from bone marrow stroma: conditions that maximize the yields of early progenitors and evaluate their quality," *Stem Cells*, vol. 20, no. 6, pp. 530–541, 2002.

[110] J. Campisi, "Replicative senescence: an old lives' tale?" *Cell*, vol. 84, no. 4, pp. 497–500, 1996.

[111] J. Campisi, "From cells to organisms: can we learn about aging from cells in culture?" *Experimental Gerontology*, vol. 36, no. 4–6, pp. 607–618, 2001.

[112] G. Lepperdinger, R. Brunauer, A. Jamnig, G. Laschober, and M. Kassem, "Controversial issue: is it safe to employ mesenchymal stem cells in cell-based therapies?" *Experimental Gerontology*, vol. 43, no. 11, pp. 1018–1023, 2008.

[113] P. R. Crisostomo, M. Wang, G. M. Wairiuko et al., "High passage number of stem cells adversely affects stem cell activation and myocardial protection," *Shock*, vol. 26, no. 6, pp. 575–580, 2006.

[114] S. Jiang, H. K. Haider, R. P. H. Ahmed, N. M. Idris, A. Salim, and M. Ashraf, "Transcriptional profiling of young and old mesenchymal stem cells in response to oxygen deprivation and reparability of the infarcted myocardium," *Journal of Molecular and Cellular Cardiology*, vol. 44, no. 3, pp. 582–596, 2008.

[115] C. Fehrer and G. Lepperdinger, "Mesenchymal stem cell aging," *Experimental Gerontology*, vol. 40, no. 12, pp. 926–930, 2005.

[116] M. E. Menezes, S. Bhatia, P. Bhoopathi et al., "MDA-7/IL-24: multifunctional cancer killing cytokine," in *Anticancer Genes*, vol. 818 of *Advances in Experimental Medicine and Biology*, pp. 127–153, Springer, London, UK, 2014.

[117] P. Dent, A. Yacoub, H. A. Hamed et al., "MDA-7/IL-24 as a cancer therapeutic: from bench to bedside," *Anti-Cancer Drugs*, vol. 21, no. 8, pp. 725–731, 2010.

[118] M. Sauane, R. V. Gopalkrishnan, D. Sarkar et al., "MDA-7/IL-24: novel cancer growth suppressing and apoptosis inducing cytokine," *Cytokine and Growth Factor Reviews*, vol. 14, no. 1, pp. 35–51, 2003.

[119] I. A. Droujinine, M. A. Eckert, and W. Zhao, "To grab the stroma by the horns: from biology to cancer therapy with mesenchymal stem cells," *Oncotarget*, vol. 4, no. 5, pp. 651–664, 2013.

[120] N. Serakinci, U. Fahrioglu, and R. Christensen, "Mesenchymal stem cells, cancer challenges and new directions," *European Journal of Cancer*, vol. 50, no. 8, pp. 1522–1530, 2014.

[121] M. Rodrigues, L. G. Griffith, and A. Wells, "Growth factor regulation of proliferation and survival of multipotential stromal cells," *Stem Cell Research and Therapy*, vol. 1, no. 4, article 32, 2010.

[122] C. Toma, M. F. Pittenger, K. S. Cahill, B. J. Byrne, and P. D. Kessler, "Human mesenchymal stem cells differentiate to a cardiomyocyte phenotype in the adult murine heart," *Circulation*, vol. 105, no. 1, pp. 93–98, 2002.

[123] C. Toma, W. R. Wagner, S. Bowry, A. Schwartz, and F. Villanueva, "Fate of culture-expanded mesenchymal stem cells in the microvasculature: in vivo observations of cell kinetics," *Circulation Research*, vol. 104, no. 3, pp. 398–402, 2009.

[124] L. von Bahr, I. Batsis, G. Moll et al., "Analysis of tissues following mesenchymal stromal cell therapy in humans indicates limited long-term engraftment and no ectopic tissue formation," *Stem Cells*, vol. 30, no. 7, pp. 1575–1578, 2012.

[125] G. L. Semenza, "Oxygen-dependent regulation of mitochondrial respiration by hypoxia-inducible factor 1," *Biochemical Journal*, vol. 405, no. 1, pp. 1–9, 2007.

[126] W. L. Grayson, F. Zhao, B. Bunnell, and T. Ma, "Hypoxia enhances proliferation and tissue formation of human mesenchymal stem cells," *Biochemical and Biophysical Research Communications*, vol. 358, no. 3, pp. 948–953, 2007.

[127] K. Tamama, H. Kawasaki, S. S. Kerpedjieva, J. Guan, R. K. Ganju, and C. K. Sen, "Differential roles of hypoxia inducible factor subunits in multipotential stromal cells under hypoxic condition," *Journal of Cellular Biochemistry*, vol. 112, no. 3, pp. 804–817, 2011.

[128] L. Song, N. E. Webb, Y. Song, and R. S. Tuan, "Identification and functional analysis of candidate genes regulating mesenchymal stem cell self-renewal and multipotency," *Stem Cells*, vol. 24, no. 7, pp. 1707–1718, 2006.

[129] D. J. Barbeau, K. T. La, D. S. Kim, S. S. Kerpedjieva, G. V. Shurin, and K. Tamama, "Early growth response-2 signaling mediates immunomodulatory effects of human multipotential stromal cells," *Stem Cells and Development*, vol. 23, no. 2, pp. 155–166, 2014.

[130] K. A. Hogquist, M. A. Nett, E. R. Unanue, and D. D. Chaplin, "Interleukin 1 is processed and released during apoptosis," *Proceedings of the National Academy of Sciences of the United States of America*, vol. 88, no. 19, pp. 8485–8489, 1991.

[131] R. J. Kaufman and J. D. Malhotra, "Calcium trafficking integrates endoplasmic reticulum function with mitochondrial bioenergetics," *Biochimica et Biophysica Acta—Molecular Cell Research*, vol. 1843, no. 10, pp. 2233–2239, 2014.

[132] S. Orrenius, B. Zhivotovsky, and P. Nicotera, "Regulation of cell death: the calcium-apoptosis link," *Nature Reviews Molecular Cell Biology*, vol. 4, no. 7, pp. 552–565, 2003.

[133] P. Pinton, C. Giorgi, R. Siviero, E. Zecchini, and R. Rizzuto, "Calcium and apoptosis: ER-mitochondria Ca^{2+} transfer in the control of apoptosis," *Oncogene*, vol. 27, no. 50, pp. 6407–6418, 2008.

[134] R. Bonasio, S. Tu, and D. Reinberg, "Molecular signals of epigenetic states," *Science*, vol. 330, no. 6004, pp. 612–616, 2010.

[135] H. Cedar and Y. Bergman, "Linking DNA methylation and histone modification: patterns and paradigms," *Nature Reviews Genetics*, vol. 10, no. 5, pp. 295–304, 2009.

[136] G. Egger, G. Liang, A. Aparicio, and P. A. Jones, "Epigenetics in human disease and prospects for epigenetic therapy," *Nature*, vol. 429, no. 6990, pp. 457–463, 2004.

[137] A. Watanabe, Y. Yamada, and S. Yamanaka, "Epigenetic regulation in pluripotent stem cells: a key to breaking the epigenetic barrier," *Philosophical transactions of the Royal Society of London. Series B, Biological sciences*, vol. 368, no. 1609, Article ID 20120292, 2013.

[138] H. Nishida, T. Suzuki, S. Kondo, H. Miura, Y.-I. Fujimura, and Y. Hayashizaki, "Histone H3 acetylated at lysine 9 in promoter is associated with low nucleosome density in the vicinity of transcription start site in human cell," *Chromosome Research*, vol. 14, no. 2, pp. 203–211, 2006.

Hindawi Publishing Corporation
Stem Cells International
Volume 2016, Article ID 9062638, 11 pages
http://dx.doi.org/10.1155/2016/9062638

Research Article

Three-Dimensional Aggregates Enhance the Therapeutic Effects of Adipose Mesenchymal Stem Cells for Ischemia-Reperfusion Induced Kidney Injury in Rats

Xiaozhi Zhao,[1,2] Xuefeng Qiu,[1,2,3] Yanting Zhang,[3] Shiwei Zhang,[1,2] Xiaoping Gu,[4] and Hongqian Guo[1,2]

[1]*Department of Urology, Affiliated Drum Tower Hospital, School of Medicine, Nanjing University, Nanjing 210008, China*
[2]*Institute of Urology, Nanjing University, Nanjing 210093, China*
[3]*State Key Laboratory of Pharmaceutical Biotechnology, Nanjing University, Nanjing 210093, China*
[4]*Department of Anesthesiology, Affiliated Drum Tower Hospital, School of Medicine, Nanjing University, Nanjing 210008, China*

Correspondence should be addressed to Xiaoping Gu; xiaopinggu1@gmail.com and Hongqian Guo; dr.guohongqian@gmail.com

Received 31 December 2014; Accepted 27 February 2015

Academic Editor: Kenichi Tamama

It has been shown that administration of adipose derived mesenchymal stem cells (AdMSCs) enhanced structural and functional recovery of renal ischemia-reperfusion (IR) injury. Low engraftment of stem cells, however, limits the therapeutic effects of AdMSCs. The present study was designed to enhance the therapeutic effects of AdMSCs by delivering AdMSCs in a three-dimensional (3D) aggregates form. Microwell was used to produce 3D AdMSCs aggregates. In vitro data indicated that AdMSCs in 3D aggregates were less susceptible to oxidative and hypoxia stress induced by 200 μM peroxide and hypoxia/reoxygenation, respectively, compared with those cultured in two-dimensional (2D) monolayer. Furthermore, AdMSCs in 3D aggregates secreted more proangiogenic factors than those cultured in 2D monolayer. 2D AdMSCs or 3D AdMSCs aggregates were injected into renal cortex immediately after induction of renal IR injury. In vivo data revealed that 3D aggregates enhanced the effects of AdMSCs in recovering function and structure after renal IR injury. Improved grafted AdMSCs were observed in kidney injected with 3D aggregates compared with AdMSCs cultured in 2D monolayer. Our results demonstrated that 3D AdMSCs aggregated produced by microwell enhanced the retention and therapeutic effects of AdMSCs for renal IR injury.

1. Introduction

Mesenchymal stem cells (MSCs) are multipotent progenitor cells which could be isolated from several tissues, in particular bone marrow and adipose tissue [1, 2]. The ease of isolation and expansion in culture, the immunomodulatory properties, and the multilineage differentiation potential make MSCs promising resource for cell therapy. Several studies have demonstrated that administration of MSCs enhanced structural and functional recovery of renal ischemia-reperfusion (IR) injury [3–5]. The beneficial effect of injected MSCs was suggested to be mainly related to the secretion of cytokines from transplanted MSCs, which is defined as paracrine effect [4, 6].

Although the therapeutic effects of MSCs for renal IR injury have been well described, a lack of initial engraftment and retention due to early cell death is a major roadblock to achieving clinical significance [7]. This might be due to the "harsh environment" including oxidative stress, hypoxia in the injured kidney. Several strategies have been developed to improve the survival of engrafted stem cells in ischemic kidney. These strategies include genetic modification of stem cells [8, 9], pretreatment of MSCs [7, 10], and the use of tissue engineering scaffolds [11]. Despite the improved survival of stem cells in ischemic kidney, the strategies still have problems for further clinical application.

Recently, many researchers demonstrated that delivering MSCs in an aggregate form could serve as an effective method to solve these problems. It has been shown that three-dimensional (3D) aggregates enhanced the survival of engrafted cells as well as the microenvironment of injured organs. For example, delivery of cardiac progenitor cells in the

form of 3D aggregates improved in vivo survival of implanted cells in cardiac ischemia-reperfusion injury [12]. Following intramuscular transplantation to ischemic limbs, 3D MSCs aggregates showed improved cell survival and limb survival [13]. However, few researches have focused on the application of 3D MSCs aggregates in stem cell-base therapy of renal IR injury. Several 3D cell culture techniques including porous scaffolds, hydrogel, and cellular aggregates have been developed. Among them, cellular aggregates have drawn rising attention because they are free of exogenous biomaterials [14]. Microwell has been reported as an effective technique to produce scale cell aggregates [12, 15]. The present study was designed to examine the therapeutic effects of 3D adipose derived MSCs (AdMSCs) aggregates produced by microwell for renal IR injury using a rat model. We hypothesize that delivery of AdMSCs in the form of aggregates could enhance the survival of AdMSCs in injured kidney and therefore improve the therapeutic effects of AdMSCs. To the best of our knowledge, this is the first study designed to explore the feasibility of using 3D AdMSCs aggregates to enhance the therapeutic effects of AdMSCs for renal IR injury.

2. Materials and Methods

2.1. Cell Culture. AdMSCs were isolated from paratesticular fat of Sprague-Dawley rats and cultured according to our previously described protocol [16, 17]. Briefly, adipose tissue was minced into small pieces and then incubated with 0.075% type I collagenase (Sigma-Aldrich, St. Louis, MO, USA) for 1 h at 37°C. After centrifuging at 220 g for 10 min, the top lipid layer was removed and the remaining cells were suspended in Dulbecco's modified Eagle's medium (DMEM, Life Technologies, Shanghai, China) supplemented with 10% fetal bovine serum (FBS, Life Technologies), and plated at a density of 1×10^6 cells in a 10 cm dish. AdMSCs were passed under the same conditions through no more than five passages before being used for assays. All procedures were approved by Institutional Animal Care and Use Committee of Nanjing University.

2.2. Microwell Assembly and Generation of AdMSCs Aggregates. Microwells were generated using micromolding on UV-photocrosslinkable polyethylene glycol dimethacrylate (PEG, MW = 1000, 20% in PBS) (Sigma-Aldrich) with 1% photoinitiator 2-hydroxy-1-[4-(hydroxyethoxy) phenyl]-2-methyl-L-propanone (Irgacure D2959, Ciba Specialty Chemicals Inc., Florham Park, NJ, USA) according to the previously described protocol [12, 15]. Briefly, PEG macromer solution was pipette on glass slide coated with 3-(trimethoxysilyl) propylmethacrylate (TMSPMA) (Sigma-Aldrich). Thereafter, a patterned PDMS stamp was placed on PEG solution to make PEG solution distribute evenly between PDMS stamp and TMSPMA coated glass slide. After 10 seconds of irradiation with UV (l = 350–500 nm, 10 mW/cm^2; OmniCure Series 2000 curing station, EXFO, Mississauga, Canada), the PEG was photocrosslinked with microwells on it. For generation of AdMSCs aggregation, AdMSCs were seeded onto microwells by using a previously developed method [18]. Briefly, AdMSCs suspension (1×10^6 cells/mL) was pipetted on the surface of the microwell array evenly (100 μL/cm^2). Two hours later, the array was immersed in media in a culture dish. AdMSCs formed 3D aggregates in microwell. A schematic summarizing the protocol is shown in Figure S.1 (see Supplementary Material available online at http://dx.doi.org/10.1155/2016/9062638).

2.3. Hydrogen Peroxide (H_2O_2) and Hypoxia/Reoxygenation Treatment. To determine the sensitivity of the cells to stress including oxidative stress and hypoxia, AdMSCs cultured in 2D monolayer or in 3D aggregates were treated with 200 μM H_2O_2 or hypoxia followed reoxygenation. Briefly, cells were incubated with culture medium containing 200 μM H_2O_2 or vehicle for 2 hours to mimic oxidative stress. For the induction of hypoxia/reoxygenation, cells were subjected to hypoxia for 24 h followed by 2 hours of reoxygenation. Hypoxia (2% O_2) was achieved by using a multigas incubator (Sanyo, Pfaffenhofen, German) that maintained a gas mixture of 2% O_2, 5% CO_2, and 93% N_2 at 37°C. Cells cultured under regular culture conditions for the same period of time were set as control. Viability of cells was determined as described below.

2.4. Cell Viability. A rapid, simultaneous double-staining procedure using fluorescein diacetate (FDA) and propidium iodide (PI) (Sigma-Aldrich) was used in the determination of cell viability [19]. In brief, cells were stained with 5 μg/mL PI and 4 μg/mL FDA and observed under the fluorescent microscopy with an appropriate barrier filter set.

2.5. Real Time Polymerase Chain Reaction (PCR). Gene expression of extracellular matrix (ECM) and proangiogenic growth factors were determined by real time PCR. Briefly, total RNA was isolated from cells using TRIzol Reagent (Life Technologies, Shanghai, China). RNA was reverse-transcribed (RT) to cDNA by using a commercial available transcription Kit (Applied Biosystems, Carlsbad, CA, USA). Quantitative RT-PCR was performed using the Power SYBR Green PCR Master Mix (Life Technologies). All experiments were performed in triplicate for each sample and each gene. The primer sequence was listed in Table S.1.

2.6. Immunofluorescent Analysis. After rinsed with PBS and fixed with 4% paraformaldehyde for 10 min, cells were rinsed with PBS and permeabilized with 0.05% triton X-100 for 10 min. After incubated with 5% horse serum for 30 min and then with primary antibody over night at 4°C, the cells were incubated with secondary antibodies for 1 h at room temperature. The primary antibodies included anti-fibronectin (1 : 100, Santa Cruz Biotechnology, Santa Cruz, CA, USA), anti-laminin (1 : 100, Santa Cruz Biotechnology). The secondary antibody is Alexa-594-conjugated secondary antibodies (1 : 500; Life Technologies). Nuclei were stained with 4′,6-diamidino-2-phenylindole (DAPI; Life Technologies).

2.7. Animals and Treatment. All experimental protocols conducted on animals were performed in accordance with the

standards established by the Institution Animal Care and Use Committee at Nanjing University. Male Sprague-Dawley rats weighing 200–250 g were housed in stainless steel cages and given free access to food and water. Rats were randomly divided into four groups. The sham group received sham surgery ($n = 6$); the IR group received injection of PBS immediately after the induction of renal IR ($n = 10$); the IR + AdMSCs group received injection of 2D AdMSCs after the induction of renal IR ($n = 10$); the IR + aggregates group received injection of 3D AdMSCs aggregates after the induction of renal IR ($n = 10$). Rats were euthanized 24 h after surgery. Blood samples were collected for measurement of renal function while kidneys were collected for molecular analysis.

2.8. Rat Model of Renal IR Injury. Rats were anesthetized intraperitoneally with a mixture of ketamine (100 mg/kg) and midazolam (5 mg/kg). After anesthetization, Rats were subjected to renal IR injury as previously described [20]. Briefly, after abdominal laparotomy, right kidney was exposed and removed. Left renal pedicle was exposed and clamped with vascular clamp for 50 min to induce ischemia. After clamp, vascular clamp was removed to induce reperfusion and the incision was closed in 2 layers. Sham-operated control animals underwent right nephrectomy only.

2.9. Cell Labeling and Injection. For the cell tracking, AdMSCs were labeled with EdU (Life Technologies, Shanghai, China) for 48 hr according to the instructions provided by the manufacturer. Since it takes about 24 h for AdMSCs to form 3D aggregates in microwell, a total of 1×10^6 EdU labeled AdMSCs were seeded onto 2D cultural dish or microwell. Twenty-four hours later, cells or aggregates were isolated from 2D cultural dish or microwell for injection. AdMSCs or 3D AdMSCs aggregates in 90 μL PBS were injected into the kidney cortex using a 28 G needle (three injections: poles and middle area) according to a previously published protocol [11].

2.10. Measurement of Renal Function. Serum was separated by centrifuging blood samples and stored at −80°C until analysis of blood serum urea nitrogen (BUN) and urine creatinine (Cr). The concentrations of BUN and Cr were assessed in duplicated with a commercially available assay kit (BioAssay System, Hayward, CA, USA) according to the instructions.

2.11. Histological Analysis. Middle part of kidney was fixed in 4% formaldehyde, dehydrated, and paraffin embedded. Tissue sections (5 μm) were stained with hematoxylin and eosin (HE). Kidney sections were examined in a blinded manner and scored to evaluate the degree of injury. The score reflected the grading of tubular necrosis, cast formation, tubular dilation, and loss of brush border in 10 randomly selected, nonoverlapping fields (200x) as follows: 0: none; 1: ≤10%; 2: 11 to 25%; 3: 26 to 45%; 4: 46 to 75%; and 5: ≥76% [20, 21].

2.12. Detection of Apoptosis. Quantitative determination of apoptosis in kidney sections was assessed by a terminal transferase-mediated dUTP nick-end labeling (TUNEL) assay using an in situ cell death detection kit (Roche, Basel, Switzerland). After dewaxing and rehydration, the tissue sections were permeabilized with 0.1% Triton X-100 for 10 min. Incubation with label solution was used to detect the apoptotic cells according to the instructions. Apoptotic score was achieved by counting the number of positive nuclei in 10 random fields.

2.13. Detection of EdU Positive Cells. Quantitative determination of EdU positive cells in kidney sections was assessed. Briefly, after dewaxing and rehydration, the tissue sections were permeabilized with 0.1% Triton X-100 for 10 min. Incubation with Click-iT@ reaction cocktails was used to detect the apoptotic cells according to the instructions (Invitrogen). Cell engraftment was determined by counting the number of positive nuclei in 10 random fields.

2.14. Statistical Analysis. All statistical analysis was performed using Prism 4 (GraphPad Software, San Diego, CA, USA). One-way analysis of variance (ANOVA) followed by the Tukey-Kramer test for post hoc comparisons was used for analyzing difference between groups. Statistical significance was set at $P < 0.05$.

3. Results

3.1. Construction of 3D AdMSCs Aggregates. AdMSCs aggregated and formed well defined 3D aggregates 24 h following seeding. The AdMSC aggregates did not disassemble for culture time up to 14 days (data not shown). The size of AdMSCs aggregates was homogenous with low variation (Figure 1(c)).

3.2. Characterization of 3D AdMSCs Aggregates. As shown in Figure 2(b), most cells in 3D aggregates were positive for FDA and negative for PI staining, suggesting high viability in the aggregates for at least 7 days (Figures 2(a) and 2(b)). 3D AdMSCs aggregates showed well-preserved ECM compared to the 2D AdMSCs. After culture in microwell for 7 days, cells expressed significantly increased the level of fibronectin and laminin (Figures 2(c)–2(e)) compared with 2D cells, partly indicating the significantly increased secretion of ECM in 3D AdMSCs aggregates.

3.3. 3D AdMSCs Aggregates Are Less Susceptible to Oxidative and Hypoxia Stress. To verify that cells in 3D aggregates enhance protection against hypoxia, AdMSCs in either 2D monolayer culture or 3D aggregates were subjected to 24 h of hypoxia followed by 2 h reoxygenation. As shown in Figures 3(a) and 3(b), cells grown in 3D aggregates were less susceptible to hypoxia/reoxygenation-induced stress compared to those cultured in 2D monolayer as determined by PI/FDA ratio. In addition, we examined the response of 2D AdMSCs or 3D aggregates to oxidative stress mimicked by 200 μM H_2O_2. Similar to results obtained following hypoxia/reoxygenation, reduced cell death, as determined by PI/FDA, was observed in 3D aggregates (Figures 3(a) and 3(c)).

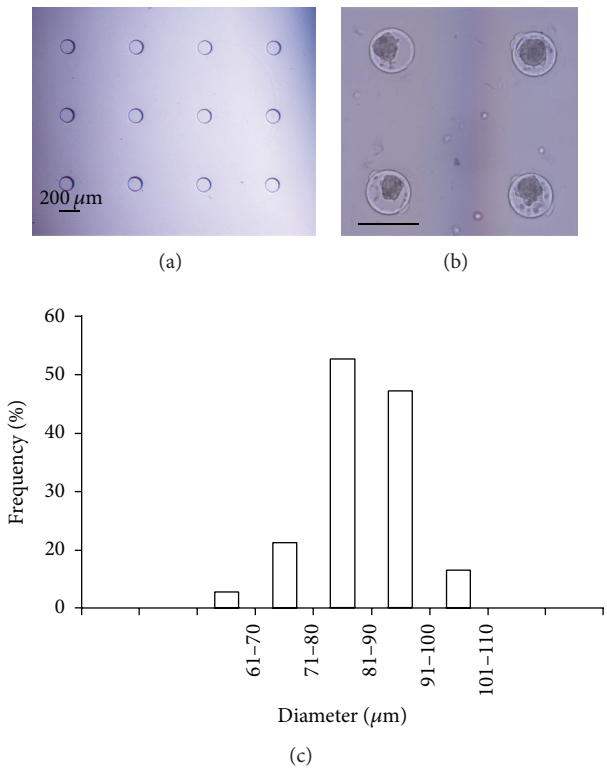

Figure 1: Microwells for culturing AdMSCs derived aggregates. (a) Phase contrast image of microwell. (b) Phase contrast image of AdMSCs aggregates formed in microwell. Black bar indicates 200 μm. (c) Frequency distribution of diameter of aggregates formed in microwell.

3.4. Enhanced Secretion of Proangiogenic Growth Factors from 3D AdMSCs Aggregates. Real time PCR was used to detect the mRNA expression of proangiogenic factors in 2D AdMSCs or 3D aggregates. 3D aggregates showed considerable expressions of proangiogenic growth factors. As shown in Figure 3(d), the expressions of vascular endothelial growth factor (VEGF), fibroblast growth factor-2 (FGF2), and hepatocyte growth factor (HGF) were much greater than those of 2D AdMSCs monolayer (Figure 3(d)).

3.5. 3D AdMSCs Aggregates Preserve Renal Function and Renal Histology. Serum levels of BUN and Cr were selected to determine the renal function. As shown in Figures 4(a) and 4(b), both BUN and Cr levels were significantly higher in IR group than sham group. Injection of AdMSCs, either 2D monolayer culture or 3D aggregates, showed positive effects in preserving renal function, reflected by significantly reduced BUN and Cr levels compared to the IR group. More importantly, the levels of BUN and Cr in IR + aggregates group were significantly lower compared with those in 2D AdMSCs group. These findings implicated that 3D aggregates showed significantly improved protective effects compared with 2D AdMSCs.

To determine the effect of AdMSCs on IR-induced renal injury, a histological scoring system bases on the typical microscopic features of acute tubular damage was adopted (Figure 4(c)). At 24 hours after the IR procedure, the injury score was highest in IR group, significantly higher than sham group. The injury scores in IR + AdMSCs and IR + aggregates group were significantly reduced compared with IR group. The injury score in IR + aggregates group was significantly lower compared with that in IR + AdMSCs group (Figure 4(d)). These findings suggested that 3D aggregates offered more protection than 2D AdMSCs.

3.6. 3D Aggregates Reduced Apoptosis in Kidney after IR Procedure. To investigate IR associated apoptotic cells, we measured TUNEL positive cells in kidney tissues. As shown in Figure 5, 24 hours after IR, no apoptotic cells were observed in the kidney from sham group. The number of apoptotic cells increased significantly in IR group compared with sham group. In contrast, tissues from AdMSCs and aggregates groups contain a significantly smaller number of TUNEL positive apoptotic cells. Furthermore, the number of apoptotic cells in 3D aggregates group reduced significantly in 3D aggregates group compared with that in 2D AdMSCs.

3.7. 3D Aggregates Improved In Vivo Survival of AdMSCs. The number of EdU positive AdMSCs in the renal section was counted to determine cell engraftment after injection. As shown in Figure 6, the number of EdU positive cells in the renal section from 3D aggregates group was significantly greater compared with that in 2D monolayer, suggesting that the form of 3D aggregates exhibit greater survival when implanted in vivo following renal IR injury.

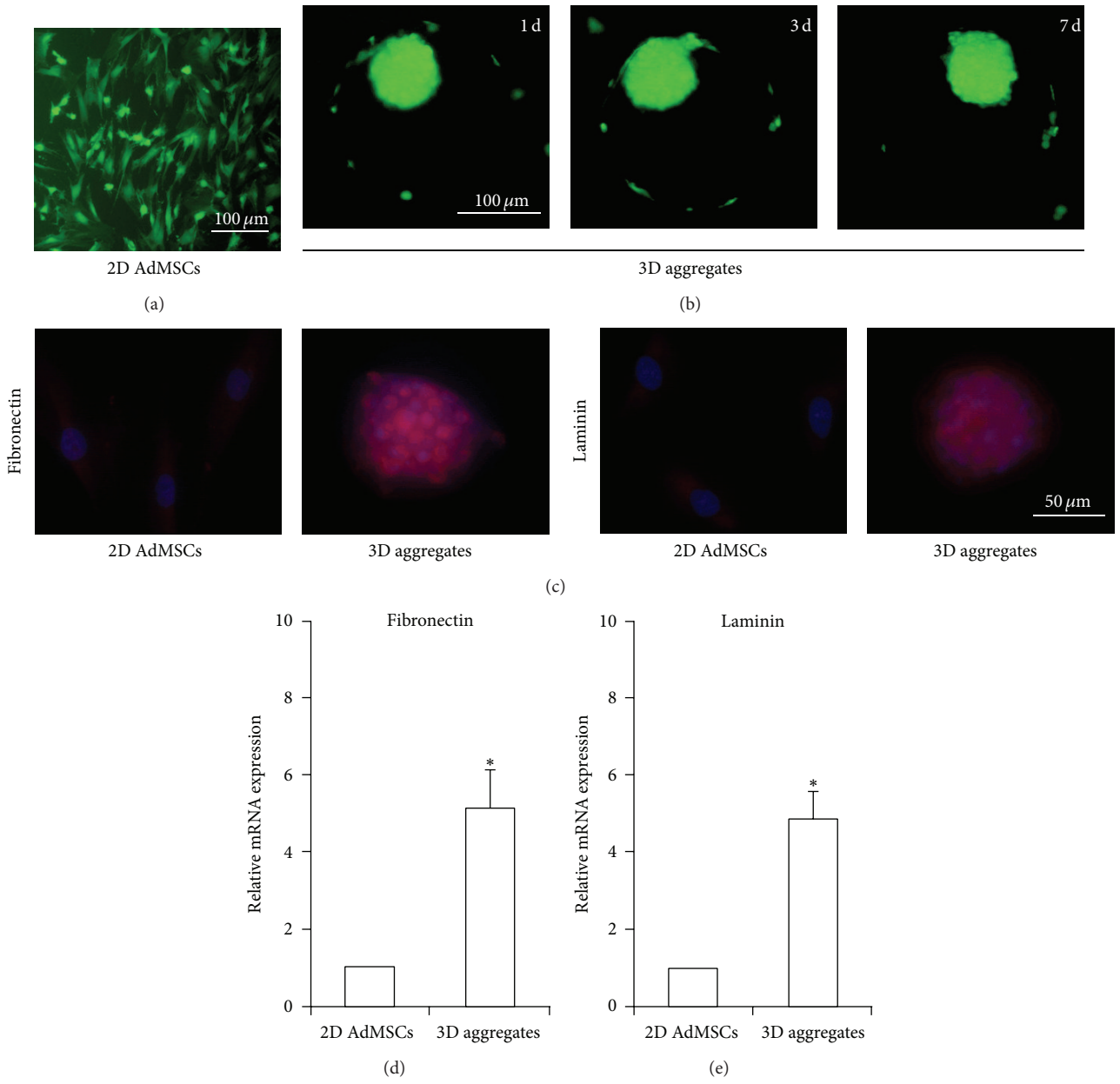

Figure 2: Characters of 3D AdMSCs aggregates. (a) Viability of AdMSCs cultured in 2D monolayer. (b) Viability of 3D AdMSCs aggregates 1 d, 3 d, and 7 d after seeding in microwell. Live or dead cells were stained with FDA (live, green) PI (dead, red). (c) Fluorescent images of 2D AdMSCs or 3D aggregates stained with fibronectin and laminin. (d) mRNA expression of fibronectin and laminin in 2D AdMSCs or 3D aggregates. $^{*}P < 0.05$ compared with 2D AdMSCs.

4. Discussion

Our results show for the first time that microwell produced 3D AdMSCs aggregates improved renal function by suppressing IR-induced elevation of BUN and Cr, restoring IR-damaged renal histological structures, and decreasing tubular cell apoptosis compared with 2D AdMSCs monolayer.

Renal IR injury is one of serious and common diseases with high morbidity and mortality in clinical nephropathy. It is often an unavoidable side effect in renal transplantation and frequently occurs as a result of shock or surgery [22]. Unfortunately, innovative interventions beyond supportive therapy are not yet available. Therefore, it is urgent to develop a new and effective approach for renal IR injury repair.

In the last several years, many studies have shown that transplantation of MSCs is an effective strategy for renal IR injury [5, 23]. MSCs isolated from different tissues including bone marrow [24], adipose [25, 26], Wharton's jelly [27], fetal membrane [28], and umbilical cord [29] have been transplanted to protect against renal IR injury. Among them, AdMSCs were one of the most promising seeding cells because of their abundance in existence, ease in harvesting.

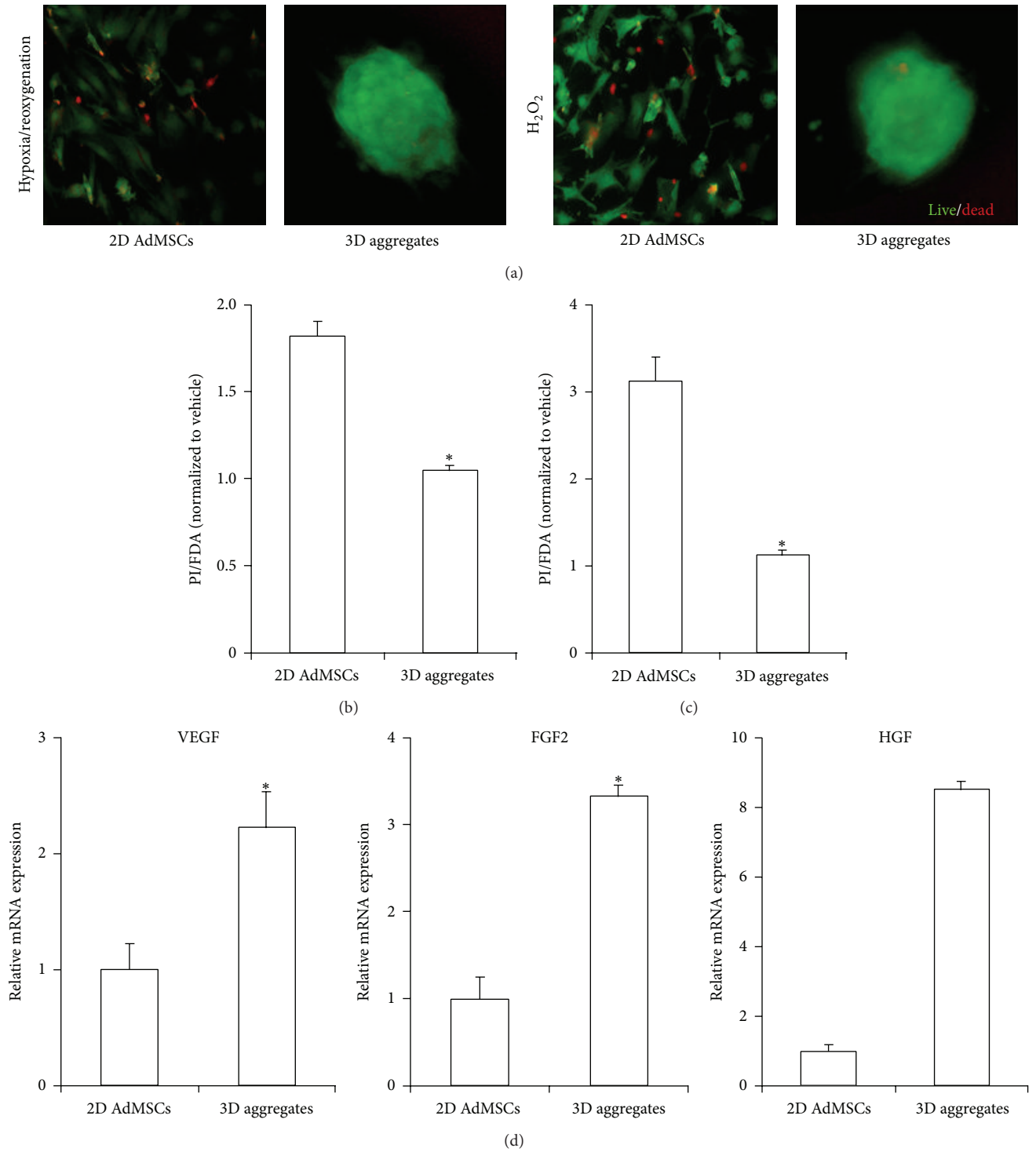

Figure 3: 3D aggregates decrease the susceptibility of AdMSCs to stress and enhance the expression of proangiogenic factors in AdMSCs. (a) Representative FDA/PI stained images of 2D AdMSCs or 3D aggregates subjected to hypoxia/reoxygenation or 200 μM-H_2O_2 treatment. (b) Quantification of dead cells in 2D AdMSCs or 3D aggregates subjected to hypoxia/reoxygenation treatment using PI/FDA ratio. Data were normalized to the vehicle group of 2D monolayer culture. (c) Quantification of dead cells in 2D AdMSCs or 3D aggregates subjected to 200 μM-H_2O_2 treatment using PI/FDA ratio. Data were normalized to the vehicle group of 2D monolayer culture. (d) Relative mRNA expression of VEGF, FGF2, and HGF in 2D AdMSCs and 3D aggregates. $^*P < 0.05$ compared with 2D AdMSCs.

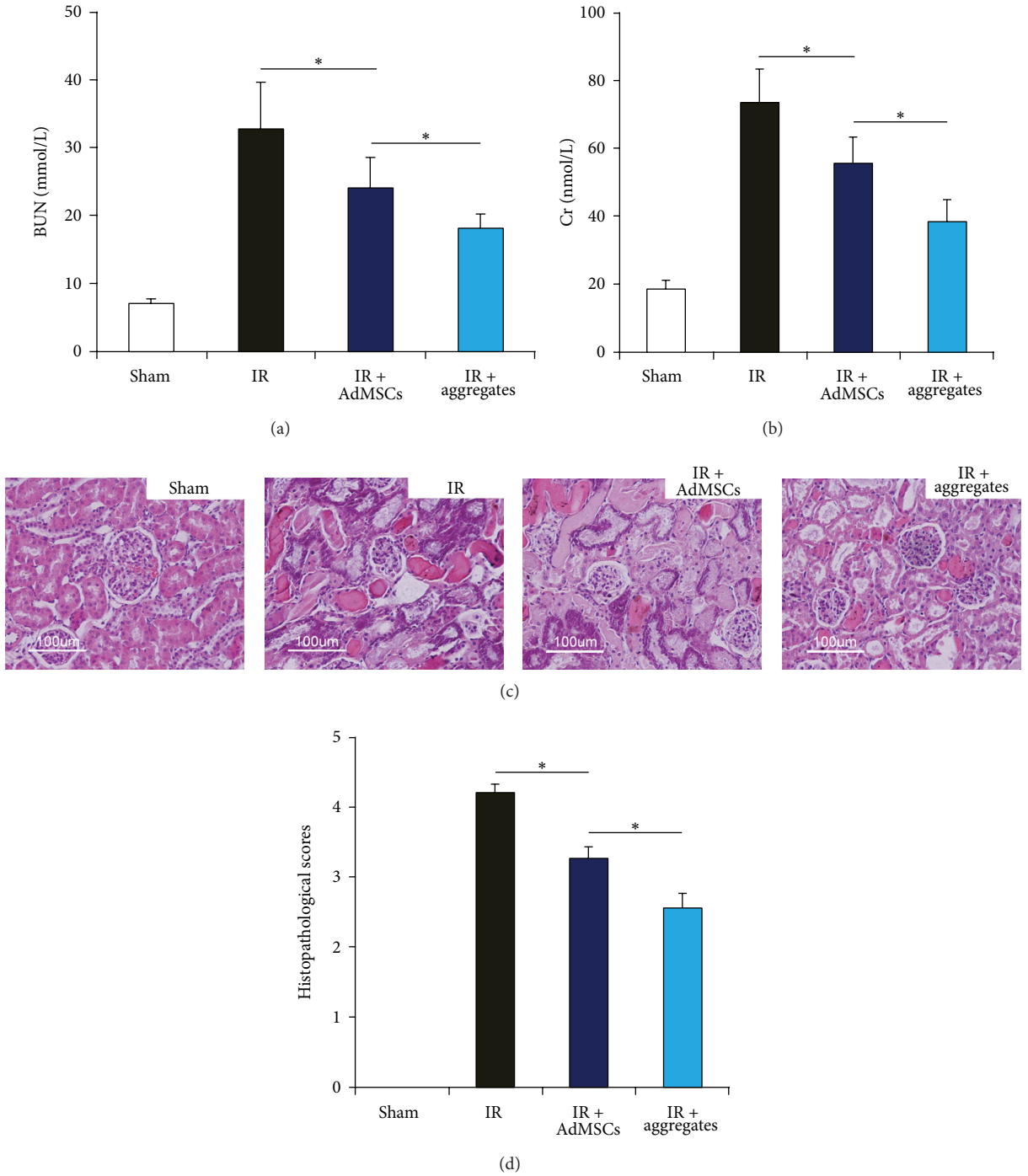

Figure 4: 2D AdMSCs or 3D aggregate preserves renal function and histology after IR. ((a)-(b)) Circulating levels of urea nitrogen (BUN) and creatinine (Cr) in different experimental groups ($n = 6$ in each group). (c) Representative images of HE staining of kidney sections in each experimental group, showing significantly higher degree of tubular damage including tubular necrosis, cast formation, dilatation of tubules, and loss of brush border in IR group. (d) Results of total histopathological scores reflecting tubular damage in each group. $^{*}P < 0.05$.

Several comparison studies have shown that AdMSCs are similar in cell surface expression profiles, differentiation potential and therapeutic efficacy with MSCs derived from bone marrow [30–32]. Most importantly, sufficient number of AdMSCs for clinical application could be obtained with minimal side effects under local anesthesia [33], making AdMSC an alternative cell source for repair of renal IR injury. Despite the advance of AdMSCs-based therapy for renal IR injury, low retention and extensive early death of grafted cells had been one of the remaining problems.

Recently, delivering MSCs in a 3D form has been demonstrated to be an effective strategy to enhance the survival and

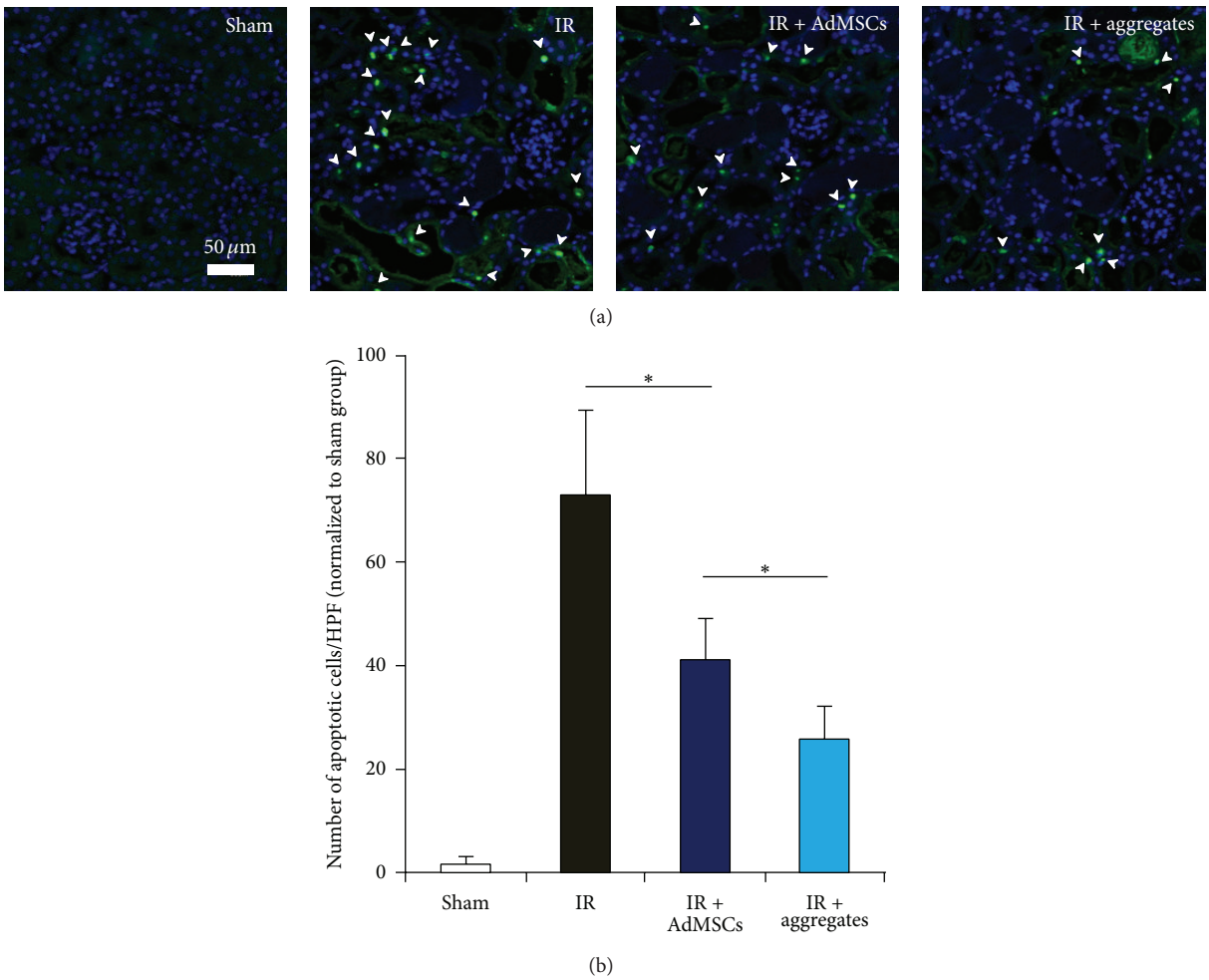

Figure 5: 2D AdMSCs or 3D aggregate reduces tubular apoptosis after IR. (a) Representative images of TUNEL staining of kidney sections in each experimental group. White arrow indicated apoptotic cells in tubules. (b) Results of the number of apoptotic cells in kidney sections in each group. $^{*}P < 0.05$.

therapeutic effects of stem cells [14]. Compared to traditional 2D substrates, 3D culture mimics the in vivo microenvironment and maximizes the cell-cell communication required for stem cell function. In the present study, 3D AdMSCs aggregates were used to promote the survival rate of grafted AdMSCs. Several approaches such as porous scaffolds, hydrogel, and cellular aggregates have been successfully applied to provide 3D culture environment for a variety of cells types, including MSCs [14]. Among these techniques, cellular aggregates have drawn increasing attention because they are free of exogenous biomaterials that may cause untoward responses upon cell transplantation [34, 35]. As a main technique of cellular aggregates, hanging drop has been widely used for stem cell culture [14]. However, hanging drop is ineffective in producing large scale of aggregates. In the present study, we used PEG derived microwell array as a 3D culture system to form AdMSCs aggregates. As shown in Figure 1, the size of AdMSCs aggregates was homogenous with low variation. Most importantly, microwell is effective in producing large scale of AdMSCs aggregates compared with hanging drop. Furthermore, medium change for microwell array is as easy as for regular 2D cell culture, which makes it feasible for longer in vitro culture. Additionally, many in vitro tests can be directly performed within microwell array without having to transfer cells to another container.

In the present study, less susceptibility to oxidative and hypoxia stress was observed in 3D AdMSCs aggregates compared with AdMSCs cultured in 2D monolayer. Being consistent with the in vitro data, significantly increased grafted AdMSCs were also observed in IR kidney. The protective effects of 3D aggregates against stress, such as oxidative stress and hypoxia, might be due to the preconditioning of AdMSCs in the 3D microenvironment [14]. It has been described that 3D aggregates structure could create a heterogeneous microenvironment which provides a size-dependent gradient of nutrients, oxygen, and cytokines. Oxygen is suggested to be a primary factor that affects the biological properties of MSCs within the aggregates. 3D AdMSCs aggregates have been demonstrated to provide a mild hypoxic environment and promote the secretion of hypoxia-inducible factor (HIF) [13, 36]. It has been demonstrated that stem cells underwent apoptosis immediately after exposing to harsh environment

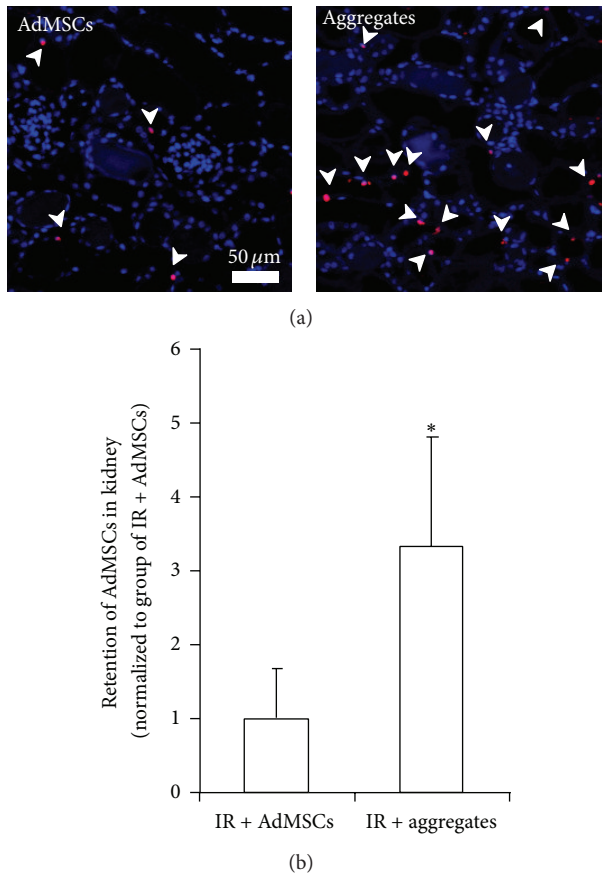

Figure 6: Retention of AdMSCs in kidney. (a) Representative images of EdU-labeled AdMSCs (indicated by white arrow) identified in kidney of rats underwent injection of 2D AdMSCs or 3D aggregates. (b) Results of EdU positive AdMSCs quantification in each high power field (HPF). Data were normalized to IR + AdMSCs group. $^*P < 0.05$ compared to IR + AdMSCs group.

including oxidative stress, hypoxia. Transplantation of 3D aggregates may inhibit apoptosis by preconditioning AdMSCs to hypoxic microenvironment and by stimulating expression of hypoxia-induced survival factors such as HIF.

It is generally accepted that the main therapeutic mechanism of AdMSCs for IR-induced renal injury is through the expressions of cytokine, which is defined as paracrine effect. Increased grafted stem cells are responsible for the enhanced therapeutic effects of AdMSCs. Furthermore, it has been demonstrated that 3D aggregates upregulated secretion of proangiogenic factors such as VEGF, FGF-2, and HGF from MSCs, which is suggested to be induced by a mild hypoxic environment in 3D aggregates [13, 36]. From our in vitro results, the secretion of proangiogenic factors was promoted in 3D AdMSCs aggregates, which is consistent with previously reported results [13]. In addition, transplantation of 3D AdMSCs aggregates to ischemic kidney inhibited tubular apoptosis when compared with 2D AdMSCs grown in monolayer. This may due to the upregulated expressions of proangiogenic factors, which could protect tubular epithelium against IR-induced injury.

Our study has some limitations. First, the retention of AdMSCs aggregates was observed only 24 h followed IR procedure. It would be interesting to detect the retention of AdMSCs aggregates at longer time points. We have started experiments aimed at identifying retention of AdMSCs in kidney at longer time points after IR injury. Second, 3D AdMSCs aggregates were delivered directly into the injured kidney. Despite the therapeutic effects, this delivery method is not suitable in clinical application. Further study would be conducted to investigate the effect of AdMSCs aggregates injected intravenously.

5. Conclusion

Our data provides for the first time that 3D AdMSCs aggregates possess survival benefits when implanted into rat kidney following IR injury. Microwell is effective in producing scale of 3D AdMSCs aggregates, which could be utilized to advance the efficacy of AdMSCs therapy for renal IR injury.

Conflict of Interests

The authors declare that there is no conflict of interests regarding the publication of this paper.

Authors' Contribution

Xiaozhi Zhao, Xuefeng Qiu, and Yanting Zhang contributed equally.

Acknowledgments

This study was supported by a grant from the National Natural Science Foundation of China (81302542, 81371207, and 81171047), China Postdoctoral Science Foundation (2014M551562), and Fundamental Research Funds for the Central Universities (20620140532).

References

[1] Y. Jiang, B. N. Jahagirdar, R. L. Reinhardt et al., "Pluripotency of mesenchymal stem cells derived from adult marrow," *Nature*, vol. 418, no. 6893, pp. 41–49, 2002.

[2] M. F. Pittenger, A. M. Mackay, S. C. Beck et al., "Multilineage potential of adult human mesenchymal stem cells," *Science*, vol. 284, no. 5411, pp. 143–147, 1999.

[3] C. Lange, F. Tögel, H. Ittrich et al., "Administered mesenchymal stem cells enhance recovery from ischemia/reperfusion-induced acute renal failure in rats," *Kidney International*, vol. 68, no. 4, pp. 1613–1617, 2005.

[4] F. Tögel, Z. Hu, K. Weiss, J. Isaac, C. Lange, and C. Westenfelder, "Administered mesenchymal stem cells protect against ischemic acute renal failure through differentiation-independent mechanisms," *The American Journal of Physiology—Renal Physiology*, vol. 289, no. 1, pp. F31–F42, 2005.

[5] Y. Wang, J. He, X. Pei, and W. Zhao, "Systematic review and meta-analysis of mesenchymal stem/stromal cells therapy for impaired renal function in small animal models," *Nephrology*, vol. 18, no. 3, pp. 201–208, 2013.

[6] F. Tögel, K. Weiss, Y. Yang, Z. Hu, P. Zhang, and C. Westenfelder, "Vasculotropic, paracrine actions of infused mesenchymal stem cells are important to the recovery from acute kidney injury," *American Journal of Physiology: Renal Physiology*, vol. 292, no. 5, pp. F1626–F1635, 2007.

[7] C. Mias, E. Trouche, M.-H. Seguelas et al., "Ex vivo pretreatment with melatonin improves survival, proangiogenic/mitogenic activity, and efficiency of mesenchymal stem cells injected into ischemic kidney," *Stem Cells*, vol. 26, no. 7, pp. 1749–1757, 2008.

[8] Y. Chen, H. Qian, W. Zhu et al., "Hepatocyte growth factor modification promotes the amelioration effects of human umbilical cord mesenchymal stem cells on rat acute kidney injury," *Stem Cells and Development*, vol. 20, no. 1, pp. 103–113, 2011.

[9] M. Hagiwara, B. Shen, L. Chao, and J. Chao, "Kallikrein-modified mesenchymal stem cell implantation provides enhanced protection against acute ischemic kidney injury by inhibiting apoptosis and inflammation," *Human Gene Therapy*, vol. 19, no. 8, pp. 807–819, 2008.

[10] M. S. Masoud, S. S. Anwar, M. Z. Afzal, A. Mehmood, S. N. Khan, and S. Riazuddin, "Pre-conditioned mesenchymal stem cells ameliorate renal ischemic injury in rats by augmented survival and engraftment," *Journal of Translational Medicine*, vol. 10, no. 1, article 243, 2012.

[11] J. Gao, R. Liu, J. Wu et al., "The use of chitosan based hydrogel for enhancing the therapeutic benefits of adipose-derived MSCs for acute kidney injury," *Biomaterials*, vol. 33, no. 14, pp. 3673–3681, 2012.

[12] M. Bauer, L. Kang, Y. Qiu et al., "Adult cardiac progenitor cell aggregates exhibit survival benefit both in vitro and in vivo," *PLoS ONE*, vol. 7, no. 11, Article ID e50491, 2012.

[13] S. H. Bhang, S.-W. Cho, W.-G. La et al., "Angiogenesis in ischemic tissue produced by spheroid grafting of human adipose-derived stromal cells," *Biomaterials*, vol. 32, no. 11, pp. 2734–2747, 2011.

[14] S. Sart, A. C. Tsai, Y. Li, and T. Ma, "Three-dimensional aggregates of mesenchymal stem cells: cellular mechanisms, biological properties, and applications," *Tissue Engineering Part B: Reviews*, vol. 20, no. 5, pp. 365–380, 2014.

[15] Y.-S. Hwang, G. C. Bong, D. Ortmann, N. Hattori, H.-C. Moeller, and A. Khademhosseinia, "Microwell-mediated control of embryoid body size regulates embryonic stem cell fate via differential expression of WNT5a and WNT11," *Proceedings of the National Academy of Sciences of the United States of America*, vol. 106, no. 40, pp. 16978–16983, 2009.

[16] H. Ning, G. Liu, G. Lin, R. Yang, T. F. Lue, and C.-S. Lin, "Fibroblast growth factor 2 promotes endothelial differentiation of adipose tissue-derived stem cell," *Journal of Sexual Medicine*, vol. 6, no. 4, pp. 967–979, 2009.

[17] X. Qiu, J. Villalta, L. Ferretti et al., "Effects of intravenous injection of adipose-derived stem cells in a rat model of radiation therapy-induced erectile dysfunction," *Journal of Sexual Medicine*, vol. 9, no. 7, pp. 1834–1841, 2012.

[18] L. Kang, M. J. Hancock, M. D. Brigham, and A. Khademhosseini, "Cell confinement in patterned nanoliter droplets in a microwell array by wiping," *Journal of Biomedical Materials Research—Part A*, vol. 93, no. 2, pp. 547–557, 2010.

[19] D. Li, Q. Liu, Y. Gong, Y. Huang, and X. Han, "Cytotoxicity and oxidative stress study in cultured rat Sertoli cells with Methyl *tert*-butyl ether (MTBE) exposure," *Reproductive Toxicology*, vol. 27, no. 2, pp. 170–176, 2009.

[20] Y.-T. Chen, C.-C. Yang, Y.-Y. Zhen et al., "Cyclosporine-assisted adipose-derived mesenchymal stem cell therapy to mitigate acute kidney ischemia-reperfusion injury," *Stem Cell Research and Therapy*, vol. 4, no. 3, article 62, 2013.

[21] V. Y. Melnikov, S. Faubel, B. Siegmund, M. Scott Lucia, D. Ljubanovic, and C. L. Edelstein, "Neutrophil-independent mechanisms of caspase-1- and IL-18-mediated ischemic acute tubular necrosis in mice," *The Journal of Clinical Investigation*, vol. 110, no. 8, pp. 1083–1091, 2002.

[22] F. Gueler, W. Gwinner, A. Schwarz, and H. Haller, "Long-term effects of acute ischemia and reperfusion injury," *Kidney International*, vol. 66, no. 2, pp. 523–527, 2004.

[23] D. K. de Vries, A. F. Schaapherder, and M. E. Reinders, "Mesenchymal stromal cells in renal ischemia/reperfusion injury," *Frontiers in Immunology*, vol. 3, article 162, 2012.

[24] F. Tögel, A. Cohen, P. Zhang, Y. Yang, Z. Hu, and C. Westenfelder, "Autologous and allogeneic marrow stromal cells are safe and effective for the treatment of acute kidney injury," *Stem Cells and Development*, vol. 18, no. 3, pp. 475–485, 2009.

[25] K. Furuichi, H. Shintani, Y. Sakai et al., "Effects of adipose-derived mesenchymal cells on ischemia-reperfusion injury in kidney," *Clinical and Experimental Nephrology*, vol. 16, no. 5, pp. 679–689, 2012.

[26] Y.-T. Chen, C.-K. Sun, Y.-C. Lin et al., "Adipose-derived mesenchymal stem cell protects kidneys against ischemia-reperfusion injury through suppressing oxidative stress and inflammatory reaction," *Journal of Translational Medicine*, vol. 9, article 51, 2011.

[27] T. Du, X. Zou, J. Cheng et al., "Human Wharton's jelly-derived mesenchymal stromal cells reduce renal fibrosis through induction of native and foreign hepatocyte growth factor synthesis in injured tubular epithelial cells," *Stem Cell Research and Therapy*, vol. 4, no. 3, article 59, 2013.

[28] H. Tsuda, K. Yamahara, K. Otani et al., "Transplantation of allogenic fetal membrane-derived mesenchymal stem cells protects against ischemia/reperfusion-induced acute kidney injury," *Cell Transplantation*, vol. 23, no. 7, pp. 889–899, 2014.

[29] W. Li, Q. Zhang, M. Wang et al., "Macrophages are involved in the protective role of human umbilical cord-derived stromal cells in renal ischemia-reperfusion injury," *Stem Cell Research*, vol. 10, no. 3, pp. 405–416, 2013.

[30] D. A. De Ugarte, K. Morizono, A. Elbarbary et al., "Comparison of multi-lineage cells from human adipose tissue and bone marrow," *Cells Tissues Organs*, vol. 174, no. 3, pp. 101–109, 2003.

[31] A. Winter, S. Breit, D. Parsch et al., "Cartilage-like gene expression in differentiated human stem cell spheroids: a comparison of bone marrow-derived and adipose tissue-derived stromal cells," *Arthritis & Rheumatism*, vol. 48, no. 2, pp. 418–429, 2003.

[32] A. Dicker, K. Le Blanc, G. Åström et al., "Functional studies of mesenchymal stem cells derived from adult human adipose tissue," *Experimental Cell Research*, vol. 308, no. 2, pp. 283–290, 2005.

[33] X. Qiu, T. M. Fandel, L. Ferretti et al., "Both immediate and delayed intracavernous injection of autologous adipose-derived stromal vascular fraction enhances recovery of erectile function in a rat model of cavernous nerve injury," *European Urology*, vol. 62, pp. 720–727, 2012.

[34] W.-Y. Lee, Y.-H. Chang, Y.-C. Yeh et al., "The use of injectable spherically symmetric cell aggregates self-assembled in a thermo-responsive hydrogel for enhanced cell transplantation," *Biomaterials*, vol. 30, no. 29, pp. 5505–5513, 2009.

[35] Y.-C. Yeh, W.-Y. Lee, C.-L. Yu et al., "Cardiac repair with injectable cell sheet fragments of human amniotic fluid stem cells in an immune-suppressed rat model," *Biomaterials*, vol. 31, no. 25, pp. 6444–6453, 2010.

[36] Q. Zhang, A. L. Nguyen, S. Shi et al., "Three-dimensional spheroid culture of human gingiva-derived mesenchymal stem cells enhances mitigation of chemotherapy-induced oral mucositis," *Stem Cells and Development*, vol. 21, no. 6, pp. 937–947, 2012.

Hindawi Publishing Corporation
Stem Cells International
Volume 2016, Article ID 4831524, 9 pages
http://dx.doi.org/10.1155/2016/4831524

Research Article

Encapsulated Whole Bone Marrow Cells Improve Survival in Wistar Rats after 90% Partial Hepatectomy

Carolina Uribe-Cruz,[1,2] Carlos Oscar Kieling,[3,4] Mónica Luján López,[1,2] Alessandro Osvaldt,[5] Gustavo Ochs de Muñoz,[1,6] Themis Reverbel da Silveira,[3,6] Roberto Giugliani,[1,2] and Ursula Matte[1,2,5]

[1]*Gene Therapy Center, Hospital de Clínicas de Porto Alegre, Ramiro Barcelos 2350, 90035-903 Porto Alegre, RS, Brazil*
[2]*Post-Graduation Program on Genetics and Molecular Biology, Federal University of Rio Grande do Sul, Porto Alegre, RS, Brazil*
[3]*Experimental Hepatology and Gastroenterology Laboratory, Experimental Research Center, Hospital de Clínicas de Porto Alegre, Ramiro Barcelos 2350, 90035-903 Porto Alegre, RS, Brazil*
[4]*Post-Graduation Program in Science of Gastroenterology and Hepatology, Federal University of Rio Grande do Sul, Porto Alegre, RS, Brazil*
[5]*Post-Graduation Program in Surgery, Federal University of Rio Grande do Sul, Porto Alegre, RS, Brazil*
[6]*Post-Graduation Program in Adolescent and Child Health, Federal University of Rio Grande do Sul, Porto Alegre, RS, Brazil*

Correspondence should be addressed to Ursula Matte; umatte@hcpa.ufrgs.br

Received 10 December 2014; Revised 18 January 2015; Accepted 28 January 2015

Academic Editor: Kenichi Tamama

Background and Aims. The use of bone marrow cells has been suggested as an alternative treatment for acute liver failure. In this study, we investigate the effect of encapsulated whole bone marrow cells in a liver failure model. *Methods*. Encapsulated cells or empty capsules were implanted in rats submitted to 90% partial hepatectomy. The survival rate was assessed. Another group was euthanized at 6, 12, 24, 48, and 72 hours after hepatectomy to study expression of cytokines and growth factors. *Results*. Whole bone marrow group showed a higher than 10 days survival rate compared to empty capsules group. Gene expression related to early phase of liver regeneration at 6 hours after hepatectomy was decreased in encapsulated cells group, whereas genes related to regeneration were increased at 12, 24, and 48 hours. Whole bone marrow group showed lower regeneration rate at 72 hours and higher expression and activity of caspase 3. In contrast, lysosomal-β-glucuronidase activity was elevated in empty capsules group. *Conclusions*. The results show that encapsulated whole bone marrow cells reduce the expression of genes involved in liver regeneration and increase those responsible for ending hepatocyte division. In addition, these cells favor apoptotic cell death and decrease necrosis, thus increasing survival.

1. Introduction

Acute liver failure (ALF) is characterized by the sudden loss of liver function that results in jaundice, coagulopathy, and hepatic encephalopathy in a previously healthy individual. If not treated it can lead to renal and multiple organ failure, coma, and death [1]. Orthotropic liver transplantation is the treatment of choice for ALF although the lack of a suitable donor in a short period of time can limit the success of this therapy [2]. In addition to that, the lifelong use of immunosuppressant after the transplant possesses side effects in the short and long term [3, 4]. These observations and the high costs of the procedure and its complications have led to the search for alternative approaches to ALF that do not include liver transplant.

The use of bone marrow-derived cells in regenerative medicine has grown in the past years. Their efficacy has been shown in animal models of both chronic [5, 6] and acute liver disease [7–9]. They present several advantages when compared to hepatocytes as they are readily available and can be expanded *in vivo* or *in vitro* [10]. In addition, the use of autologous cells would eliminate the need for immunosuppressants [11]. In animal models, heterologous transplantation of mesenchymal stem cells [12] or encapsulated bone

marrow cells [13] is also performed without immunosuppressants. However the mechanisms by which these cells exert their beneficial effect on liver regeneration are not completely well understood. They may involve an increase in the number of hepatocytes by either transdifferentiation, fusion, and/or the secretion of paracrine factors that stimulate cell division, inhibit apoptosis, or modulate local and systemic inflammatory state [10, 14].

Several proinflammatory factors are involved in the early phase of liver regeneration. After partial hepatectomy, the increased amounts of enteric lipopolysaccharides (LPS) that bind to Tlr-4 (toll like receptor 4) on Kupffer cells activate the MYD88 (myeloid differentiation factor) pathway and trigger the activation of Nfκ-B (nuclear factor kappa B) and the release of Tnf-α (tumor necrosis factor-α) and Il-6 (interleukin-6) [15]. Il-6 plays a key role in liver regeneration, activating acute phase genes and priming hepatocytes to growth factors [16, 17]. Hgf (hepatocyte growth factor) then stimulates hepatocytes to pass from G0 to G1, thus initiating the cell cycle [18, 19]. The increase in molecules such as Socs3 (suppressor of cytokine signaling 3) and Tgf-β1 (transforming growth factor-beta) contributes to the decrease in stimulating factors and the halt of liver regeneration [18, 20].

After partial hepatectomy, there is a complex remodeling of the liver tissue with a transient disruption of the lobular architecture [21]. Agglomerates of poorly vascularized hepatocytes are formed in the periportal area before invasion of sinusoidal cells [20, 22]. Some authors have suggested that at the early stages of liver regeneration a very fine tuning in the rate of proliferation of parenchymal and nonparenchymal cells is needed. Ninomiya et al. [22] showed that a slowed hepatocyte regeneration rate increased the survival in a model of 90% partial hepatectomy.

Our goal was to investigate the paracrine effects of bone marrow cells and the mechanisms by which they increase survival in a rat model of 90% partial hepatectomy.

2. Methods

2.1. Animals. Two-month-old male outbred Wistar rats, weighing 310.5 ± 33 g, were housed under controlled temperature (between 18 and 22°C) in light-dark cycles of 12 h with free access to water and standard chow at the Experimental Animal Unit at Hospital de Clínicas de Porto Alegre (HCPA). Handling, care, and processing of animals were carried out according to regulations approved by our local ethics committee (protocol number 10-0062) and complied with the National Guidelines on Animal Care.

2.2. Experimental Design. Animals were submitted to 90% partial hepatectomy (90% PH) and randomly divided in two groups. Treated group received encapsulated whole bone marrow cells (WBM, $n = 11$) and control group ($n = 15$) received empty capsules (EC). Survival was observed for up to 10 days after 90% PH. An additional set of animals from both groups was sacrificed at 6, 12, 24, 48, and 72 hours after 90% PH ($n = 6$/group/time point) to evaluate the early effects of treatments.

2.3. Isolation of Whole Bone Marrow Cells and Encapsulation. Thirty-three animals without liver injury were used as donors of WBM cells. In a sterile environment, the femurs and tibias were isolated and WBM from each bone was flushed with 3 mL complete medium: DMEM (Dulbecco's Modified Eagle Medium, LGC, Brazil) supplemented with 10% fetal bovine serum (Gibco, USA), 1% penicillin/streptomycin (Gibco, USA). Cell viability was determined by Trypan's Blue exclusion.

Cell encapsulation was performed according to our laboratory protocol, previously described [23]. Briefly, WBM cells were mixed with 1.5% sodium alginate (Sigma-Aldrich, USA) in complete medium and extruded through an Encapsulation Unit type J1 (Nisco, Switzerland), attached to JMS Syringe Pump. Droplets were sheared off with an air flow of 5 L/min delivered to the tip of a 27 G needle and the rate of infusion was 40 mL/h. The droplets fell into a bath of 125 mM $CaCl_2$ and ionically cross-linked with $Ca_2{}^+$ to form solid spherical hydrogel beads containing embedded WBM cells. For control group, empty capsules were produced using the same approach, although without cells. The resulting capsules were maintained under normal cell culture conditions with complete medium at 37°C and 5% CO_2 for 24 h prior to transplantation.

2.4. Surgical Procedure and Capsules Transplantation. Ninety percent hepatectomy was performed by a single operator as described by Gaub and Iversen [24]. In brief, the left lateral (30%), left median (40%), and right superior lobes (20%) were removed, leaving only the caudate lobes. Hepatectomy was carried out under isoflurane (Forane, Abbott SA, Argentina) anesthesia [25]. Immediately after 90% PH and before complete suture, microcapsules (containing 3×10^7 WBM cells [26] or empty) were placed into the peritoneal cavity and glucose was supplemented i.p. (5% of body weight). Postoperatively, animals were given i.p. glucose (5% of body weight) until day seven and received 20% glucose in their drinking water and standard chow *ad libitum*.

2.5. Euthanasia. Euthanasia was performed in CO_2 chambers. To evaluate survival, the animals were euthanized 10 days after 90% HP. To evaluate the early effects of treatments the animals were euthanized 6, 12, 24, 48, and 72 h after 90% HP and immediately blood was collected, the liver was removed and weighed, and part was flash frozen in liquid nitrogen or set at paraffin.

2.6. Quantitative Real-Time PCR. Total RNA was extracted from 50 mg of liver tissue using TRIzol reagent (Invitrogen, USA) according to the manufacturer's instructions. Two micrograms of RNA was reverse-transcribed using High Capacity cDNA Reverse Transcription Kit (Life Technologies, USA). Gene expression was measured using TaqMan assays (Life Technologies, USA) for genes involved in hepatic regeneration (Table 1). The percentage of a test RNA to that of β-actin was calculated by subtracting the cycle to reach the threshold (CT) for a gene from the CT for a separate assay using β-actin assay to determine the ΔCT and the following

Table 1: TaqMan (Life Technologies, USA) ID assays for genes analyzed in this study.

Gene symbol	Assay ID
Act-β	Rn00667869_m1
Hgf	Rn00566673_m1
Il-6	Rn01410330_m1
Myd88	Rn01640049_m1
Nfκ-B	Rn01399583_m1
Socs3	Rn00585674_m1
Tgf-β	Rn01475963_m1
Tlr-4	Rn00569848_m1
Tnf-α	Rn00562055_m1
Casp3	Rn00563902_m1

formula: percent β-actin = (100) $\times$ $2^{\Delta CT}$ [27]. The percent β-actin for hepatectomized animals was divided by the percent β-actin in normal animals to determine the ratio of the gene in both treatments after 90% PH to normal rats. Livers of animals without injury were used as calibrator group ($n = 5$).

2.7. Liver Regeneration Rate. The liver regeneration rate was calculated as follows: liver regeneration rate (%) = $100 \times [C - (A - B)]/A$, where A is the estimated liver weight before PH, B is the excised liver weight at the time of PH, and C is the weight of the regenerated liver at the time of sacrifice [28].

2.8. Histology. Paraffin-embedded liver specimens were cut in 4 μm sections and stained with hematoxylin and eosin (H-E). To assess the rate of hepatocyte proliferation, the number of hepatocytes undergoing mitosis was counted in 10 high-power fields (HPF) in 72 hs after HP (mitotic index) [29].

To determine the number and the size of parenchymal cells per slide, the hepatocytes nuclei were counted and internuclear distance was measured in 5 HPF using Cell Imaging Software for Life Science Microscopy (Olympus) at 72 h after HP.

2.9. Enzyme Assays. Fluorimetric caspase activity (Sigma-Aldrich, USA) assays were performed according to manufacturer's instruction. Briefly, approximately 100 μg of liver was placed in an opaque 96-well plate and 200 μL of mixture reaction solution (containing acetyl-Asp-Glu-Val-Asp-7-amido-4-methylcoumarin) was added in each well. The plate was incubated in dark at 25°C and every 10 minutes the fluorescence was read at 360 nm of excitation and 460 of emission. Caspase activity was normalized by protein.

For lysosomal-β-glucuronidase (Gusb) measurement, livers were homogenized in PBS buffer with proteases inhibitor cocktail 1%. Assays were performed using the chromogenic substrates 4-methylumbelliferyl-β-L-glucuronide (Sigma-Aldrich) at pH 4.5. One unit of enzyme activity converts 1 nmol of substrate to product per hour at 37°C.

2.10. Statistical Analysis. Results were expressed as means ± standard deviation (SD) or medians when required. Statistical differences were assessed by Student's t-test and for nonparametric variables Mann-Whitney test was used. The survival rate was analyzed by Kaplan-Meier curve. The comparison of survival rates in different groups was tested by the log rank test. P values less than .05 were considered statistically significant.

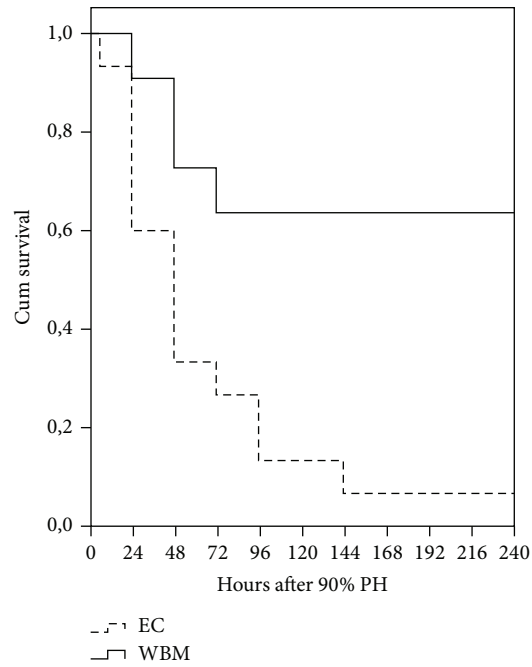

Figure 1: Spontaneous survival according to therapeutic regimen in rats after 90% partial hepatectomy (PH). EC: empty capsules, WBM: whole bone marrow, and Cum: cumulative. Log rank = .002.

3. Results

3.1. Survival Rate. Overall survival rate was observed during 10 days after hepatectomy. The survival rate was higher for the WBM group (63.6%) than for EC group (6.7%) ($P = .002$). Animals in WBM group died predominantly during the first three days, whereas in the other group deaths occurred over time after surgery (Figure 1). Therefore, to evaluate the effect of encapsulated WBM on the regeneration pathway the remaining analyses were performed in the first 72 hours after 90% PH.

3.2. Expression of Genes Involved in Liver Regeneration. First we assessed the expression levels of genes related to the early phase of liver regeneration. The expression of *Tnf-α* ($P = .01$) and *Nfκ-B* ($P = .01$) was markedly decreased in WBM group at 6 hours after 90% PH (Figures 2(a) and 2(b)). As a result, the expression of *Il-6* was also decreased ($P = .04$) in the WBM group compared to EC group (Figure 2(c)). Interestingly, LPS receptor (*Tlr-4*) and its mediator (*Myd88*) showed no differences in gene expression between groups 6 hours after 90% HP (Figures 2(d) and 2(e)).

We then analyzed genes related to the progress of liver regeneration. At 12, 24, and 48 hours after 90% PH other

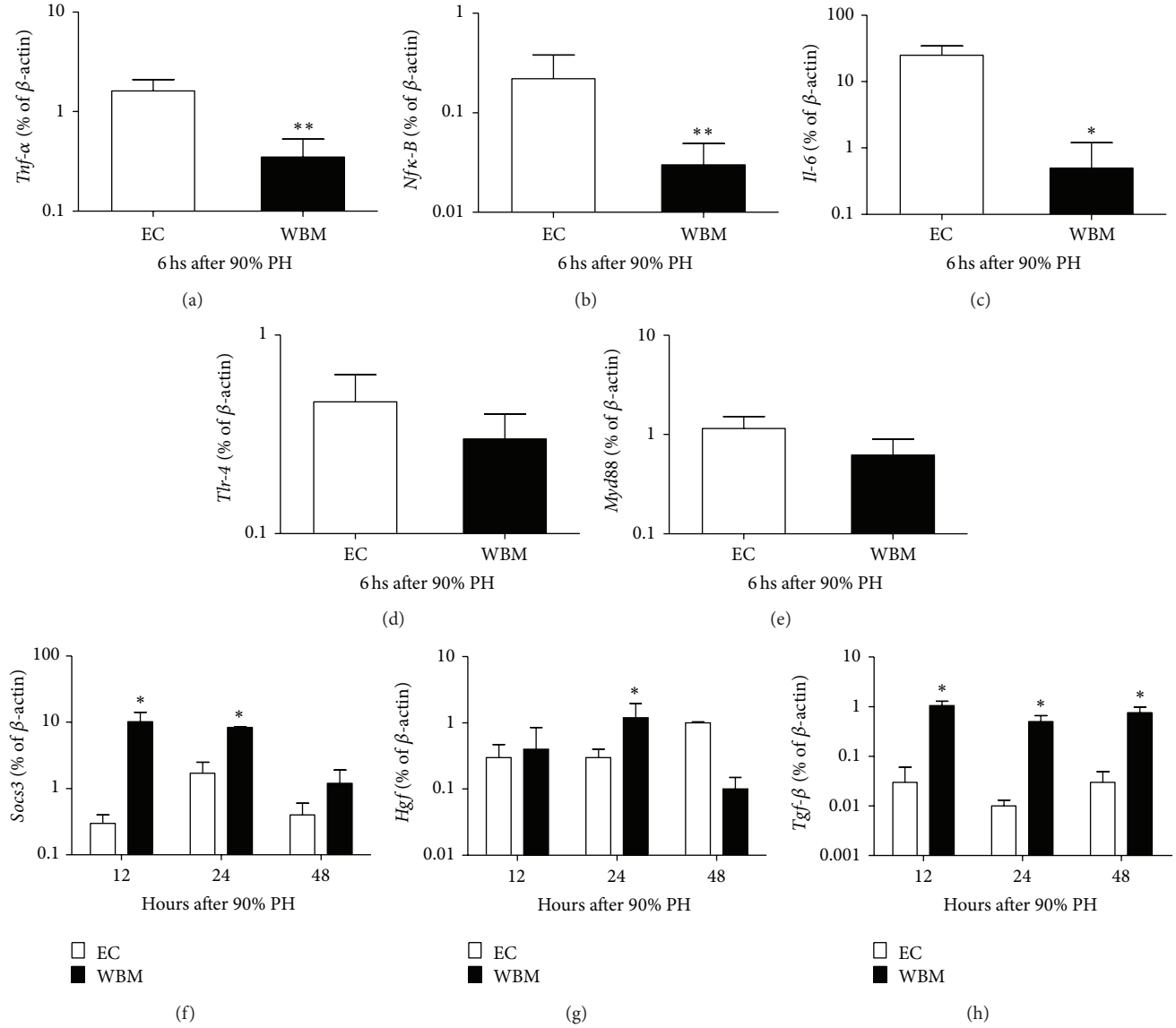

FIGURE 2: Liver gene expression after 90% partial hepatectomy (PH). Liver gene expression of *Tnf-α* (a), *Nfκ-B* (b), *Il-6* (c), *Tlr-4* (d), and *Myd88* (e) 6 hours after 90% partial hepatectomy and *Socs3* (f), *Hgf* (g), and *Tgf-β* (h) 12, 24, and 48 hours after 90% partial hepatectomy. WBM: whole bone marrow; EC: empty capsules. Values are expressed as means ± SD in log scale. Student's *t*-test, $^{*}P < .05$, $^{**}P < .01$.

genes were also differently expressed between WBM and EC groups. *Socs3*, which inhibits signaling via *Il-6*, was increased in the WBM group at 12 and 24 hours after 90% PH ($P \leq .05$, Figure 2(f)). *Hgf* was slightly increased in WBM only 24 hours after 90% PH ($P = .04$, Figure 2(g)), whereas the expression of *Tgf-β* was increased in WBM group in 12–48 hrs ($P \leq .03$, Figure 2(h)).

3.3. Liver Regeneration Rate and Histology Analysis. Interestingly, genes that promote liver regeneration were decreased in WBM group, whereas genes that halt hepatocyte division were increased. On the other hand, liver regeneration rate increased gradually after surgery, but without differences between groups at 6, 12, 24, or 48 hours. However, as shown in Figure 3(a), at 72 hours WBM group showed a lower regeneration rate compared to EC group (44% versus 59%, $P = .003$). Nevertheless, no differences were found in the number of mitotic cells in both groups (Figure 3(b)) and the number of hepatocytes at 72 hours after PH was also similar (Figure 3(c)). Surprisingly, the internuclear distance among hepatocytes was higher in EC group compared to WBM group at 72 hours ($P = .003$; Figure 3(d)), indicating that hepatocytes in WBM group were smaller than in EC group, resembling that of normal liver (data not shown). This could explain the lower regeneration rate, measured by changes in the remnant liver weight.

3.4. Mechanisms of Cell Death. Since no differences were found regarding cell proliferation, we then investigated if encapsulated WBM cells could lead to differential cell death.

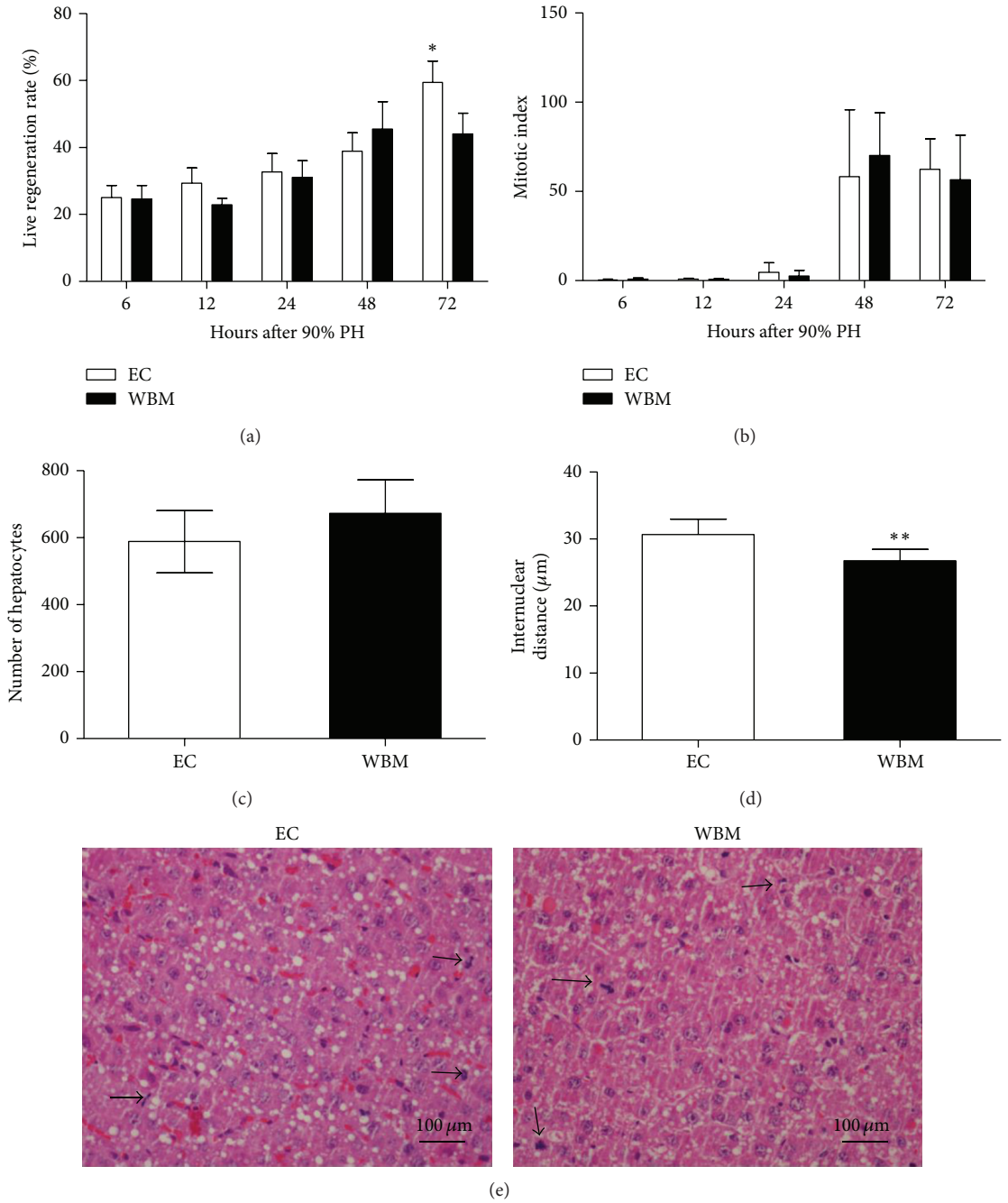

Figure 3: Liver regeneration rate after 90% partial hepatectomy (a). Mitotic index of hepatocytes after 90% partial hepatectomy (b). Number of hepatocytes (c) and internuclear distance (d) at 72 hours after partial hepatectomy. (e) Histology of mitotic hepatocytes (arrows) 72 hours after 90% partial hepatectomy; liver slides were stained with H-E. WBM: whole bone marrow; EC: empty capsules. Values are expressed as means ± SD. Student's t-test, $^{*}P < .05$, $^{**}P < .01$.

In order to assess possible mechanisms of cell death associated with our results, we quantified Caspase 3 as a measure of apoptosis and Gusb activity as an indicator of necrosis. We observed that WBM group had higher levels of *Casp3* at all times points ($P < .05$, Figure 4(a)), except at 72 hours where there was no difference between groups. Caspase 3 activity was also assessed in liver homogenates at 24, 48, and 72 hours. It was increased in WBM compared to EC group only at 48 hours ($P = .013$; Figure 4(b)), suggesting that cells from WBM group are dying by apoptosis. Interestingly when we evaluated Gusb activity at the same time point, WBM group presented less activity at 72 hours than EC group ($P = .009$; Figure 4(c)) suggesting that hepatocytes from EC group are dying by necrosis.

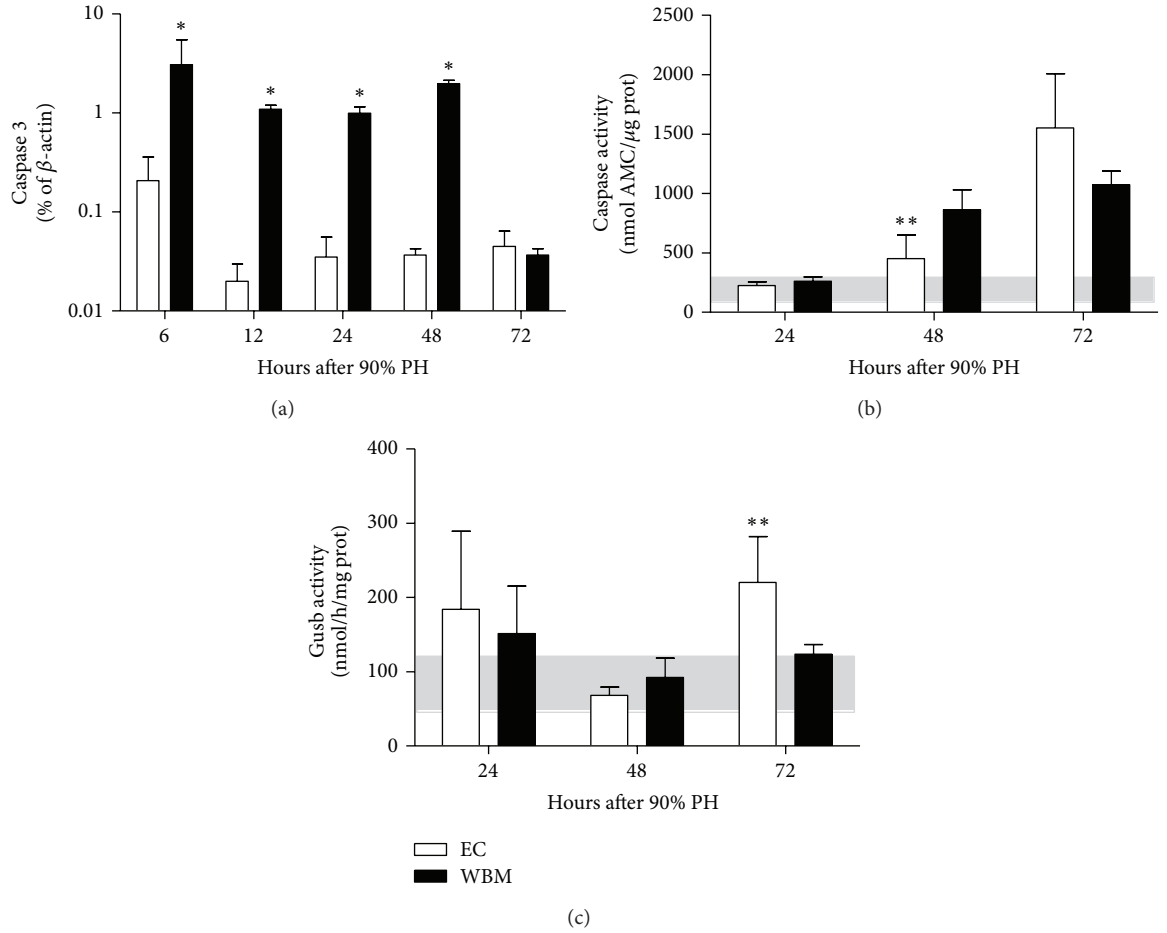

FIGURE 4: Mechanisms of cell death after 90% partial hepatectomy (PH). (a) Liver gene expression of *Caspase 3* at 6, 12, 24, 48, and 72 hours after 90% PH. (b) Caspase 3 activity and (c) lysosomal-β-glucuronidase (Gusb) activity at 24, 48, and 72 hours after 90% PH. Gray bar indicates normal values. WBM: whole bone marrow; EC: empty capsules. Values are expressed as means ± SD. Student's t-test, $^{*}P < .05$; $^{**}P < .01$.

4. Discussion

In the present study we showed that encapsulated WBM cells increase ten-day survival in a model of 90% PH by acting very early in the regenerative process. At 6 hours after 90% PH the synthesis of inflammatory cytokines in the liver was reduced. Moreover, the expression of factors abrogating liver regeneration (such as *Tgf β* and *Socs3*) was increased from 12 hours on, thus suggesting a decrease in the pace of liver regeneration through the secretion of paracrine factors. Our results corroborate the findings of Liu and Chang [13, 28, 29, 32], who showed that encapsulated WBM cells increased survival in rats after 90% PH.

The increase in 10-day survival rate from 6.7% in EC group to 63.6% in the treated group may not be directly comparable to other data in the literature. Indeed the survival rate after 90% PH is quite variable. It depends on many factors, including the surgeon's experience, the use of glucose, and the type of anesthesia [25]. In fact, some authors report 100% survival in one week [30] whereas others have 0% survival after 2 days [31], both using glucose supplementation as in the present study. Therefore, it is important to compare the differences between treated and untreated animals within the same research group, as all animals are submitted to the same surgeon, anesthetic protocol, and glucose administration. Also, there is no group without empty capsules (EC); therefore an influence of alginate itself in the survival curve cannot be ruled out. Yet, the results reported here can be compared to those of Liu and Chang [32] who reported 35% survival in empty capsules group in 10 days (and 100% in those treated with whole bone marrow cells). However, they showed an increase in the secretion of Hgf suggesting that it stimulated liver regeneration [32].

We evaluated the expression of inflammatory cytokines *Il-6*, *Tnf-α*, and *Nfκ-B* that are pivotal for the beginning of liver regeneration [33]. We observed that these cytokines were all decreased in WBM group at 6 hours after 90% PH. We then hypothesized that this reduction could be, at least in part, due to a decreased signaling by Kupffer cells. It is known that after partial hepatectomy Kupffer cells are overloaded with enteric antigens and that LPS-binding to Tlr-4 triggers the regenerative process [34]. However, no differences in

expression of *Tlr-4* and its mediator *Myd88* were detected between groups. It is worth noticing that such differences may have occurred at earlier time points and therefore would not be detected by this study.

Consistent with this decrease in genes related to the promotion of early regenerative phase, *Hgf* was also not increased in WBM group, except at 24 hours after 90% PH. On the other hand, the expression of *Tgf-β*, an inhibitor of Hgf [35], was markedly increased in WBM group between 12 and 48 hours. In addition to that, the expression of *Socs3*, an important negative regulator of IL-6 that blocks Stat3 phosphorylation [36, 37], was also increased in WBM group. Taken together, these data suggest that encapsulated WBM cells are increasing survival by decreasing liver regeneration rate.

Nevertheless, the liver regeneration rate was similar in both groups until 48 hours. Only at 72 hours did WBM group show a decreased regeneration rate compared to EC group. Ninomiya et al. [22] suggested that the abrupt regenerative response after PH causes a derangement of the lobular architecture that is damaging to hepatocytes. In their work, the deceleration of liver regeneration increases survival rate after 90% PH. Accordingly, in the present study WBM group survival rate was 63% compared to 6.7% in EC group at 10 days after surgery.

It is important to stress that the rate of regeneration mentioned above is evaluated by the weight of the remaining liver. Thus, a more precise measure of regeneration rate would be mitotic index or hepatocyte number. However, when we evaluate these parameters we found no differences between the WBM group and EC group. Nevertheless, the internuclear distance was smaller in WBM group, suggesting that hepatocytes were smaller when compared with EC group. Therefore, these results point to the fact that hepatocytes of EC group are swelled and this may contribute to an increase in the reminiscent liver weight.

Cell swelling is an indication of hydropic degeneration, as observed by López et al. [37] in the 90% PH model. This led us to hypothesize that WBM group's hepatocytes are healthier than EC group's hepatocytes, maybe due to protective cell death. Both *Caspase 3* gene expression and activity were increased in the WBM group. Furthermore, Gusb activity, a marker of necrosis [38], was lower in WBM group. These results indicate that in the WBM group the predominant mechanism of cell death is apoptosis whereas in the EC group it is necrosis.

Apoptosis may be considered a controlled process to eliminate malfunctioning cells and results in apoptotic bodies that will be phagocyte by other cells [39]. Necrosis, on the other hand, is a traumatic cell death in which cells swell until the lysis and spread of intracellular components, which will trigger the immune response, leading to inflammation [39]. We observed that in both groups liver cells died as a consequence of injury; nonetheless in WBM group the death is cleaned and controlled.

It is worth noticing that donor and recipient animals were not related, as our experiments were performed in Wistar rats, which are outbred animals. However, as the cells are encapsulated in alginate beads no immune reaction against the cells is expected; that is the function of the capsules. The allograft model seems to be a better option as in a clinical setting one may not expect a patient in acute liver failure to be able to provide cells for transplantation or to wait for a match donor to be found.

In summary the results presented here show that encapsulated WBM cells increase survival in a model of 90% PH, reduce the expression of genes involved in liver regeneration, such as *Tnf-α*, *Nfκ-B*, *Il-6*, and *Hgf*, and increase those responsible for ending hepatocyte division, such as *Tgf-β* and *Socs3*. In addition to that, these cells favor apoptotic cell death and decrease necrosis, thus increasing long term survival. Although there is no definitive answer on how these cells exert their beneficial effects, a few hypotheses may be ruled out. There is no immunomodulatory effect of stem cells, as data on systemic cytokine levels did not differ between groups (Supplementary Figure 1 in Supplementary Material available online at http://dx.doi.org/10.1155/2016/4831524). Differences related to genes involved in liver regeneration were found but point to the opposite direction (as one would expect survival to be related to a faster regeneration). Also, no difference was found on cell proliferation. Unfortunately we were unable to retrieve enough RNA from recovered capsules in order to investigate what kind of changes happened in WBM cells, although preliminary data from an ongoing study from our group suggest that they may be compensating for some liver function, as well as which specific cell types are involved in this response.

Abbreviations

ALF: Acute liver failure
WBM: Whole bone marrow
EC: Empty capsules
PH: Partial hepatectomy
LPS: Lipopolysaccharides
Tlr-4: Toll like receptor 4
MYD88: Myeloid differentiation factor
Tnf: Tumor necrosis factor
Il-6: Interleukin-6
Hgf: Hepatocyte growth factor
Tgf-β: Transforming growth factor-beta
Nfκ-B: Nuclear factor kappa B
Socs3: Suppressor of cytokine signaling 3
Gusb: Lysosomal-β-glucuronidase
SD: Standard deviation.

Conflict of Interests

The authors have no conflict of interests to declare.

Authors' Contribution

Carolina Uribe-Cruz and Carlos Oscar Kieling contributed equally to this work.

Acknowledgment

This work was supported by FIPE/HCPA, PRONEX/FAPERGS 10/0039-3.

References

[1] R. T. Chung, R. T. Stravitz, R. J. Fontana et al., "Pathogenesis of liver injury in acute liver failure," *Gastroenterology*, vol. 143, no. 3, pp. e1–e7, 2012.

[2] A. Canbay, F. Tacke, J. Hadem, C. Trautwein, G. Gerken, and M. P. Manns, "Acute liver failure—a life-threatening disease," *Deutsches Arzteblatt*, vol. 108, no. 42, pp. 714–720, 2011.

[3] A. Strauss, E. Grabhorn, M. Sornsakrin et al., "Liver transplantation for fulminant hepatic failure in infancy: a single center experience," *Pediatric Transplantation*, vol. 13, no. 7, pp. 838–842, 2009.

[4] P. Mahadeb, J. Gras, E. Sokal et al., "Liver transplantation in children with fulminant hepatic failure: the UCL experience," *Pediatric Transplantation*, vol. 13, no. 4, pp. 414–420, 2009.

[5] A. C. Lyra, M. B. P. Soares, L. F. M. da Silva et al., "Infusion of autologous bone marrow mononuclear cells through hepatic artery results in a short-term improvement of liver function in patients with chronic liver disease: a pilot randomized controlled study," *European Journal of Gastroenterology and Hepatology*, vol. 22, no. 1, pp. 33–42, 2010.

[6] L. Y. Ghanem, M. M. Nosseir, A. A. Lotfi et al., "Hematopoietic stem cell mobilization into the peripheral circulation in patients with chronic liver diseases: stem cell mobilization in liver diseases," *Journal of Digestive Diseases*, vol. 13, no. 11, pp. 571–578, 2012.

[7] M. C. Belardinelli, F. Pereira, G. Baldo et al., "Adult derived mononuclear bone marrow cells improve survival in a model of acetaminophen-induced acute liver failure in rats," *Toxicology*, vol. 247, no. 1, pp. 1–5, 2008.

[8] H. Tokai, Y. Kawashita, Y. Ito et al., "Efficacy and limitation of bone marrow transplantation in the treatment of acute and subacute liver failure in rats," *Hepatology Research*, vol. 39, no. 11, pp. 1137–1143, 2009.

[9] G. Baldo, R. Giugliani, C. Uribe et al., "Bone marrow mononuclear cell transplantation improves survival and induces hepatocyte proliferation in rats after CCl_4 acute liver damage," *Digestive Diseases and Sciences*, vol. 55, no. 12, pp. 3384–3392, 2010.

[10] G. Almeida-Porada, E. D. Zanjani, and C. D. Porada, "Bone marrow stem cells and liver regeneration," *Experimental Hematology*, vol. 38, no. 7, pp. 574–580, 2010.

[11] P. A. Lysy, D. Campard, F. Smets, M. Najimi, and E. M. Sokal, "Stem cells for liver tissue repair: current knowledge and perspectives," *World Journal of Gastroenterology*, vol. 14, no. 6, pp. 864–875, 2008.

[12] I. Moscoso, J. Barallobre, Ó. M. de Ilarduya et al., "Analysis of different routes of administration of heterologous 5-azacytidine-treated mesenchymal stem cells in a porcine model of myocardial infarction," *Transplantation Proceedings*, vol. 41, no. 6, pp. 2273–2275, 2009.

[13] Z. C. Liu and T. M. S. Chang, "Transplantation of bioencapsulated bone marrow stem cells improves hepatic regeneration and survival of 90% hepatectomized rats: a preliminary report," *Artificial Cells, Blood Substitutes, and Immobilization Biotechnology*, vol. 33, no. 4, pp. 405–410, 2005.

[14] D. D. Houlihan and P. N. Newsome, "Critical review of clinical trials of bone marrow stem cells in liver disease," *Gastroenterology*, vol. 135, no. 2, pp. 438–450, 2008.

[15] J. Vaquero, K. J. Riehle, N. Fausto, and J. S. Campbell, "Liver regeneration after partial hepatectomy is not impaired in mice with double deficiency of *Myd88* and *IFNAR* genes," *Gastroenterology Research and Practice*, vol. 2011, Article ID 727403, 8 pages, 2011.

[16] T. Wuestefeld, C. Klein, K. L. Streetz et al., "Interleukin-6/glycoprotein 130-dependent pathways are protective during liver regeneration," *The Journal of Biological Chemistry*, vol. 278, no. 13, pp. 11281–11288, 2003.

[17] R. Taub, "Liver regeneration: from myth to mechanism," *Nature Reviews Molecular Cell Biology*, vol. 5, no. 10, pp. 836–847, 2004.

[18] N. Fausto and K. J. Riehle, "Mechanisms of liver regeneration and their clinical implications," *Journal of Hepato-Biliary-Pancreatic Surgery*, vol. 12, no. 3, pp. 181–189, 2005.

[19] K. Sudo, Y. Yamada, K. Saito et al., "TNF-α and IL-6 signals from the bone marrow derived cells are necessary for normal murine liver regeneration," *Biochimica et Biophysica Acta—Molecular Basis of Disease*, vol. 1782, no. 11, pp. 671–679, 2008.

[20] G. K. Michalopoulos, "Liver regeneration," *Journal of Cellular Physiology*, vol. 213, no. 2, pp. 286–300, 2007.

[21] K. E. Wack, M. A. Ross, V. Zegarra, L. R. Sysko, S. C. Watkins, and D. B. Stolz, "Sinusoidal ultrastructure evaluated during the revascularization of regenerating rat liver," *Hepatology (Baltimore, Md.)*, vol. 33, no. 2, pp. 363–378, 2001.

[22] M. Ninomiya, K. Shirabe, T. Terashi et al., "Deceleration of regenerative response improves the outcome of rat with massive hepatectomy: the pathogenesis of small-for-size syndrome," *The American Journal of Transplantation*, vol. 10, no. 7, pp. 1580–1587, 2010.

[23] V. L. Lagranha, G. Baldo, T. G. de Carvalho et al., "*In vitro* correction of ARSA deficiency in human skin fibroblasts from Metachromatic Leukodystrophy patients after treatment with microencapsulated recombinant cells," *Metabolic Brain Disease*, vol. 23, no. 4, pp. 469–484, 2008.

[24] J. Gaub and J. Iversen, "Rat liver regeneration after 90% partial hepatectomy," *Hepatology*, vol. 4, no. 5, pp. 902–904, 1984.

[25] C. O. Kieling, A. N. Backes, R. L. Maurer et al., "The effects of anesthetic regimen in 90% hepatectomy in rats," *Acta Cirurgica Brasileira*, vol. 27, no. 10, pp. 702–706, 2012.

[26] Z. C. Liu and T. M. S. Chang, "Transdifferentiation of bioencapsulated bone marrow cells into hepatocyte-like cells in the 90% hepatectomized rat model," *Liver Transplantation*, vol. 12, no. 4, pp. 566–572, 2006.

[27] G. Baldo, S. Wu, R. A. Howe et al., "Pathogenesis of aortic dilatation in mucopolysaccharidosis VII mice may involve complement activation," *Molecular Genetics and Metabolism*, vol. 104, no. 4, pp. 608–619, 2011.

[28] L. Zhang, J.-S. Ye, V. Decot, J.-F. Stoltz, and L. Zheng, "Research on stem cells as candidates to be differentiated into hepatocytes," *Bio-Medical Materials and Engineering*, vol. 22, no. 1–3, pp. 105–111, 2012.

[29] K. Tryfonidis, M. Kafousi, M. Perraki et al., "Detection of circulating cytokeratin-19 mRNA-positive cells in the blood and the mitotic index of the primary tumor have independent prognostic value in early breast cancer," *Clinical Breast Cancer*, vol. 14, no. 6, pp. 442–450, 2014.

[30] K. Watanabe, S. Togo, T. Takahashi et al., "PAI-1 plays an important role in liver failure after excessive hepatectomy in the rat," *Journal of Surgical Research*, vol. 143, no. 1, pp. 13–19, 2007.

[31] Y. Panis, D. M. McMullan, and J. C. Emond, "Progressive necrosis after hepatectomy and the pathophysiology of liver failure after massive resection," *Surgery*, vol. 121, no. 2, pp. 142–149, 1997.

[32] Z. C. Liu and T. M. S. Chang, "Preliminary study on intrasplenic implantation of artificial cell bioencapsulated stem cells to increase the survival of 90% hepatectomized rats," *Artificial Cells, Blood Substitutes, and Biotechnology*, vol. 37, no. 1, pp. 53–55, 2009.

[33] G. Garcea and G. J. Maddern, "Liver failure after major hepatic resection," *Journal of Hepato-Biliary-Pancreatic Surgery*, vol. 16, no. 2, pp. 145–155, 2009.

[34] J. Vaquero, J. S. Campbell, J. Haque et al., "Toll-like receptor 4 and myeloid differentiation factor 88 provide mechanistic insights into the cause and effects of interleukin-6 activation in mouse liver regeneration," *Hepatology*, vol. 54, no. 2, pp. 597–608, 2011.

[35] Y. Arakawa, M. Shimada, H. Uchiyama et al., "Beneficial effects of splenectomy on massive hepatectomy model in rats," *Hepatology Research*, vol. 39, no. 4, pp. 391–397, 2009.

[36] K. J. Riehle, Y. Y. Dan, J. S. Campbell, and N. Fausto, "New concepts in liver regeneration," *Journal of Gastroenterology and Hepatology*, vol. 26, no. 1, pp. 203–212, 2011.

[37] M. L. López, C. O. Kieling, C. Uribe Cruz et al., "Platelet increases survival in a model of 90% hepatectomy in rats," *Liver International*, vol. 34, no. 7, pp. 1049–1056, 2014.

[38] H. Ohta, "Measurement of serum immunoreactive beta-glucuronidase: a possible serological marker for histological hepatic cell necrosis and to predict the histological progression of hepatitis," *Hokkaido Igaku Zasshi*, vol. 66, no. 4, pp. 545–557, 1991.

[39] S. L. Fink and B. T. Cookson, "Apoptosis, pyroptosis, and necrosis: mechanistic description of dead and dying eukaryotic cells," *Infection and Immunity*, vol. 73, no. 4, pp. 1907–1916, 2005.

Hindawi Publishing Corporation
Stem Cells International
Volume 2016, Article ID 2018474, 11 pages
http://dx.doi.org/10.1155/2016/2018474

Research Article

Effects of Magnetically Guided, SPIO-Labeled, and Neurotrophin-3 Gene-Modified Bone Mesenchymal Stem Cells in a Rat Model of Spinal Cord Injury

Rui-Ping Zhang,[1] Ling-Jie Wang,[1] Sheng He,[1] Jun Xie,[2] and Jian-Ding Li[1]

[1]*Department of Radiology, First Hospital of Shanxi Medical University, Taiyuan 030001, China*
[2]*Department of Molecular Biology, Shanxi Medical University, Taiyuan, Shanxi 030001, China*

Correspondence should be addressed to Jun Xie; 1900547207@qq.com and Jian-Ding Li; 4617784@qq.com

Received 9 February 2015; Revised 30 March 2015; Accepted 31 March 2015

Academic Editor: Jianjun Guan

Despite advances in our understanding of spinal cord injury (SCI) mechanisms, there are still no effective treatment approaches to restore functionality. Although many studies have demonstrated that transplanting *NT3* gene-transfected bone marrow-derived mesenchymal stem cells (BMSCs) is an effective approach to treat SCI, the approach is often low efficient in the delivery of engrafted BMSCs to the site of injury. In this study, we investigated the therapeutic effects of magnetic targeting of *NT3* gene-transfected BMSCs via lumbar puncture in a rat model of SCI. With the aid of a magnetic targeting cells delivery system, we can not only deliver the engrafted BMSCs to the site of injury more efficiently, but also perform cells imaging in vivo using MR. In addition, we also found that this composite strategy could significantly improve functional recovery and nerve regeneration compared to transplanting *NT3* gene-transfected BMSCs without magnetic targeting system. Our results suggest that this composite strategy could be promising for clinical applications.

1. Introduction

On a worldwide scale, a total of 2.5 million people have suffered spinal cord injury (SCI), which has placed a significant burden on societal resources [1]. Over the past two decades, the understanding of the pathophysiology of SCI has been greatly improved, and significant advances have been made in approaches employing various cell types (e.g., embryonic stem cells, mesenchymal stem cells, and neural stem cells) for transplantation to treat SCI [2]. Many studies have focused on bone marrow mesenchymal stem cell (BMSC) transplantation for SCI because of the pluripotent differentiation capabilities of these cells [3] and because they are associated with fewer ethical issues. Engrafted BMSCs can promote nerve fiber regeneration and functional recovery in animal studies [4]. In addition, neurotrophins play a significant role in modulating neuronal survival, neurogenesis, and synapse formation following SCI [5]. These neurotrophins include brain-derived neurotrophic factor (BDNF), nerve growth factor (NGF), neurotrophin-3 (*NT3*), neurotrophin-4/5 (*NT4/5*), and neurotrophin-6 (*NT6*), many of which can be secreted by BMSCs.

However, BMSC transplantation for SCI cannot always achieve the desired outcome, partly because the number of surviving transplanted cells in injured spinal cord lesions and the secreted neurotrophins can directly influence the effect of cell transplantation [6]. Therefore, we designed an approach that is able to not only improve the efficiency of the delivery of BMSCs to the site of injury but also promote the secretion of neurotrophins.

Magnetic targeting systems with magnetically labeled cells have been evaluated as a more efficient and effective method for the delivery of cells to target sites [6–10]. A previous study by our group demonstrated that transplantation of *NT3*-expressing BMSCs has beneficial effects on functional recovery and nerve regeneration after SCI in a rat model [11]. Therefore, we attempted to combine the two strategies for the treatment of SCI.

The present study was designed to evaluate the therapeutic effects of a magnetic targeting system guiding magnetically labeled BMSCs, combined with *NT3* gene overexpression, as a novel approach for the treatment of SCI.

2. Materials and Methods

This study was approved by the Institutional Animal Use and Care Committee of Shanxi Medical University. Eight-week-old female Sprague-Dawley rats (Animal Center of Chinese People's Army Military Medical and Scientific Academy, Beijing, China, SCXK2007-004) were used in our study.

2.1. BMSC Isolation and Culture. Donor rats were euthanized with an overdose of pentobarbital sodium administered via intraperitoneal injection. The tibiae and femurs, including both ends of the bones, were harvested. After the proximal and distal ends of the bones were removed, the bone marrow cavities were exposed and flushed repeatedly with 6 mL of Dulbecco's modified essential medium (DMEM; Hyclone, Logan, UT, USA) using a 25-gauge needle. The collected bone marrow suspension was seeded into 25 cm^2 culture flasks in DMEM containing 10% fetal bovine serum (Hyclone), penicillin (100 U/mL; Invitrogen, Carlsbad, CA, USA), and streptomycin (100 μg/mL, Invitrogen), and the suspension was cultured at 37°C in a 5% CO_2 incubator (NAPCO, Thermo Scientific, Waltham, MA, USA). After 48 h, nonadherent cells and tissue fragments were discarded by replacing the medium. The medium was subsequently changed at intervals of 2 or 3 days. At approximately 2 weeks after the initiation of seeding, the adherent cells usually reached confluence. Then, the cells were resuspended in a trypsin/EDTA solution (Hyclone, USA) and passaged 1 : 3 at a density of 6,000/cm^2. After the cells were passaged three times, BMSCs from passage 3 were used for the present study. Details of identification of BMSCs are provided as supplementary data (in Supplementary Material available online at http://dx.doi.org/10.1155/2016/2018474).

2.2. Lentiviral Infection of BMSCs. The rat *NT3* gene (reference sequence: NM_031073.2) was synthesized by Nanjing GenScript Bioengineering Technology and Services Co., Ltd. (Nanjing, China), and was confirmed via sequencing. The target plasmids pLV.EX3d.P/puro-EF1α > *NT3* > IRES/DsRed Express2 and pLV.EX2d.P/puro-EF1α > DsRed Express2 were constructed by Cyagen Biosciences Inc. (Suzhou, China). The target plasmids, three helper plasmids (pLV/helper-SL3, pLV/helper-SL4, and pLV/helper-SL5) and Lipofectamine 2000 were used to create NTF3-DsRed lentivirus and DsRed lentivirus in 293T cells. The titers of the *NT3*-DsRed lentivirus and the DsRed lentivirus ranged from 1 to 1.8×10^8 TU/mL and 3.5 to 3.8×10^8 TU/mL, respectively, and were determined by the plate counting test dilution method.

The packaged lentiviruses were added to passage 3 BMSCs with complete culture medium and then incubated at 37°C in a 5% CO_2 and 95% relative humidity incubator (NAPCO, Thermo Scientific, Waltham, MA, USA). After 16 h, the medium was replaced. After 48 h, the BMSCs containing the *NT3-DsRed* or *DsRed* gene were harvested, and the *NT3-DsRed* and *DsRed* genes were detected using a fluorescence microscope (IX71, Olympus, Tokyo, Japan). The *NT3* gene was detected via real-time Q-PCR (AB7500, Applied Biosystems, USA).

2.3. BMSC Labeling with Superparamagnetic Iron Oxide (SPIO). In total, 25 μg Fe/mL SPIO (0.5 mmol/mL; Resovist, Schering, Germany) and 375 ng/mL poly-L-lysine (PLL; Sigma, USA) were added to the complete culture medium and incubated at room temperature for 60 min. Then, this medium was added to transfected BMSCs containing the *NT3-DsRed* gene. After the cells were cultured for 24 h at 37°C in a 5% CO_2 incubator, this medium was discarded. The BMSCs were subsequently washed 3 times with phosphate-buffered saline (PBS) to remove the unlabeled SPIO. Following trypsinization, the BMSCs were suspended in culture medium as the injection solution for transplantation. Details of induction of SPIO-labeled BMSCs are provided as supplementary data.

2.4. SCI Model Preparation. We used 8–10-week-old adult female Sprague-Dawley rats (weight 180–240 g) for the present in vivo study. After the rats were anesthetized via intraperitoneal injection of pentobarbital sodium (50 mg/kg), laminectomies were performed microscopically on the T7-8 vertebrae through the midline, with the dura mater intact. A weight-drop device was used to generate the SCI model [12]. To induce a contusion of the spinal cord, a 25 g metal rod with a 2 mm diameter was dropped from a height of 3 cm vertically onto the exposed spinal cord, after which the metal rod was immediately removed from the impact point. Simultaneously, the hind limbs of the rats relaxed completely after twitching, indicating that the SCI model had been successfully generated. Then, the incision was sutured tightly in layers. To prevent postoperative infection, the rats were given 2×10^5 U of penicillin via intramuscular injection every day after surgery. In addition, manual emptying of the bladders of the rats after surgery was performed twice a day by squeezing the lower abdomen until recovery of the micturition reflex was observed. Rats without postoperative hind-limb paralysis were excluded from the present study.

2.5. Rat Group Allocation and Cell Transplantation via Lumbar Puncture (LP). One-week after operation, 36 rats were selected as recipients and were randomly assigned to the following 3 groups: (1) BMSC group (BMSC, $n = 12$); (2) *NT3*-BMSC group (*NT3*, $n = 12$); and (3) Magnet and *NT3*-BMSC group (M-*NT3*, $n = 12$). After the rats were anesthetized again, BMSCs were transplanted via lumbar puncture (LP) as described previously [13]. Briefly, the L5 spinous process and the L4-5 ligamentum flavum were partially resected, and the dura was exposed. Then, at the L4-L5 intervertebral space, a microsyringe was advanced into the subarachnoid space, and 40 μL of culture medium containing 1×10^6 cells was injected into the CSF. In the *NT3* and M-*NT3* groups, the rats received SPIO-labeled *NT3*-BMSCs. In the BMSC group, the rats received unlabeled BMSCs. After injection, each rat was kept in the head-down position at

a 30° slope for approximately 30 min [8]. Additionally, a slab of neodymium magnet (0.57 T, length 10 mm, width 8 mm, and height 2 mm) was attached to the spine of the rats at the T7 level with medical adhesive tape in the M-*NT3* group, whereas nothing was placed on the back of the rats in the other two groups. After 24 h, the magnets were removed.

2.6. Magnetic Resonance Imaging. After the magnets were removed, the rats were anesthetized via intraperitoneal injection of pentobarbital sodium (50 mg/kg), and MR imaging of the spinal cord was performed using a 1.5 T clinical MR imager (GE Medical System, Signa Infinity Twin Speed & Excite Technology, USA) with a circular surface coil (diameter 11 cm). Axial images were obtained using a standard T2-weighted turbo spin-echo sequence. The imaging sequence parameters were as follows: field of view (FOV), $80 \times 80\,mm^2$; slice thickness, 2 mm; spacing, 0.5 mm; base resolution matrix, 256×256; repetition time (TR), 2,000 ms; and effective echo time (TE), 70 ms. To quantify the signal intensity (SI) in the MR images of the injured spinal cord, signal to noise ratios (SNRs) were calculated as $SNR = S - S_b/SD$, where S represents the SI of the region of interest (ROI); S_b represents the mean SI of the background; and SD represents the standard deviation of the ROI [14].

2.7. Evaluation of Hind-Limb Motor Function. After transplantation, the hind-limb motor function of all of the rats was assessed using the Basso, Beattie, and Bresnahan (BBB) locomotor rating scale [15]. The averaged BBB scores were recorded independently on days 1–7 and then every week up to the fifth week by two examiners who were not aware of the group allocation information.

2.8. Tissue Harvesting and Preparation for Histological Assessment. On day 35 after cell transplantation, the rats were perfused intracardially with 100 mL of normal saline (NS), followed by 4% paraformaldehyde in a state of deep anesthesia, through intraperitoneal injection of pentobarbital sodium (100 mg/kg). After the spinal cord tissues were dissected, they were placed in 4% paraformaldehyde overnight for postfixation and were then transferred successfully to 10% and 20% sucrose solutions overnight. Each of the spinal cord tissues at the lesion site was resected as a 10 mm long block. The obtained tissue blocks were frozen, and 20 μm and 5 μm thick longitudinal sections were then cut using a cryostat (CM3050, Leica, Wetzlar, Germany). Next, the sections were mounted on glass slides for histological assessment. For western blot analysis, the rats were not perfused, and the spinal cords tissues were freshly harvested.

2.9. Hematoxylin-Eosin (HE) Staining for Cystic Cavity Measurements. Five-micrometer-thick longitudinal sections were stained with HE for measurements of the cystic cavity. After the slices were fixed in cold acetone for 30 min, they were sequentially placed in xylene, ethanol, and distilled water. The slices were stained with hematoxylin for 5 min, rinsed with running water, and then placed in HCL-ethanol for 30 s. After the slices were soaked in running water for 15 min, they were counterstained in eosin and rinsed. Finally, the slices were dehydrated in an ascending series of ethanol, cleared in xylene, air-dried, and enveloped with balata (Sinopharm, Shanghai, China). The area of the cystic cavity was measured using a phase-contrast microscope (E100, Nikon, Tokyo, Japan).

2.10. Immunofluorescence Staining. Five-micrometer-thick longitudinal frozen sections were used for immunofluorescence staining. After the slices were fixed in cold acetone for 30 min, they were immersed in 0.3% Triton X-100 for 30 min at room temperature and then treated with 10% goat serum for 1 h at room temperature. Next, the slices were incubated overnight at 4°C with a primary antibody against either neurofilament-200 (NF200) or glial fibrillary acidic protein (GFAP) and then incubated for 1 h at room temperature with a secondary goat anti-mouse antibody (DyLight 488 AffiniPure, Earthox Biotechnology, San Francisco, CA, USA). After the slices were rinsed, they were enveloped with DAPI, and 10 min later, the slices were observed under a fluorescence microscope (IX70, Olympus).

2.11. Prussian Blue Staining. To identify iron particles in the SPIO-labeled cells, Prussian blue staining was performed on adjacent sections of the same spinal cord tissues. After the slices were fixed in cold acetone for 30 min, they were incubated in Perl's solution for 30 min at 37°C. Next, the slices were cooled, washed three times with PBS, and then counterstained with nuclear fast red. After the slices were washed and air-dried, they were enveloped with balata.

2.12. Statistical Analysis. All results are presented as the means ± standard deviation (SD). The BBB scores were analyzed through repeated measures analysis of variance (ANOVA). The data obtained from Prussian blue staining were analyzed with the Mann-Whitney U test. All other data were analyzed using one-way ANOVA to identify significant differences among the three groups. Statistical significance was inferred when the p value was less than 0.05. All statistical analyses were performed using the SAS 6.12 software program (SAS Institute, Cary, NC, USA).

3. Results

3.1. In Vitro Expression of DsRed and NT3 in BMSCs. After puromycin screening, red fluorescence was identified in the cytoplasm of >95% of the *NT3*-DsRed BMSCs and >99% of the DsRed BMSCs (Figure 1), which indicated a high transfection efficiency for BMSCs in the present study.

NT3 mRNA expression was assessed via real-time Q-PCR (Figure 1). The *NT3* mRNA expression levels in the DsRed BMSCs and untransfected BMSCs were nearly equal. The *NT3* mRNA expression level in the *NT3*-DsRed BMSCs was approximately 13-fold that in the DsRed BMSCs or untransfected BMSCs.

3.2. Successful Labeling of BMSCs with SPIO. After the BMSCs were labeled with SPIO, Prussian blue staining was performed to identify the SPIO labeling rate of BMSCs. Blue

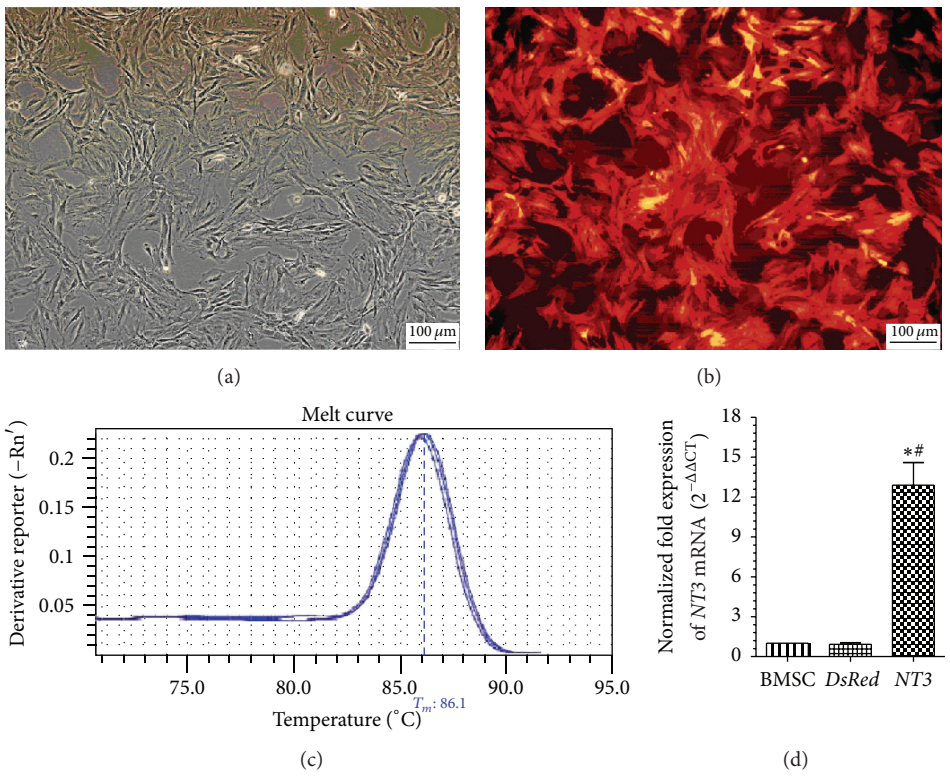

Figure 1: Stable transfection of the *NT3-DsRed* gene into BMSCs using a lentivirus ((a), (b)) and Q-PCT detection of *NT3* mRNA ((c), (d)). (a) Before transfection. (b) After transfection. (c) *NT3* mRNA Q-PCR melting curve. (d) The normalized fold change in *NT3* mRNA expression ($2^{-\Delta\Delta CT}$). Magnification, ×100 ((a), (b)). Scale bar, 100 μm ((a), (b)).

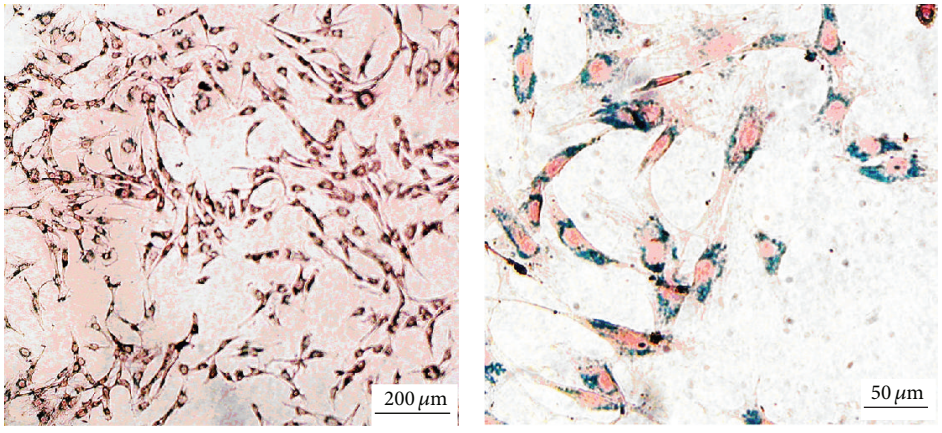

Figure 2: Prussian blue staining of the SPIO-labeled and gene-transfected BMSCs ((a), (b)). Magnification, ×100 (a), ×400 (b). Scale bar, 200 μm (a), 50 μm (b).

iron particles were observed in the cytoplasm of the SPIO-labeled BMSCs, and the SPIO labeling rate of the BMSCs was nearly 100% (Figure 2).

3.3. MR Imaging after Cell Transplantation. The SI was obtained using T2*-weighted gradient-echo sequences in the injured spinal cord because T2*-weighted imaging is sensitive to SPIO (Figure 3). The injured spinal cord SIs of the M-*NT3* and *NT3* groups decreased after transplantation, whereas no apparent change in the SI was observed in the BMSC group. Analysis of the SNR further revealed that the injured spinal cord SNRs of the M-*NT3* group were significantly decreased compared with those of the *NT3* group, and the SNRs for the injured spinal cords of the *NT3* group were significantly decreased compared with those of the BMSC group.

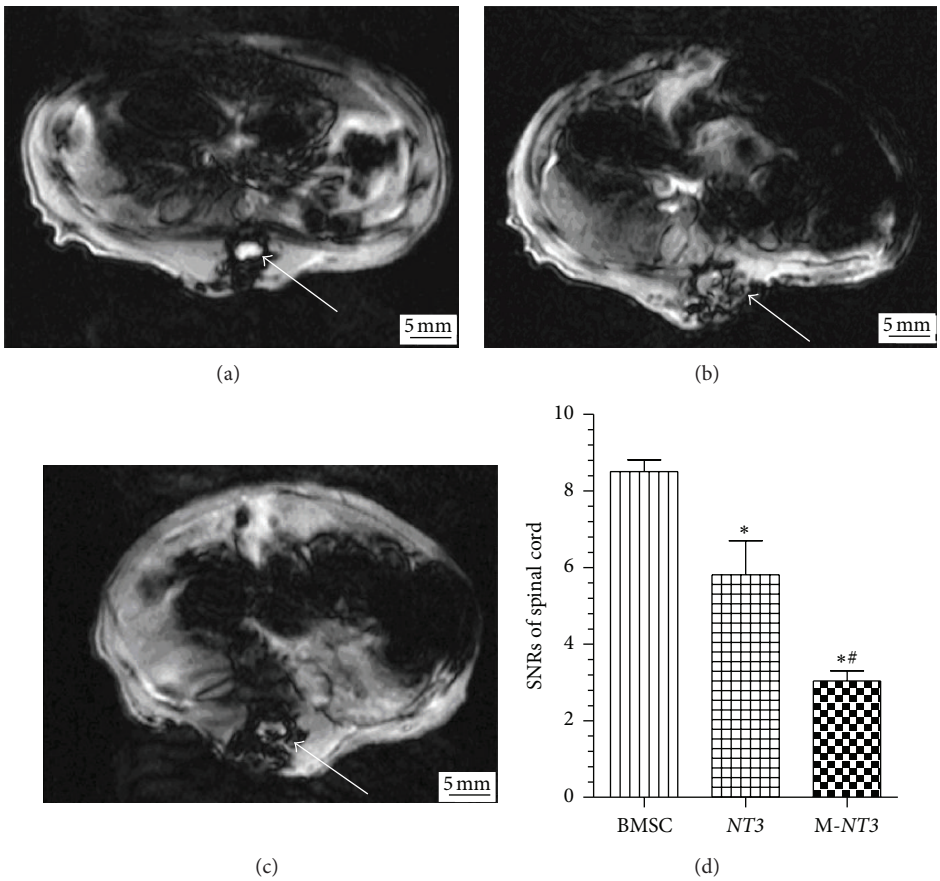

Figure 3: T2*-weighted MR images of the injured spinal cord on day 1 after cell transplantation in the BMSC group (a), *NT3* group (b), and M-*NT3* group (c). A bar graph showing the SNRs in the injured spinal cord MR images from each group (d). The data, which are presented as the means ± SD ($n = 12$), were analyzed using one-way ANOVA. $^{*}p < 0.05$ versus the BMSC group, $^{\#}p < 0.05$ versus the *NT3* group.

3.4. Locomotor Behavioral Assessment. The hind-limb locomotor functions in each group were assessed using the BBB scores on days 1, 3, 7, 14, 21, 28, and 35 after cell transplantation (Figure 4). On days 1 and 3 after cell transplantation, the BBB scores of the M-*NT3* group did not improve significantly compared with those of the other two groups. However, the BBB scores of the M-*NT3* group were the highest among the three groups on days 7, 14, 21, 28, and 35 after cell transplantation, which indicated that hind-limb locomotor functional recovery was enhanced and accelerated in the M-*NT3* group compared with the other two groups. The BBB scores of the *NT3* group were also significantly higher than those of the BMSC group on days 7, 14, 21, 28, and 35 after cell transplantation. Moreover, significant differences ($p < 0.05$) were observed among the three groups at these time points.

3.5. Prussian Blue Staining of the Injured Spinal Cord Tissues. After Prussian blue staining was performed on the injured spinal cord tissue sections, significantly more blue-stained cells were observed in the M-*NT3* group than in the *NT3* group, whereas no blue-stained cells could be observed in the BMSC group (Figure 5).

3.6. Cystic Cavity Area Measurements. At 7 weeks after the spinal cord was injured, the mean values of the cystic cavity area in the BMSC, *NT3*, and M-*NT3* groups were 0.64 ± 0.14 mm^2, 0.51 ± 0.11 mm^2, and 0.39 ± 0.10 mm^2, respectively. Statistically significant differences were observed among the three groups ($p < 0.05$, Figure 6), with the cystic cavity area in the M-*NT3* group being the smallest.

3.7. Expression of the NT3 Protein in the Injured Spinal Cord after Cell Transplantation. On day 35 after cell transplantation, *NT3* protein expression was investigated through western blot analysis (Figure 7). Although *NT3* protein overexpression was observed in both the M-*NT3* group and the *NT3* group, the *NT3* protein level in the M-*NT3* group was significantly higher than in the *NT3* group. In addition, the *NT3* protein level in the BMSC group was significantly lower than in the *NT3* group. The magnetic targeting system significantly enhanced *NT3* protein expression in the injured spinal cord lesions.

3.8. Axon Regeneration and Glial Scar Inhibition in the Injured Spinal Cord. NF200 is a NF protein that is found in axons under normal conditions [16]. Increased expression of NF200 indicates axon regeneration in the injured spinal cord. In contrast, GFAP is expressed primarily in astrocytes, and a reduction of its expression indicates glial scar inhibition

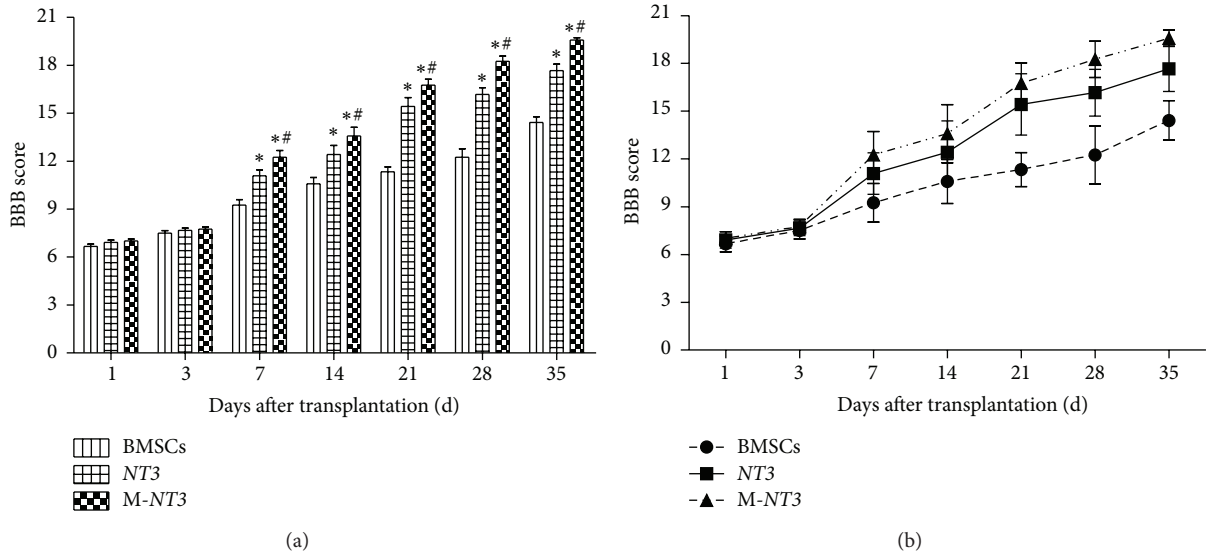

Figure 4: The BBB scores of the hind-limb locomotor functions in each group on days 1, 3, 7, 14, 21, 28, and 35 after cell transplantation ((a), (b)). The data, which are presented as the means ± SD ($n = 12$), were analyzed using repeated measures ANOVA. $^{*}p < 0.05$ versus the BMSC group, $^{\#}p < 0.05$ versus the *NT3* group.

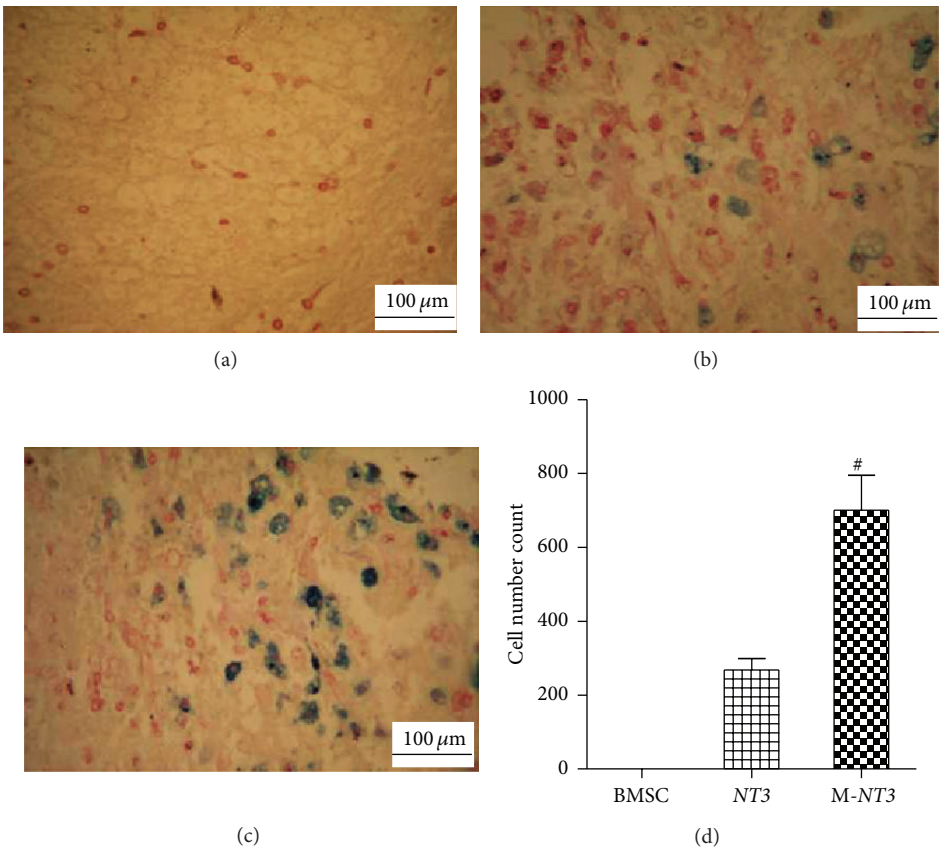

Figure 5: Prussian blue staining of tissues around the injured spinal cord lesion on day 35 after transplantation in the BMSC group (a), *NT3* group (b), and M-*NT3* group (c). Magnification, ×200 ((a), (b), and (c)). Scale bar, 100 μm ((a), (b), and (c)). (d) The data, which are presented as the means ± SD ($n = 12$), were analyzed using the Mann-Whitney U test. $^{\#}p < 0.05$ versus the *NT3* group.

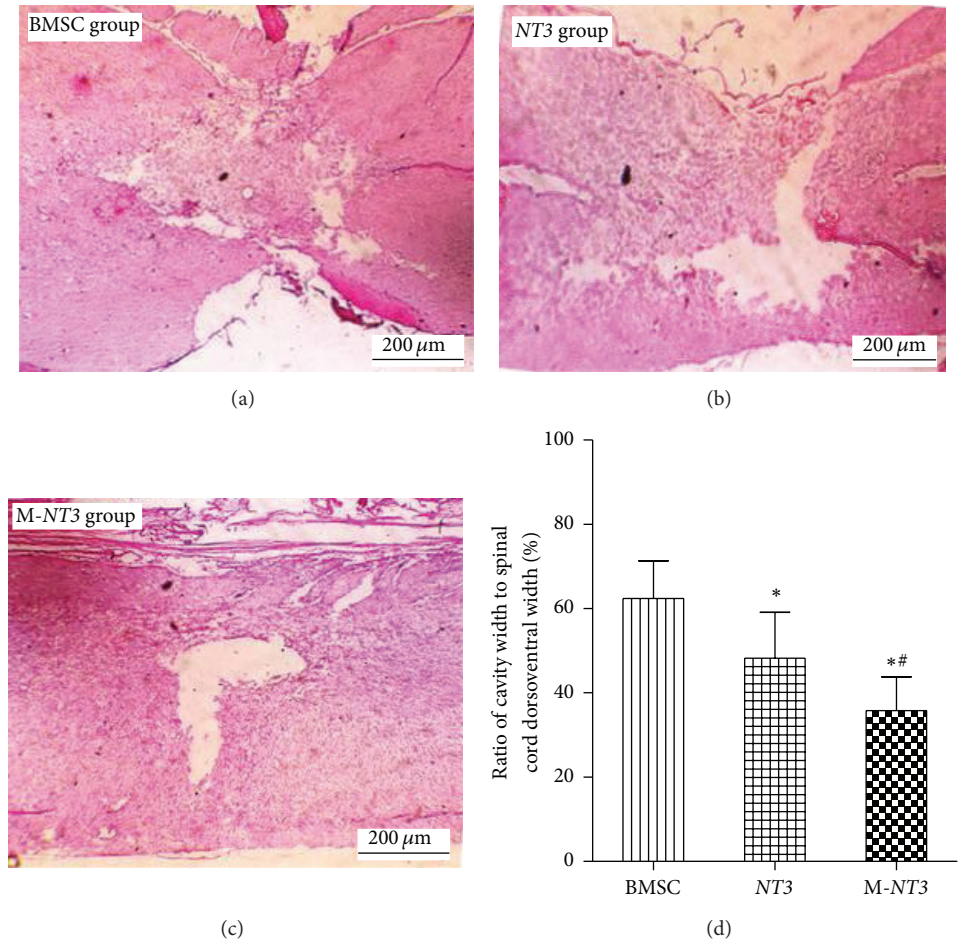

Figure 6: The cystic cavity area of the injured spinal cords on day 35 after cell transplantation in the BMSC group (a), *NT3* group (b), and M-*NT3* group (c). Magnification, ×40 ((a), (b), and (c)). Scale bar, 200 μm ((a), (b), and (c)). The data, which are presented as the means ± SD ($n = 12$), were analyzed using one-way ANOVA. $^{*}p < 0.05$ versus the BMSC group, $^{\#}p < 0.05$ versus the *NT3* group.

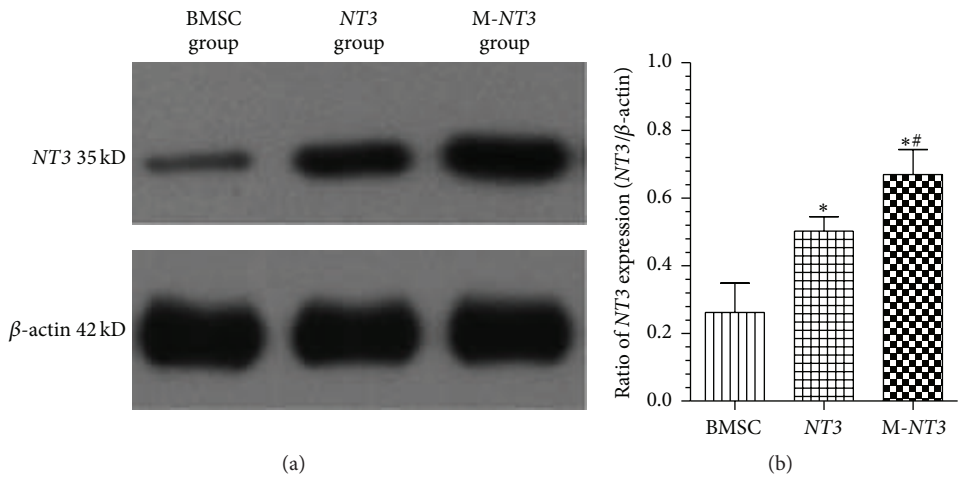

Figure 7: Western blot detection of *NT3* protein expression in the injured spinal cords on day 35 after cell transplantation in each group (a). Ratio of the lane density of the *NT3* protein to the lane density of the β-actin protein in each group (b). The data, which are presented as the means ± SD ($n = 12$), were analyzed using one-way ANOVA. $^{*}p < 0.05$ versus the BMSC group, $^{\#}p < 0.05$ versus the *NT3* group.

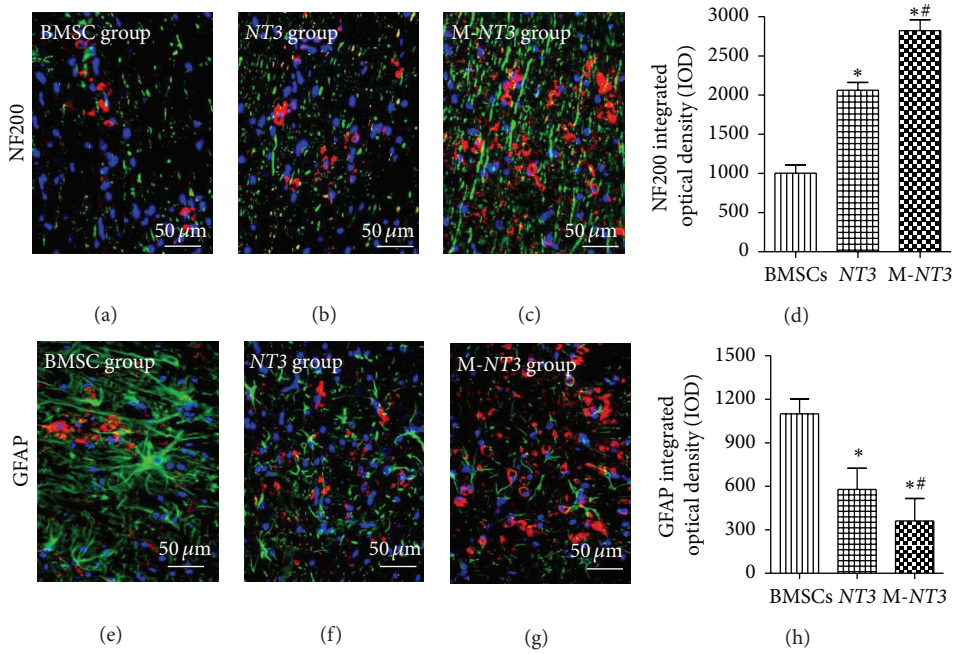

Figure 8: Immunofluorescence labeling of NF200 ((a), (b), and (c)) and GFAP ((e), (f), and (g)) in sagittal sections of the injured spinal cords from each group on day 35 after cell transplantation. Double labeling for NF200/GFAP (green) and BMSCs (red). Magnification, ×400 ((a)–(c), (e)–(g)). Scale bar, 50 μm ((a)–(c), (e)–(g)). Integrated optical density (IOD) bar graphs showing NF200 (g) and GFAP (h) expression in each group. All microscopic images were captured under identical conditions. The data, which are presented as the means ± SD ($n = 12$), were analyzed using one-way ANOVA. $^{*}p < 0.05$ versus the BMSC group, $^{\#}p < 0.05$ versus the *NT3* group.

in the injured spinal cord. As shown in Figure 8, the level of NF200 expression in the M-*NT* group was significantly increased compared with that in the other two groups, whereas the GFAP expression level in the M-*NT* group was significantly decreased compared with that in the other two groups. Moreover, the NF200 expression level in the *NT3* group was higher than in the BMSC group, whereas the GFAP expression level in the *NT3* group was lower than in the BMSC group.

4. Discussion

In the present study, we investigated the effects of a magnet-guided SPIO-labeled BMSC transplantation method combined with gene therapy for the treatment of spinal cord injury in rats. We found that this approach not only was more effective for repairing SCI but also allowed the engrafted cells to be tracked in vivo.

SCI is a complex pathological process for which effective treatment strategies are currently lacking [17]. Cell replacement therapy is a promising approach for repairing the injured spinal cord. In particular, BMSCs have been extensively studied in animal models of SCI because these cells are easily isolated and cultured, exhibit pluripotent differentiation capabilities, and are associated with fewer ethical issues [2, 3, 8, 18, 19]. Although many experimental studies have demonstrated that BMSC transplantation can promote nerve regeneration and enhance functional recovery in animal models of SCI [20], the desired outcome (full recovery) cannot be obtained. The possible reasons for these poor outcomes include the lack of adequate neurotropic factors and surviving stem cells in injured spinal cord lesions.

Neurotropic factors, such as nerve growth factor (NGF), brain-derived neurotrophic factor (BDNF), neurotrophin-3 (*NT3*), neurotrophin-4/5 (*NT4/5*), and neurotrophin-6 (*NT6*), play crucial roles in nerve regeneration after SCI [21, 22]. Although BMSCs can express many neurotropic factors in vitro [23, 24], engrafted BMSCs do not express *NT3* in vivo [23, 25, 26]. However, *NT3* is an extremely important neuroregenerative protein involved in guiding stem cell migration, mediating engrafted BMSC survival, inducing neuronal differentiation, promoting axonal regeneration, and facilitating angiogenesis after SCI [22, 27–31]. Considering these *NT3* protein activities, stably *NT3*-transfected BMSCs were obtained using lentivirus vectors to produce BMSCs that could overexpress the *NT3* protein in vivo.

The present study showed that stable transfection of BMSCs with the *NT3* gene was possible, and the resulting cells were more effective than conventional BMSCs in vivo for promoting axonal regeneration, enhancing functional recovery, and maintaining the survival of engrafted cells. Although the *NT3* protein could be detected in the BMSC group, it was expressed at a much lower level than in the other two groups. This low-level expression may be attributed to the presence of inflammatory cells (i.e., macrophages, lymphocytes, and mast cells), microglia/macrophages, astrocytes, oligodendrocytes, and neural progenitor cells that are present following spinal cord injury and can express the *NT3* protein [32–36]. All of these findings are consistent with a previous study by our group [11]. In addition, our previous study demonstrated that

NT3 gene-modified BMSC transplantation was superior to BMSC transplantation in promoting neuronal regeneration, inhibiting glial scar formation, and increasing BDNF and VEGF secretion after SCI [11].

The survival of the engrafted stem cells in the lesion has a direct effect on the repair outcome of stem cell transplantation strategies [6, 37]. Although BMSCs have been shown to home to injured spinal cord lesions [38, 39], this homing effect does not result in an adequate number of BMSCs homing to the lesion for clinical efficacy. Direct injection, lumbar subdural injection, and intravessel injection are the traditional methods used for cell transplantation. Many recent studies have shown that lumbar subdural injection is a safe, less invasive (compared to the other methods), and repeatable method of cell transplantation [8, 13, 40, 41]. However, the direct injection of cells is more efficient than lumbar subdural injection [8], although this method is more invasive than intravessel injection.

A highly efficient and less invasive cell delivery system is particularly important for cell transplantation to treat SCI. To achieve a compromise between efficiency and invasiveness, we chose to transplant cells via lumbar subdural injection in the present study. To improve the efficiency of cell delivery, a magnetic targeting system was used. Some previous studies demonstrated that SPIO-labeled BMSCs transplanted via lumbar puncture were delivered to the spinal cord injury site efficiently through the CSF using a magnetic targeting system [6, 8, 10]. In addition, SPIO nanoparticles can significantly shorten T1 and T2 relaxation times and particularly the $T2^*$ relaxation time. Therefore, SPIO nanoparticles can cause a significant reduction of the $T2^*$ SI observed under MRI. In the present study, many more blue-stained cells could be observed following Prussian blue staining, and the injured spinal cord SNRs of the $T2^*$-weighted MR images were significantly decreased in the magnet group compared with the other two nonmagnet groups; both of these findings indicated that more BMSCs homed to the injured spinal cord lesions in the magnet group than in the other two, nonmagnet groups.

NF200 is one of the NF proteins that can be found in axons under normal conditions [15]. After SCI, astrocytosis will increase GFAP expression following glial scar formation in the lesion. The immunofluorescence experiments performed in the present study showed that NF200 expression around the injured site was much higher in the magnet group than in the other two, nonmagnet groups, whereas GFAP expression around the injured site was much lower in the magnet group than in the other two, nonmagnet groups. These findings indicate that transplantation of *NT3* gene-modified BMSCs with the aid of a magnetic targeting system can significantly promote neuronal regeneration and inhibit glial scar formation.

Locomotor testing was also performed in the present study to assess hind-limb motor function using the BBB score. At day 35 after cell transplantation, the BBB scores of the magnet group did not appear to be markedly improved compared with the *NT3*-BMSC group from our previous study [11], which was mainly attributed to the different researchers involved in the two studies and the subjectivity of the BBB scoring system. Although the BBB scores of the magnet group were improved by only approximately 10% at day 35 after cell transplantation in the present study, the dynamic variation of BBB scores in the three groups indicated that hind-limb locomotor functional recovery was enhanced and accelerated in the magnet group compared with the other two, nonmagnet groups. All of these findings could be attributed primarily to the magnetic targeting system effectively delivering the engrafted BMSCs to the injured spinal cord lesion [10].

In summary, the present study demonstrated that the Magnet-*NT3* group showed a significantly better efficiency of cell delivery, nerve regeneration, and functional recovery than the *NT3*-BMSC group. Thus, transplantation of *NT3* gene-modified BMSCs via lumbar puncture combined with a magnetic targeting system is a highly effective and minimally invasive therapeutic method for treating spinal cord injury and is promising for monitoring engrafted BMSCs in vivo through MR.

Disclosure

Rui-Ping Zhang and Ling-Jie Wang are co-first authors.

Conflict of Interests

There is no conflict of interests to declare.

Authors' Contribution

Rui-Ping Zhang and Ling-Jie Wang contributed equally to this work.

Acknowledgments

This study was supported by grants from the Scientific and Technological Projects of Shanxi Province (20120321028-02) to Rui-Ping Zhang, from the China Postdoctoral Foundation to Rui-Ping Zhang (2013M541206 and 2014T70233), and from the NSFC (National Nature Science Foundation of People's Republic of China, 81371628) to Jian-Ding Li.

References

[1] M. G. Fehlings, J. R. Wilson, and M. O'Higgins, "Introduction: spinal cord injury at the cutting edge of clinical translation: a focus issue collaboration between NACTN and AOSpine North America," *Journal of Neurosurgery. Spine*, vol. 17, no. 1, pp. 1–3, 2012.

[2] A. M. Parr, I. Kulbatski, X.-H. Wang, A. Keating, and C. H. Tator, "Fate of transplanted adult neural stem/progenitor cells and bone marrow-derived mesenchymal stromal cells in the injured adult rat spinal cord and impact on functional recovery," *Surgical Neurology*, vol. 70, no. 6, pp. 600–607, 2008.

[3] C. D. Porada, E. D. Zanjani, and G. Almeida-Porad, "Adult mesenchymal stem cells: a pluripotent population with multiple applications," *Current Stem Cell Research and Therapy*, vol. 1, no. 3, pp. 365–369, 2006.

[4] C. P. Hofstetter, E. J. Schwarz, D. Hess et al., "Marrow stromal cells form guiding strands in the injured spinal cord and promote recovery," *Proceedings of the National Academy of Sciences of the United States of America*, vol. 99, no. 4, pp. 2199–2204, 2002.

[5] G. C. Sieck and C. B. Mantilla, "Role of neurotrophins in recovery of phrenic motor function following spinal cord injury," *Respiratory Physiology & Neurobiology*, vol. 169, no. 2, pp. 218–225, 2009.

[6] V. Vaněček, V. Zablotskii, S. Forostyak et al., "Highly efficient magnetic targeting of mesenchymal stem cells in spinal cord injury," *International Journal of Nanomedicine*, vol. 7, pp. 3719–3730, 2012.

[7] R. Egle, M. Milek, I. Mlinarič-Raščan, A. Fahr, and J. Kristl, "A novel gene delivery system for stable transfection of thiopurine-S-methyltransferase gene in versatile cell types," *European Journal of Pharmaceutics and Biopharmaceutics*, vol. 69, no. 1, pp. 23–30, 2008.

[8] K. Nishida, N. Tanaka, K. Nakanishi et al., "Magnetic targeting of bone marrow stromal cells into spinal cord: through cerebrospinal fluid," *NeuroReport*, vol. 17, no. 12, pp. 1269–1272, 2006.

[9] T. Hamasaki, N. Tanaka, N. Kamei et al., "Magnetically labeled neural progenitor cells, which are localized by magnetic force, promote axon growth in organotypic cocultures," *Spine*, vol. 32, no. 21, pp. 2300–2305, 2007.

[10] H. Sasaki, N. Tanaka, K. Nakanishi et al., "Therapeutic effects with magnetic targeting of bone marrow stromal cells in a rat spinal cord injury model," *Spine*, vol. 36, no. 12, pp. 933–938, 2011.

[11] L.-J. Wang, R.-P. Zhang, and J.-D. Li, "Transplantation of neurotrophin-3-expressing bone mesenchymal stem cells improves recovery in a rat model of spinal cord injury," *Acta Neurochirurgica*, vol. 156, no. 7, pp. 1409–1418, 2014.

[12] S. Constantini and W. Young, "The effects of methylprednisolone and the ganglioside GM1 on acute spinal cord injury in rats," *Journal of Neurosurgery*, vol. 80, no. 1, pp. 97–111, 1994.

[13] A. Bakshi, C. Hunter, S. Swanger, A. Lepore, and I. Fischer, "Minimally invasive delivery of stem cells for spinal cord injury: advantages of the lumbar puncture technique," *Journal of Neurosurgery: Spine*, vol. 1, no. 3, pp. 330–337, 2004.

[14] R. R. Price, L. Axel, T. Morgan et al., "Quality assurance methods and phantoms for magnetic resonance imaging: report of AAPM nuclear magnetic resonance Task Group No. 1," *Medical Physics*, vol. 17, no. 2, pp. 287–295, 1990.

[15] D. M. Basso, M. S. Beattie, and J. C. Bresnahan, "A sensitive and reliable locomotor rating scale for open field testing in rats," *Journal of Neurotrauma*, vol. 12, no. 1, pp. 1–21, 1995.

[16] W.-G. Liu, Z.-Y. Wang, and Z.-S. Huang, "Bone marrow-derived mesenchymal stem cells expressing the bFGF transgene promote axon regeneration and functional recovery after spinal cord injury in rats," *Neurological Research*, vol. 33, no. 7, pp. 686–693, 2011.

[17] J. Shen, X.-M. Zhong, X.-H. Duan et al., "Magnetic resonance imaging of mesenchymal stem cells labeled with dual (MR and fluorescence) agents in rat spinal cord injury," *Academic Radiology*, vol. 16, no. 9, pp. 1142–1154, 2009.

[18] E. Syková and P. Jendelová, "Magnetic resonance tracking of implanted adult and embryonic stem cells in injured brain and spinal cord," *Annals of the New York Academy of Sciences*, vol. 1049, pp. 146–160, 2005.

[19] M. Chopp and Y. Li, "Treatment of neural injury with marrow stromal cells," *Lancet Neurology*, vol. 1, no. 2, pp. 92–100, 2002.

[20] S. Wu, Y. Suzuki, Y. Ejiri et al., "Bone marrow stromal cells enhance differentiation of cocultured neurosphere cells and promote regeneration of injured spinal cord," *Journal of Neuroscience Research*, vol. 72, no. 3, pp. 343–351, 2003.

[21] J. L. Goldberg and B. A. Barres, "The relationship between neuronal survival and regeneration," *Annual Review of Neuroscience*, vol. 23, pp. 579–612, 2000.

[22] A. Patapoutian and L. F. Reichardt, "Trk receptors: mediators of neurotrophin action," *Current Opinion in Neurobiology*, vol. 11, no. 3, pp. 272–280, 2001.

[23] L. Crigler, R. C. Robey, A. Asawachaicharn, D. Gaupp, and D. G. Phinney, "Human mesenchymal stem cell subpopulations express a variety of neuro-regulatory molecules and promote neuronal cell survival and neuritogenesis," *Experimental Neurology*, vol. 198, no. 1, pp. 54–64, 2006.

[24] B. Neuhuber, B. Timothy Himes, J. S. Shumsky, G. Gallo, and I. Fischer, "Axon growth and recovery of function supported by human bone marrow stromal cells in the injured spinal cord exhibit donor variations," *Brain Research*, vol. 1035, no. 1, pp. 73–85, 2005.

[25] M. M. Yaghoobi and S. J. Mowla, "Differential gene expression pattern of neurotrophins and their receptors during neuronal differentiation of rat bone marrow stromal cells," *Neuroscience Letters*, vol. 397, no. 1-2, pp. 149–154, 2006.

[26] N. Kamei, N. Tanaka, Y. Oishi et al., "Bone marrow stromal cells promoting corticospinal axon growth through the release of humoral factors in organotypic cocultures in neonatal rats," *Journal of Neurosurgery: Spine*, vol. 6, no. 5, pp. 412–419, 2007.

[27] M. Douglas-Escobar, C. Rossignol, D. Steindler, T. Zheng, and M. D. Weiss, "Neurotrophin-induced migration and neuronal differentiation of multipotent astrocytic stem cells *in vitro*," *PLoS ONE*, vol. 7, no. 12, Article ID e51706, 2012.

[28] A. D. Pyle, L. F. Lock, and P. J. Donovan, "Neurotrophins mediate human embryonic stem cell survival," *Nature Biotechnology*, vol. 24, no. 3, pp. 344–350, 2006.

[29] Z.-H. Zhang, R.-Z. Wang, G.-L. Li et al., "Transplantation of neural stem cells modified by human neurotrophin-3 promotes functional recovery after transient focal cerebral ischemia in rats," *Neuroscience Letters*, vol. 444, no. 3, pp. 227–230, 2008.

[30] B. Cristofaro, O. A. Stone, A. Caporali et al., "Neurotrophin-3 is a novel angiogenic factor capable of therapeutic neovascularization in a mouse model of limb ischemia," *Arteriosclerosis, Thrombosis, and Vascular Biology*, vol. 30, no. 6, pp. 1143–1150, 2010.

[31] I. Jean, C. Lavialle, A. Barthelaix-Pouplard, and C. Fressinaud, "Neurotrophin-3 specifically increases mature oligodendrocyte population and enhances remyelination after chemical demyelination of adult rat CNS," *Brain Research*, vol. 972, no. 1-2, pp. 110–118, 2003.

[32] M. Besser and R. Wank, "Cutting edge: clonally restricted production of the neurotrophins brain-derived neurotrophic factor and neurotrophin-3 mRNA by human immune cells and Th1/Th2-polarized expression of their receptors," *Journal of Immunology*, vol. 162, no. 11, pp. 6303–6306, 1999.

[33] M. A. Laurenzi, G. Barbany, T. Timmusk, J. A. Lindgren, and H. Persson, "Expression of mRNA encoding neurotrophins and neurotrophin receptors in rat thymus, spleen tissue and immunocompetent cells. Regulation of neurotrophin-4 mRNA expression by mitogens and leukotriene B4," *European Journal of Biochemistry*, vol. 223, no. 3, pp. 733–741, 1994.

[34] A. G. Rabchevsky and W. J. Streit, "Role of microglia in post injury repair and regeneration of the CNS," *Mental Retardation and Developmental Disabilities Research Reviews*, vol. 4, no. 3, pp. 187–192, 1998.

[35] K. D. Dougherty, C. F. Dreyfus, and I. B. Black, "Brain-derived neurotrophic factor in astrocytes, oligodendrocytes, and microglia/macrophages after spinal cord injury," *Neurobiology of Disease*, vol. 7, no. 6, pp. 574–585, 2000.

[36] N. Kamei, N. Tanaka, Y. Oishi et al., "BDNF, NT-3, and NGF released from transplanted neural progenitor cells promote corticospinal axon growth in organotypic cocultures," *Spine*, vol. 32, no. 12, pp. 1272–1278, 2007.

[37] E.-S. Kang, K.-Y. Ha, and Y.-H. Kim, "Fate of transplanted bone marrow derived mesenchymal stem cells following spinal cord injury in rats by transplantation routes," *Journal of Korean Medical Science*, vol. 27, no. 6, pp. 586–593, 2012.

[38] B.-R. Son, L. A. Marquez-Curtis, M. Kucia et al., "Migration of bone marrow and cord blood mesenchymal stem cells in vitro is regulated by stromal-derived factor-1-CXCR4 and hepatocyte growth factor-c-met axes and involves matrix metalloproteinases," *Stem Cells*, vol. 24, no. 5, pp. 1254–1264, 2006.

[39] J. F. Ji, J. B. P. He, S. T. Dheen, and S. S. W. Tay, "Interactions of chemokines and chemokine receptors mediate the migration of mesenchymal stem cells to the impaired site in the brain after hypoglossal nerve injury," *Stem Cells*, vol. 22, no. 3, pp. 415–427, 2004.

[40] M. Ohta, Y. Suzuki, T. Noda et al., "Bone marrow stromal cells infused into the cerebrospinal fluid promote functional recovery of the injured rat spinal cord with reduced cavity formation," *Experimental Neurology*, vol. 187, no. 2, pp. 266–278, 2004.

[41] K. Satake, J. Lou, and L. G. Lenke, "Migration of mesenchymal stem cells through cerebrospinal fluid into injured spinal cord tissue," *Spine*, vol. 29, no. 18, pp. 1971–1979, 2004.

Hindawi Publishing Corporation
Stem Cells International
Volume 2016, Article ID 5831276, 14 pages
http://dx.doi.org/10.1155/2016/5831276

Research Article

Ciprofloxacin Improves the Stemness of Human Dermal Papilla Cells

Chayanin Kiratipaiboon,[1] Parkpoom Tengamnuay,[2] and Pithi Chanvorachote[3,4]

[1] *Pharmaceutical Technology (International) Program, Faculty of Pharmaceutical Sciences, Chulalongkorn University, Bangkok 10330, Thailand*
[2] *Department of Pharmaceutics and Industrial Pharmacy, Faculty of Pharmaceutical Sciences, Chulalongkorn University, Bangkok 10330, Thailand*
[3] *Department of Pharmacology and Physiology, Faculty of Pharmaceutical Sciences, Chulalongkorn University, Bangkok 10330, Thailand*
[4] *Cell-Based Drug and Health Product Development Research Unit, Faculty of Pharmaceutical Sciences, Chulalongkorn University, Bangkok 10330, Thailand*

Correspondence should be addressed to Pithi Chanvorachote; pithi_chan@yahoo.com

Received 12 January 2015; Revised 18 March 2015; Accepted 19 March 2015

Academic Editor: Kenichi Tamama

Improvement in the expansion method of adult stem cells may augment their use in regenerative therapy. Using human dermal papilla cell line as well as primary dermal papilla cells as model systems, the present study demonstrated that ciprofloxacin treatment could prevent the loss of stemness during culture. Clonogenicity and stem cell markers of dermal papilla cells were shown to gradually decrease in the culture in a time-dependent manner. Treatment of the cells with nontoxic concentrations of ciprofloxacin could maintain both stem cell morphology and clonogenicity, as well as all stem cells markers. We found that ciprofloxacin exerted its effect through ATP-dependent tyrosine kinase/glycogen synthase kinase3β dependent mechanism which in turn upregulated β-catenin. Besides, ciprofloxacin was shown to induce epithelial-mesenchymal transition in DPCs as the transcription factors ZEB1 and Snail were significantly increased. Furthermore, the self-renewal proteins of Wnt/β-catenin pathway, namely, Nanog and Oct-4 were significantly upregulated in the ciprofloxacin-treated cells. The effects of ciprofloxacin in preserving stem cell features were confirmed in the primary dermal papilla cells directly obtained from human hair follicles. Together, these results revealed a novel application of ciprofloxacin for stem cell maintenance and provided the underlying mechanisms that are responsible for the stemness in dermal papilla cells.

1. Introduction

Based on the fact that dermal papilla cells (DPCs) interaction with epithelial stem cells can induce generation of new hair follicles [1–3], the cell therapy using DPCs has emerged as a potentially new approach for hair transplantation [4, 5]. DPCs have been intensively investigated to possess many advantages for cell therapy approaches. However, many studies also demonstrated the loss of their stemness and inductive activity during the *in vitro* passages [4, 6–8].

The hair follicle is composed of epithelial and mesenchymal compartments. DPCs, the major cell population existing in the mesenchymal compartments, are located at the base of the hair follicle and function as a signaling center in the hair follicle morphogenesis and growth cycle [9]. These cells instruct the epithelial stem cells through specific signals to proliferate and differentiate into multiple layers of the growing hair shaft [1–3]. Interestingly, DPCs have been characterized as multipotent stem cells and the stemness of such cells is tightly associated with the ability to induce hair follicle formation. With comprehensive knowledge of the stem cell biology, the evidence suggested that CD133, a protein marker of human stem cells, contributes to the hair inductive property of DPCs in transgenic mice [10, 11]. In addition, an ablation of stem cell-related transcription factors including Sox2 in DPCs leads to the impairment of the hair shaft

outgrowth [12]. Although the molecular features that regulate stemness as well as hair inductive function in these specialized DPCs are still largely unknown, the Wnt/β-catenin signaling appears to lend strong support to hair follicle morphogenesis and regeneration [13–15]. Indeed, β-catenin was shown to regulate crucial signaling pathways in hair follicle formation in response to several stimuli, including fibroblast growth factor (FGF) and insulin-like growth factor (IGF) [13]. In transgenic mice model, the suppression of β-catenin in the DPCs resulted in the inhibition of hair follicle formation [13], as epithelial-mesenchymal transition (EMT) lately has been shown to play an important role in the stem cell behaviors and the activation of Wnt/β-catenin signaling was shown to activate the transition of the epithelial cells toward mesenchymal stem cells. Together with the concept that transcription factors presenting in the cell undergoing EMT like Snail were found to be important for the accomplishment of stem cell functions [16–18], it is likely that these β-catenin and EMT could impact the stemness and stem cell activity in the DPCs.

Ciprofloxacin (CIP) has been used as an antibiotic prophylaxis for the prevention of bacterial infection in patients receiving stem cell transplant and in stem cell research [19, 20]. Also, this considerably safe drug is widely used in the treatment of certain infection in cell culture [21]. So far, the molecular basis of CIP on human cell biology has not been fully investigated, especially in the area of stem cell research. The present study therefore aimed to elucidate the possible role of CIP for its possible effect on the stemness of DPCs using human dermal papilla cell line and primary human dermal papilla cells as models.

2. Material and Methods

2.1. Cells and Reagents. Immortalized dermal papilla cells (DPCs) were obtained from Applied Biological Materials Inc. (Richmond, BC, Canada). The cells were cultured in Prigrow III medium (Richmond, BC, Canada) supplemented with 10% fetal bovine serum (FBS) and 100 units/mL of penicillin/streptomycin (Life technologies, MD, USA) at 37°C in a 5% CO_2 atmosphere. For primary human DPCs, they were obtained from PromoCell (Heidelberg, Germany). The cells were cultured in medium containing bovine pituitary extract 4 μL/mL, fetal calf serum 0.05 mL/mL, basic fibroblast growth factor 1 ng/mL, recombinant human insulin 5 μg/Ml and phenol red 0.62 ng/mL from PromoCell (Heidelberg, Germany), and 100 units/mL of penicillin/streptomycin at 37°C in a 5% CO_2 atmosphere. Ciprofloxacin (CIP) and dimethylsulfoxide (DMSO) were purchased from Sigma (St. Louis, MO, USA). Hoechst 33342 and propidium iodide (PI) were obtained from Molecular Probes Inc. (Eugene, OR, USA). 3-(4,5-Dimethylthiazol-2-yl)-2,5-diphenyltetrazolium bromide (MTT) and Alexa Fluor 488/594 conjugated secondary antibody were from Invitrogen (Carlsbad, CA, USA). Rabbit monoclonal antibodies for integrinβ1, phosphorylated ATP-dependent tyrosine kinase (Akt, Ser 473), Akt, phosphorylated glycogen synthase kinase3β (GSK3β, Ser 9), GSK3β, ZEB1, Nanog, Oct-4, Slug, Snail, Vimentin, N-cadherin, phosphorylated extracellular signal-regulated kinase (Erk), Erk, β-actin, and peroxidase conjugated anti-rabbit IgG were obtained from Cell Signaling (Denver, MA, USA). Rabbit CD133 antibody was bought from Cell Applications Inc. (San Diego, CA, USA). Rabbit procollagen type I antibody, goat aldehyde dehydrogenase 1A1 antibody (ALDH1A1), and peroxidase conjugated anti-goat IgG were obtained from Santa Cruz Biotechnology Inc. (Dallas, Texas, USA). Immobilon Western Chemiluminescent HRP substrate was from Millipore Corp. (Billerica, MA) and Thermo Fisher Scientific Inc. (Rockford, IL).

2.2. Cell Viability Assay. MTT viability assay was used to evaluate cell viability. Cells were seeded at a density of 1×10^4 cells/well and cultivated for 12 h in 96-well plate. Afterward, the cells were incubated with various concentrations of CIP (0–10 μg/mL) for 24 h. The cells were then incubated with 5 mg/mL MTT for 4 h at 37°C. Then, the supernatant was removed and replaced with 100 μL of DMSO to dissolve the formazan crystal. The intensity of MTT product was measured at 570 nm using a microplate reader (Anthos, Durham, NC). Cell viability was calculated by the following formula and presented as a percentage to untreated control value

$$\text{Cell viability}\,(\%) = \frac{\text{A570 of treatment}}{\text{A570 of control}} \times 100. \quad (1)$$

2.3. Nuclear Staining Assay. Hoechst 33342 and PI costaining was used to detect apoptotic and necrosis cell death. Cells were seeded at a density of 1×10^4 cells/well and cultivated for 12 h. Subsequently, the cells were treated with various concentrations of CIP (0–10 μg/mL) for further 24 h. After treatments, the cells were stained with 10 μM of Hoechst and 5 μg/mL of PI for 30 min at 37°C and visualized by fluorescence microscope (Olympus IX 51 with DP70, Olympus America Inc., Center valley, PA).

2.4. Cell Morphology and Aggregation Behavior Evaluation. DP cells were seeded at a density of 6×10^3 cells/well onto 24-well plate and incubated for 12 h. The cells were treated with various concentrations of CIP (0–10 μg/mL) for 72 h, and cell morphology was observed at 0, 24, 48, and 72 h. The aggregation behavior of the cells was determined at 72 h. Morphology and aggregation behaviors of cells were photographed by a phase-contrast microscope (Olympus IX51 with DP70, Olympus America Inc., Center valley, PA).

2.5. Cell Cycle Analysis. Cells were seeded at a density of 3×10^4 cells/well onto 6-well plate and incubated overnight. The cells were cultured in the presence or absence of CIP (10 μg/mL) for 72 h. After indicated treatment, the cells were incubated in the absence of growth factors for 24 h. The cells were then incubated with complete media for 12 h, trypsinized and fixed with 70% absolute ethanol at −20°C overnight. The cells were washed with cold PBS and incubated in PI solution containing 0.1% Triton-X, 1 μg/mL RNase, and 1 mg/mL propidium iodide at 37°C for 30 min. The cells at the early passages (passages 2-3) without serum-starvation were used as an untreated control at 0 h. DNA in whole cells

was stained with PI, and cell cycle profile was analyzed using flow cytometry (FACSort, Becton Dickinson, Rutherford, NJ, USA).

2.6. Immunofluorescence. Cells were seeded at a density of 3×10^4 cells/well onto coverslips in 6-well plate and incubated overnight. The cells were cultured in the presence or absence of ciprofloxacin (10 μg/mL) for 72 h. The cells at the early passages were used as an untreated control at 0 h. The coverslips were fixed with 4% paraformaldehyde for 20 min and permeabilized with 0.1% Triton-X for 10 min at room temperature. Thereafter, the coverslips were incubated with 3% bovine serum albumin (BSA) for 30 min at room temperature to prevent nonspecific binding. The coverslips were washed and incubated with CD133 or procollagen type I rabbit monoclonal antibodies at 1 : 100 dilution overnight at 4°C. After primary antibody incubation, the coverslips were washed with PBS and subsequently incubated with Alexa Fluor 488 or 594 conjugated secondary antibodies for 1 h at room temperature. Samples were examined with Confocal Laser Scanning Microscopy (Zeiss LSM 510) to analyze expression of CD133 and procollagen type I.

2.7. Western Blot Analysis. Cells were seeded at a density of 5×10^4 cells/well onto 6-well plate for 12 h and cultured in the presence of various concentrations of CIP (2.5–10 μg/mL) for 72 h. After washing the cells with PBS, cell lysates were prepared by incubating the cells in ice-cold lysis buffer containing 20 mM Tris·HCl (pH 7.5), 0.5% Triton X, 10% glycerol, 150 mM sodium chloride, 50 mM sodium fluoride, 1 mM sodium orthovanadate, 1 mM phenylmethylsulfonyl fluoride, and commercial protease inhibitor cocktail (Roche Molecular Biochemicals) for 45 min on ice. Subsequently, cell lysates were collected and determined for protein content by the Bradford method (Bio-Rad, Hercules, CA). Equal amounts of proteins of each sample (50 μg) were boiled in Laemmli loading buffer at 95°C for 5 min. The proteins were subsequently loaded on 10% SDS-polyacrylamide electrophoresis. After separation, proteins were transferred onto 0.45 μm nitrocellulose membranes (Bio-Rad). Following blocking with 5% nonfat milk in TBST [25 mM Tris·HCl (pH 7.5), 0.05% Tween-20, and 125 mM NaCl] for 2 h, membranes were then incubated with appropriate primary antibodies for 10 h at 4°C. Membranes were washed three times with TBST for 15 min and incubated with horseradish peroxidase-coupled secondary antibodies for 1 h at room temperature. The immune complexes were detected with Chemiluminescence substrate (SuperSignal West Pico, Pierce, Rockford, IL) and quantified using analyst/PC densitometry software (Bio-Rad).

2.8. Statistical Analysis. Data were obtained from at least four independent experiments and presented as means ± standard deviation (SD). Statistical analysis was performed using one-way ANOVA with post hoc test at a significance level (α) of 0.05. These analyses were performed using SPSS Version 19 (SPSS Inc., Chicago, IL).

3. Results

3.1. Effect of CIP on Viability of DPCs. To study the role of CIP on the stem cell property of DPCs, we first characterized cell viability and cell death response to CIP treatment in DPCs using MTT and Hoechst 33342/propidium iodide (PI) costaining assays. Treatment of the cells with CIP at the concentrations of 0–10 μg/mL for 24 h caused no significant change in cell viability compared with control levels (Figure 1(a)). Consistent with the Hoechst/PI apoptosis assay, our results indicated that the treatment drug at such concentrations caused neither apoptosis nor necrosis detected by Hoechst and PI, respectively (Figure 1(b)). This information may help to clarify that the following effects of CIP on DPCs were not a consequence of cytotoxic effect or cell stress.

3.2. CIP Maintains Stem Cell-Like Characteristics in DPCs. DPCs have been reported to function as multipotent stem cells and the stemness of DPCs was linked to their ability to induce hair follicles [10–12]. However, DPCs lose their hair follicle inductive ability during culture [4, 6–8]. We found that, after culturing the DPCs for 5 days, the shape and appearance of DPCs are spontaneously altered toward fibroblast-like morphology. The primitive DPCs usually appearing as spindle-shaped cells changed to flat multipolar cells with elongated shapes (Figure 2(a)). Besides, the DPCs at the beginning showed an aggregative growth pattern in culture and such pattern was lost during the extended time of culturing. In order to test whether CIP affects the change in morphology of these DPCs, the cells were treated with CIP at the concentrations of 0–10 μg/mL for 0–72 h, and morphology of the cells as well as aggregative pattern was determined. Figure 2(a) shows that most of untreated control cells exhibited fibroblast-like morphology at 48 and 72 h. Meanwhile, the morphology of CIP treated cells remained unaltered (Figure 2(a)). Because the hair follicle inductive property of the DPCs has been shown to relate with their aggregate behaviors [22], we further investigated the effect of CIP treatments on the aggregative growth pattern of the cells. The DPCs at early passages (passages 2-3) were cultured in the presence or absence of CIP for 72 h and the aggregate size and number were determined. Figures 2(b), 2(c), and 2(d) show that CIP at the concentration of 5 and 10 μg/mL significantly increased the size as well as the number of cell aggregation in comparison to those of untreated control at 72 h.

As mesenchymal cells have been shown to be slow-cycling cells, we next investigated the effect of CIP on the proliferation and the cell cycle distribution of DPCs. The DPCs were cultured in the presence or absence of CIP for 72 h and subjected to cell cycle evaluation. The cells were incubated in the absence of growth factors for 24 h. Then, the cells were incubated with complete media for 12 h and the cell cycle progression was analyzed by PI and flow cytometer. Also, the DPCs at the early passages without serum-starvation were used as a control. Figures 2(e) and 2(f) show that, at 12 h after the cells receive growth factors, the untreated control cells at 72 h proceeded to M phase of the cell cycle. Importantly, treatment of the cells with 10 μg/mL CIP attenuated the cell cycle progression as the cells cannot enter

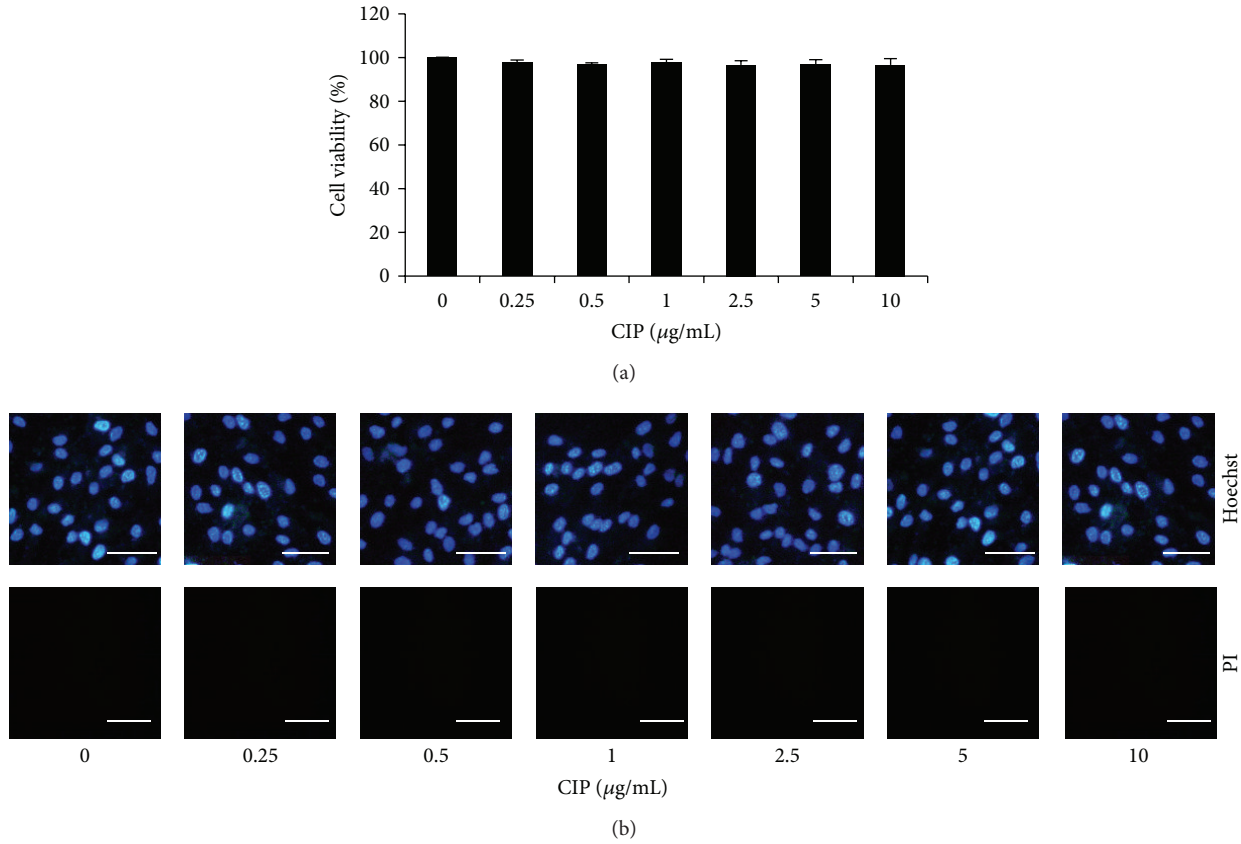

Figure 1: Cytotoxicity of CIP on DPCs. (a) Cells were treated with CIP (0–10 μg/mL) for 24 h. Cytotoxicity was determined by MTT assay. (b) After indicated treatment for 24 h, mode of cell death was examined by Hoechst 33342/PI costaining assay. Scale bar is 100 μm. The data represent the means of four independent samples ± SD.

to M phase. Further, the cell cycle distribution was quantified as described in Section 2.5. The results confirmed the above findings that the treatment of the cells with CIP significantly decreased the cell population in G2/M phase (Figures 2(e) and 2(f)).

3.3. CIP Prevents the Downregulation of Stem Cell Markers in DPCs. Having shown that culture of the DPCs caused the spontaneous decline of stem cell-like phenotypes, we next clarify the mentioned conception by detecting stem cell markers in such cells. Because the CD133 and procollagen type I expressions have been recognized as the dermal papilla cell and fibroblast indicators, respectively [11, 23, 24], we analyzed the expression of such proteins in the DPCs treated with CIP at the concentrations of 10 μg/mL for 72 h and the control cells. Immunocytochemistry showed that the expression of CD133 with CIP was suppressed in the DPCs cells after being cultivated for 72 h in comparison to that of control cells (DPCs at the early passages at 0 h, Figure 3(a)). Treatment of the cells with CIP could dramatically prevent such a loss of CD133 expression in the cells (Figure 3(a)). These results suggested that CIP preserve the stemness of DPCs during culture. Also, the expression level of fibroblast marker procollagen type I was significantly increased in the untreated DPCs cells at 72 h, whereas the increase in fibroblast marker could be prevented by CIP at the concentration of 10 μg/mL (Figure 3(a)).

We further exploited the information to show that CIP prevents the loss of stemness in cultured DPCs. By utilizing CD133, integrin β1, and ALDH1A1 as dermal papilla markers and procollagen type I as a fibroblast marker, the cells cultured in the presence or absence of CIP were analyzed for the proteins by western blot analysis. Figure 3(b) shows that the expression of procollagen type I was upregulated in a time-dependent manner, whereas treatment with CIP could prevent the increase of such a protein. As expected, all mesenchymal related proteins including CD133, integrin β1, and ALDH1A1 were gradually decreased in the untreated control cells in a time-dependent fashion and treatment of the cells with CIP inhibited the reduction of the protein markers (Figure 3(b)). We also performed the dose-dependent experiment to assure the effect of the drug on DPCs stemness. The results indicated that CIP increased the stem cell markers in these cells while it decreased fibroblast marker in a dose-dependent manner (Figure 3(c)).

3.4. CIP Activates Wnt/β-Catenin Signaling and Epithelial-Mesenchymal Transition (EMT) in DPCs. Activation of

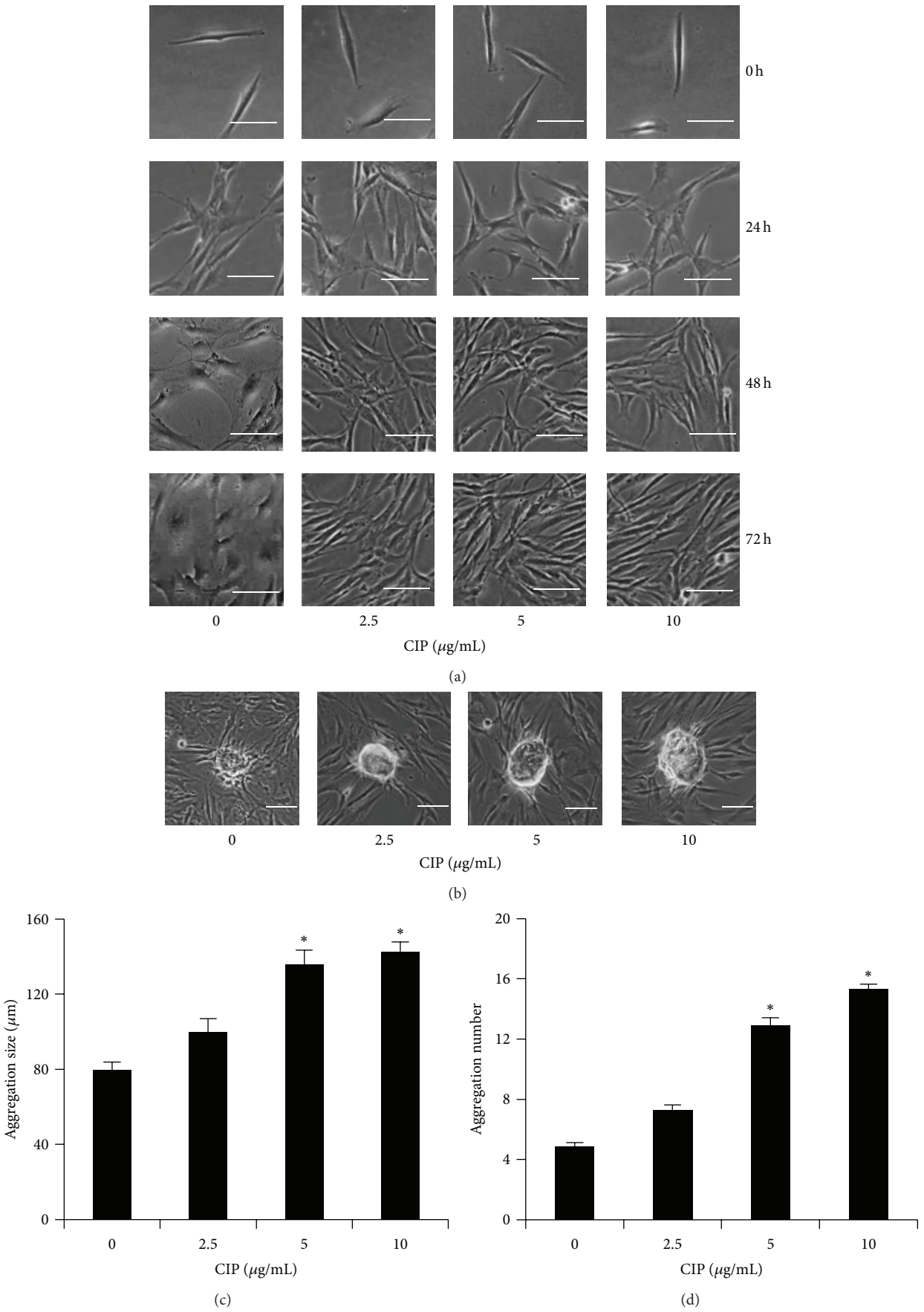

Figure 2: Continued.

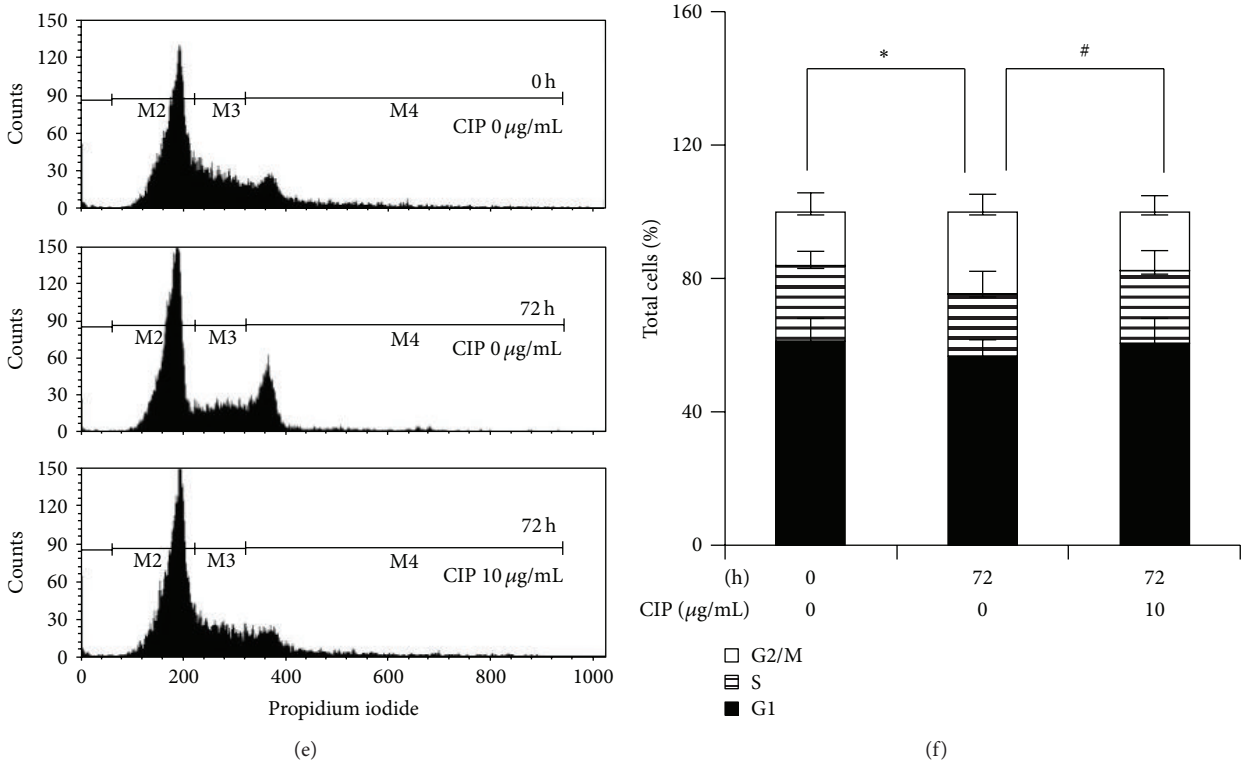

Figure 2: Effects of CIP on stem cell-like characteristics in DPCs. (a) Cells were treated with CIP (0–10 μg/mL) for various times (0–72 h). After indicated treatment, morphology of DPCs was observed. Scale bar is 100 μm. (b) Aggregation behavior of cells was determined after indicated treatment for 72 h. Scale bar is 100 μm. ((c)-(d)) Aggregation size and aggregation number were determined by image analyzer. The data represent the means of four independent samples ± SD. $^{*}P < 0.05$ versus untreated control. ((e)-(f)) Cells were cultured in the presence or absence of CIP (10 μg/mL) for 72 h and serum-starved for 24 h. After serum-starvation, cells were incubated with complete media for 12 h. The cells at the early passages (passages 2-3) without serum-starvation were also used as an untreated control at 0 h. Cell cycle distribution was determined by PI staining and flow cytometry. The data represent the means of four independent samples ± SD. $^{*}P < 0.05$ versus untreated control at 0 h; $^{\#}P < 0.05$ versus untreated control at 72 h.

Wnt/β-catenin signaling was shown to play a critical role in stem cell maintenance [25–27] and hair regeneration [13–15]. In addition, the hair follicle inductive effect in cultured DPCs could be prolonged by exposing the cells to Wnt/β-catenin activator [14, 15]. Based on these data, it is promising that CIP may exert its positive role in stemness in DPCs through this pathway. The signaling proteins related to Wnt/β-catenin including activated Akt (phosphorylated Akt at Ser 473), total Akt, inactivated glycogen synthase kinase3β (phosphorylated GSK3β at Ser 9), parental GSK3β, and β-catenin were determined by western blot analysis.

The results showed that activated Akt was significantly enhanced by treatment of the cells with CIP at 2.5–10 μg/mL in a dose-dependent manner (Figure 4(a)). Consequently, the downstream GSK3β was inactivated by the treatment of CIP as indicated by an increase in phosphorylated GSK3β (Figure 4(a)). As GSK3β was shown to inhibit the degradation process of β-catenin, we found corresponding results that phosphorylated GSK3β leads to an increase of cellular β-catenin in CIP treated DPCs (Figure 4(a)). These data suggested that CIP maintains stemness in DPCs at least in part by increased cellular β-catenin via Akt/GSK3β pathway.

Recently, the process of the cell transition from epithelial-mesenchymal phenotypes (EMT) has garnered increased attention in cell biology as it is linked with the stem cell-like properties in various cells [16–18]. Furthermore, the transcription factors upregulated during EMT like Snail were shown to maintain the stem cell-like phenotypes in many cells [16–18]. In order to clarify whether this EMT plays a part in stem cell maintenance of CIP, the EMT-activating transcription factors including ZEB1, Slug, and Snail were determined in the CIP treated cells by western blotting. After incubation with CIP for 72 h, the cellular levels of ZEB1 and Snail were significantly upregulated; however, we found only minimal change in case of Slug (Figure 4(b)). Moreover, we have determined the levels of downstream gene targets of Snail including N-cadherin and vimentin [28, 29]. The results indicated that such proteins are significantly upregulated in the CIP-treated cells (Figure 4(c)). It is worth noting herein that p-Erk (Thr 202/Tyr 204), an activation downstream target of Snail [30], was also found to be increased in CIP-treated cells. Taken together, our results revealed the novel molecular mechanism by which CIP mediates the stem cell-like phenotypes in the DPCs through β-catenin and EMT.

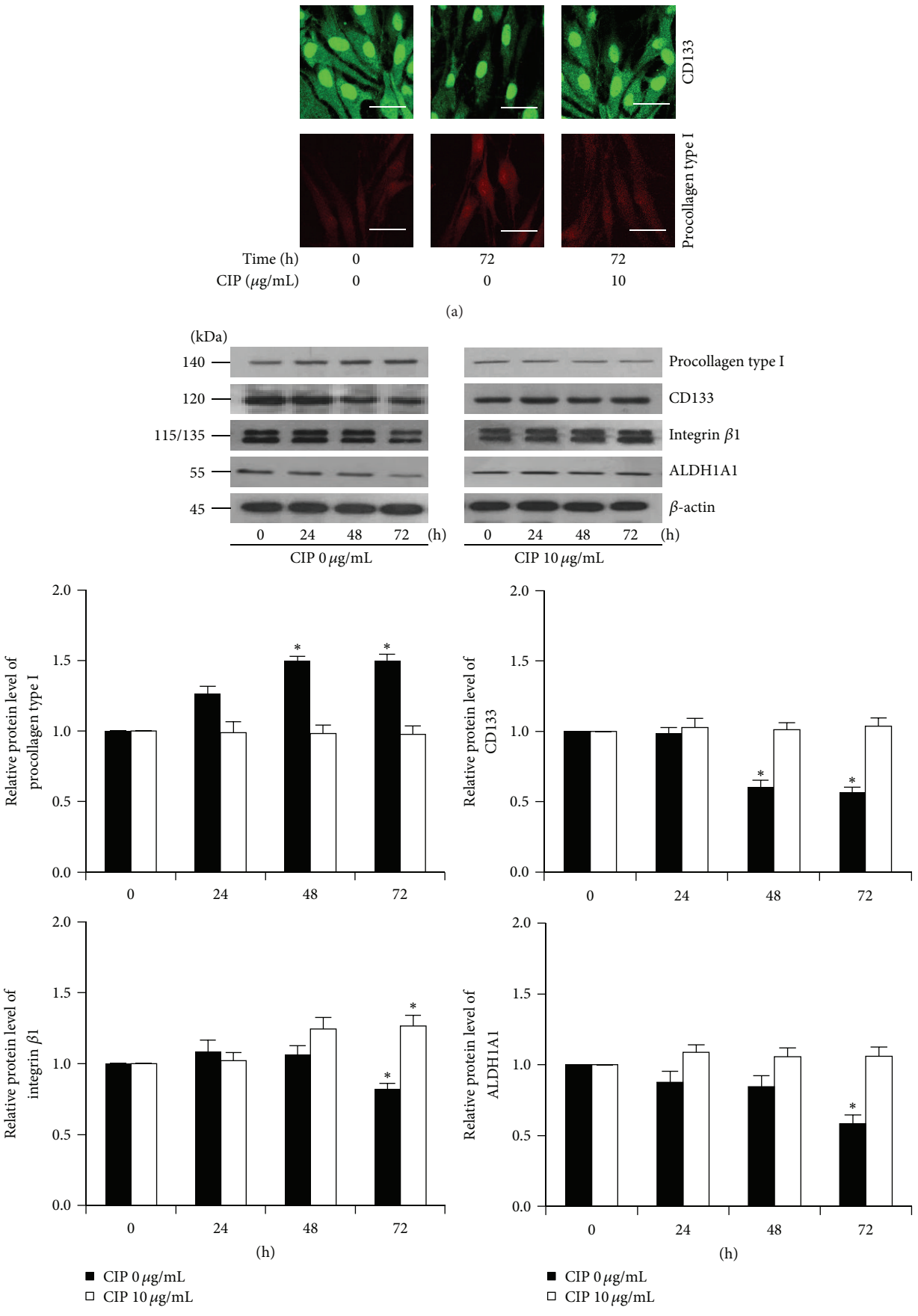

Figure 3: Continued.

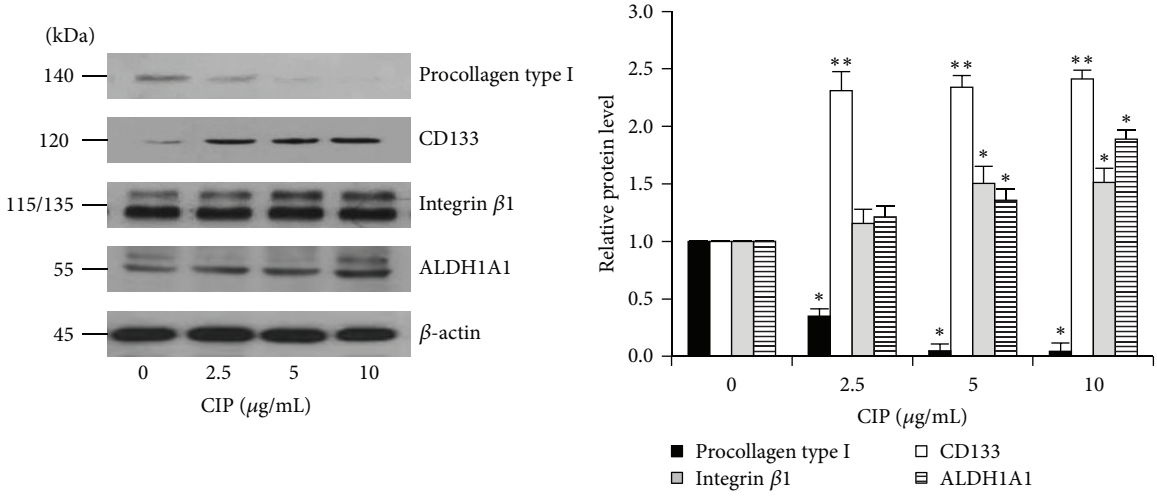

(c)

Figure 3: Effects of CIP on stem cell markers in DPCs. (a) Cells were cultured in the presence or absence of CIP (10 μg/mL) for 72 h. The cells at the early passages were used as an untreated control at 0 h. Expression of CD133 and procollagen type I were analyzed by immunofluorescence staining. Scale bar is 50 μm. (b) Time-dependent effects of CIP treatment on the expression of stem cell markers were determined. Cells were cultured in the presence or absence of CIP (10 μg/mL) for 0–72 h. The levels of procollagen type I, CD133, integrin β1, and ALDH1A1 were determined by western blot analysis. Blots were reprobed with β-actin to confirm equal loading. The immunoblot signals were quantified by densitometry and the mean data from independent experiments were normalized to the results. The data represent the means of four independent samples ± SD. $^{*}P < 0.05$ versus untreated control at 0 h. (c) Cells were treated with CIP (0–10 μg/mL) for 72 h. After indicated treatment, levels of procollagen type I, CD133, integrin β1, and ALDH1A1 were analyzed by western blot. β-actin was served as the loading control. The immunoblot signals were quantified by densitometry and the mean data from independent experiments were normalized to the results. The data represent the means of four independent samples ± SD. $^{*}P < 0.05$ and $^{**}P < 0.01$ versus untreated control.

3.5. CIP Increases the Self-Renewal Transcription Factors in DPCs. Self-renewal is an important signature of stem cells [31–33]. To provide supportive data on the effects of CIP on DPCs stemness, critical transcription factors that maintain pluripotency and self-renewal in stem cells, including Nanog and Oct-4, were determined [34, 35]. After treatment of the cells with 5 and 10 μg/mL of CIP (Figure 4(b)), the cells exhibited dramatic increases of Nanog and Oct-4 in a dose-dependent manner, suggesting that the treatments induced the self-renewal machinery in these cells.

3.6. CIP Maintains the Stem Cell-Like Phenotypes of Primary Human DPCs. To determine the extent to which primary human DPCs will respond to the CIP treatment by the same manner, we treated the isolated human DPCs with 0–10 μg/mL CIP and evaluated stem cell characteristics, accordingly. Figures 5(a) and 5(b) indicate that treatment of the cells with 0–10 μg/mL CIP caused no direct cytotoxicity in these cells. We next tested the signature characteristics of stem cells to assess whether CIP sustained the stemness in these primary cells. The cells were cultured in the presence or absence of CIP for 72 h and the expression of stem cells as well as fibroblast markers was determined as described previously. Western blot analysis revealed that the levels of CD133, integrin β1, and ALDH1A1 were significantly increased in response to CIP treatment in a dose-dependent manner, whereas the expression of procollagen type I was significantly suppressed (Figure 5(c)). Furthermore, the Wnt/β-catenin and EMT were evaluated by western blotting. Figure 5(d) shows that treatment of the cells with CIP significantly increased the level of activated Akt level, inactivated GSK3β, and β-catenin. Besides, the EMT transcription factors ZEB1 and Snail were found to be upregulated in response to the treatment (Figure 5(e)). Taken together, these data supported our earlier findings that CIP maintains the stemness of DPCs via β-catenin and EMT.

4. Discussion

DPCs have been shown to exhibit phenotypic plasticity by differentiating to different cell types [36]. Interestingly, multipotency of DPCs is accepted to be an important factor determining an ability to induce hair follicle formation [10–12]. Although advancement in research facilitates the culture of these specialized cells, previous study has shown that the hair inducing property of DPCs is gradually declined during culture [4, 6, 7]. In an attempt to evaluate the possible ways to maintain the DPCs signature *in vitro*, we have discovered for the first time that CIP was able to prevent the loss of DPCs stemness during culture. Treatment of the DPCs with nontoxic concentration of CIP prevented the spontaneous alteration of cell morphology toward fibroblast-like cells (Figure 2(a)). Also, our immunocytochemistry as well as protein analysis revealed that the cultured DPCs decreased the stem cell markers, and that could be prevented by an addition of CIP (Figures 3(a) and 3(b)). In addition, we found

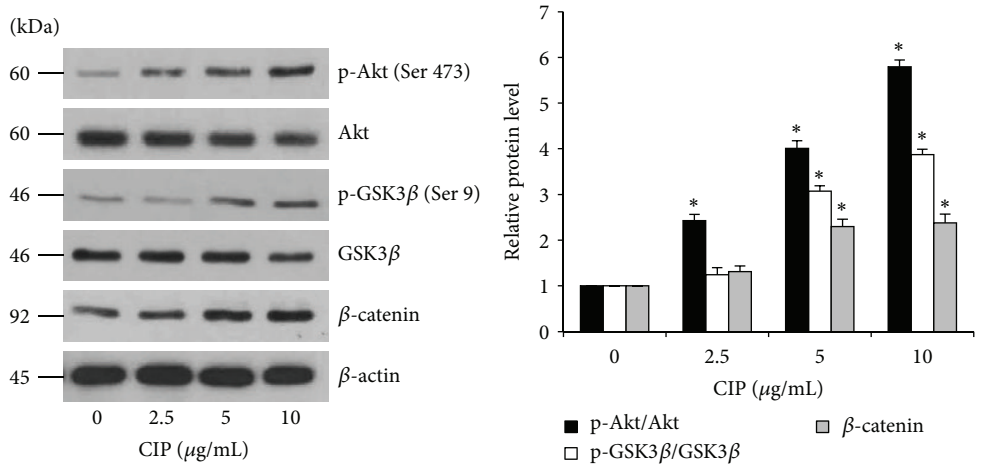

(a)

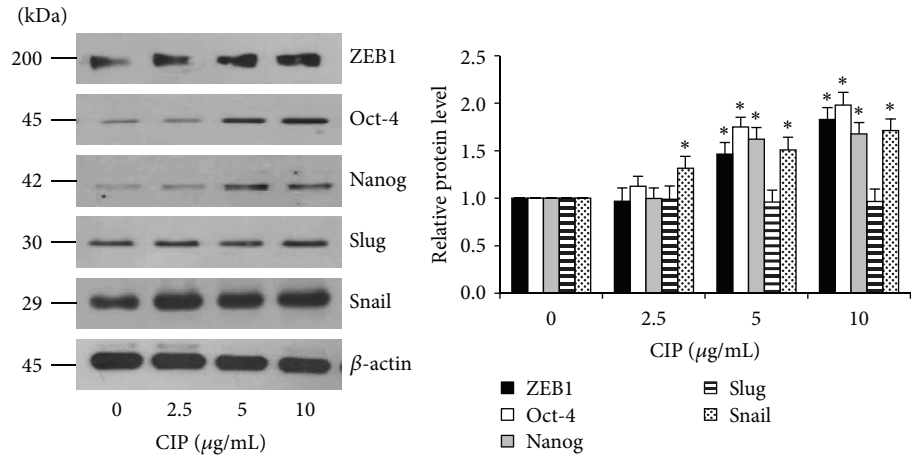

(b)

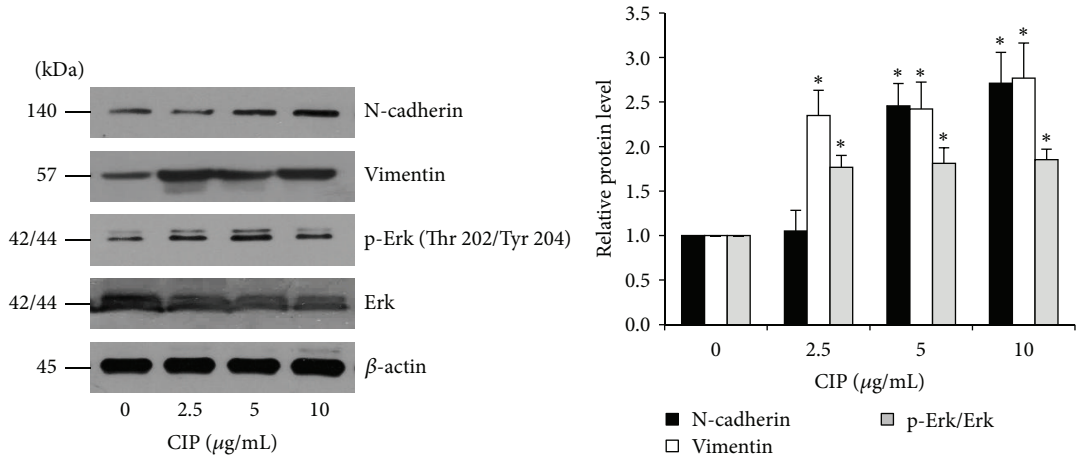

(c)

Figure 4: Effects of CIP on Wnt/β-catenin signaling, EMT, and self-renewal transcription factors in DPCs. (a) Cells were treated with CIP (1–10 μg/mL) for 72 h. After indicated treatment, the levels of Wnt/β-catenin signaling (Akt, p-Akt (Ser 473), GSK3β, p-GSK3β (Ser 9), and β-catenin) were analyzed by western blot analysis. The immunoblot signals were quantified by densitometry and mean data from independent experiments were normalized to the results. (b) EMT and self-renewal transcription factors (ZEB1, Oct-4, Nanog, Slug, and Snail) were determined by western blot analysis. (c) Downstream targets of Snail including N-cadherin, vimentin, total Erk, and p-Erk (Thr 202/Tyr 204) were analyzed by western blot analysis. β-actin was used as the loading control. The western blot signals were quantified by densitometry and mean data from independent experiments were normalized to the results. The data represent the means of four independent samples ± SD. $^*P < 0.05$ versus untreated control.

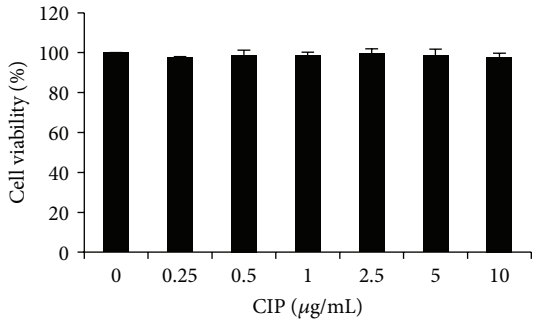

(a)

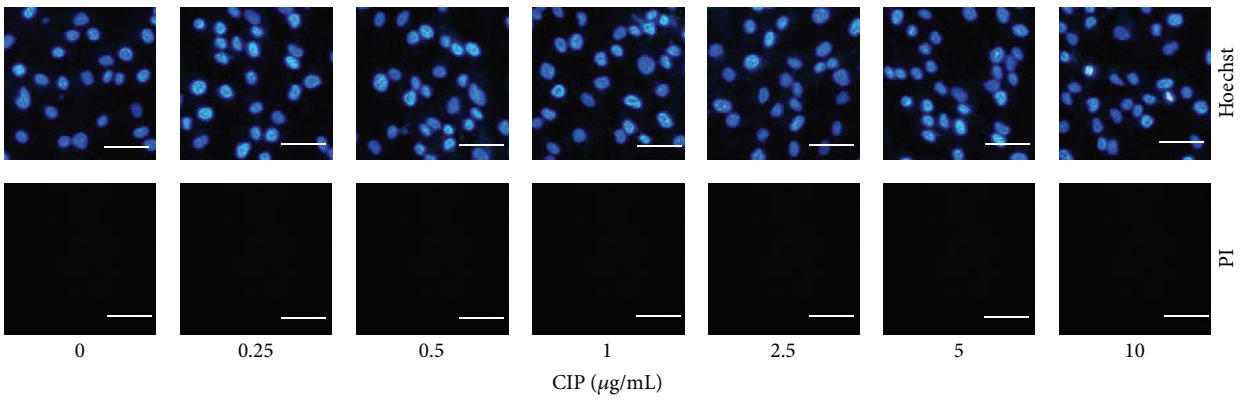

(b)

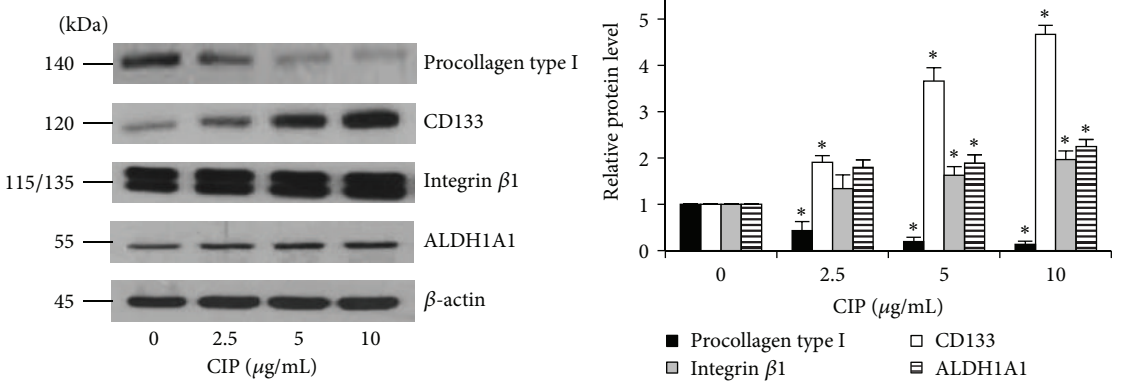

(c)

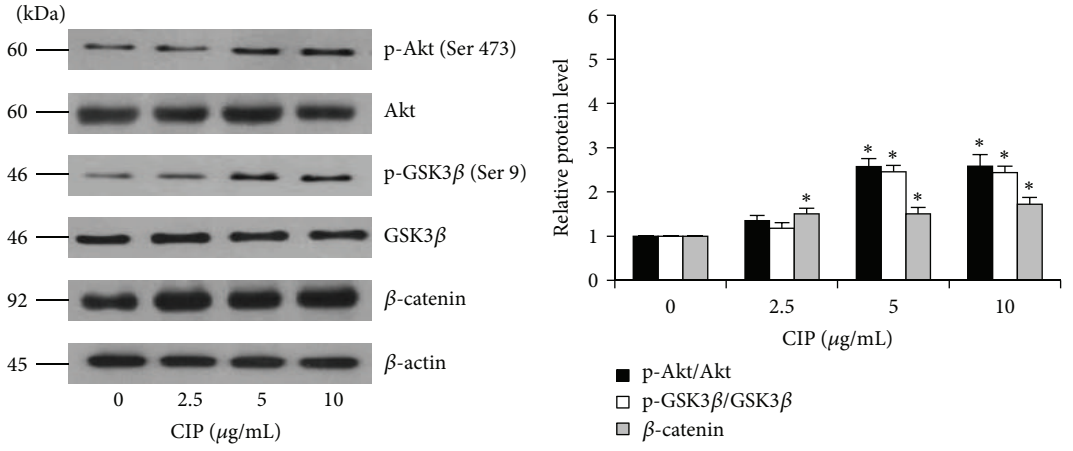

(d)

Figure 5: Continued.

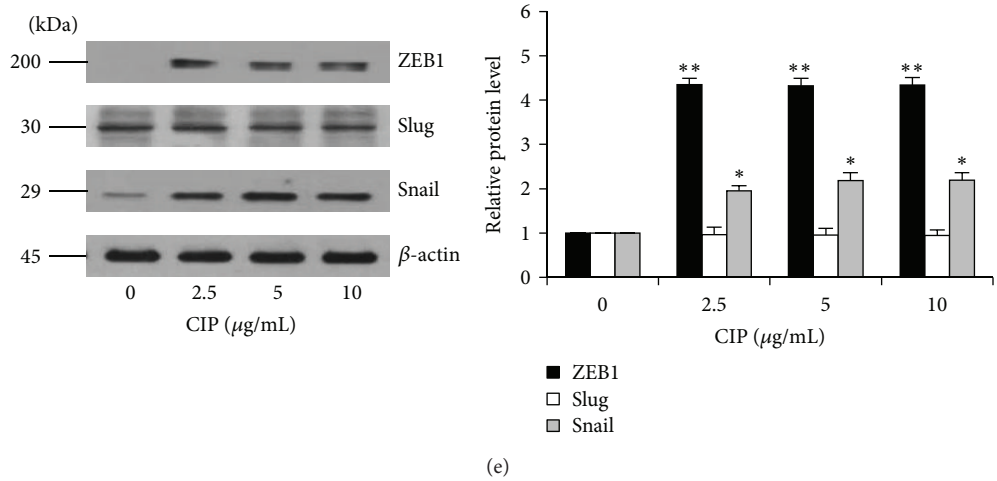

Figure 5: Effects of CIP on stem cell-like phenotypes in primary human DPCs. (a) Cells were treated with CIP (0–10 μg/mL) for 24 h. Cytotoxicity was determined by MTT assay. The data represent the means of four independent triplicate samples ± SD. (b) After indicated treatment, mode of cell death was examined by Hoechst 33342/PI costaining assay. Scale bar is 100 μm. ((c)–(e)) Cells were treated with CIP (0–10 μg/mL) for 72 h. After indicated treatment, the levels of stem cell markers (procollagen type I, CD133, integrin β1, and ALDH1A1), Wnt/β-catenin signaling (Akt, p-Akt, GSK3β, p-GSK3β, and β-catenin), and EMT transcription factors (ZEB1, Slug, and Snail) were determined by western blot analysis, respectively. β-actin was served as the loading control. The immunoblot signals were quantified by densitometry and mean data from independent experiments were normalized to the results. The data represent the means of four independent samples ± SD. $^{*}P < 0.05$ and $^{**}P < 0.01$ versus untreated control.

the increase of procollagen type I in the DPCs, suggesting that the DPCs can instinctively differentiate to fibroblast-like cells (Figure 3(b)). This observation is in agreement with the previous reports indicating that DPCs differentiate toward fibroblast-like cells [23, 24].

Regarding stem cell research, CD133, a transmembrane glycoprotein, has been widely used as a standard biomarker of stem cells [37]. We found that DPCs at the early passages exhibited high level of CD133; however, the expression of this protein was found to decline in a time-dependent manner during the time of cultivation, indicating that the cells have lost their stemness. Together with other stem cell markers, CIP was shown to sustain stemness of DPCs as indicated by the steady level of CD133, ALDH1A, and integrin β1 (Figure 3(b)). Besides, the presence of ALDH1A1, a detoxifying enzyme highly expressed in stem cells, was shown to regulate stem cell function [38]. Thus the increase of the proteins in response to CIP treatment could support our finding that CIP maintains the stemness of the cells.

In the past decade, considerable progress has been obtained in elucidating stem cell signaling pathways, in particular Wnt/β-catenin that is critical for maintaining stem cell features as well as function [25–27]. Previously, studies reported that an ablation of β-catenin in DPCs causes the suppression of hair growth and regeneration [13]. The β-catenin functions as a cotranscription factor of T-cell factor/lymphoid enhancing factor (TCF/LEF) and consequently regulates expression of proteins facilitating stem cell functions [39]. The cellular level of β-catenin is tightly controlled by GSK3β. The phosphorylation of β-catenin by the function of GSK3β resulted in ubiquitination and proteasomal degradation of β-catenin. The activated Akt is shown to inhibit such a function of GSK3β by phosphorylating the GSK3β at serine 9 [39]. Therefore, the activation of Akt increases cellular level of β-catenin. As a consequence, β-catenin accumulates in cytoplasm and translocates into nucleus leading to stimulation of target genes. Here, we showed that the levels of activated Akt and inactivated GSK3β were upregulated consistently with the increase of β-catenin in CIP treated cells (Figures 4(a) and 5(d)). These results suggested that the stemness sustaining effect of CIP is due to the activation of Akt/β-catenin pathway.

Indeed, the DPCs require stemness in terms of molecular signals rather than pluripotency for the production of cytokines and growth factors functioning in the keratinocyte recruitment and proliferation. In this regard, activation of Wnt/β-catenin signaling was shown to induce hair follicle formation and hair growth through stem cell signals that drive cytokine synthesis [7, 13, 40, 41]. For the focus points of this study, the upregulation of stemness signals including β-catenin, Nanog, Oct4, Slug, and Snail described the mechanism of ciprofloxacin in driving the DPCs to functioning in enhancing the growth of hair (Figures 4 and 5).

Recent evidences have suggested that β-catenin interacts with many signaling pathways involved in pluripotency and EMT [25–27, 35, 42]. Furthermore, Wnt/β-catenin signaling activation was shown to increase the expression of EMT proteins and pluripotent activating transcription factors [43–47]. Consistent with previous reports that the transcription factors Snail and ZEB1 play an important role in EMT process [16, 18], we found significant increase of such proteins in the DPCs treated with CIP (Figures 4(b) and 5(e)), and

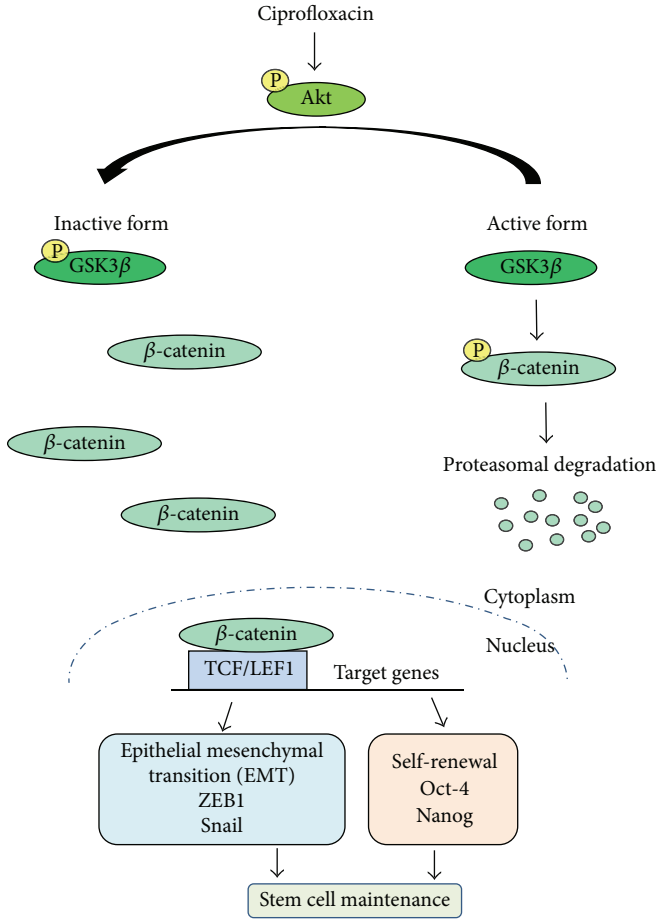

Figure 6: Schematic diagram summarizes the effects of CIP for improvement of the stemness in human DPCs. CIP improved the stemness of human DPCs through Akt activation which accounts for GSK3β inactivation, resulting in the increase of cellular β-catenin. As a consequence, β-catenin accumulates in cytoplasm and translocates into nucleus leading to stimulation of target genes, including transcription factors associated with EMT and self-renewal that might exert the stemness sustaining effect of CIP.

the increase of EMT markers was found to be corresponding to the stem cell-like morphology and aggregative behavior. Our findings also lend strong support to the view that Akt/GSK3β-dependent β-catenin upregulation is important for the DPCs to maintain their stemness. We unveiled that the transcription factors which are downstream targets of Wnt/β-catenin, namely, Nanog and Oct4, were upregulated in the CIP-treated cells.

In closing, we systemically evaluated the positive role of CIP treatment for the maintenance of stemness in cultured DPCs. We identified a novel finding on the stemness regulatory effect of CIP in DPCs, that is, through Akt/GSK3β-dependent β-catenin signal resulting in an upregulation of transcription factors associated with EMT and self-renewal (Figure 6). This information may open the door to further investigations and make this new application of the drug in culture be useful for the cell therapeutic approaches.

Abbreviations

DPCs: Dermal papilla cells
GSK3β: Glycogen synthase kinase3β
Akt: ATP-dependent tyrosine kinase
EMT: Epithelial-mesenchymal transition
FGF: Fibroblast growth factor
IGF: Insulin-like growth factor
CIP: Ciprofloxacin
TCF: T-cell factor
LEF: Lymphoid enhancing factor.

Conflict of Interests

The authors declare that there is no conflict of interests regarding the publication of this paper.

Acknowledgments

This research has been supported by the Ratchadaphisek-somphot Endowment Fund of Chulalongkorn University (CU-57-003-HR) and The Thailand Research Fund through a Research and Researchers for Industries program. The funders had no role in study design, data collection and analysis, decision to publish, or preparation of the paper.

References

[1] G. Cotsarelis, "Epithelial stem cells: a folliculocentric view," *The Journal of Investigative Dermatology*, vol. 126, no. 7, pp. 1459–1468, 2006.

[2] M. R. Schneider, R. Schmidt-Ullrich, and R. Paus, "The hair follicle as a dynamic miniorgan," *Current Biology*, vol. 19, no. 3, pp. R132–R142, 2009.

[3] K. S. Stenn and R. Paus, "Controls of hair follicle cycling," *Physiological Reviews*, vol. 81, no. 1, pp. 450–481, 2001.

[4] C. A. B. Jahoda, K. A. Horne, and R. F. Oliver, "Induction of hair growth by implantation of cultured dermal papilla cells," *Nature*, vol. 311, no. 5986, pp. 560–562, 1984.

[5] J. Teumer and J. Cooley, "Follicular cell implantation: an emerging cell therapy for hair loss," *Seminars in Plastic Surgery*, vol. 19, no. 2, pp. 193–200, 2005.

[6] K. A. Horne, C. A. B. Jahoda, and R. F. Oliver, "Whisker growth induced by implantation of cultured vibrissa dermal papilla cells in the adult rat," *Journal of Embryology and Experimental Morphology*, vol. 97, pp. 111–124, 1986.

[7] R. R. Driskell, A. Giangreco, K. B. Jensen, K. W. Mulder, and F. M. Watt, "Sox2-positive dermal papilla cells specify hair follicle type in mammalian epidermis," *Development*, vol. 136, no. 16, pp. 2815–2823, 2009.

[8] J. H. Shim, T. R. Lee, and D. W. Shin, "Novel in vitro culture condition improves the stemness of human dermal stem/progenitor cells," *Molecules and Cells*, vol. 36, no. 6, pp. 556–563, 2013.

[9] T. J. van Raay, K. B. Moore, I. Iordanova et al., "Frizzled 5 signaling governs the neural potential of progenitors in the developing *Xenopus* retina," *Neuron*, vol. 46, no. 1, pp. 23–36, 2005.

[10] A. N. Ziegler, J. S. Schneider, M. Qin et al., "IGF-II promotes stemness of neural restricted precursors," *Stem Cells*, vol. 30, no. 6, pp. 1265–1276, 2012.

[11] Y. Ito, T. S. Hamazaki, K. Ohnuma, K. Tamaki, M. Asashima, and H. Okochi, "Isolation of murine hair-inducing cells using the cell surface marker prominin-1/CD133," *Journal of Investigative Dermatology*, vol. 127, no. 5, pp. 1052–1060, 2007.

[12] L. Armstrong, O. Hughes, S. Yung et al., "The role of PI3K/AKT, MAPK/ERK and NFkappabeta signalling in the maintenance of human embryonic stem cell pluripotency and viability highlighted by transcriptional profiling and functional analysis," *Human Molecular Genetics*, vol. 15, no. 11, pp. 1894–1913, 2006.

[13] D. Enshell-Seijffers, C. Lindon, M. Kashiwagi, and B. A. Morgan, "Beta-catenin activity in the dermal papilla regulates morphogenesis and regeneration of hair," *Developmental Cell*, vol. 18, no. 4, pp. 633–642, 2010.

[14] J. Kishimoto, R. E. Burgeson, and B. A. Morgan, "Wnt signaling maintains the hair-inducing activity of the dermal papilla," *Genes & Development*, vol. 14, no. 10, pp. 1181–1185, 2000.

[15] H. Shimizu and B. A. Morgan, "Wnt signaling through the β-catenin pathway is sufficient to maintain, but not restore, anagen-phase characteristics of dermal papilla cells," *Journal of Investigative Dermatology*, vol. 122, no. 2, pp. 239–245, 2004.

[16] S. A. Mani, W. Guo, M.-J. Liao et al., "The epithelial-mesenchymal transition generates cells with properties of stem cells," *Cell*, vol. 133, no. 4, pp. 704–715, 2008.

[17] W. Guo, Z. Keckesova, J. L. Donaher et al., "Slug and Sox9 cooperatively determine the mammary stem cell state," *Cell*, vol. 148, no. 5, pp. 1015–1028, 2012.

[18] Y. Shimono, M. Zabala, R. W. Cho et al., "Downregulation of miRNA-200c links breast cancer stem cells with normal stem cells," *Cell*, vol. 138, no. 3, pp. 592–603, 2009.

[19] K. A. Sepkowitz, "Antibiotic prophylaxis in patients receiving hematopoietic stem cell transplant," *Bone Marrow Transplantation*, vol. 29, no. 5, pp. 367–371, 2002.

[20] I. Gabanyi, F. H. Lojudice, P. M. Kossugue, E. Rebelato, M. A. Demasi, and M. C. Sogayar, "VP22 herpes simplex virus protein can transduce proteins into stem cells," *Brazilian Journal of Medical and Biological Research*, vol. 46, no. 2, pp. 121–127, 2013.

[21] J. M. Mowles, "The use of ciprofloxacin for the elimination of mycoplasma from naturally infected cell lines," *Cytotechnology*, vol. 1, no. 4, pp. 355–358, 1988.

[22] A. Osada, T. Iwabuchi, J. Kishimoto, T. S. Hamazaki, and H. Okochi, "Long-term culture of mouse vibrissal dermal papilla cells and de novo hair follicle induction," *Tissue Engineering*, vol. 13, no. 5, pp. 975–982, 2007.

[23] J. A. McDonald, T. J. Broekelmann, M. L. Matheke, E. Crouch, M. Koo, and C. Kuhn III, "A monoclonal antibody to the carboxyterminal domain of procollagen type I visualizes collagen-synthesizing fibroblasts. Detection of an altered fibroblast phenotype in lungs of patients with pulmonary fibrosis," *The Journal of Clinical Investigation*, vol. 78, no. 5, pp. 1237–1244, 1986.

[24] Y. Riaz, H. T. Cook, A. Wangoo, B. Glenville, and R. J. Shaw, "Type 1 procollagen as a marker of severity of scarring after sternotomy: effects of topical corticosteroids," *Journal of Clinical Pathology*, vol. 47, no. 10, pp. 892–899, 1994.

[25] J. Li, J. Li, and B. Chen, "Oct4 was a novel target of Wnt signaling pathway," *Molecular and Cellular Biochemistry*, vol. 361, no. 1-2, pp. 233–240, 2012.

[26] B. J. Merrill, "Wnt pathway regulation of embryonic stem cell self-renewal," *Cold Spring Harbor Perspectives in Biology*, vol. 4, Article ID a007971, pp. 1–17, 2012.

[27] T. Miki, S. Y. Yasuda, and M. Kahn, "Wnt/beta-catenin signaling in embryonic stem cell self-renewal and somatic cell reprogramming," *Stem Cell Reviews and Reports*, vol. 7, no. 4, pp. 836–846, 2011.

[28] L. D. M. Derycke and M. E. Bracke, "N-cadherin in the spotlight of cell-cell adhesion, differentiation, invasion and signalling," *The International Journal of Developmental Biology*, vol. 48, no. 5-6, pp. 463–476, 2004.

[29] D. Olmeda, M. Jordá, H. Peinado, Á. Fabra, and A. Cano, "Snail silencing effectively suppresses tumour growth and invasiveness," *Oncogene*, vol. 26, no. 13, pp. 1862–1874, 2007.

[30] A. Barrallo-Gimeno and M. A. Nieto, "The Snail genes as inducers of cell movement and survival: Implications in development and cancer," *Development*, vol. 132, no. 14, pp. 3151–3161, 2005.

[31] C. Blanpain, W. E. Lowry, A. Geoghegan, L. Polak, and E. Fuchs, "Self-renewal, multipotency, and the existence of two cell populations within an epithelial stem cell niche," *Cell*, vol. 118, no. 5, pp. 635–648, 2004.

[32] S. He, D. Nakada, and S. J. Morrison, "Mechanisms of stem cell self-renewal," *The Annual Review of Cell and Developmental Biology*, vol. 25, pp. 377–406, 2009.

[33] S. P. Medvedev, A. I. Shevchenko, and S. M. Zakain, "Molecular basis of mammalian embryonic stem cell pluripotency and self-renewal," *Acta Naturae*, vol. 2, no. 3, pp. 30–46, 2010.

[34] Y.-H. Loh, Q. Wu, J.-L. Chew et al., "The Oct4 and Nanog transcription network regulates pluripotency in mouse embryonic stem cells," *Nature Genetics*, vol. 38, no. 4, pp. 431–440, 2006.

[35] T. Su, S. Dan, and Y. Wang, "Akt-Oct4 regulatory circuit in pluripotent stem cells," *Chinese Science Bulletin*, vol. 59, no. 10, pp. 936–943, 2014.

[36] G. D. Richardson, E. C. Arnott, C. J. Whitehouse et al., "Plasticity of rodent and human hair follicle dermal cells: implications for cell therapy and tissue engineering," *Journal of Investigative Dermatology Symposium Proceedings*, vol. 10, no. 3, pp. 180–183, 2005.

[37] Z. Li, "CD133: a stem cell biomarker and beyond," *Experimental Hematology & Oncology*, vol. 2, no. 1, pp. 1–8, 2013.

[38] B. P. Levi, Ö. H. Yilmaz, G. Duester, and S. J. Morrison, "Aldehyde dehydrogenase 1a1 is dispensable for stem cell function in the mouse hematopoietic and nervous systems," *Blood*, vol. 113, no. 8, pp. 1670–1680, 2009.

[39] S. Fukumoto, C.-M. Hsieh, K. Maemura et al., "Akt participation in the Wnt signaling pathway through Dishevelled," *The Journal of Biological Chemistry*, vol. 276, no. 20, pp. 17479–17483, 2001.

[40] R. R. Driskell, V. R. Juneja, J. T. Connelly, K. Kretzschmar, D. W.-M. Tan, and F. M. Watt, "Clonal growth of dermal papilla cells in hydrogels reveals intrinsic differences between Sox2-positive and -Negative cells in vitro and in vivo," *Journal of Investigative Dermatology*, vol. 132, no. 4, pp. 1084–1093, 2012.

[41] C. Clavel, L. Grisanti, R. Zemla et al., "Sox2 in the dermal papilla niche controls hair growth by fine-tuning BMP signaling in differentiating hair shaft progenitors," *Developmental Cell*, vol. 23, no. 5, pp. 981–994, 2012.

[42] K. Kim, Z. Lu, and E. D. Hay, "Direct evidence for a role of beta-catenin/LEF-1 signaling pathway in induction of EMT," *Cell Biology International*, vol. 26, no. 5, pp. 463–476, 2002.

[43] M. F. Cole, S. E. Johnstone, J. J. Newman, M. H. Kagey, and R. A. Young, "Tcf3 is an integral component of the core regulatory circuitry of embryonic stem cells," *Genes & Development*, vol. 22, no. 6, pp. 746–755, 2008.

[44] E. Lambertini, T. Franceschetti, E. Torreggiani et al., "SLUG: a new target of lymphoid enhancer factor-1 in human osteoblasts," *BMC Molecular Biology*, vol. 11, article 13, 12 pages, 2010.

[45] L. Pereira, F. Yi, and B. J. Merrill, "Repression of Nanog gene transcription by Tcf3 limits embryonic stem cell self-renewal," *Molecular and Cellular Biology*, vol. 26, no. 20, pp. 7479–7491, 2006.

[46] D. ten Berge, W. Koole, C. Fuerer, M. Fish, E. Eroglu, and R. Nusse, "Wnt signaling mediates self-organization and axis formation in embryoid bodies," *Cell Stem Cell*, vol. 3, no. 5, pp. 508–518, 2008.

[47] K. Wu, J. Fan, L. Zhang et al., "PI3K/Akt to GSK3β/β-catenin signaling cascade coordinates cell colonization for bladder cancer bone metastasis through regulating ZEB1 transcription," *Cellular Signalling*, vol. 24, no. 12, pp. 2273–2282, 2012.